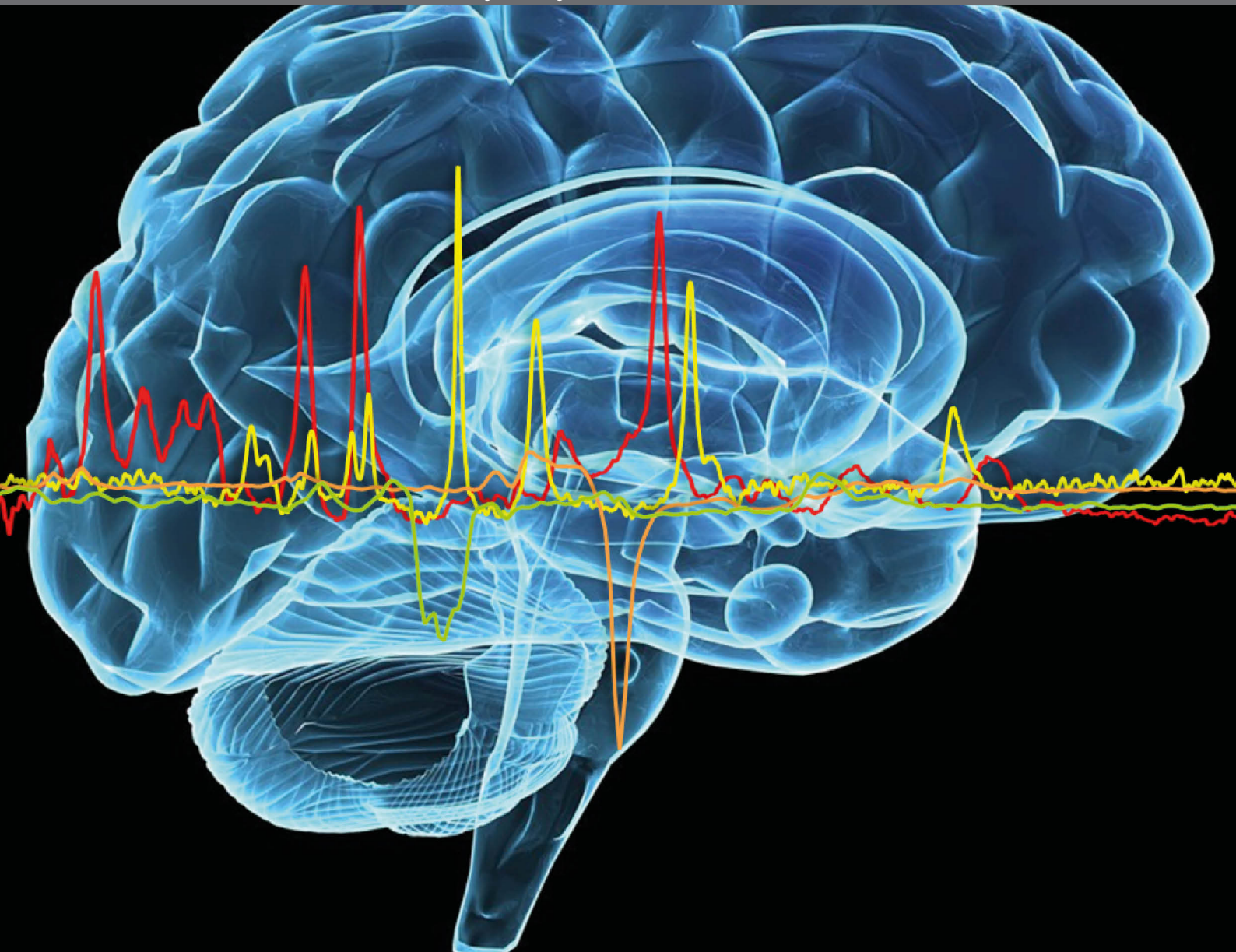


# MR SPECTROSCOPY IN NEUROPSYCHIATRY

EDITED BY: Anouk Marsman, Alice Egerton, Brian V. Broberg and

Hilleke E. Hulshoff Pol

PUBLISHED IN: Frontiers in Psychiatry





#### Frontiers Copyright Statement

© Copyright 2007-2018 Frontiers Media SA. All rights reserved.

All content included on this site, such as text, graphics, logos, button icons, images, video/audio clips, downloads, data compilations and software, is the property of or is licensed to Frontiers Media SA ("Frontiers") or its licensees and/or subcontractors. The copyright in the text of individual articles is the property of their respective authors, subject to a license granted to Frontiers.

The compilation of articles constituting this e-book, wherever published, as well as the compilation of all other content on this site, is the exclusive property of Frontiers. For the conditions for downloading and copying of e-books from Frontiers' website, please see the Terms for Website Use. If purchasing Frontiers e-books from other websites or sources, the conditions of the website concerned apply.

Images and graphics not forming part of user-contributed materials may not be downloaded or copied without permission.

Individual articles may be downloaded and reproduced in accordance with the principles of the CC-BY licence subject to any copyright or other notices. They may not be re-sold as an e-book.

As author or other contributor you grant a CC-BY licence to others to reproduce your articles, including any graphics and third-party materials supplied by you, in accordance with the Conditions for Website Use and subject to any copyright notices which you include in connection with your articles and materials.

All copyright, and all rights therein, are protected by national and international copyright laws.

The above represents a summary only. For the full conditions see the Conditions for Authors and the Conditions for Website Use.

ISSN 1664-8714

ISBN 978-2-88945-524-9

DOI 10.3389/978-2-88945-524-9

#### About Frontiers

Frontiers is more than just an open-access publisher of scholarly articles: it is a pioneering approach to the world of academia, radically improving the way scholarly research is managed. The grand vision of Frontiers is a world where all people have an equal opportunity to seek, share and generate knowledge. Frontiers provides immediate and permanent online open access to all its publications, but this alone is not enough to realize our grand goals.

#### Frontiers Journal Series

The Frontiers Journal Series is a multi-tier and interdisciplinary set of open-access, online journals, promising a paradigm shift from the current review, selection and dissemination processes in academic publishing. All Frontiers journals are driven by researchers for researchers; therefore, they constitute a service to the scholarly community. At the same time, the Frontiers Journal Series operates on a revolutionary invention, the tiered publishing system, initially addressing specific communities of scholars, and gradually climbing up to broader public understanding, thus serving the interests of the lay society, too.

#### Dedication to quality

Each Frontiers article is a landmark of the highest quality, thanks to genuinely collaborative interactions between authors and review editors, who include some of the world's best academicians. Research must be certified by peers before entering a stream of knowledge that may eventually reach the public - and shape society; therefore, Frontiers only applies the most rigorous and unbiased reviews.

Frontiers revolutionizes research publishing by freely delivering the most outstanding research, evaluated with no bias from both the academic and social point of view. By applying the most advanced information technologies, Frontiers is catapulting scholarly publishing into a new generation.

#### What are Frontiers Research Topics?

Frontiers Research Topics are very popular trademarks of the Frontiers Journals Series: they are collections of at least ten articles, all centered on a particular subject. With their unique mix of varied contributions from Original Research to Review Articles, Frontiers Research Topics unify the most influential researchers, the latest key findings and historical advances in a hot research area! Find out more on how to host your own Frontiers Research Topic or contribute to one as an author by contacting the Frontiers Editorial Office: [researchtopics@frontiersin.org](mailto:researchtopics@frontiersin.org)

# MR SPECTROSCOPY IN NEUROPSYCHIATRY

Topic Editors:

**Anouk Marsman**, Danish Research Centre for Magnetic Resonance, Denmark

**Alice Egerton**, King's College London, United Kingdom

**Brian V. Broberg**, Mental Health Centre Glostrup, University of Copenhagen, Denmark

**Hilleke E. Hulshoff Pol**, Brain Center Rudolf Magnus, Netherlands

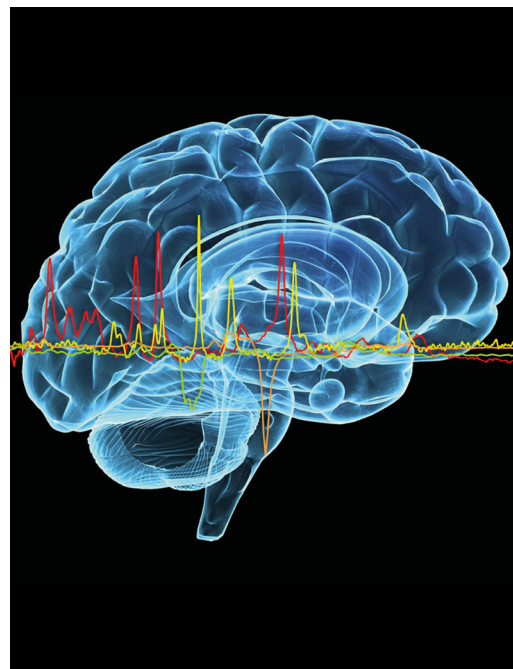


Image: Anouk Marsman and Brian Villumsen Broberg

Neuropsychiatric disorders, covering both psychotic and depressive disorders, but also autism and attention-deficit hyperactivity disorder (ADHD), are characterized by abnormal behavior and brain structure. Accumulating evidence suggests that altered neurochemistry plays a role in these disorders and may have a causal relationship with the observed behavioral and structural abnormalities. To improve the understanding of neurochemical anomalies and (patho)physiological changes in psychiatric conditions, *in vivo* assessment of the affected tissue, the brain, is wanted and needed. Magnetic resonance spectroscopy (MRS) is a non-invasive technique which allows *in vivo* assessment of the molecular composition of brain tissues and identification of metabolites involved in physiological and pathological processes, which is otherwise virtually impossible. Only in the last decade with the development of high field MR methodologies, MRS has become sensitive enough for broader use in clinical studies. The implications are many, but proper guidance and elucidation of the pros and cons for the specific methods is needed to optimally exploit the potential. This Research Topic updates the reader on the possibilities and pitfalls of MRS today and highlights methodologies and applications for the future.

**Citation:** Marsman, A., Egerton, A., Broberg, B. V., Hulshoff Pol, H. E., eds. (2018). MR Spectroscopy in Neuropsychiatry. Lausanne: Frontiers Media. doi: 10.3389/978-2-88945-524-9

# Table of Contents

## 04 Editorial: MR Spectroscopy in Neuropsychiatry

Alice Egerton, Anouk Marsman, Brian V. Broberg and Hilleke E. Hulshoff Pol

## SECTION 1

### STATE-OF-THE-ART

#### 06 Ultra-High-Field Magnetic Resonance Spectroscopy in Psychiatry

Beata R. Godlewska, Stuart Clare, Philip J. Cowen and Uzay E. Emir

#### 15 Detection of Glutamate Alterations in the Human Brain Using $^1\text{H}$ -MRS: Comparison of STEAM and sLASER at 7 T

Anouk Marsman, Vincent O. Boer, Peter R. Luijten, Hilleke E. Hulshoff Pol, Dennis W. J. Klomp and René C. W. Mandl

#### 23 Functional Magnetic Resonance Spectroscopy: The "New" MRS for Cognitive Neuroscience and Psychiatry Research

Jeffrey A. Stanley and Naftali Raz

#### 35 Intelligence and Brain Efficiency: Investigating the Association between Working Memory Performance, Glutamate, and GABA

Anouk Marsman, René C. W. Mandl, Dennis W. J. Klomp, Wiepke Cahn, René S. Kahn, Peter R. Luijten and Hilleke E. Hulshoff Pol

## SECTION 2

### MRS APPLICATIONS IN PSYCHIATRIC RESEARCH

#### 44 Risk-Conferring Glutamatergic Genes and Brain Glutamate Plus Glutamine in Schizophrenia

Juan R. Bustillo, Veena Patel, Thomas Jones, Rex Jung, Nattida Payaknait, Clifford Qualls, Jose M. Canive, Jingyu Liu, Nora Irma Perrone-Bizzozero, Vince D. Calhoun, Jessica A. Turner and Charles Gasparovic

#### 53 Effects of Antipsychotic Administration on Brain Glutamate in Schizophrenia: A Systematic Review of Longitudinal $^1\text{H}$ -MRS Studies

Alice Egerton, Akarmi Bhachu, Kate Merritt, Grant McQueen, Agata Szulc and Philip McGuire

#### 60 Glutamate Levels and Resting Cerebral Blood Flow in Anterior Cingulate Cortex Are Associated at Rest and Immediately Following Infusion of S-Ketamine in Healthy Volunteers

Kirsten Borup Bojesen, Kasper Aagaard Andersen, Sophie Nordahl Rasmussen, Lone Baandrup, Line Malmer Madsen, Birte Yding Glenthøj, Egill Rostrup and Brian Villumsen Broberg

#### 70 GABAergic Mechanisms in Schizophrenia: Linking Postmortem and In Vivo Studies

Jeroen C. de Jonge, Christiaan H. Vinkers, Hilleke E. Hulshoff Pol and Anouk Marsman

#### 82 Antigliadin Antibodies (AGA IgG) Are Related to Neurochemistry in Schizophrenia

Laura M. Rowland, Haley K. Demyanovich, S. Andrea Wijtenburg, William W. Eaton, Katrina Rodriguez, Frank Gaston, Daniela Cihakova, Monica V. Talor, Fang Liu, Robert R. McMahon, L. Elliot Hong and Deanna L. Kelly



# Editorial: MR Spectroscopy in Neuropsychiatry

**Alice Egerton<sup>1\*</sup>, Anouk Marsman<sup>2</sup>, Brian V. Broberg<sup>3</sup> and Hilleke E. Hulshoff Pol<sup>4</sup>**

<sup>1</sup> Department of Psychosis Studies, King's College London, Institute of Psychiatry, Psychology and Neuroscience, London, United Kingdom, <sup>2</sup> Danish Research Centre for Magnetic Resonance, Centre for Functional and Diagnostic Imaging and Research, Copenhagen University Hospital Hvidovre, Hvidovre, Denmark, <sup>3</sup> Centre for Neuropsychiatric Schizophrenia Research, Centre for Clinical Intervention and Neuropsychiatric Schizophrenia Research, Mental Health Centre Glostrup, Mental Health Services, Capital Region of Denmark, University of Copenhagen, Glostrup, Denmark, <sup>4</sup> Department of Psychiatry, Brain Center Rudolf Magnus, University Medical Center Utrecht, Utrecht, Netherlands

**Keywords:** **MR spectroscopy, neurochemistry, neuroimaging, schizophrenia, glutamate, GABA, 7 tesla MRI, functional MRS**

## Editorial on the Research Topic

### MR Spectroscopy in Neuropsychiatry

Magnetic resonance spectroscopy (MRS) is a non-invasive neuroimaging technique with the unique ability to reveal the role of neurometabolites in brain physiological and pathophysiological processes. MRS-visible metabolites include the neurotransmitters glutamate and GABA, as well as compounds implicated in oxidative stress or inflammation, such as glutathione and myo-inositol. Optimal application of MRS techniques therefore has significant potential for revealing brain pathophysiological mechanisms in psychiatric disorders.

The last decade has seen substantial developments in MRS capability. These advances have been driven by the availability of high field strength MR scanners, in parallel with new MRS acquisition and data analysis methods. It is now possible to accurately detect previously indistinguishable MRS metabolites, such as GABA and glutathione, or to measure dynamic changes in metabolite levels occurring during behavioral challenges or in response to other stimuli. The articles in this research topic together provide an update on the current state-of-the-art MRS methodology, and, using schizophrenia as an example, illustrate how MRS may be applied to increase understanding of neurochemical abnormalities across the psychiatric disorders.

Three articles in this research topic focus on current state-of-the-art MRS methodology. Godlewska et al. provide an overview of ultra-high-field (UHF) MRS. In UHF MRS, data are acquired at MR field strengths of 7 Tesla (7T) or more, resulting in high sensitivity and resolution, and allowing quantification of numerous metabolites in the MR spectra. This review provides a practical guide to the advantages and disadvantages of UHF MRS, together with examples of its application in psychiatric disorders. Development of UHF methodology is further described in the article of Marsman et al. which presents a comparison of two different acquisition sequences for glutamate quantification at 7T; the more common approach of STEAM vs the recent approach of sLASER. Comparing test-retest reproducibility in healthy volunteers, this study demonstrates advantage of sLASER acquisition in robustly and sensitively determining glutamate levels in the frontal cortex.

In the third article of the research topic focussing on methodology, Stanley and Raz describe the emerging and innovative approach of functional MRS (fMRS). Typically, MRS is used to measure metabolite levels while the subject is at rest in the scanner. In contrast, fMRS can measure the dynamic changes in metabolites, particularly glutamate, which occur while subjects perform a behavioral task. This review provides a summary of the technological advances, strengths and

## OPEN ACCESS

**Edited and reviewed by:**  
Stefan Borgwardt,  
Universität Basel, Switzerland

**\*Correspondence:**  
Alice Egerton  
alice.egerton@kcl.ac.u

**Specialty section:**  
This article was submitted to  
Neuroimaging and Stimulation,  
a section of the journal  
*Frontiers in Psychiatry*

**Received:** 24 April 2018  
**Accepted:** 27 April 2018  
**Published:** 31 May 2018

**Citation:**  
Egerton A, Marsman A, Broberg BV  
and Hulshoff Pol HE (2018) Editorial:  
MR Spectroscopy in Neuropsychiatry.  
*Front. Psychiatry* 9:197.  
doi: 10.3389/fpsyg.2018.00197

limitations of fMRS, and describes how this approach is contributing to our understanding of the glutamatergic basis of cognitive impairments in psychiatric disorders.

Marsman et al. then bring together the themes of UHF MRS and the role of glutamate in cognition in their study at 7T examining the relationship between working memory and the level of glutamate and GABA in the frontal and occipital cortex. The results indicate that working memory performance in healthy individuals is related to the balance between these excitatory and inhibitory neurotransmitters.

The remaining articles in the research topic relate to schizophrenia, and provide complementary examples of MRS application in psychiatric research. A principal focus of MRS research in schizophrenia has been on the measurement of brain glutamate levels, due to its core implication in schizophrenia pathophysiology. Bustillo et al. provide a significant step forward, by combining glutamate genetic data with MRS imaging in schizophrenia, and thereby linking two fields of glutamatergic research. This study found that in younger patients with schizophrenia, the combined score for three single nucleotide polymorphisms in glutamatergic genes associated with schizophrenia risk partially contributes to elevated levels of Glx (the combined MRS signal from glutamate and glutamine) in gray matter. Interestingly this association was not apparent in older patients, which suggests that other factors affect Glx levels during the course of schizophrenic illness.

There is some debate as to whether antipsychotic medication may alter brain glutamate levels, and the article of Egerton et al. provided a systematic review of longitudinal MRS studies that have addressed this question. Although these studies have used a range of methodological approaches and have investigated different brain regions, the majority report a numerical reduction in Glx levels over the course of antipsychotic treatment, suggesting that to at least some degree antipsychotics may reduce glutamate elevation in schizophrenia.

The study of Bojesen et al. addresses potential associations between schizophrenia-related abnormalities in glutamate levels and brain activity, measured as regional cerebral blood flow (rCBF). To avoid the potential confounds of medication or prolonged illness that may be present in a patient sample, this study used administration of the N-methyl-D-aspartate (NMDA) antagonist ketamine in healthy volunteers as a glutamatergic experimental model of schizophrenia pathophysiology. The

observed associations between glutamate and rCBF in the anterior cingulate cortex may suggest a mechanistic link between these neurobiological features relevant to schizophrenia.

The development of MRS techniques to accurately measure GABA has permitted investigation of GABA abnormalities in schizophrenia *in vivo*, which were previously mainly understood on the basis of post-mortem data. The review of de Jonge et al. summarizes the findings to date from GABA MRS studies in relation to post-mortem evidence, and suggests key future directions for this emerging field. Finally, included in this research topic is the study of Rowland et al. which used levels of the MRS metabolites myo-inositol and choline-containing compounds as an innovative proxy measure of brain inflammation in schizophrenia. This exploratory study found correlations between antiglandin antibody levels and the MRS “inflammation measures,” and may open new avenues for MRS application in testing inflammatory theories of brain disorders.

Through these examples from schizophrenia research, these articles demonstrate how MRS can be applied to increase our understanding of neurochemical abnormalities or inflammation across neurological and psychiatric disorders. Recent advances in MRS technology will play a major role in achieving this goal, and this research topic provides a practical guide to the emerging MRS technologies of UHF MRS and fMRS. Together these articles provide a resource for researchers interested in MRS approaches and understanding their strengths and limitations, and also some inspiration for future research applications.

## AUTHOR CONTRIBUTIONS

All authors listed have made a substantial, direct and intellectual contribution to the work, and approved it for publication.

**Conflict of Interest Statement:** The authors declare that the research was conducted in the absence of any commercial or financial relationships that could be construed as a potential conflict of interest.

Copyright © 2018 Egerton, Marsman, Broberg and Hulshoff Pol. This is an open-access article distributed under the terms of the Creative Commons Attribution License (CC BY). The use, distribution or reproduction in other forums is permitted, provided the original author(s) and the copyright owner are credited and that the original publication in this journal is cited, in accordance with accepted academic practice. No use, distribution or reproduction is permitted which does not comply with these terms.



# Ultra-High-Field Magnetic Resonance Spectroscopy in Psychiatry

Beata R. Godlewska<sup>1</sup>, Stuart Clare<sup>2</sup>, Philip J. Cowen<sup>1</sup> and Uzay E. Emir<sup>2\*</sup>

<sup>1</sup> Department of Psychiatry, University of Oxford, Warneford Hospital, Oxford, United Kingdom, <sup>2</sup> Oxford Centre for Functional MRI of the Brain, Nuffield Department of Clinical Neurosciences, University of Oxford, John Radcliffe Hospital, Oxford, United Kingdom

## OPEN ACCESS

### Edited by:

Anouk Marsman,  
Copenhagen University  
Hospital Hvidovre,  
Denmark

### Reviewed by:

Jeffrey A. Stanley,  
Wayne State University School  
of Medicine, United States  
Kim M. Cecil,  
Cincinnati Children's  
Hospital Medical Center,  
United States

### \*Correspondence:

Uzay E. Emir  
uzay.emir@ndcn.ox.ac.uk

### Specialty section:

This article was submitted to  
Neuroimaging and Stimulation,  
a section of the journal  
*Frontiers in Psychiatry*

Received: 13 February 2017

Accepted: 26 June 2017

Published: 11 July 2017

### Citation:

Godlewska BR, Clare S, Cowen PJ  
and Emir UE (2017) Ultra-High-Field  
Magnetic Resonance Spectroscopy in Psychiatry.  
*Front. Psychiatry* 8:123.  
doi: 10.3389/fpsy.2017.00123

The advantages of ultra-high-field (UHF  $\geq 7\text{T}$ ) MR have been demonstrated in a variety of MR acquisition modalities. Magnetic resonance spectroscopy (MRS) can particularly benefit from substantial gains in signal-to-noise ratio (SNR) and spectral resolution at UHF, enabling the quantification of numerous metabolites, including glutamate, glutamine, glutathione, and  $\gamma$ -aminobutyric acid that are relevant to psychiatric disorders. The aim of this review is to give an overview about the advantages and advances of UHF MRS and its application to psychiatric disorders. In order to provide a practical guide for potential applications of MRS at UHF, a literature review is given, surveying advantages and disadvantages of MRS at UHF. Key concepts, emerging technologies, practical considerations, and applications of UHF MRS are provided. Second, the strength of UHF MRS is demonstrated using some examples of its application in psychiatric disorders.

**Keywords:** **ultra-high-field, magnetic resonance spectroscopy, psychiatric disorders, neurochemicals, magnetic resonance spectroscopic imaging**

Psychiatric disorders are related to substantial personal, public, and economic burdens and are responsible for nearly 13% of the global burden of disease in terms of disability-adjusted life years, and a staggering 32% of years lived with disability (1). Multiple lines of research, including brain imaging, analysis of post-mortem brain tissue, and genetic studies have resulted in the identification of potential dysfunctions in psychiatric disorders, including schizophrenia (SCZ) (2), major depressive disorders (MDD) (3), bipolar disorder (BD) (2), anxiety disorders (4), autism spectrum disorder (5), and anorexia nervosa (6). In addition, the development and research application of newer imaging modalities such as mapping the “human connectome” employing magnetic resonance imaging (MRI) is opening new avenues to study brain mechanisms underlying psychological processes non-invasively in the living brain (7).

Most MRI-based imaging modalities (for example, structural imaging) are sensitive to macroscopic alterations. Complementary to MRI, magnetic resonance spectroscopy (MRS) techniques may be utilized to reveal abnormalities before any visible macroscopic changes in brain anatomy and physiology occur, since they provide unique information on the neurochemical composition of the brain tissue (8–10). For instance, neurochemicals that can be measured non-invasively in human brain include (1) endogenous neurotransmitters; glutamate (Glu) and gamma-aminobutyric acid (GABA) (11) (2), psychotropic medications, such as lithium (12) and fluorinated drugs (13). Thus, when applied to *in vivo* brain imaging, MRS can be used to measure the neurochemical composition of brain in order to characterize metabolic processes and identify aberrant neurochemical or metabolic relationships related to psychiatric disorders.

The recent progress in MRI technology such as the use of ultra-high-field (UHF  $\geq 7\text{ T}$ ) magnets, advanced magnetic field ( $B_0$ ) shim coils, improved gradient systems, and radio frequency (RF) coils have been enabling robust *in vivo* application of MRS techniques by providing the improved sensitivity and resolution. Specifically, using MRS at UHF, it is possible to measure the signals from 10 to 15 metabolites that might be a marker of different pathophysiological processes of psychiatric disorders (Figure 1) (14). Signal-to-noise ratio (SNR) (defined as peak height divided by root mean square noise) is approximately 1.6 times higher at 7 T relative to 3 T (Figure 2) (15). From 3 T to 7 T, gains in sensitivity are particularly prominent for Glu, glutamine (Gln), and GABA (16). As a result, metabolites are quantified with lower errors (lower Cramér-Rao Lower Bounds) at 7 T than at 3 T, which can be translated to improved quantification metabolite concentrations. Thus, UHF MRS methods have the potential to improve the understanding of the etiology, progression, and the response to therapy in psychiatric disorders due to the improved quantification of metabolites, such as Glu, Gln, and GABA that are relevant to psychiatric disorders.

The aim of this review is to give a comprehensive overview of the advantages, challenges, and advances of UHF MRS with regard to methodological development, discoveries, and applications in psychiatric research from its beginnings around 15 years ago up to the current state. At lower magnetic field strengths, MRS has been used *in vivo* for different nuclei, including  $^1\text{H}$ ,  $^{31}\text{P}$ ,  $^{13}\text{C}$ ,  $^{15}\text{N}$ ,  $^{19}\text{F}$ , and  $^{23}\text{Na}$ ; however, psychiatric disorder applications of UHF MRS are limited to  $^1\text{H}$ . For this reason, this review will focus on the use of  $^1\text{H}$  for MRS at 7 T.

## CHALLENGES AT UHF

*In vivo* MRS at UHF is ready to make important contributions not only in the evaluation of disease (19) but also more importantly because it may assist to study disease progression and treatment (20, 21). Despite this potential, implementing MRS in the human brain at UHF involves multiple challenges, such as magnetic field and RF inhomogeneity, increased spectral bandwidth and short relaxation times of metabolites.

At UHF, the interaction between the brain tissue and RF pulse results in strong inhomogeneities since the RF wavelength is in the order of human head. For instance, at 7 T, the wavelength of the RF pulse used in the human brain is around 12 cm and generates varying destructive interferences throughout the brain, resulting in RF pulse inhomogeneity. As a result, the insufficient transmit power with conventional volume head coils requires increased RF pulse durations with smaller bandwidths and this in turn introduces a large chemical shift displacement error in the spectra. This problem is worsened in many regions of the brain since volume coils can only provide high enough transmit power in the central region of human head compared with the periphery region (22).

Recent noteworthy investigations demonstrated the feasibility of the use of multiple transmit array coils used to control the distribution of electromagnetic fields and overcome this limitation. It has been demonstrated that such adjusting of RF amplitude and phase to each transmit array coil (RF shimming)

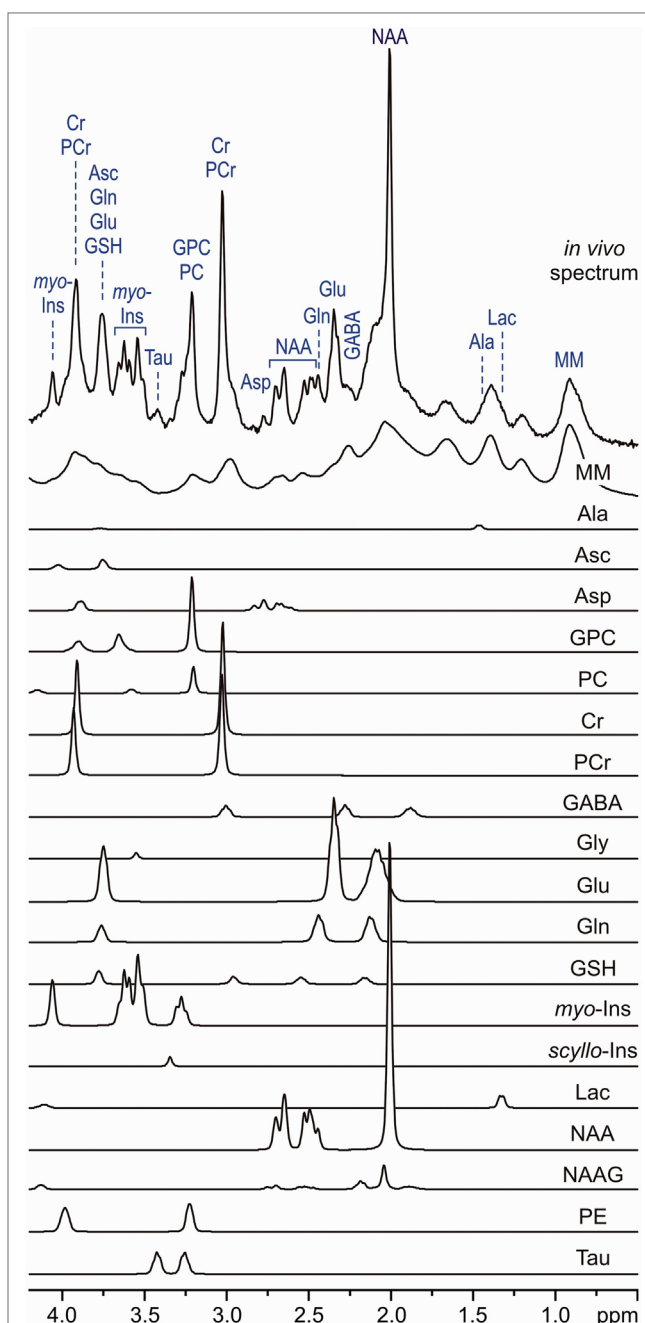
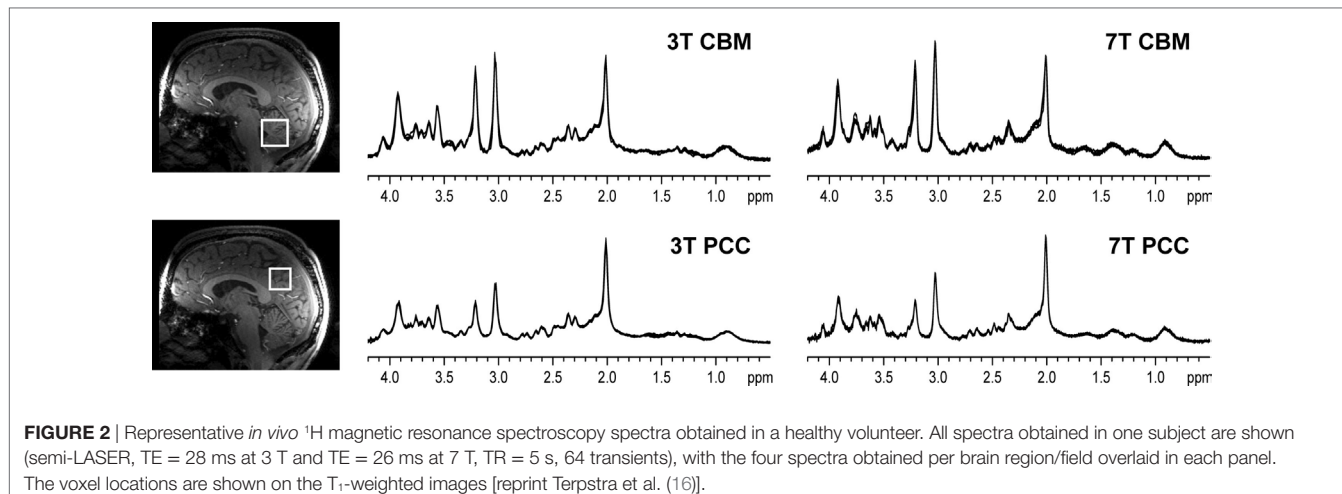


**FIGURE 1 |** *In vivo* stimulated echo acquisition mode spectrum (volume of interest, 8 ml, TE = 6 ms, TR = 5 s and number of transients, 160) and LCModel fit, modeling metabolite contributions to the neurochemical profile. Model spectra for glycerophosphocholine, phosphocholine, creatine, phosphocreatine,  $\gamma$ -aminobutyric acid, glucose, glutamine, Glutamate, glutathione, lactate, myo-inositol, *N*-acetylaspartate, *N*-acetylaspartylglutamate, scyllo-inositol, and taurine were imported into LCModel (17) and used for spectroscopic quantification [reprint McKay and Tkác (18)].

results in considerable gains in the efficiency of RF pulses used in single-voxel MRS and magnetic resonance spectroscopic imaging (MRSI) localizations in the brain at 7 T (23). Data quality has been further improved with dynamic RF shimming,



especially for MRSI, and several MRSI studies have already demonstrated this approach by utilizing several RF shim settings generated to ensure optimal transmit fields for a VOI-specific homogeneous excitation, a ring-shaped excitation of the skull area for lipid suppression and a global uniform excitation for water suppression (24).

Problems resulting from limitations in available RF magnitude can be partially avoided by utilizing dedicated new excitation and saturation pulses without modifying any hardware at UHF. These pulses should have a high degree of tolerance to RF inhomogeneity with broadband sharp slice-selection profiles. It has been demonstrated that broadband frequency-modulated RF pulses can partially overcome these problems, as in semi-localization by adiabatic selective refocusing (semi-LASER) and localization by adiabatic selective refocusing (LASER) pulse sequences, albeit with a cost of long echo times [50 and 80 ms, respectively (25, 26)]. Alternatively, composite broadband refocusing pulse designs can be used (27). For example, MRSI data can be obtained using the free induction decay acquisition localized by outer volume suppression (FIDLOVS) technique (28), based on 2D pre-localization by outer volume suppression and frequency-modulated excitation pulse for slice-selection.

In addition to RF inhomogeneity, significant main magnetic field ( $B_0$ ) inhomogeneity will be introduced as the subject is placed in the scanner due to the magnetic susceptibility of the different tissues. At UHF, the effect is even more marked, since the magnitude of the  $B_0$  shift is proportional to static field (29). The process of  $B_0$  shimming usually mitigates these effects. However, for the size of voxels used in single-voxel MRS at UHF, the vendor-provided approaches are not always optimum. At UHF, it is better to use an approach focusing on the volume of interest to minimize strong  $B_0$  inhomogeneities. One approach is to acquire a  $B_0$  field map using two gradient-echo images with different echo times. When choosing the difference in echo time to use for  $B_0$  shimming, there is a balance between long evolution times giving the best sensitivity and short evolution times giving better signal and avoiding phase wraps. Typically, an evolution time of 2–4 ms is appropriate (30) or it can be better to use multiple evolution times (31). An alternative approach is to use the

FASTMAP and its echo-planar-based derivative (32, 33), which measures  $B_0$  field plots along projections around the voxel of interest. This approach is faster and can be run at a higher resolution than an imaging-based method. For both methods, iterations minimize the  $B_0$  inhomogeneities.

For MRSI at UHF, where a larger volume of interest needs to be shimmed, it appears to be most beneficial to use higher order (third or fourth) shim terms (34) to achieve narrow linewidths. However, even with these extra terms, it is not possible to completely remove all  $B_0$  variation. An alternative approach that has shown much promise for MRSI is dynamic  $B_0$  shimming (35); however, this again requires specialist hardware for the scanner. A number of researchers have shown the benefits of using diamagnetic or paramagnetic passive shims, such as those placed in the mouth (36); however, these approaches are often less comfortable to the subject and require a much more involved optimization procedure. More recently shim coil designs that are not based on spherical harmonics, but that can drive current in an arbitrary pattern, have been proposed (37). These solutions are again technically complex and are some way from being routine.

Transverse relaxation times,  $T_2$ , of metabolites in the human brain decrease as the magnetic field increase (38, 39) and the SNR advantages quickly disappear with increasing echo times. Therefore, short echo times are critical for not only minimizing  $T_2$  losses and preserving intensity from J-modulation but also when using UHF to study patient populations, who potentially have different metabolite  $T_2$  values (40).

Recent developments have demonstrated that challenges can be overcome, and the gap between bench and their potential for clinical application can get narrower. As clinical UHF systems become increasingly available, *in vivo* MRS detection of metabolites at UHF benefits from gains in SNR and chemical shift dispersion, which may enable the detection of subtle changes in metabolite levels. MRS allows detection of a variety of metabolites, including *N*-acetylaspartate (NAA) as a marker of neuronal loss/dysfunction, total creatine [ $t\text{Cr}$ , creatine (Cr) + phosphocreatine (PCr)] as a marker for deficits in energy metabolism, total choline (phosphocholine + glycerophosphocholine) as a

marker for cell membrane turnover, and Glu and GABA, the primary excitatory and inhibitory brain neurotransmitters, respectively. The improved detection of these metabolites at UHF is of potential value in understanding the neuropathology or biochemical abnormalities in mental health disorders as well as in evaluating disease progression and response to therapeutic interventions. In the following sections, we will review clinically relevant and MRS-detectable metabolites and illustrate potential applications in psychiatric conditions. Furthermore, if applicable, we will provide examples from translational research as they relate to psychiatric disorders.

## WHY UHF MRS CAN BE USEFUL IN PSYCHIATRIC RESEARCH

As stated above, one of the clear advantages of UHF MRS is an increased SNR, which can allow for a more precise assessment of molecules that would not pass the quality threshold at lower fields due to sensitivity issues. Yet, possibly the greatest advantage for clinical research is the higher spectral resolution that UHF offers and which allows for a more reliable measurement of metabolites that cannot be resolved at lower magnetic fields and are relevant to the pathogenesis of psychiatric symptoms. Up to date, there have only been a few MRS studies at UHF, which we will report in the context of UHF benefits and with a short summary of findings at lower fields.

## Glu, Gln, AND GABA

Effective separation of Glu and Gln may be one of the most important advantages derived from the use of UHF in the context of psychiatric disorders (41). While the role of Glu and Gln has been postulated in the pathogenesis of major psychiatric conditions, the clear separation of Glu and Gln resonances at UHF compared to lower magnetic fields (Figure 3) might shed light on understanding their plausible mechanisms (41). Glu is the main

excitatory neurotransmitter in the brain, present in about 80% of synapses, and it is one of the key components of cellular energy metabolism. It has an average concentration of 6–13  $\mu\text{mol/g}$  with significant differences between gray and white matter (42). Released Glu is taken up into astrocytes where it is converted to Gln. This process prevents the toxic effect of excess Glu on neurons. Subsequently, Gln is released into the extracellular space, to be taken into the presynaptic terminals and converted back into Glu. Gln concentrations are around 2–4  $\mu\text{mol/g}$  (42). GABA, the main inhibitory neurotransmitter, is closely linked to the Glu and Gln molecules. It is produced from Glu by glutamate decarboxylase and has concentration of circa 1– $\mu\text{mol/g}$  (42). GABA plays an important role in maintaining the correct excitation–inhibition balance of cortical networks. Due to its low natural concentrations and proximity of more abundant metabolites of NAA at 2 ppm, tCr at 3 ppm, and Glu and Gln at 2.3 ppm, reliable quantification of GABA benefits from improved SNR and increased resolution offered by UHF compared to lower magnetic fields (43).

To our knowledge, only a few studies have assessed the glutamatergic system at UHF, and most of them focused on SCZ. One study has shown no differences in Glu levels between patients with SCZ and healthy controls in medial prefrontal cortex (mPFC) and parieto-occipital cortex (OCC) (44). There was, however, an effect of age and gender on mPFC Glu concentration, with lower Glu in older participants and in males, irrespective of disease. These are also found lower GABA/Cr ratio in patients in mPFC but not in parieto-OCC.

Another 7 T study explored differences between medicated patients with SCZ, their healthy relatives and healthy non-related controls – finding reduced cortical Glu in patients with SCZ compared to healthy controls, as well as reduced Glu in healthy relatives, suggesting that Glu concentrations were associated with genetic load for illness (45). They also found reduced cortical GABA in patients compared with both healthy relatives and the pooled sample of healthy individuals (relatives and non-relatives), suggesting an association of altered GABA concentrations in SCZ with either illness state or medication effects. There were no differences in metabolite concentrations in basal ganglia.

One other 7 T study has showed an effect of age in relation to illness, with higher Glu levels in ACC in patients with SCZ under the age of 40 compared to controls, with no differences between patients over 40 and controls (46). An inverse correlation of Glu with age was found for patients but not controls, suggesting an ongoing pathological process during which Glu might decline through the course of the disease. There were no differences in Glu, Gln, Glu/Gln ratio, or GABA when comparing all patients to all controls.

To our knowledge, there has been only one UHF study in mood disorders—a 7 T MRSI investigation in MDD, which showed no statistically significant difference in Glu, Gln, and GABA levels across the number of regions, although there was an increase in Glu after 8 weeks of mindfulness-based cognitive therapy (MBCT) (47).

A pilot 7 T study has shown widespread reductions in Glu in anorexia patients as compared to healthy controls (48). Previous studies at 3 T in this group of patients measured Glx (a combined measure of Glu and Gln), and some, although not

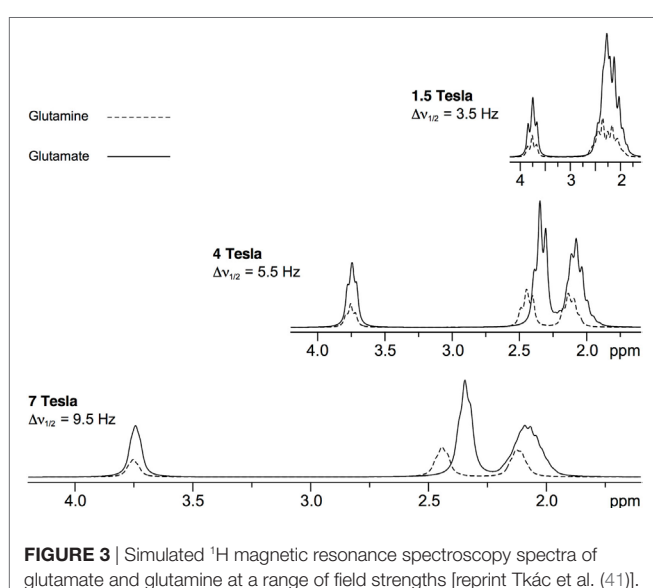


**FIGURE 3 |** Simulated  $^1\text{H}$  magnetic resonance spectroscopy spectra of glutamate and glutamine at a range of field strengths [reprint Tkác et al. (41)].

all of them, reporting a decrease. A separation enabled by UHF MRS allowed for the identification of the likely key contributor to this change.

Complementary to the fMRI, functional MRS (fMRS) could help relate functional impairments to psychiatric disorder. The potential of fMRS has been demonstrated by detecting metabolic changes in the brain induced by different types of physiological interventions (49–52). For instance, a recent study has demonstrated a correlation between Glu and BOLD-fMRI time courses using a novel combined fMRI-MRS sequence (53). Thus, fMRS could be used to measure neurochemical levels to study glutamatergic response and/or energy metabolism in psychiatric disorders during different physiological interventions. A recent fMRS study at 7 T has successfully demonstrated differential response of the glutamatergic system to a Stroop task in patients with SCZ, MDD, and healthy controls (54).

Ultra-high-field studies are a potentially useful tool in drug discovery. They can help to understand more precisely mechanisms of action of medications and explore their potential in the context of known pathophysiology of psychiatric conditions. This would apply to both existing treatments, with the view of repurposing, and new ones, whose mode of action may suggest their potential use in known pathologies. Two UHF studies on medication effect can serve as a good example. One of them studied the effect of gabapentin, indicated for treatment of focal seizures, peripheral neuropathic pain, and migraine prophylaxis, which has also been used as an adjunctive treatment in mood disorders. In a 7 T study Cai et al. (20) found a mean 55.7% increase in occipital GABA in response to gabapentin challenge in healthy volunteers. This was consistent with another study in healthy volunteers performed at 4.1 T (55). Given that a decrease in GABA in MDD has been postulated (56), this effect, although obtained in healthy volunteers, is of potential interest to MDD treatment. Another study in healthy participants has shown a decrease in Glu and Gln under the influence of ebselen, a potential lithium-mimetic and glutaminase inhibitor, in healthy volunteers (57). This finding supports its further exploration as treatment for BD in the light of postulated increased in Glx levels in this condition (the effect of ebselen on *myo*-inositol (*myo*-Ins) is described below).

These findings at UHF would be important for interpretation of lower magnetic field studies in psychiatric disorders where there are many conflicting results, partly because distinguishing Glu, Gln, and GABA is difficult due to the lower SNR and spectral resolution. For instance, a meta-analysis by Merritt et al. (58) in SCZ suggested elevations in glutamatergic metabolites across several brain regions, including limbic areas and frontal regions. Another meta-analysis (59) suggested reduced Glu and elevated Gln in frontal regions in patients, with their levels decreasing with age but only in the patient group. A review by Poels et al. (60) suggested that Glu activity (as indexed by Glu and Glx levels) might be elevated in medication-free early-stage patients with psychosis, while they decrease after treatment and in chronic patients.

Again at conventional magnetic fields, GABA-related findings in SCZ show increase, decrease, and no difference (61). One meta-analysis showed a trend toward lower GABA in patients,

which, however, did not reach significance (56). This, however, would be consistent with two of the 7 T studies in SCZ noted above (44, 45).

Findings from 3 T studies suggest, to a reasonably consistent degree, decreased Glu and Glx levels in MDD and increased levels in BD, as suggested by meta-analyses (62–64) and reviews (65–68). The changes were shown across a number of regions important for mood processing, such as prefrontal cortex, the hippocampus and the amygdala, across different ages (69), and, in BD, seemed to be independent of the current mood state or medication status. Only a few studies attempted discrimination between Glu, Gln, and GABA at 3 T using J-resolved (70) and J-editing MRS sequences (71) in depressed patients. Both a decrease (71) and no change in GABA (70) levels were reported. A recent meta-analysis (56) has shown reduced GABA concentration in currently depressed MDD patients but not in remitted MDD patients compared with healthy controls, while there were no differences between patients with BD and controls.

## NAA AND N-ACETYLASPARTYLGLUTAMIC ACID (NAAG)

Another two molecules that can benefit from increased separation at UHF are NAA and NAAG (15). NAA is mainly found in neurons, it is considered a marker of neuronal integrity/function, and its concentration is in the range of 8–14  $\mu\text{mol/g}$  under normal conditions (42). NAAG is a derivate of NAA and Glu and acts as an agonist at metabotropic Glu receptor type 3 (72). Animal studies indicate that it may play a role in psychiatric conditions. For instance, it has been demonstrated that an alteration of synaptic NAAG levels represents a new therapeutic approach to treating the positive and negative symptoms of SCZ (73). Rare reports on NAAG encourage further exploration, showing differences in its concentration between patients with SCZ and healthy controls (74). The singlet of NAA at 2.02 ppm is the most prominent metabolite signal, whereas the detection of NAAG in human brain by MRS is challenging at lower magnetic field due to its relatively low concentration and the overlap with intense signals of NAA and Glu. Similar to the separation of Glu and Gln at UHF, the separation of NAA and NAAG also benefits from improved resolution and increased SNR at UHF. Interestingly, a recent 7 T study has shown a reduction in NAA/tCr levels in patients with MDD, which normalized after 8 weeks of MBCT treatment (47).

Large meta-analyses of lower field studies in SCZ, reported possibly disease stage-related NAA reductions in frontal and medial temporal regions (75, 76) and in basal ganglia (75). In BD, a large meta-analysis (76) found an NAA decrease in basal ganglia only, while there were elevations in dorso-lateral pre-frontal cortex; in this second region, data heterogeneity across the included studies was high, however. It was suggested that in BD, medication status, particularly with lithium, might be a confounder. Indeed, some studies showed a decrease in NAA in drug-free BD patients, with some of NAA increases after treatment with lithium (63). There is no convincing evidence of NAA changes in MDD (62, 69, 77).

## Cr AND PCr

Total Cr, a combined measure of Cr and PCr ( $t\text{Cr}$ ,  $\text{Cr} + \text{PCr}$ ), is often used as a reference molecule in MRS analysis. However,  $t\text{Cr}$  level should be used with caution as an internal concentration reference since it might change with disease, complicating the interpretation of changes in ratios relative to  $t\text{Cr}$  (78, 79). Cr and PCr have an important physiological role acting as a system for quick generation and storage of energy by moving phosphate groups between ATP and ADP in anaerobic processes in tissues and organs with high and quickly changing energy demands, such as the brain. Changes in their concentration may be linked to disturbances in energy metabolism and their assessment can provide important information about underlying pathologies. Most studies assessing PCr-Cr cycle used  $^{31}\text{P}$  MRS, with changes reported in a number of psychiatric conditions, such as SCZ (80). While this is an informative way of assessing PCr-Cr cycle activity, information on other metabolites of interest cannot be acquired simultaneously, which would be the main benefit of UHF in this context (81). A discussion of  $^{31}\text{P}$  studies is beyond the scope of this paper.

## *myo*-Ins AND GLYCINE (Gly)

The main, resolved resonance of *myo*-Ins is at 3.56 ppm (42). This resonance, at lower magnetic field strength also contains contributions from the amino acid, Gly (42). *myo*-Ins is one of the larger signals in short echo time spectra, with a concentration of 5–10  $\mu\text{mol/g}$  whereas Gly present in normal human brain at up to a 1  $\mu\text{mol/g}$  concentration (42). *myo*-Ins is a precursor for the phosphatidylinositol second messenger system. Predominantly located in astrocytes, it is often considered to be a glial marker. It also has an established role in osmoregulation. Gly is a co-agonist of Glu for the NMDA receptor and is necessary for Glu effect. Due to this, it may play an important role in the pathogenesis of disorders for which dysfunction of the glutamatergic system has been postulated, such as mood disorders and SCZ. In addition, it has been shown that Gly administration to SCZ patients improves the efficacy of conventional antipsychotic drugs, such as olanzapine and risperidone (82).

At lower magnetic fields, Gly detection requires specific MRS sequences to separate *myo*-Ins and Gly signals, such as the two-dimensional J-PRESS (83) and TE-optimized triple refocusing (84). At UHF, the improvement in separation of *myo*-Ins and Gly resonances has been demonstrated without requiring any specific MRS sequence (85). Thus, the use of UHF creates a unique opportunity for the separation of these two molecules, a finding potentially important for treatment development.

As for *myo*-Ins, two recent 7 T studies have reported decreased levels of *myo*-Ins in MDD, one in the insula (47), with levels correlating with depression severity as measured by Hamilton Depression Rating Scale (HAMD-17), and one in ACC and thalamus (86). Another 7 T study has shown a reduction in *myo*-Ins in the ACC and OCC of patients with anorexia nervosa (48). Two studies in patients with SCZ that reported *myo*-Ins found no differences in ACC (44) and thalamus (86) between patients and controls. As for Gly, a recent 7 T study (86) found reductions in

the thalamus but not ACC of patients with SCZ as compared to healthy controls and patients with MDD.

*myo*-inositol is perhaps most interesting in the therapeutic context, given that lithium, an effective mood stabilizer, has an ability to diminish its levels and potentially thereby lower signaling through synapses employing the PI cycle as a second messenger system. A 3 T study in healthy volunteers aimed to assess the effect of ebselen, a putative lithium-mimetic and IMPase inhibitor and found a decrease in ACC *myo*-Ins under its influence (78); the finding was then replicated on a 7 T scanner (57), with the additional benefit of providing information on Glu and Gln changes, described above.

Only a few studies at lower fields showed differences in *myo*-Ins levels between patient populations and healthy controls, e.g. decreased *myo*-Ins in frontal areas of the brain in MDD (87). However, due to signal overlap between *myo*-Ins and Gly, Gly has not been reported in low-field MRS studies of psychiatric disorders.

## GLUTATHIONE (GSH)

The importance of GSH relates to its role as a major endogenous antioxidant removing free radicals and, hence, protecting cells against the effect of oxidative stress. GSH peaks appear as a singlet at 3.77 ppm, multiplets at 2.15 and 2.55 ppm, and doublet of doublets at 2.93, 2.98, and 4.56 ppm (42). It has relatively high concentrations in the brain (2–3  $\mu\text{mol/g}$ ) (42). However, it is challenging to measure *in vivo* due to significant resonance overlap with other metabolites. GSH can be detected using selective editing techniques at lower magnetic fields. In addition, a reasonably robust measurement from non-edited short echo spectra using fitting routines such as LCModel has been demonstrated (88). Recent MRS studies without special editing techniques at UHF demonstrated improved GSH quantification providing valuable new insights into psychiatrist disorders (89).

The role of increased oxidative stress has been postulated in the pathogenesis of major psychiatric conditions. Measurement of GSH is challenging at lower fields and it was reported in only a few 3 T studies (90, 91). MRS at UHF improves GSH quantification providing (89). A 7 T study in MDD observed a decrease in GSH in the putamen, in line with the findings of a 3 T study (47), which has shown a decrease in the OCC of MDD patients. The aforementioned 7 T study on the effect of ebselen has shown a decrease in GSH under the influence of the drug (57). Two other 7 T studies, one in SCZ (46) and one in anorexia (48) did not observe any differences between patients and healthy controls.

## LIMITATIONS AND POTENTIAL

Scanning at UHF, although in many ways advantageous, is not free from limitations, which can hamper its use for clinical applications. One such limitation is potential safety hazards. While no physiological health hazards have been identified in connection to UHF, there are potential dangers related to higher magnetic fields, such as the potential for tissue heating, and effects of UHF on implanted devices, such as surgical clips, coils,

and stimulation effects. More research is underway in the centers across the world to assess dangers related to specific devices. In practical terms, however, safety protocols lead to a significant proportion of patients being excluded from studies, which may make results from 7 T investigations difficult to generalize. Another issue is the cost of scanning, which is likely to change with time but currently can make clinical applications impractical. Last but not least, UHF studies share some of the limitations with lower field studies. Such limitations include, among others, differences between volunteers in different studies, the lack of clinically relevant stratification, for instance in terms of disorder severity or stage of the condition, medication status, differences in study design or MRS signal acquisition, and post processing, which can make results difficult to compare. The emerging, albeit at this point limited, picture of UHF studies suggests that they may not be free from inconsistencies characterizing lower field studies.

Despite these limitations, UHF MRS may offer important advantages over lower fields, thanks to which it could become a useful and powerful tool in the clinical context. It can provide

information about molecules crucial to both physiological functions of the brain and pathogenesis of psychiatric conditions, assessment of which could not be reliably performed at lower fields. In the future, UHF MRS may explore approaches based on other nuclei, such as  $^{31}\text{P}$ , which will increase the amount of information that can be obtained. Importantly, UHF MRS may also be useful as a tool for drug discovery in terms of both understanding existing treatments and testing the neurochemical effects of novel pharmacological approaches.

## AUTHOR CONTRIBUTIONS

Conception and design: UE and BG. Writing, review, and/or revision of the manuscript: UE, BG, PC, and SC.

## FUNDING

The authors would like to acknowledge the following: the Wellcome Trust (UE, 097813/Z/11/Z) and Medical Research Council (PC, MR/K022202/1).

## REFERENCES

- Vigo D, Thornicroft G, Atun R. Estimating the true global burden of mental illness. *Lancet Psychiatry* (2016) 3(2):171–8. doi:10.1016/S2215-0366(15)00505-2
- Birur B, Kraguljac NV, Shelton RC, Lahti AC. Brain structure, function, and neurochemistry in schizophrenia and bipolar disorder—a systematic review of the magnetic resonance neuroimaging literature. *NPJ Schizophr* (2017) 3(1):15. doi:10.1038/s41537-017-0013-9
- Treadway MT, Pizzagalli DA. Imaging the pathophysiology of major depressive disorder – from localist models to circuit-based analysis. *Biol Mood Anxiety Disord* (2014) 4(1):5. doi:10.1186/2045-5380-4-5
- Reinecke A, Filippini N, Berna C, Western DG, Hanson B, Cooper MJ, et al. Effective emotion regulation strategies improve fMRI and ECG markers of psychopathology in panic disorder: implications for psychological treatment action. *Transl Psychiatry* (2015) 5:e673. doi:10.1038/tp.2015.160
- Hampson DR, Blatt GJ. Autism spectrum disorders and neuropathology of the cerebellum. *Front Neurosci* (2015) 9:420. doi:10.3389/fnins.2015.00420
- Vogel K, Timmers I, Kumar V, Nickl-Jockschat T, Bastiani M, Roebroek A, et al. White matter microstructural changes in adolescent anorexia nervosa including an exploratory longitudinal study. *Neuroimage Clin* (2016) 11:614–21. doi:10.1016/j.nicl.2016.04.002
- Van Essen DC, Barch DM. The human connectome in health and psychopathology. *World Psychiatry* (2015) 14(2):154–7. doi:10.1002/wps.20228
- Godbolt AK, Waldman AD, MacManus DG, Schott JM, Frost C, Cipolotti L, et al. MRS shows abnormalities before symptoms in familial Alzheimer disease. *Neurology* (2006) 66(5):718–22. doi:10.1212/01.wnl.0000201237.05869.df
- Dydak U, Jiang YM, Long LL, Zhu H, Chen J, Li WM, et al. In vivo measurement of brain GABA concentrations by magnetic resonance spectroscopy in smelters occupationally exposed to manganese. *Environ Health Perspect* (2011) 119(2):219–24. doi:10.1289/ehp.1002192
- Emir UE, Tianmeng L, Deelchand DK, Joers JM, Hutter D, Gomez CM, et al. Diagnostic accuracy of MRS for hereditary neurodegeneration at 3T and 7T. *ISM RM. Singapore* (2016).
- Maddock RJ, Buonocore MH. MR spectroscopic studies of the brain in psychiatric disorders. *Curr Top Behav Neurosci* (2012) 11:199–251. doi:10.1007/7854\_2011\_197
- Lee JH, Adler C, Norris M, Chu WJ, Fugate EM, Strakowski SM, et al. 4-T 7Li 3D MR spectroscopy imaging in the brains of bipolar disorder subjects. *Magn Reson Med* (2012) 68(2):363–8. doi:10.1002/mrm.24361
- Wolf W, Presant CA, Waluch V. 19F-MRS studies of fluorinated drugs in humans. *Adv Drug Deliv Rev* (2000) 41(1):55–74. doi:10.1016/S0169-409X(99)00056-3
- Emir UE, Auerbach EJ, Van De Moortele PF, Marjanska M, Ugurbil K, Terpstra M, et al. Regional neurochemical profiles in the human brain measured by (1)H MRS at 7 T using local B(1) shimming. *NMR Biomed* (2012) 25(1):152–60. doi:10.1002/nbm.1727
- Pradhan S, Bonekamp S, Gillen JS, Rowland LM, Wijtenburg SA, Edden RA, et al. Comparison of single voxel brain MRS AT 3T and 7T using 32-channel head coils. *Magn Reson Imaging* (2015) 33(8):1013–8. doi:10.1016/j.mri.2015.06.003
- Terpstra M, Cheong I, Lyu T, Deelchand DK, Emir UE, Bednarik P, et al. Test-retest reproducibility of neurochemical profiles with short-echo, single-voxel MR spectroscopy at 3T and 7T. *Magn Reson Med* (2016) 76(4):1083–91. doi:10.1002/mrm.26022
- Provencher SW. Automatic quantitation of localized in vivo 1H spectra with LCModel. *NMR Biomed* (2001) 14(4):260–4. doi:10.1002/nbm.698
- McKay J, Tkáč I. Quantitative in vivo neurochemical profiling in humans: where are we now? *Int J Epidemiol* (2016) 45(5):1339–50. doi:10.1093/ije/dyw235
- Trattning S, Springer E, Bogner W, Hanel G, Strasser B, Dymerska B, et al. Key clinical benefits of neuroimaging at 7T. *Neuroimage* (2016). doi:10.1016/j.neuroimage.2016.11.031
- Cai K, Nanga RP, Lamprou L, Schinstine C, Elliott M, Hariharan H, et al. The impact of gabapentin administration on brain GABA and glutamate concentrations: a 7T (1)H-MRS study. *Neuropsychopharmacology* (2012) 37(13):2764–71. doi:10.1038/npp.2012.142
- Pan JW, Duckrow RB, Spencer DD, Avdievich NI, Hetherington HP. Selective homonuclear polarization transfer for spectroscopic imaging of GABA at 7T. *Magn Reson Med* (2013) 69(2):310–6. doi:10.1002/mrm.24283
- Collins CM, Liu W, Schreiber W, Yang QX, Smith MB. Central brightening due to constructive interference with, without, and despite dielectric resonance. *J Magn Reson Imaging* (2005) 21(2):192–6. doi:10.1002/jmri.20245
- Deelchand DK, Van de Moortele PF, Adriany G, Iltis I, Andersen P, Strupp JP, et al. In vivo 1H NMR spectroscopy of the human brain at 9.4 T: initial results. *J Magn Reson* (2010) 206(1):74–80. doi:10.1016/j.jmr.2010.06.006
- Boer VO, Klomp DW, Juchem C, Luijten PR, de Graaf RA. Multislice (1)H MRSI of the human brain at 7 T using dynamic B(0) and B(1) shimming. *Magn Reson Med* (2012) 68(3):662–70. doi:10.1002/mrm.23288
- Garwood M, Delabarre L. The return of the frequency sweep: designing adiabatic pulses for contemporary NMR. *J Magn Reson* (2001) 153(2):155–77. doi:10.1006/jmre.2001.2340

26. Scheenen TW, Heerschap A, Klomp DW. Towards  $^1\text{H}$ -MRSI of the human brain at 7T with slice-selective adiabatic refocusing pulses. *MAGMA* (2008) 21(1–2):95–101. doi:10.1007/s10334-007-0094-y
27. Moore J, Jankiewicz M, Zeng H, Anderson AW, Gore JC. Composite RF pulses for B1+-insensitive volume excitation at 7 Tesla. *J Magn Reson* (2010) 205(1):50–62. doi:10.1016/j.jmr.2010.04.002
28. Henning A, Fuchs A, Murdoch JB, Boesiger P. Slice-selective FID acquisition, localized by outer volume suppression (FIDLOVS) for  $(1)\text{H}$ -MRSI of the human brain at 7 T with minimal signal loss. *NMR Biomed* (2009) 22(7):683–96. doi:10.1002/nbm.1366
29. Schenck JF. The role of magnetic susceptibility in magnetic resonance imaging: MRI magnetic compatibility of the first and second kinds. *Med Phys* (1996) 23(6):815–50. doi:10.1118/1.597854
30. Wilson JL, Jenkinson M, de Araujo I, Kringselbach ML, Rolls ET, Jezzard P. Fast, fully automated global and local magnetic field optimization for fMRI of the human brain. *Neuroimage* (2002) 17(2):967–76. doi:10.1006/nimg.2002.1172
31. Chen NK, Wyrwicz AM. Correction for EPI distortions using multi-echo gradient-echo imaging. *Magn Reson Med* (1999) 41(6):1206–13. doi:10.1002/(SICI)1522-2594(199906)41:6<1206::AID-MRM17>3.3.CO;2-C
32. Gruetter R, Tkáć I. Field mapping without reference scan using asymmetric echo-planar techniques. *Magn Reson Med* (2000) 43(2):319–23. doi:10.1002/(SICI)1522-2594(200002)43:2<319::AID-MRM22>3.3.CO;2-T
33. Gruetter R. Automatic, localized *in vivo* adjustment of all first- and second-order shim coils. *Magn Reson Med* (1993) 29(6):804–11. doi:10.1002/mrm.1910290613
34. Pan JW, Lo KM, Hetherington HP. Role of very high order and degree B0 shimming for spectroscopic imaging of the human brain at 7 Tesla. *Magn Reson Med* (2012) 68(4):1007–17. doi:10.1002/mrm.24122
35. Koch KM, Sacolick LI, Nixon TW, McIntyre S, Rothman DL, de Graaf RA. Dynamically shimmed multivoxel  $^1\text{H}$  magnetic resonance spectroscopy and multislice magnetic resonance spectroscopic imaging of the human brain. *Magn Reson Med* (2007) 57(3):587–91. doi:10.1002/mrm.21141
36. Wilson JL, Jenkinson M, Jezzard P. Optimization of static field homogeneity in human brain using diamagnetic passive shims. *Magn Reson Med* (2002) 48(5):906–14. doi:10.1002/mrm.10298
37. Harris CT, Handler WB, Chronik BA. A new approach to shimming: the dynamically controlled adaptive current network. *Magn Reson Med* (2014) 71(2):859–69. doi:10.1002/mrm.24724
38. Li Y, Xu D, Ozturk-Isik E, Lupo JM, Chen AP, Vigneron DB, et al. T1 and T2 metabolite relaxation times in normal brain at 3T and 7T. *J Mol Imaging Dynam* (2012) S1:002. doi:10.4172/2155-9937.S1-002-002
39. Michaeli S, Garwood M, Zhu XH, Delabarre L, Andersen P, Adriany G, et al. Proton T2 relaxation study of water, N-acetylaspartate, and creatine in human brain using Hahn and Carr-Purcell spin echoes at 4T and 7T. *Magn Reson Med* (2002) 47(4):629–33. doi:10.1002/mrm.10135
40. Marjanska M, Emir UE, Deelchand DK, Terpstra M. Faster metabolite  $(1)\text{H}$  transverse relaxation in the elder human brain. *PLoS One* (2013) 8(10):e77572. doi:10.1371/journal.pone.0077572
41. Tkáć I, Andersen P, Adriany G, Merkle H, Ugurbil K, Gruetter R. In vivo  $^1\text{H}$  NMR spectroscopy of the human brain at 7 T. *Magn Reson Med* (2001) 46(3):451–6. doi:10.1002/mrm.1213
42. Govindaraju V, Young K, Maudsley AA. Proton NMR chemical shifts and coupling constants for brain metabolites. *NMR Biomed* (2000) 13(3):129–53. doi:10.1002/1099-1492(200005)13:3<129::AID-NBM619>3.3.CO;2-M
43. Puts NA, Edden RA. In vivo magnetic resonance spectroscopy of GABA: a methodological review. *Prog Nucl Magn Reson Spectrosc* (2012) 60:29–41. doi:10.1016/j.pnmrs.2011.06.001
44. Marsman A, Mandl RC, Klomp DW, Bohlken MM, Boer VO, Andreychenko A, et al. GABA and glutamate in schizophrenia: a 7 T (1) H-MRS study. *Neuroimage Clin* (2014) 6:398–407. doi:10.1016/j.nicl.2014.10.005
45. Thakkar KN, Rosler L, Wijnen JP, Boer VO, Klomp DW, Cahn W, et al. 7T proton magnetic resonance spectroscopy of gamma-aminobutyric acid, glutamate, and glutamine reveals altered concentrations in patients with schizophrenia and healthy siblings. *Biol Psychiatry* (2017) 81(6):525–35. doi:10.1016/j.biopsych.2016.04.007
46. Brandt AS, Unschuld PG, Pradhan S, Lim IA, Churchill G, Harris AD, et al. Age-related changes in anterior cingulate cortex glutamate in schizophrenia: a (1)H MRS Study at 7 Tesla. *Schizophr Res* (2016) 172(1–3):101–5. doi:10.1016/j.schres.2016.02.017
47. Li Y, Jakary A, Gillung E, Eisendrath S, Nelson SJ, Mukherjee P, et al. Evaluating metabolites in patients with major depressive disorder who received mindfulness-based cognitive therapy and healthy controls using short echo MRSI at 7 Tesla. *MAGMA* (2016) 29(3):523–33. doi:10.1007/s10334-016-0526-7
48. Godlewski BR, Pike A, Sharpley AL, Ayton A, Park RJ, Cowen PJ, et al. Brain glutamate in anorexia nervosa: a magnetic resonance spectroscopy case control study at 7 Tesla. *Psychopharmacology (Berl)* (2017) 234(3):421–6. doi:10.1007/s00213-016-4477-5
49. Lin Y, Stephenson MC, Xin L, Napolitano A, Morris PG. Investigating the metabolic changes due to visual stimulation using functional proton magnetic resonance spectroscopy at 7 T. *J Cereb Blood Flow Metab* (2012) 32(8):1484–95. doi:10.1038/jcbfm.2012.33
50. Mangia S, Tkáć I, Gruetter R, Van de Moortele PF, Maraviglia B, Ugurbil K. Sustained neuronal activation raises oxidative metabolism to a new steady-state level: evidence from  $^1\text{H}$  NMR spectroscopy in the human visual cortex. *J Cereb Blood Flow Metab* (2007) 27(5):1055–63. doi:10.1038/sj.jcbfm.9600401
51. Schaller B, Mekle R, Xin L, Kunz N, Gruetter R. Net increase of lactate and glutamate concentration in activated human visual cortex detected with magnetic resonance spectroscopy at 7 Tesla. *J Neurosci Res* (2013) 91(8):1076–83. doi:10.1002/jnr.23194
52. Bednarik P, Tkáć I, Giove F, DiNuzzo M, Deelchand DK, Emir UE, et al. Neurochemical and BOLD responses during neuronal activation measured in the human visual cortex at 7 Tesla. *J Cereb Blood Flow Metab* (2015) 35(4):601–10. doi:10.1038/jcbfm.2014.233
53. Betina Ip I, Berrington A, Hess AT, Parker AJ, Emir UE, Bridge H. Combined fMRI-MRS acquires simultaneous glutamate and BOLD-fMRI signals in the human brain. *Neuroimage* (2017) 155:113–9. doi:10.1016/j.neuroimage.2017.04.030
54. Taylor R, Neufeld RW, Schaefer B, Densmore M, Rajakumar N, Osuch EA, et al. Functional magnetic resonance spectroscopy of glutamate in schizophrenia and major depressive disorder: anterior cingulate activity during a color-word Stroop task. *NPJ Schizophr* (2015) 1:15028. doi:10.1038/njpschz.2015.28
55. Kuzniecky R, Ho S, Pan J, Martin R, Gilliam F, Faught E, et al. Modulation of cerebral GABA by topiramate, lamotrigine, and gabapentin in healthy adults. *Neurology* (2002) 58(3):368–72. doi:10.1212/WNL.58.3.368
56. Schur RR, Draisma LW, Wijnen JP, Boks MP, Koevoets MG, Joels M, et al. Brain GABA levels across psychiatric disorders: a systematic literature review and meta-analysis of (1) H-MRS studies. *Hum Brain Mapp* (2016) 37(9):3337–52. doi:10.1002/hbm.23244
57. Masaki C, Sharpley AL, Godlewski BR, Berrington A, Hashimoto T, Singh N, et al. Effects of the potential lithium-mimetic, ebselen, on brain neurochemistry: a magnetic resonance spectroscopy study at 7 Tesla. *Psychopharmacology (Berl)* (2016) 233(6):1097–104. doi:10.1007/s00213-015-4189-2
58. Merritt K, Egerton A, Kempton MJ, Taylor MJ, McGuire PK. Nature of glutamate alterations in schizophrenia: a meta-analysis of proton magnetic resonance spectroscopy studies. *JAMA Psychiatry* (2016) 73(7):665–74. doi:10.1001/jamapsychiatry.2016.0442
59. Marsman A, van den Heuvel MP, Klomp DW, Kahn RS, Luijten PR, Hulshoff Pol HE. Glutamate in schizophrenia: a focused review and meta-analysis of (1)H-MRS studies. *Schizophr Bull* (2013) 39(1):120–9. doi:10.1093/schbul/sbr069
60. Poels EM, Kegeles LS, Kantrowitz JT, Javitt DC, Lieberman JA, Abi-Dargham A, et al. Glutamatergic abnormalities in schizophrenia: a review of proton MRS findings. *Schizophr Res* (2014) 152(2–3):325–32. doi:10.1016/j.schres.2013.12.013
61. Taylor SF, Tso IF. GABA abnormalities in schizophrenia: a methodological review of *in vivo* studies. *Schizophr Res* (2015) 167(1–3):84–90. doi:10.1016/j.schres.2014.10.011
62. Yildiz-Yesiloglu A, Ankerst DP. Review of  $^1\text{H}$  magnetic resonance spectroscopy findings in major depressive disorder: a meta-analysis. *Psychiatry Res* (2006) 147(1):1–25. doi:10.1016/j.psychresns.2005.12.004
63. Yildiz-Yesiloglu A, Ankerst DP. Neurochemical alterations of the brain in bipolar disorder and their implications for pathophysiology: a systematic review of the *in vivo* proton magnetic resonance spectroscopy findings. *Prog Neuropsychopharmacol Biol Psychiatry* (2006) 30(6):969–95. doi:10.1016/j.pnpbp.2006.03.012

64. Arnone D, Mumuni AN, Jauhar S, Condon B, Cavanagh J. Indirect evidence of selective glial involvement in glutamate-based mechanisms of mood regulation in depression: meta-analysis of absolute prefrontal neuro-metabolic concentrations. *Eur Neuropsychopharmacol* (2015) 25(8):1109–17. doi:10.1016/j.euroneuro.2015.04.016
65. Luykx JJ, Laban KG, van den Heuvel MP, Boks MP, Mandl RC, Kahn RS, et al. Region and state specific glutamate downregulation in major depressive disorder: a meta-analysis of (1)H-MRS findings. *Neurosci Biobehav Rev* (2012) 36(1):198–205. doi:10.1016/j.neubiorev.2011.05.014
66. Yuksel C, Ongur D. Magnetic resonance spectroscopy studies of glutamate-related abnormalities in mood disorders. *Biol Psychiatry* (2010) 68(9):785–94. doi:10.1016/j.biopsych.2010.06.016
67. Gigante AD, Bond DJ, Lafer B, Lam RW, Young LT, Yatham LN. Brain glutamate levels measured by magnetic resonance spectroscopy in patients with bipolar disorder: a meta-analysis. *Bipolar Disord* (2012) 14(5):478–87. doi:10.1111/j.1399-5618.2012.01033.x
68. Szulc A, Galinska-Skok B, Waszkiewicz N, Bibulowicz D, Konarzewska B, Tarasow E. Proton magnetic resonance spectroscopy changes after anti-psychotic treatment. *Curr Med Chem* (2013) 20(3):414–27. doi:10.2174/092986713804870783
69. Kondo DG, Hellein TL, Sung YH, Kim N, Jeong EK, Delmastro KK, et al. Review: magnetic resonance spectroscopy studies of pediatric major depressive disorder. *Depress Res Treat* (2011) 2011:650450. doi:10.1155/2011/650450
70. Walter M, Henning A, Grimm S, Schulte RF, Beck J, Dydak U. The relationship between aberrant neuronal activation in the pregenual anterior cingulate, altered glutamatergic metabolism, and anhedonia in major depression. *Arch Gen Psychiatry* (2009) 66(5):478–86. doi:10.1001/archgenpsychiatry.2009.39
71. Sanacora G, Gueorguieva R, Epperson CN, Wu YT, Appel M, Rothman DL, et al. Subtype-specific alterations of gamma-aminobutyric acid and glutamate in patients with major depression. *Arch Gen Psychiatry* (2004) 61(7):705–13. doi:10.1001/archpsyc.61.7.705
72. NealeJH, Bzduga T, WroblewskaB. N-acetylaspartylglutamate: the most abundant peptide neurotransmitter in the mammalian central nervous system. *J Neurochem* (2000) 75(2):443–52. doi:10.1046/j.1471-4159.2000.0750443.x
73. Olszewski RT, Wegorzewska MM, Monteiro AC, Krolkowski KA, Zhou J, Kozikowski AP, et al. Phencyclidine and dizocilpine induced behaviors reduced by N-acetylaspartylglutamate peptidase inhibition via metabotropic glutamate receptors. *Biol Psychiatry* (2008) 63(1):86–91. doi:10.1016/j.biopsych.2007.04.016
74. Rowland LM, Kontson K, West J, Edden RA, Zhu H, Wijtenburg SA, et al. In vivo measurements of glutamate, GABA, and NAAG in schizophrenia. *Schizophr Bull* (2013) 39(5):1096–104. doi:10.1093/schbul/sbs092
75. Steen RG, Hamer RM, Lieberman JA. Measurement of brain metabolites by 1H magnetic resonance spectroscopy in patients with schizophrenia: a systematic review and meta-analysis. *Neuropsychopharmacology* (2005) 30(11):1949–62. doi:10.1038/sj.npp.1300850
76. Kraguljac NV, Reid M, White D, Jones R, den Hollander J, Lowman D, et al. Neurometabolites in schizophrenia and bipolar disorder – a systematic review and meta-analysis. *Psychiatry Res* (2012) 203(2–3):111–25. doi:10.1016/j.psychresns.2012.02.003
77. Capizzano AA, Jorge RE, Acion LC, Robinson RG. In vivo proton magnetic resonance spectroscopy in patients with mood disorders: a technically oriented review. *J Magn Reson Imaging* (2007) 26(6):1378–89. doi:10.1002/jmri.21144
78. Singh N, Sharpley AL, Emir UE, Masaki C, Herzallah MM, Gluck MA, et al. Effect of the putative lithium mimetic ebselen on brain myo-inositol, sleep, and emotional processing in humans. *Neuropsychopharmacology* (2016) 41(7):1768–78. doi:10.1038/npp.2015.343
79. Li BS, Wang H, Gonen O. Metabolite ratios to assumed stable creatine level may confound the quantification of proton brain MR spectroscopy. *Magn Reson Imaging* (2003) 21(8):923–8. doi:10.1016/S0730-725X(03)00181-4
80. Jensen JE, Miller J, Williamson PC, Neufeld RW, Menon RS, Malla A, et al. Focal changes in brain energy and phospholipid metabolism in first-episode schizophrenia: <sup>31</sup>P-MRS chemical shift imaging study at 4 Tesla. *Br J Psychiatry* (2004) 184:409–15. doi:10.1192/bj.p.184.5.409
81. Lei H, Zhu XH, Zhang XL, Ugurbil K, Chen W. In vivo <sup>31</sup>P magnetic resonance spectroscopy of human brain at 7 T: an initial experience. *Magn Reson Med* (2003) 49(2):199–205. doi:10.1002/mrm.10379
82. Heresco-Levy U, Ermilov M, Lichtenberg P, Bar G, Javitt DC. High-dose glycine added to olanzapine and risperidone for the treatment of schizophrenia. *Biol Psychiatry* (2004) 55(2):165–71. doi:10.1016/S0006-3223(03)00707-8
83. Schulte RF, Boesiger P. ProFit: two-dimensional prior-knowledge fitting of J-resolved spectra. *NMR Biomed* (2006) 19(2):255–63. doi:10.1002/nbm.1027
84. Choi C, Bhardwaj PP, Seres P, Kalra S, Tibbo PG, Coupland NJ. Measurement of glycine in human brain by triple refocusing <sup>1</sup>H-MRS *in vivo* at 3.0T. *Magn Reson Med* (2008) 59(1):59–64. doi:10.1002/mrm.21450
85. Gambarota G, Mekle R, Xin L, Hergt M, van der Zwaag W, Krueger G, et al. In vivo measurement of glycine with short echo-time <sup>1</sup>H MRS in human brain at 7 T. *MAGMA* (2009) 22(1):1–4. doi:10.1007/s10334-008-0152-0
86. Taylor R, Osuch EA, Schaefer B, Rajakumar N, Neufeld RWJ, Théberge J, et al. Neurometabolic abnormalities in schizophrenia and depression observed with magnetic resonance spectroscopy at 7 T. *BJPsych Open* (2017) 3:6–11. doi:10.1192/bjpo.bp.116.003756
87. Coupland NJ, Ogilvie CJ, Hegadoren KM, Seres P, Hanstock CC, Allen PS. Decreased prefrontal myo-inositol in major depressive disorder. *Biol Psychiatry* (2005) 57(12):1526–34. doi:10.1016/j.biopsych.2005.02.027
88. Wijtenburg SA, Gaston FE, Spicker EA, Korenic SA, Kochunov P, Hong LE, et al. Reproducibility of phase rotation STEAM at 3T: focus on glutathione. *Magn Reson Med* (2014) 72(3):603–9. doi:10.1002/mrm.24959
89. Deelchand DK, Marjanska M, Hodges JS, Terpstra M. Sensitivity and specificity of human brain glutathione concentrations measured using short-TE <sup>1</sup>H MRS at 7 T. *NMR Biomed* (2016) 29(5):600–6. doi:10.1002/nbm.3507
90. Godlewska BR, Near J, Cowen PJ. Neurochemistry of major depression: a study using magnetic resonance spectroscopy. *Psychopharmacology (Berl)* (2015) 232(3):501–7. doi:10.1007/s00213-014-3687-y
91. Poels EM, Kegeles LS, Kantrowitz JT, Slifstein M, Javitt DC, Lieberman JA, et al. Imaging glutamate in schizophrenia: review of findings and implications for drug discovery. *Mol Psychiatry* (2014) 19(1):20–9. doi:10.1038/mp.2013.136

**Conflict of Interest Statement:** The authors declare that the research was conducted in the absence of any commercial or financial relationships that could be construed as a potential conflict of interest.

Copyright © 2017 Godlewska, Clare, Cowen and Emir. This is an open-access article distributed under the terms of the Creative Commons Attribution License (CC BY). The use, distribution or reproduction in other forums is permitted, provided the original author(s) or licensor are credited and that the original publication in this journal is cited, in accordance with accepted academic practice. No use, distribution or reproduction is permitted which does not comply with these terms.



# Detection of Glutamate Alterations in the Human Brain Using $^1\text{H}$ -MRS: Comparison of STEAM and sLASER at 7 T

Anouk Marsman<sup>1</sup>, Vincent O. Boer<sup>2</sup>, Peter R. Luijten<sup>2</sup>, Hilleke E. Hulshoff Pol<sup>1</sup>, Dennis W. J. Klompen<sup>2</sup> and René C. W. Mandl<sup>1\*</sup>

<sup>1</sup>Psychiatry, Brain Center Rudolf Magnus, University Medical Center Utrecht, Utrecht, Netherlands, <sup>2</sup>Radiology, Brain Center Rudolf Magnus, University Medical Center Utrecht, Utrecht, Netherlands

## OPEN ACCESS

### Edited by:

Paul Croarkin,  
Mayo Clinic, USA

### Reviewed by:

Kim M. Cecil,  
Cincinnati Children's Hospital  
Medical Center, USA  
Frank P. MacMaster,  
University of Calgary, Canada

### \*Correspondence:

René C. W. Mandl  
r.mandl@umcutrecht.nl

### Specialty section:

This article was submitted to  
Neuroimaging and Stimulation,  
a section of the journal  
*Frontiers in Psychiatry*

Received: 01 March 2017

Accepted: 04 April 2017

Published: 21 April 2017

### Citation:

Marsman A, Boer VO, Luijten PR, Hulshoff Pol HE, Klompen DWJ and Mandl RCW (2017) Detection of Glutamate Alterations in the Human Brain Using  $^1\text{H}$ -MRS: Comparison of STEAM and sLASER at 7 T. *Front. Psychiatry* 8:60. doi: 10.3389/fpsy.2017.00060

**Purpose:** To assess reproducibility of glutamate measurement in the human brain by two short echo time (TE)  $^1\text{H}$ -MRS sequences [stimulated echo acquisition mode (STEAM) and semi-localized by adiabatic selective refocusing (sLASER)] at 7 T. Reliable assessment of glutamate is important when studying a variety of neurological and neuropsychiatric disorders. At 7 T, the glutamate signal can be separated from the glutamine signal and hence more accurately measured as compared to lower field strengths. A sLASER sequence has been developed for 7 T, using field focusing at short TE, resulting in twice as much signal as can be obtained using STEAM and improved localization accuracy due to a decreased chemical shift artifact.

**Materials and methods:** Eight subjects were scanned twice using both STEAM and sLASER. Data were acquired from the frontal and occipital brain region. Subsequently, intraclass correlations were computed for the estimated metabolite concentrations.

**Results:** sLASER has higher ICC's for glutamate concentration as compared to STEAM in both the frontal and occipital VOI, which is probably due to the higher sensitivity and localization accuracy.

**Conclusion:** We conclude that sLASER  $^1\text{H}$ -MRS at 7 T is a reliable method to obtain reproducible measures of glutamate levels in the human brain at such high accuracy that individual variability, even between age-matched subjects, is measured.

**Keywords:** glutamate, magnetic resonance spectroscopy, reproducibility, brain, 7 T

## INTRODUCTION

*In vivo*  $^1\text{H}$  magnetic resonance spectroscopy ( $^1\text{H}$ -MRS) can be used to determine glutamate levels in the human brain. Glutamate is the primary excitatory neurotransmitter in the mammalian central nervous system. Examining glutamate levels is important when studying a variety of neuropsychiatric conditions, including schizophrenia, bipolar disorder, depression, Alzheimer's dementia, and anxiety disorders (1). Up until now, the majority of studies examining glutamate in psychiatric disorders using  $^1\text{H}$ -MRS were conducted at magnetic field strengths of 4 T or lower. However, measurement of glutamate with  $^1\text{H}$ -MRS is challenging at lower field strengths, due to its spectral overlap with glutamine. A magnetic field strength of 7 T not only results in an increased signal-to-noise ratio (SNR) but also in an increased chemical shift dispersion. Therefore, the glutamate

and glutamine resonances can be adequately separated, and glutamate can be accurately determined (2). The full in-phase glutamate signal can be acquired using short echo time (TE)  $^1\text{H}$ -MRS sequences. For human brain applications, the stimulated echo acquisition mode (STEAM) sequence is the most commonly used method at 7 T for localization. For human brain applications, the stimulated echo acquisition mode (STEAM) sequence is the most commonly used method at 7 T for localization (3), in particular for metabolites with a short  $T_2$  (e.g., glutamate). However, STEAM suffers from severe SNR loss because only half of the available signal can be obtained (Figure 1). Recently, a semi-localized by adiabatic selective refocusing (sLASER) sequence has been developed for application at a magnetic field strength of 7 T. sLASER can be applied to the human brain with a conventional volume head coil, and the full signal can be acquired at short TE with a small chemical shift displacement artifact. The two transmit channels in a conventional volume head coil are driven independently, generating a maximized  $B_1^+$  field and allowing the use of short adiabatic refocusing pulses for single-voxel MRS in most of the brain (4).

When performing clinical  $^1\text{H}$ -MRS studies, it is necessary to reliably detect changes in metabolite levels caused by diseases. As mentioned above, glutamate assessment in the human brain has been challenging at low magnetic field strengths due to poor spectral resolution and SNR loss. With the introduction of the sLASER sequence at 7 T, these issues could be overcome. To determine if sLASER can be used as a standard in  $^1\text{H}$ -MRS, studies of glutamate levels in psychiatric disorders, it is needed to assess the reproducibility of glutamate measurement with the sLASER sequence. To evaluate this, experiments were performed at two time-points in eight healthy, age-matched volunteers. Both the STEAM and sLASER sequence were used to measure metabolite concentrations in the frontal as well as the occipital brain region. In addition, we fitted the data into metabolite concentrations using three models, each including a different amount of metabolite basis sets, to evaluate the robustness of the results.

## MATERIALS AND METHODS

### Subjects

Eight healthy subjects (21–29 years, mean  $\pm$  SD = 23.9  $\pm$  2.4 years, three males, five females) were scanned twice, with 2 weeks between the measurements. Written informed consent, as

approved by the institutional ethics board, was given by all volunteers prior to the examinations. Participants had no major psychiatric or neurological history and no history of drug or alcohol abuse, as tested with the Mini International Neuropsychiatric Interview Plus (MINI-Plus) (5). Participants had no first degree relatives with psychiatric or neurological disorders. We excluded the first measurement with the sLASER sequence in the occipital lobe in one subject because of low spectral quality.

### MR Acquisition

All investigations were performed on a 7 T whole body MR scanner (Philips, Cleveland, OH, USA). A birdcage transmit head coil was used in dual transmit driven by  $2 \times 4$  kW amplifiers, in combination with a 16-channel receive coil (both Nova Medical, Inc., Burlington, MA, USA). A  $T_1$ -weighted MP-RAGE sequence (450 slices, slice thickness = 0.8 mm, TR = 7 ms, TE = 3 ms, flip angle = 8°, FOV = 250 mm  $\times$  200 mm  $\times$  180 mm, 312  $\times$  312 acquisition matrix, SENSE factor 2.7, scan duration = 408 s) was obtained for anatomical reference and gray and white matter (GM and WM) tissue classification.  $^1\text{H}$ -MRS experiments were conducted with two short TE sequences, i.e., STEAM (stimulated echo acquisition mode; TE = 7.8 ms, 128 averages, TR = 2 s) and sLASER (semi-localized by adiabatic selective refocusing; TE = 28 ms, 16 averages, TR = 5 s). Voxels (2 cm  $\times$  2 cm  $\times$  2 cm) were located in the left frontal and left occipital lobe (Figure 2). Non-water suppressed spectra were obtained for quantification (carrier frequency was set to the chemical shift of  $\text{H}_2\text{O}$ , acquisition time = 10 s). Prior to the MRS exams, second order  $B_0$  shimming was applied using the FASTERMAP algorithm at the voxel of interest (6, 7). Second, at this location, a high  $B_1$  field was generated to minimize chemical shift displacement artifacts (8). The highest possible  $B_1$  field was generated by optimizing the phase of both transmit channels to locally assure constructive  $B_1$  interferences (4).

### Spectral Fitting and Quantification

Retrospective phase and frequency alignment was performed on all data sets of each measurement (9). Spectral fitting was performed with LCModel-based software implemented in Matlab (10), which uses *a priori* knowledge of the spectral components to fit metabolite resonances (11). Basis sets were generated for the STEAM and sLASER sequence. Three separate fitting procedures were performed on all data sets to examine if the amount of metabolites included in the model influences the reproducibility of the

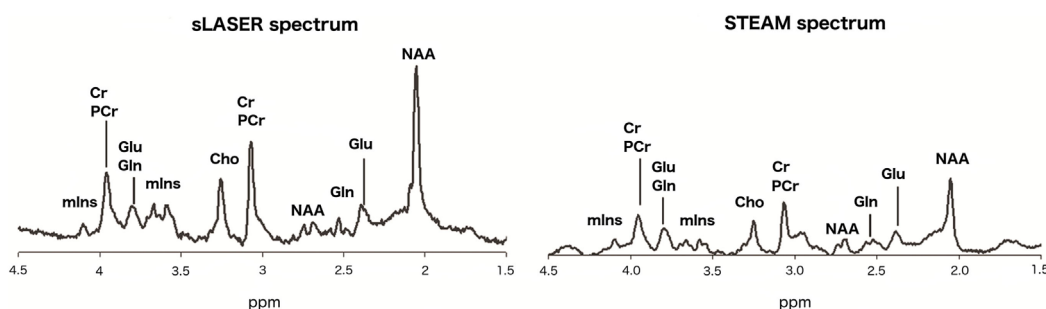


**FIGURE 1 |** Typical spectra for the semi-localized by adiabatic selective refocusing (sLASER) sequence (left) and stimulated echo acquisition mode (STEAM) sequence (right).

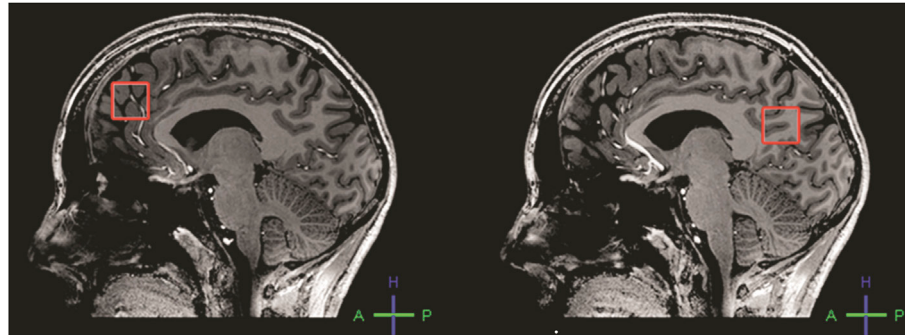


**FIGURE 2 |** Placement of the frontal (left) and occipital (right) voxel.

data. In the separate fitting procedures 8 (PC, PE, PCr, NAA, Glu, Gln, GSH, mIns), 12 (Cho, PC, GPC, PE, Cr, PCr, NAA, NAAG, Glu, Gln, GSH, mIns) or 16 (Ace, Asp, Cho, PC, GPC, PE, Cr, PCr, NAA, NAAG, GABA, Glu, Gln, GSH, mIns, Tau) metabolites and a measured macromolecular baseline (12) were fitted to the spectra (**Table 1**). Metabolite levels were estimated using the water signal as an internal reference and calculated as follows:

$$[\text{met}] = \frac{\frac{\text{signal}_{\text{met}}}{\text{signal}_{\text{water}}} * \left( \begin{array}{l} \text{volGM} * [\text{water}_{\text{GM}}] \\ + \text{volWM} * [\text{water}_{\text{WM}}] \\ + \text{volCSF} * [\text{water}_{\text{pure}}] \end{array} \right)}{\text{volGM} + \text{volWM}}$$

where [met] is the metabolite concentration,  $\text{signal}_{\text{met}}$  is the fitted signal intensity of the metabolite, accounting for the number of protons, and  $\text{signal}_{\text{water}}$  is the fitted signal intensity of water, accounting for the number of protons; volGM, volWM, and volCSF are, respectively, the GM content, WM content, and cerebrospinal fluid (CSF) content in the voxel; and  $[\text{water}_{\text{GM}}]$ ,  $[\text{water}_{\text{WM}}]$ , and  $[\text{water}_{\text{pure}}]$  are, respectively, the water concentration in GM, WM, or CSF. For determining the contribution of GM, WM, and CSF of each voxel, the software package SPM8 was used to segment the  $T_1$ -weighted image. In the  $T_1$ -weighted image, the position of the  $^1\text{H}$ -MRS voxel was determined, after which the amount of GM, WM, and CSF in the  $^1\text{H}$ -MRS voxel was computed. To account for differences in transverse relaxation between water and metabolites, a correction was applied based on reported  $T_2$  values at 7 T of 47 ms on average for water and 107 ms assumed for the metabolites (13).

## Statistical Analysis

To assess the reproducibility for glutamate, and the major spectral components total  $N$ -acetyl aspartate (NAA) (NAA + NAAG), total creatine (Cr + PCr), and total choline (Cho + PCh + GPC + PE), a test-retest reliability test was performed (SPSS 15.0, Chicago, IL, USA) for each sequence and VOI, by calculating the intraclass correlation coefficient using a two-way mixed model ANOVA. We reported the average measures intraclass correlations (ICC), since it takes into account the average of the values of the two scan sessions. A negative ICC indicates that the measurement is not reliable.

**TABLE 1 |** Metabolites that were fitted to the spectra using three different fitting procedures.

Metabolites	8-metabolite fit	12-metabolite fit	16-metabolite fit
Acetate (Ace)			x
Aspartate (Asp)			x
Choline (Cho)		x	x
Phosphorylcholine (PC)	x	x	x
Glycerophosphorylcholine (GPC)		x	x
Phosphorylethanolamine (PE)	x	x	x
Creatine (Cr)		x	x
Phosphocreatine (PCr)	x	x	x
$N$ -acetyl aspartate (NAA)	x	x	x
$N$ -acetyl aspartyl glutamate (NAAG)		x	x
Gamma-aminobutyric acid (GABA)			x
Glutamate (Glu)	x	x	x
Glutamine (Gln)	x	x	x
Glutathione (GSH)	x	x	x
Myo-inositol (mIns)	x	x	x
Taurine (Tau)			x
Macromolecules (MM)	x	x	x

## RESULTS

Glutamate concentrations for all subjects at the two scan sessions and as determined by the three different fitting procedures are shown in **Figures 3–5**. ICC's and  $p$ -values are shown in **Table 2**. Coefficients of variation values are provided in Table S7 in Supplementary Material. Average metabolite concentrations are shown in **Table 3**. In the frontal lobe, the sLASER provides significant ICC's when fitting with 8 or 16-metabolite basis sets.

To evaluate the precision of the quantification of the most commonly obtained metabolites, average metabolite concentrations, ICC's, and  $p$ -values are shown in the supplemental figures and tables (Figures S1–S3 in Supplementary Material and Tables S1 and S2 in Supplementary Material for NAA, Figures S4–S6 in Supplementary Material and Tables S3 and S4 in Supplementary Material for Cr, and Figures S7–S9 in Supplementary Material and Tables S5 and S6 in Supplementary Material for Cho).

For the occipital lobe, a significant ICC was found only for NAA measured with sLASER and fitted with the 12-metabolite

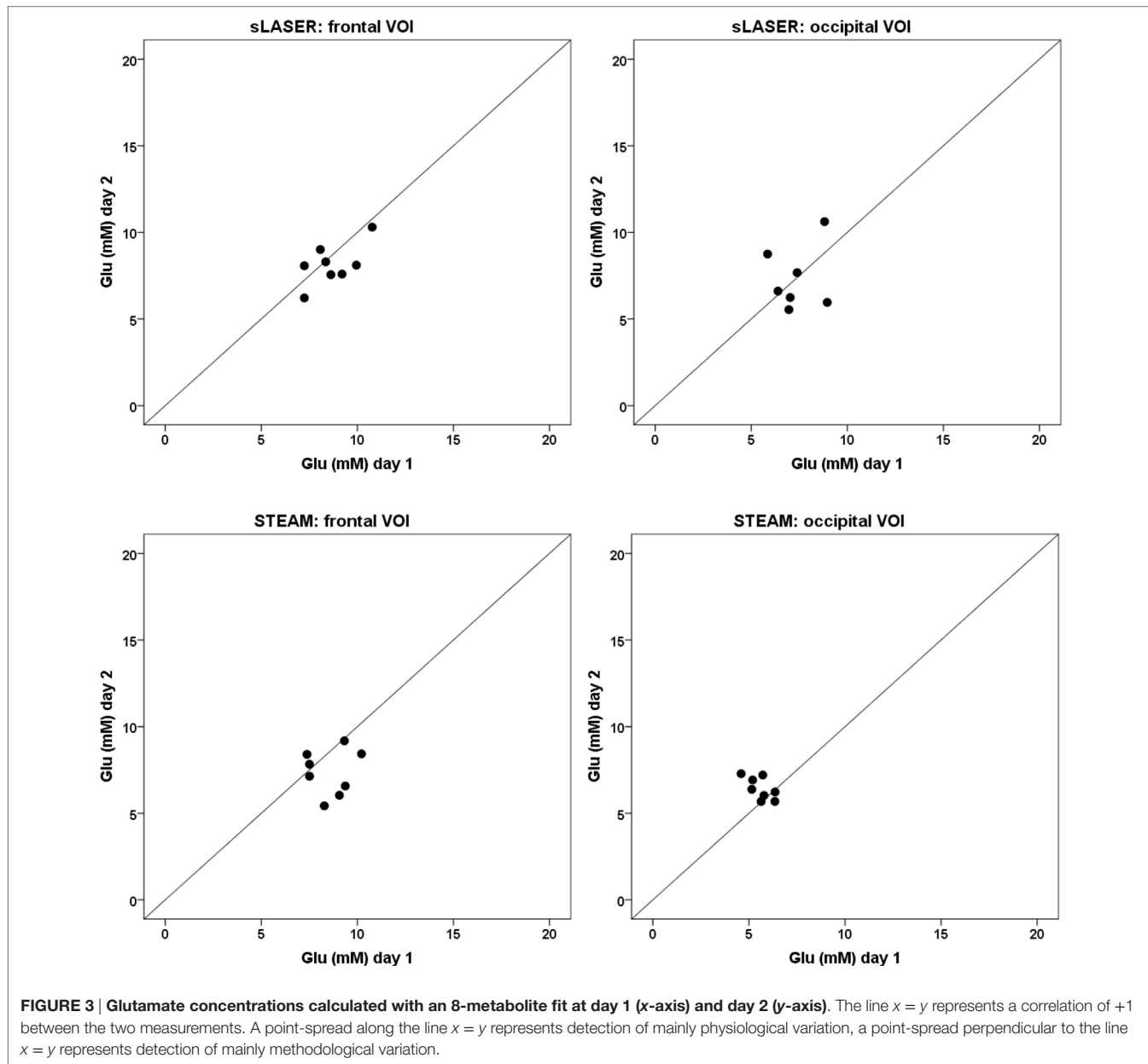


**FIGURE 3 |** Glutamate concentrations calculated with an 8-metabolite fit at day 1 (x-axis) and day 2 (y-axis). The line  $x = y$  represents a correlation of +1 between the two measurements. A point-spread along the line  $x = y$  represents detection of mainly physiological variation, a point-spread perpendicular to the line  $x = y$  represents detection of mainly methodological variation.

basis set. Bland–Altman plots for significant ICC's are shown in Figure S10 in Supplementary Material.

## DISCUSSION

In this study, we estimated the reproducibility of glutamate measurements using the STEAM and sLASER sequence at 7 T in two different areas of the human brain. As compared to the commonly used STEAM sequence, sLASER seems to be a more robust method for determining glutamate levels. It produces similar results at different time-points and is sensitive enough to detect physiological differences between subjects. Particularly, in the frontal brain region that plays an important role in psychiatric disorders (14–18), glutamate concentrations measured with sLASER show a high reproducibility.

Concentrations of NAA, creatine, and choline are expected to remain stable over subjects, particularly in the small age range used in this study (19, 20), hence one would expect lower ICC's for these metabolites, as the between subjects variance is low. The results for sLASER indeed show that the ICC's for NAA, creatine, and choline are lower than the ICC computed for glutamate. This has already been shown for sLASER at 3 T (21). In contrast to glutamate, NAA, creatine, and choline do not suffer from overlap with other metabolites at lower field strength and show low between subjects variances. Therefore, measurements of these metabolites at 7 T only result in a higher SNR, while the low ICC's remain.

We note that, in contrast to the sLASER measurements, a clear difference in variance can be observed between the two measurements using STEAM (see for instance Figure 3). This suggests

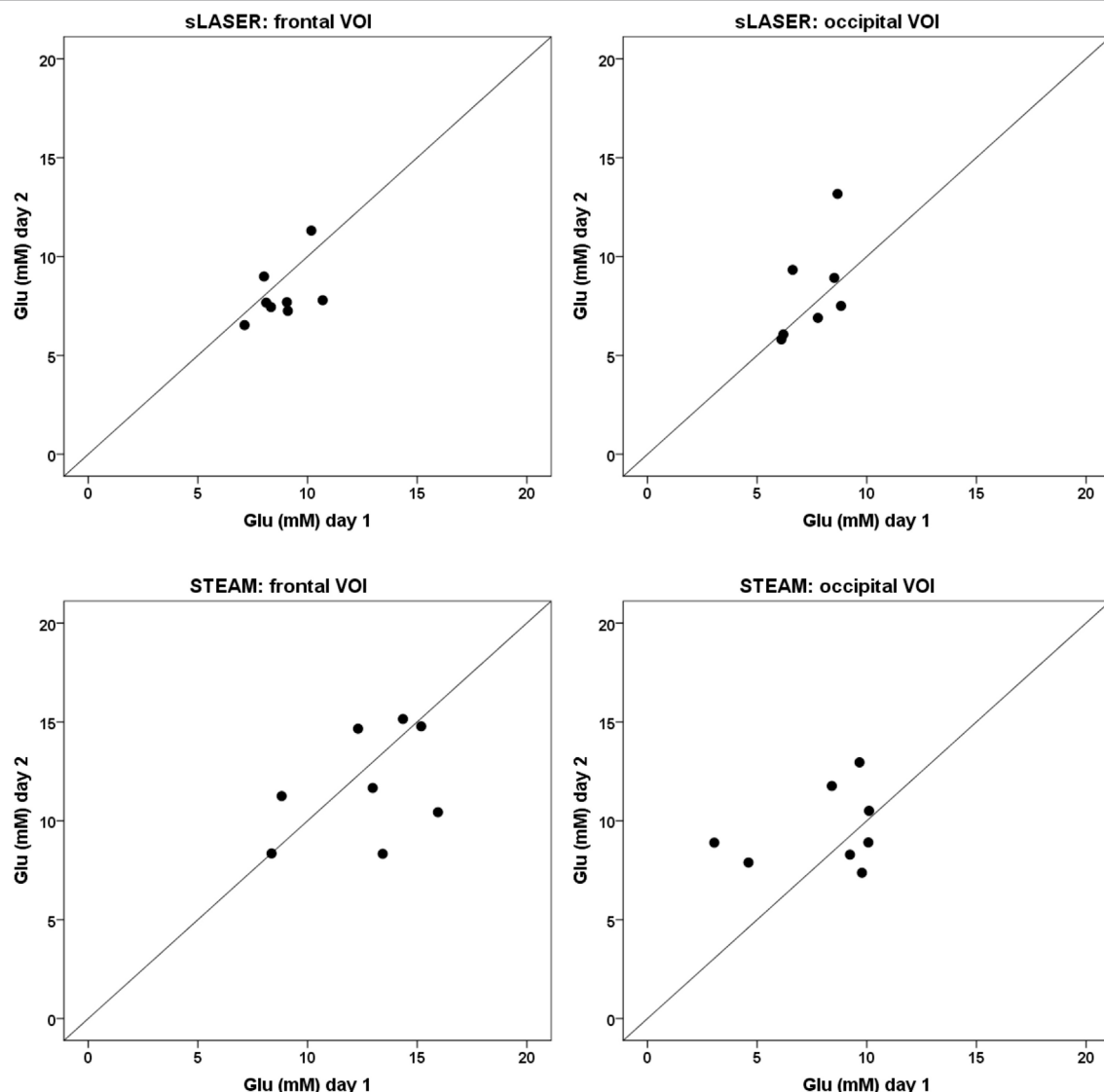


**FIGURE 4 |** Glutamate concentrations calculated with a 12-metabolite fit at day 1 (x-axis) and day 2 (y-axis). The line  $x = y$  represents a correlation of +1 between the two measurements. A point-spread along the line  $x = y$  represents detection of mainly physiological variation, a point-spread perpendicular to the line  $x = y$  represents detection of mainly methodological variation.

that the STEAM sequence is more sensitive than the sLASER sequence to external factors that are apparently difficult to control as we tried to keep the conditions in our experiments the same as much as possible. As mentioned before, STEAM suffers from reduced localization accuracy as compared to sLASER, which may compromise the precision of the measurement. Also, the longer measurements times used with the STEAM sequence to partly compensate SNR loss, may have caused reduced stability. Additionally, a fitting procedure including 12 or more metabolite basis sets seems to more robustly display measured metabolite levels. It is known that omitting basis sets from metabolites that are indeed present in the tissue of interest leads to a systematic bias and potential overlap of the fitted metabolite resonances and thereby detects physiological and methodological variations less accurately (22, 23). This seems to be the case in a fitting procedure

that includes basis sets for only eight metabolites, for which we generally observed small within and between subjects variations, whereas fitting procedures including basis sets for 12 or 16 metabolites show larger variations within and between subjects.

Several limitations have to be considered when interpreting the results of this study. First, only eight subjects were examined. Although this was not enough to establish the reliability for the STEAM sequence, it was enough to establish the reliability of the sLASER sequence. This finding speaks in favor of the sLASER sequence. On the other hand, application of the STEAM sequence in clinical studies is easier since it does not require additional hardware modifications. To reach a short TE on the system we used, the sLASER required a dual transmit option. This may not be routinely available on all 7-T MR systems, and it also requires slightly more scan preparation, e.g., determination of the optimal

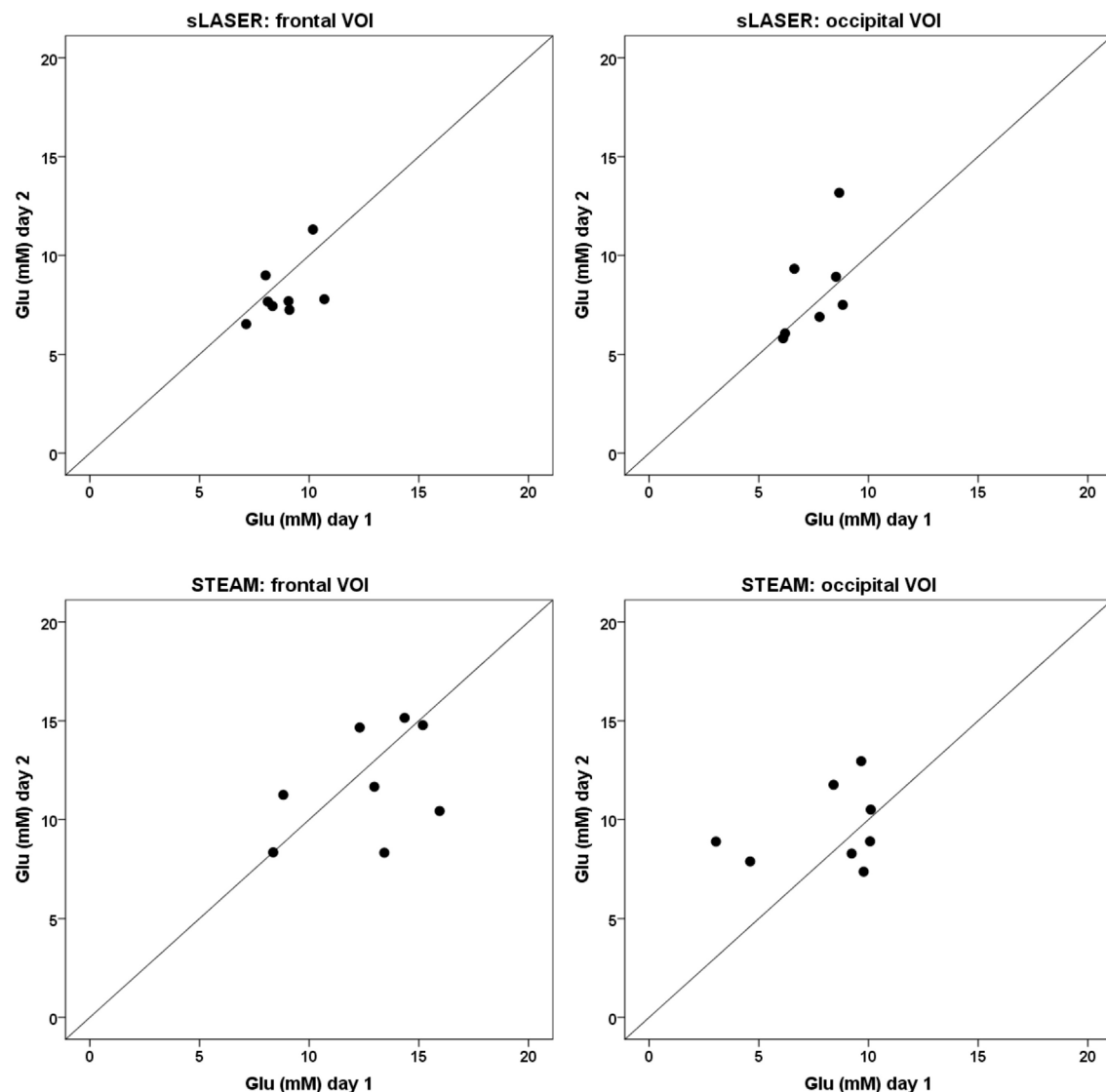


**FIGURE 5 |** Glutamate concentrations calculated with a 16-metabolite fit at day 1 (x-axis) and day 2 (y-axis). The line  $x = y$  represents a correlation of +1 between the two measurements. A point-spread along the line  $x = y$  represents detection of mainly physiological variation, a point-spread perpendicular to the line  $x = y$  represents detection of mainly methodological variation.

**TABLE 2 |** ICC's and *p*-values for measurement of glutamate concentrations, using semi-localized by adiabatic selective refocusing (sLaser) and stimulated echo acquisition mode (STEAM) in a frontal and occipital VOI, for three different fitting procedures.

	sLaser				STEAM			
	Frontal		Occipital		Frontal		Occipital	
	Intraclass correlations (ICC)	<i>p</i> -Value	ICC	<i>p</i> -Value	ICC	<i>p</i> -Value	ICC	<i>p</i> -Value
8-metabolite fit	0.77	0.04	0.28	0.35	0.17	0.41	-3.62	0.97
12-metabolite fit	0.65	0.09	0.61	0.14	0.58	0.14	0.42	0.24
16-metabolite fit	0.80	0.03	0.34	0.31	0.56	0.15	0.54	0.17

phase of the two input channels. If fully automated, however, this would only require several seconds.

A potential cause of variation between repeated measurements might be the manual positioning of the VOIs. Differences

in location may result in different contributions of GM, WM, and CSF, which may affect the measured metabolite levels (21). However, the ICC's of GM and WM content between the first and second measurement in the frontal (GM: ICC = 0.89,

**TABLE 3 | Glutamate concentrations (average  $\pm$  SD, in millimolars) at the first and second measurement, using semi-localized by adiabatic selective refocusing (sLASER) and stimulated echo acquisition mode (STEAM) in a frontal and occipital VOI, for three different fitting procedures.**

	sLASER				STEAM			
	Frontal		Occipital		Frontal		Occipital	
	Day 1	Day 2						
8-metabolite fit	8.7 $\pm$ 1.2	8.1 $\pm$ 1.2	7.3 $\pm$ 1.2	7.5 $\pm$ 1.8	8.6 $\pm$ 1.1	7.4 $\pm$ 1.3	5.6 $\pm$ 0.6	6.4 $\pm$ 0.6
12-metabolite fit	12.6 $\pm$ 1.7	11.5 $\pm$ 2.1	10.8 $\pm$ 1.7	12.1 $\pm$ 3.5	18.1 $\pm$ 4.0	16.9 $\pm$ 4.0	11.6 $\pm$ 3.9	13.7 $\pm$ 2.8
16-metabolite fit	13.6 $\pm$ 2.3	12.5 $\pm$ 2.5	11.2 $\pm$ 1.9	11.7 $\pm$ 2.1	19.8 $\pm$ 3.9	19.3 $\pm$ 5.1	12.9 $\pm$ 6.3	15.9 $\pm$ 2.4

$p < 0.01$ ; WM: ICC = 0.87,  $p < 0.01$ ) and the occipital voxel (GM: ICC = 0.69,  $p = 0.07$ ; WM: ICC = 0.67,  $p = 0.09$ ) indicate only small variations in positioning. Larger variations in positioning and thus slightly smaller ICC's for GM and WM content, could explain the fact that no significant ICC's for metabolite levels were found in the occipital region. Also, we corrected the measured metabolite levels for contribution of GM, WM, and CSF by tissue segmentation of the VOIs based on the T<sub>1</sub>-weighted image. While this corrects for the differences in water content and assumed absence of glutamate in CSF, it does not correct for differences in glutamate between GM and WM. However, it is not plausible that systematic variations in GM and WM content of the VOIs are causing high ICC's for glutamate concentrations, since we did not find significant correlations between glutamate concentrations and GM content, and including GM or WM fractions as a regressor in the analyses did not yield different results. *For completeness, the analysis was repeated on the uncorrected data (no correction for GM and WM fractions), but this did not change the nature of our findings.*

We conclude that the sLASER sequence can be successfully applied for glutamate measurements in the human brain at 7 T. MR spectra acquired at different time-points, and in a well-controlled population, are comparable and robust and the variance is mainly caused by physiological differences between subjects, since the methodological variation is reduced when using sLASER compared to STEAM. This is particularly beneficial when studying populations that are difficult to recruit, since sLASER requires a smaller sample size than STEAM to detect physiological differences between subjects.

## REFERENCES

- Javitt DC. Glutamate as a therapeutic target in psychiatric disorders. *Mol Psychiatry* (2004) 9(11):984–97. doi:10.1038/sj.mp.4001551
- Marsman A, Mandl RCW, van den Heuvel MP, Boer VO, Wijnen JP, Klomp DWJ, et al. Glutamate changes in healthy young adulthood. *Eur Neuropsychopharmacol* (2013) 23:1484–90. doi:10.1016/j.euroneuro.2012.11.003
- Tkac I, Andersen P, Adriany G, Merkle H, Ugurbil K, Gruetter R. In vivo 1H NMR spectroscopy of the human brain at 7 T. *Magn Reson Med* (2001) 46(3):451–6. doi:10.1002/mrm.1213
- Boer VO, van Lier AL, Hoogduin JM, Wijnen JP, Luijten PR, Klomp DW. 7-T (1) H MRS with adiabatic refocusing at short TE using radiofrequency focusing with a dual-channel volume transmit coil. *NMR Biomed* (2011) 24(9):1038–46. doi:10.1002/nbm.1641
- Van Vliet IM, Leroy H, Van Megen HJGM. *M.I.N.I. Plus: M.I.N.I. International Neuropsychiatric Interview*. Dutch version 5.0.0. (2000).
- Gruetter R. Automatic, localized in vivo adjustment of all first- and second-order shim coils. *Magn Reson Med* (1993) 29:804–11. doi:10.1002/mrm.1910290613
- Gruetter R, Boesch C. Fast, non-iterative shimming on spatially localized signals: in vivo analysis of the magnetic field along axes. *J Magn Reson* (1992) 96:323–34.
- Versluis MJ, Kan HE, van Buchem MA, Webb AG. Improved signal to noise in proton spectroscopy of the human calf muscle at 7 T using localized B1 calibration. *Magn Reson Med* (2010) 63(1):207–11. doi:10.1002/mrm.22195
- Waddell KW, Avison MJ, Joers JM, Gore JC. A practical guide to robust detection of GABA in human brain by J-difference spectroscopy at 3 T using a standard volume coil. *Magn Reson Imaging* (2007) 25:1032–8. doi:10.1016/j.mri.2006.11.026
- De Graaf RA. *NMR Processing Software for Spectroscopy, Imaging and Spectroscopic Imaging*. (1999).
- Govindaraju V, Young K, Maudsley AA. Proton NMR chemical shifts and coupling constants for brain metabolites. *NMR Biomed* (2000) 13(3):129–53. doi:10.1002/1099-1492(200005)13:3<129::AID-NBM619>3.3.CO;2-M
- Behar KL, Rothman DL, Spencer DD, Petroff OA. Analysis of macromolecule resonances in 1H NMR spectra of human brain. *Magn Reson Med* (1994) 32(3):294–302. doi:10.1002/mrm.1910320304

## ETHICS STATEMENT

This study was carried out in accordance with the recommendations of the institutional ethics board (METC) with written informed consent from all subjects. All subjects gave written informed consent in accordance with the Declaration of Helsinki. The protocol was approved by the institutional ethics board (METC).

## AUTHOR CONTRIBUTIONS

AM: involved in designing the experiment, acquired the data, performed the analysis of the results, and wrote the initial version of the manuscript. VB: involved in data acquisition and revising the manuscript. PL: involved in revising the manuscript. HH, DK, and RM: involved in designing the experiment, analysis of the results, and revising the manuscript.

## FUNDING

This research was funded by the Netherlands Organisation for Scientific Research (NWO) VIDI Grant 917-46-370 (to HH); and Utrecht University High Potential Grant (to HH).

## SUPPLEMENTARY MATERIAL

The Supplementary Material for this article can be found online at <http://journal.frontiersin.org/article/10.3389/fpsyg.2017.00060/full#supplementary-material>.

13. Marjanska M, Auerbach EJ, Valabregue R, Van de Moortele PF, Adriany G, Garwood M. Localized 1H NMR spectroscopy in different regions of human brain in vivo at 7 T: T2 relaxation times and concentrations of cerebral metabolites. *NMR Biomed* (2012) 25(2):332–9. doi:10.1002/nbm.1754
14. Marsman A, van den Heuvel MP, Klomp DWJ, Kahn RS, Luijten PR, Hulshoff Pol HE. Glutamate in schizophrenia: a focused review and meta-analysis of 1H-MRS studies. *Schizophr Bull* (2011) 39(1):120–9. doi:10.1093/schbul/sbr069
15. Bora E, Fornito A, Pantelis C, Yücel M. Gray matter abnormalities in major depressive disorder: a meta-analysis of voxel based morphometry studies. *J Affect Disord* (2012) 138(1–2):9–18. doi:10.1016/j.jad.2011.03.049
16. Bora E, Fornito A, Radua J, Walterfang M, Seal M, Wood SJ, et al. Neuroanatomical abnormalities in schizophrenia: a multimodal voxel-wise meta-analysis and meta-regression analysis. *Schizophr Res* (2011) 127(1–3):46–57. doi:10.1016/j.schres.2010.12.020
17. Arnone D, Cavanagh J, Gerber D, Lawrie SM, Ebmeier KP, McIntosh AM. Magnetic resonance imaging studies in bipolar disorder and schizophrenia: meta-analysis. *Br J Psychiatry* (2009) 195(3):194–201. doi:10.1192/bjp.bp.108.059717
18. Steen RG, Hamer RM, Lieberman JA. Measurement of brain metabolites by <sup>1</sup>H magnetic resonance spectroscopy in patients with schizophrenia: a systematic review and meta-analysis. *Neuropsychopharmacology* (2005) 30(11):1949–62. doi:10.1038/sj.npp.1300850
19. Saunders DE, Howe FA, Van den Boogaart A, Griffiths JR, Brown MM. Aging of the adult human brain: in vivo quantitation of metabolite content with proton magnetic resonance spectroscopy. *J Magn Reson Imaging* (1999) 9(5):711–6. doi:10.1002/(SICI)1522-2586(199905)9:5<711::AID-JMRI14>3.3.CO;2-V
20. Maudsley AA, Domenig C, Govind V, Darkazanli A, Studholme C, Arheart K, et al. Mapping of brain metabolite distributions by volumetric proton MR spectroscopic imaging (MRSI). *Magn Reson Med* (2009) 61(3):548–59. doi:10.1002/mrm.21875
21. Wijnen JB, van Asten JJ, Klomp DW, Sjoberg TE, Gribbestad IS, Scheenen TW, et al. Short echo time 1H MRSI of the human brain at 3T with adiabatic slice-selective refocusing pulses: reproducibility and variance in a dual center setting. *J Magn Reson Imaging* (2010) 31(1):61–70. doi:10.1002/jmri.21999
22. De Graaf RA. *Spectral Quantification. In Vivo NMR Spectroscopy*. 2nd ed. West Sussex: Wiley (2007). p. 445–77.
23. Hofmann L, Slotboom J, Jung B, Maloca P, Boesch C, Kreis R. Quantitative <sup>1</sup>H-magnetic resonance spectroscopy of human brain: influence of composition and parameterization of the basis set in linear combination model-fitting. *Magn Reson Med* (2002) 48(3):440–53. doi:10.1002/mrm.10246

**Conflict of Interest Statement:** The authors declare that the research was conducted in the absence of any commercial or financial relationships that could be construed as a potential conflict of interest.

Copyright © 2017 Marsman, Boer, Luijten, Hulshoff Pol, Klomp and Mandl. This is an open-access article distributed under the terms of the Creative Commons Attribution License (CC BY). The use, distribution or reproduction in other forums is permitted, provided the original author(s) or licensor are credited and that the original publication in this journal is cited, in accordance with accepted academic practice. No use, distribution or reproduction is permitted which does not comply with these terms.



# Functional Magnetic Resonance Spectroscopy: The “New” MRS for Cognitive Neuroscience and Psychiatry Research

Jeffrey A. Stanley<sup>1\*</sup> and Naftali Raz<sup>2,3,4</sup>

<sup>1</sup> Department of Psychiatry and Behavioral Neurosciences, School of Medicine, Wayne State University, Detroit, MI, United States, <sup>2</sup> Department of Psychology, Wayne State University, Detroit, MI, United States, <sup>3</sup> Institute of Gerontology, Wayne State University, Detroit, MI, United States, <sup>4</sup> Center for Lifespan Psychology, Max Planck Institute for Human Development, Berlin, Germany

## OPEN ACCESS

### Edited by:

Anouk Marsman,  
Danish Research Centre for Magnetic Resonance (DRCMR), Denmark

### Reviewed by:

Uzay Emir,  
Purdue University, United States  
Laura M. Rowland,  
University of Maryland, Baltimore,  
United States

### \*Correspondence:

Jeffrey A. Stanley  
jeffrey.stanley@wayne.edu

### Specialty section:

This article was submitted to  
Neuroimaging and Stimulation,  
a section of the journal  
Frontiers in Psychiatry

Received: 16 September 2017

Accepted: 23 February 2018

Published: 12 March 2018

### Citation:

Stanley JA and Raz N (2018)  
Functional Magnetic Resonance Spectroscopy: The “New” MRS for Cognitive Neuroscience and Psychiatry Research.  
*Front. Psychiatry* 9:76.  
doi: 10.3389/fpsy.2018.00076

Proton magnetic resonance spectroscopy (<sup>1</sup>H MRS) is a well-established technique for quantifying the brain regional biochemistry *in vivo*. In most studies, however, the <sup>1</sup>H MRS is acquired during rest with little to no constraint on behavior. Measured metabolite levels, therefore, reflect steady-state concentrations whose associations with behavior and cognition are unclear. With the recent advances in MR technology—higher-field MR systems, robust acquisition techniques and sophisticated quantification methods—<sup>1</sup>H MRS is now experiencing a resurgence. It is sensitive to task-related and pathology-relevant regional dynamic changes in neurotransmitters, including the most ubiquitous among them, glutamate. Moreover, high temporal resolution approaches allow tracking glutamate modulations at a time scale of under a minute during perceptual, motor, and cognitive tasks. The observed task-related changes in brain glutamate are consistent with new metabolic steady states reflecting the neural output driven by shifts in the local excitatory and inhibitory balance on local circuits. Unlike blood oxygen level differences-base functional MRI, this form of *in vivo* MRS, also known as functional MRS (<sup>1</sup>H fMRS), yields a more direct measure of behaviorally relevant neural activity and is considerably less sensitive to vascular changes. <sup>1</sup>H fMRS enables noninvasive investigations of task-related glutamate changes that are relevant to normal and impaired cognitive performance, and psychiatric disorders. By targeting brain glutamate, this approach taps into putative neural correlates of synaptic plasticity. This review provides a concise survey of recent technological advancements that lay the foundation for the successful use of <sup>1</sup>H fMRS in cognitive neuroscience and neuropsychiatry, including a review of seminal <sup>1</sup>H fMRS studies, and the discussion of biological significance of task-related changes in glutamate modulation. We conclude with a discussion of the promises, limitations, and outstanding challenges of this new tool in the armamentarium of cognitive neuroscience and psychiatry research.

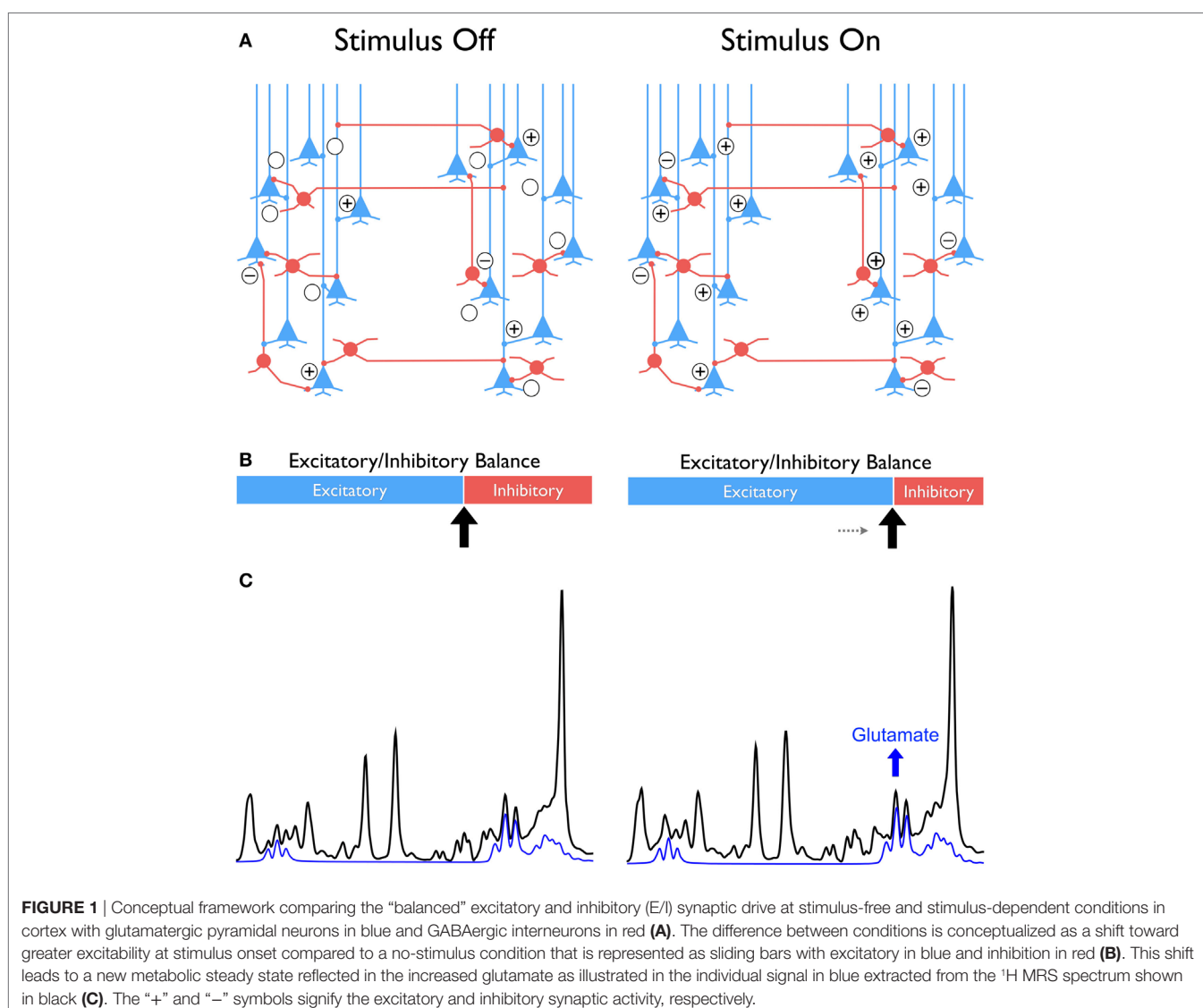
**Keywords:** MRI, <sup>1</sup>H MRS, glutamate, cognition, plasticity, schizophrenia, aging

## INTRODUCTION

Understanding of human behavior and cognition as products of their neural substrates depends on elucidation of the neural foundations of information processing. With the brain neurons comprising only about 10% of the gray matter bulk (1), allocating the lion share of brain energy supply to neurotransmission (2) suggests that deciphering the relationships between neurotransmitter dynamics and cognitive operations is key to success of that enterprise. Most (up to 80%) of cortical and hippocampal neurons are excitatory with glutamate as their dominant neurotransmitter, while the remaining 20% are inhibitory and have  $\gamma$ -aminobutyric acid (GABA) as their principal neurotransmitter (3). Therefore, understanding the dynamics of these neurotransmitter's release during cognitive operations is particularly important for elucidating the mechanisms of normal and abnormal behavior. Notably, cortical glutamatergic and GABAergic neurons do not act as separate excitatory and inhibitory entities but are highly integrated into neural ensembles within local

and long-range circuits, in which the “balanced” excitatory and inhibitory (E/I) synaptic drive serves as the functional basis of coherent networks (4–7).

In the cortex, sensory input, motor output as well as perceptual, and cognitive activity evoke temporally correlated excitation and inhibition at the synapses, thus shifting the dynamic equilibrium of E/I toward a (wide) range of excitation–inhibition patterns, as illustrated in **Figure 1**. These temporal fluctuations in E/I equilibrium eventually give rise to plasticity and synaptic reorganization by driving long-term potentiation and long-term depression, which are viewed as the neurophysiological bases of memory [see Tatti et al. (7) for a recent review]. Because of strong evidence implicating the glutamatergic and GABAergic neurotransmission in psychiatric disorders (8–10), and cognitive aging (11), it is plausible that a dysfunction in the ability to modulate E/I equilibrium of local circuits would affect function within broader networks in which complex cognition is implemented. Impairment of glutamatergic and GABAergic plasticity may underpin the development of symptomatology



that characterizes psychiatric disorders (7) and age-related cognitive dysfunction (12).

Whereas in animal models, a wide range of invasive methods of gauging glutamatergic and GABAergic activity is available, in humans, the opportunities are very limited. To date, the most popular approach to studying brain correlates and neural mechanisms of cognition *in vivo* harnesses blood oxygen level differences (BOLD) effect in an imaging paradigm known as functional MRI (fMRI). Although fMRI has good temporal and spatial properties, the BOLD signal is, however, an indirect measure of the neuronal response to stimuli. In addition, the BOLD signal cannot differentiate between inhibitory or excitatory neural activity. Moreover, the BOLD signal is influenced by major determinants of vascular tone such as dopamine (5) that depends on age (13) and are altered in psychiatric conditions (14). Given the role played by glutamate and GABA to shifting the E/I balance in cortical information processing, it is critically important to develop more specific means of *in vivo* evaluation of glutamatergic and GABAergic systems in intact, behaving humans. Such noninvasive approach to assessing regional brain concentration of these important neurotransmitters is indeed available. In the neuroimaging literature, magnetic resonance spectroscopy (MRS) is typically described as the only noninvasive technique that can reliably quantify *in vivo* concentration levels of key metabolites, including glutamate and  $\gamma$ -aminobutyric acid (GABA) (15).

<sup>1</sup>H MRS, with its ability to measure glutamate and GABA levels *in vivo* in localized cortical and subcortical areas, is well suited for testing hypotheses posited in the conceptual framework that emphasizes temporal dynamics of the E/I equilibrium (**Figure 1**). Unfortunately, the dynamic aspect of glutamate (and GABA) activity is lost in the majority of the extant <sup>1</sup>H MRS studies that are limited to measuring static neurotransmitter levels under “pseudo-” rest condition. In a typical <sup>1</sup>H MRS experiment, the data are acquired without any specific instructions or behavioral constraints aside from asking the participants to relax and keeping the head still during acquisition. Thus, the measured neurotransmitter levels are static and integrated over a time window spanning several minutes. This coarse temporal resolution and static task-free neurotransmitter assessment preclude the interpretation of findings with respect to neural correlates of synaptic plasticity. Although the <sup>1</sup>H fMRS literature is sparse, evidence shows surprising sensitivity in detecting dynamic changes in the magnitude and direction of task-related changes in glutamate and/or GABA steady-state levels in functionally relevant brain areas (**Table 1**). This ability to capture the temporal dynamics of glutamate and GABA *in vivo*, point at the emerging role of <sup>1</sup>H fMRS as the “new” <sup>1</sup>H MRS, with potentially exciting contributions to the understanding of neural mechanisms relevant to cognitive neuroscience and psychiatry research.

In this review, we focus on <sup>1</sup>H MRS findings pertaining to changes in glutamate with task in the context of <sup>1</sup>H fMRS [for a review on <sup>1</sup>H fMRS of GABA, see Duncan et al. (16)]. First, we describe the technological advancements in <sup>1</sup>H MRS that made characterization of the glutamate temporal dynamics with a temporal resolution under a min possible. Second, we survey the findings from seminal <sup>1</sup>H fMRS studies demonstrating task-related changes in glutamate (**Table 1**). Third, we discuss the

significance of observing changes in glutamate from the perspective of neurovascular and neurometabolic processes and evaluate the implication of the findings for understanding behaviorally relevant neural output driven by shifts in the E/I balance. Finally, we evaluate the pros and cons of the <sup>1</sup>H fMRS application in studying normal and impaired cognitive functions and outline the challenges ahead.

## TECHNICAL ADVANCEMENTS

The history of <sup>1</sup>H fMRS application to neuroimaging is to a large extent similar to that of the BOLD-based fMRI. Early <sup>1</sup>H fMRS studies conducted in the 1990s on 1.5 and 2.0 T MR systems demonstrated decreases in glucose and (transient) increases in lactate localized to the visual cortex during visual stimulation, and the findings were interpreted as reflecting a transient increase in non-oxidative glycolysis (17–21). However, the recent emergence of high-field MR systems including 3, 4, and 7 T (and higher), have dramatically rejuvenated the MRS field. The major advancement was the increase in the signal-to-noise ratio (S/N), which scales with the  $B_0$  field strength. The enhanced S/N at higher  $B_0$  field strengths can improve the spatial resolution of the localized single-voxel <sup>1</sup>H MRS to ~2–4 cm<sup>3</sup> as well as significantly increase the temporal resolution of the <sup>1</sup>H MRS acquisition to under a minute. In addition, the chemical-shift but not the scalar J-coupling of spin systems (e.g., CH<sub>2</sub>, CH<sub>3</sub>, etc.) scales with the  $B_0$  field strength, which in turn significantly improves in the spectral resolution or delineation of the coupled spin systems between molecules such as glutamate and glutamine (22). These advancements improve the overall accuracy and precision of quantifying glutamate and other metabolites (23, 24), minimized the partial volume effects that impeded voxel placement precision in functionally relevant brain areas, and more importantly, enabled capturing real-time task-induced changes in the brain biochemistry within the time scale of epochs often used in task-based fMRI paradigms.

In addition to the advantages of conducting high  $B_0$  field <sup>1</sup>H MRS, recent improvements in the acquisition technology enabled acquisition of highly reliable <sup>1</sup>H MRS data with minimal spectral artifacts (25). These new developments include the incorporation of  $B_1$ -insensitive adiabatic excitation and refocusing radio-frequency (RF) pulses (26) and customized phase- and amplitude-modulated RF pulses (27), which greatly improve the uniformity of the  $B_1$  field and edge profile of the defined MRS voxel. As a result, the ground was set for resurgent popularity of <sup>1</sup>H MRS acquisition sequences such as the Localization by Adiabatic SElective Refocusing (LASER) (26), semi-LASER (28), and SPIN ECho, full Intensity Acquired Localized (SPECIAL) (29). Adiabatic pulses are highly effective for outer volume suppression, which is a typical part of the acquisition sequence (30). Regarding the suppression of the water signal, the CHEmical Shift Selective (CHESS) RF pulses (31) has become common. However, optimized schemes using CHESS pulses such as the Variable Power and Optimized Relaxation delays (VAPOR) technique are robust and highly effective in suppressing the water signal and producing a cleaner spectral baseline (32).

Maximizing the homogeneity of the  $B_0$  magnetic field *via* shimming is critical for attaining optimal spectral resolution,

**TABLE 1** | Description of <sup>1</sup>H fMRS studies reporting task-related changes in glutamate.

Study	Sample size	Acquisition protocol	Task	Results	Comments
<b>Visual stimuli—visual cortex</b>					
Mangia et al. (41)	12 adults	<ul style="list-style-type: none"> <li>– 7 T</li> <li>– STEAM TE = 6ms</li> <li>– Midline visual cortex</li> <li>– 2 cm × 2.2 cm × 2 cm</li> </ul>	<ul style="list-style-type: none"> <li>– Radial red/black checkerboard covering the entire visual field (8 Hz)</li> <li>– Two protocols: (1) 2 short 5.3 min blocks interspersed by rest epochs and (2) 1 long 10.6 min block interspersed by rest epochs</li> </ul>	<ul style="list-style-type: none"> <li>– Increased glutamate (3%) during checkerboard vs rest</li> </ul>	<ul style="list-style-type: none"> <li>– The response of glutamate was delayed compared to Lac</li> <li>– The change in glutamate tended to decrease over time</li> </ul>
Lin et al. (42)	10 adults	<ul style="list-style-type: none"> <li>– 7 T</li> <li>– STEAM TE 15 ms</li> <li>– Midline visual cortex</li> <li>– 2 cm × 2 cm × 2 cm</li> </ul>	<ul style="list-style-type: none"> <li>– Visual stimulation included contrast-defined wedges, moving toward or away from the fixation cross and randomized</li> <li>– Two protocols: (1) 1 13.2 min block interspersed by rest epochs and (2) two 9.9 min blocks interspersed by rest epochs</li> </ul>	<ul style="list-style-type: none"> <li>– Increased glutamate (<math>2 \pm 1\%</math>) during single block vs rest</li> <li>– Increased glutamate (<math>3 \pm 1\%</math>) during the two blocks vs rest</li> </ul>	
Schaller et al. (43)	10 adults	<ul style="list-style-type: none"> <li>– 7 T</li> <li>– SPECIAL TE = 6 ms</li> <li>– Midline visual cortex</li> <li>– 2 cm × 2 cm × 2 cm</li> </ul>	<ul style="list-style-type: none"> <li>– Reversed black–gray checkerboard (9 Hz)</li> <li>– 2 blocks interspersed by rest epochs</li> </ul>	<ul style="list-style-type: none"> <li>– Increased glutamate (<math>4 \pm 1\%</math>) during stimulation vs rest</li> </ul>	
Bednářík et al. (44)	12 adults	<ul style="list-style-type: none"> <li>– 7 T</li> <li>– Semi-LASER TE = 26 ms</li> <li>– Midline visual cortex</li> <li>– 2 cm × 2 cm × 2 cm</li> </ul>	<ul style="list-style-type: none"> <li>– Red–black checkerboard (7.5 Hz)</li> <li>– 2 blocks interspersed by rest epochs</li> </ul>	<ul style="list-style-type: none"> <li>– Increased glutamate (~3%) during checkerboard vs rest</li> </ul>	
Apšvalka et al. (45)	19 young adults	<ul style="list-style-type: none"> <li>– 3 T</li> <li>– PRESS TE = 105 ms</li> <li>– Left lateral occipital cortex</li> <li>– 2 cm × 2 cm × 2 cm</li> </ul>	<ul style="list-style-type: none"> <li>– Three different task blocks: novel stimuli and two repeated (6 unique vs 4 unique) stimulus presentations interspersed with rest blocks</li> <li>– Presentation of novel/repeated black-line drawings representing real world objects for 700 ms</li> <li>– 4 runs of 8 task blocks per run</li> <li>– Each run, 4 novel and 4 repeated blocks</li> <li>– Each block 36 s in duration</li> </ul>	<ul style="list-style-type: none"> <li>– Increased glutamate (~12%) during novel presentations compared to both rest and repeated presentations</li> </ul>	
<b>Motor task—motor and somatosensory cortex</b>					
Schaller et al. (35)	11 adults	<ul style="list-style-type: none"> <li>– 7 T</li> <li>– SPECIAL TE = 12 ms</li> <li>– Left motor and somatosensory cortices</li> <li>– 1.7 cm × 2 cm × 1.7 cm</li> </ul>	<ul style="list-style-type: none"> <li>– Cued finger-to-thumb tapping task with both hands at a frequency of 3 Hz</li> <li>– 2 blocks interspersed by rest epochs</li> </ul>	<ul style="list-style-type: none"> <li>– Increased glutamate (<math>2 \pm 1\%</math>) during finger tapping vs rest</li> </ul>	
<b>Thermoregulation—anterior cingulate cortex (ACC) and insular cortex</b>					
Mullins et al. (47)	12 adults	<ul style="list-style-type: none"> <li>– 4 T</li> <li>– STEAM TE = 20 ms</li> <li>– Bilateral ACC</li> <li>– 2 cm × 2 cm × 2 cm</li> </ul>	<ul style="list-style-type: none"> <li>– Frozen compress (0–4°C) or sham pain was applied to the base of the left foot</li> <li>– 8:32 min task epoch preceded by a rest block and followed by two 8:32 min rest periods</li> </ul>	<ul style="list-style-type: none"> <li>– Increased glutamate (<math>9 \pm 6\%</math>) during pain condition vs rest condition</li> </ul>	
Gussew et al. (48)	6 adults	<ul style="list-style-type: none"> <li>– 3 T</li> <li>– PRESS TE = 30 ms</li> <li>– Left anterior insular cortex</li> <li>– 2.5 cm × 1 cm × 1 cm</li> </ul>	<ul style="list-style-type: none"> <li>– Heat stimuli were applied to the inner skin area of the left forearm</li> <li>– 2 blocks interspersed by rest epochs</li> </ul>	<ul style="list-style-type: none"> <li>– Increased glutamate (<math>18 \pm 8\%</math>) during heat vs rest</li> </ul>	

(Continued)

**TABLE 1** | Continued

<b>Study</b>	<b>Sample size</b>	<b>Acquisition protocol</b>	<b>Task</b>	<b>Results</b>	<b>Comments</b>
<b>Executive functions—dorsolateral prefrontal cortex (dlPFC)</b>					
Woodcock et al. (40)	16 young adults	<ul style="list-style-type: none"> <li>– 3 T</li> <li>– PRESS</li> <li>– TE = 23ms</li> <li>– left dlPFC</li> <li>– <math>1.5 \times 2.0 \times 1.5 \text{ cm}^3</math></li> </ul>	<ul style="list-style-type: none"> <li>– 2-back working memory task</li> <li>– 7 task blocks of 64 s each interspersed by 32 s rest epochs</li> </ul>	<ul style="list-style-type: none"> <li>– Increased glutamate (2.7%) during n-back vs fixation crosshair</li> </ul>	<ul style="list-style-type: none"> <li>– The control condition was a separate run fixating on a crosshair</li> </ul>
Lynn et al. (87)	16 young adults	<ul style="list-style-type: none"> <li>– 3 T</li> <li>– PRESS</li> <li>– TE = 23ms</li> <li>– left dlPFC</li> <li>– <math>1.5 \times 2.0 \times 1.5 \text{ cm}^3</math></li> </ul>	<ul style="list-style-type: none"> <li>– Four “non-task-active” conditions: relaxed eyes closed, passive visual fixation crosshair, visual flashing checkerboard, and a finger tapping task</li> <li>– Each task 3:28 min in duration</li> </ul>	<ul style="list-style-type: none"> <li>– Increased glutamate (4.7 and 3.2%) during flashing checkerboard and motor finger tapping conditions, respectively compared to visual fixation crosshair condition</li> <li>– Visual fixation crosshair and visual flashing checkerboard conditions produced the least variability in glutamate with CV's under 5%, which were both significantly lower compared to the eyes closed condition with a mean CV = 6.7%</li> </ul>	<ul style="list-style-type: none"> <li>– Conditions were chosen because the left dlPFC is not the dominant brain region engaged in these tasks</li> </ul>
<b>Learning and memory—hippocampus</b>					
Stanley et al. (36)		<ul style="list-style-type: none"> <li>– 3 T</li> <li>– PRESS TE = 23 ms</li> <li>– Right anterior hippocampus</li> <li>– <math>1.7 \text{ cm} \times 3.0 \text{ cm} \times 1.2 \text{ cm}</math></li> </ul>	<ul style="list-style-type: none"> <li>– Associative learning and memory task</li> <li>– Epochs of encoding (9 unique object–location pairs) and cued-retrieval (of those associated memoranda) and interspersed with rest epochs</li> <li>– 8 encoding-retrieval cycles were employed to allow learning to asymptote</li> </ul>	<ul style="list-style-type: none"> <li>– Increased glutamate (5.2 and 4.2%) during both encoding and retrieval, respectively</li> <li>– Applying a median split based on learning proficiency, fast learners showed increased during the early encoding trials, whereas slow learners showed increased glutamate in the later encoding trials</li> </ul>	<ul style="list-style-type: none"> <li>– Motor finger tapping task in response to a random visual stimulus was the control condition</li> </ul>
<b>Cognitive control—ACC</b>					
Taylor et al. (66)	7 adults	<ul style="list-style-type: none"> <li>– 7 T</li> <li>– STEAM TE = 10 ms</li> <li>– dACC</li> <li>– <math>2 \text{ cm} \times 2 \text{ cm} \times 2 \text{ cm}</math></li> </ul>	<ul style="list-style-type: none"> <li>– STROOP task with 4 conditions</li> <li>– One block flanked by rest epochs</li> </ul>	<ul style="list-style-type: none"> <li>– Increased glutamate (<math>2.6 \pm 1.0\%</math>) during STROOP vs rest</li> </ul>	<ul style="list-style-type: none"> <li>– Significance based on one-tailed <i>t</i>-test</li> </ul>
Taylor et al. (65)	16 controls; 16 major depressive disorder (MDD); 16 Schizo	<ul style="list-style-type: none"> <li>– 7 T</li> <li>– STEAM TE = 10 ms</li> <li>– dACC</li> <li>– <math>2 \text{ cm} \times 2 \text{ cm} \times 2 \text{ cm}</math></li> </ul>	<ul style="list-style-type: none"> <li>– STROOP task with four conditions</li> <li>– Two blocks interspersed with rest epochs</li> </ul>	<ul style="list-style-type: none"> <li>– Increased glutamate (3.2%) in controls during first STROOP vs rest</li> <li>– Decreased glutamate in MDD during second STROOP vs rest</li> </ul>	
<b>Visuospatial cognition—parietal and posterior cingulated cortices</b>					
Lindner et al. (68)	19 adults	<ul style="list-style-type: none"> <li>– 3 T</li> <li>– PRESS TE = 32 ms</li> <li>– Right or left border of parietal/occipital cortices</li> <li>– <math>1.5 \text{ cm} \times 1.5 \text{ cm} \times 1.5 \text{ cm}</math></li> </ul>	<ul style="list-style-type: none"> <li>– Visuospatial attention task</li> <li>– Button press in response to the tilt orientation of the grating that appeared on the side of the screen cued by an arrow</li> <li>– 3 conditions (ipsi, contra, and control) randomized</li> <li>– 3 blocks interspersed with rest epochs</li> </ul>	<ul style="list-style-type: none"> <li>– No trial condition effect on glutamate</li> </ul>	

especially in brain areas with extreme  $B_0$  susceptibility (e.g., the hippocampus or orbital frontal cortex). Techniques such as the Fast Automatic Shim Technique using Echo-planar Signal readouT for Mapping Along Projections (FASTESTMAP) (33) and its predecessor, FASTMAP (34), have brought significant improvement in the spectral quality, including increased S/N (35, 36). These acquisition sequences are readily available by most manufacturers on current MR systems and should be utilized [for review see Duarte et al. (37)].

Finally, reliable voxel placement across subjects and within subjects over time is an often-overlooked aspect of single-voxel <sup>1</sup>H MRS acquisition protocols (25). Unreliable voxel placement adds error variance to the outcome measurements by increasing the variability of the partial volume effect. Recently introduced automated approaches have demonstrated significant improvements in consistency of voxels placement, between subjects, even in anatomical brain areas, in which partial voluming is difficult to avoid, such as the dorsolateral prefrontal cortex (dlPFC) (38, 39). For example, Woodcock et al. (40) reported an improvement from 68% voxel overlap with manual placement to 98% overlap using an automated approach. In all, these major technological advancements provide the necessary tools to fully exploit the characterization of the task-related temporal dynamics of glutamate and GABA with <sup>1</sup>H fMRS, which is fueling the resurgence of *in vivo* <sup>1</sup>H fMRS as a powerful tool for cognitive neuroscience and psychiatry research.

## EVIDENCE OF TASK-INDUCED GLUTAMATE MODULATION

### Visual Stimuli—Visual Cortex

As in BOLD-based fMRI, the visual cortex is one of the most studied brain regions with <sup>1</sup>H fMRS (Table 1). Studies of response to flashing checkerboard stimuli compared to a non-visual stimulation (i.e., a blank screen) have shown a consistent stimulus-bound increases of ~2–4% in steady-state glutamate levels (41–44). The magnitude of the average task-related increase in glutamate may be less consistent as it depends on task duration and cognitive processing demands. Shorter stimulus blocks were associated with a 3% increase in glutamate, compared to 2% for longer ones (42). With a temporal resolution of ~1 min, a delay in the increased stimulus-dependent modulation of glutamate was consistently observed, whereas smaller and earlier elevations in lactate were noted (41, 43, 44). The mechanism of these two temporal effects is not fully understood. Finally, sensitivity of glutamate levels to stimulus characteristics was illustrated by a <sup>1</sup>H fMRS study that found an almost 12% increase within the left occipital cortex during passive viewing of novel pictures compared to a (pseudo-) rest control condition, but no change during repeated picture presentation (45).

### Motor Task—Motor and Somatosensory Cortex

To date, only a single <sup>1</sup>H fMRS study, at 7 T, investigated neurochemical changes in the motor cortex during a motor task (35). As expected, a periodic cued finger-to-thumb tapping induced a significant (2%) glutamate increase in the motor/somatosensory

cortices relative to a non-tapping “rest” condition (Table 1). In that study, the <sup>1</sup>H fMRS voxel was co-localized with BOLD fMRI activation. Thus, task-related changes in glutamate can be detected in other functionally relevant cortical areas besides the visual cortex and can be used in investigating interesting research questions pertaining to neural activity during implicit vs explicit motor learning or periodic vs randomly cued stimuli (46).

### Thermoregulation and Pain Perception—Anterior Cingulate Cortex (ACC) and Insular Cortex

Motivated by the involvement of the ACC in thermal sensory responses, Mullins et al. (47) investigated glutamate response to a 10 min cold-pressor stimulation of the foot compared to the baseline rest without the cold exposure. They observed a substantial (9.3%) condition-related increase in glutamate within the ACC. With acute heat exposure, Gussew et al. (48) reported an even greater, 18%, glutamate increase in the anterior insular cortex. The manipulation involved acute 5 s cycles of heat exposure to the forearm compared to the no heat exposure condition. These findings lay the foundation of further investigation of the brain’s thermoregulatory system and its relationship to temperature perception with greater temporal resolution, made possible by current improvements in <sup>1</sup>H MRS.

### Working Memory (WM)—dlPFC

The construct of WM refers to the ability to hold information in memory for a duration of a few seconds while manipulating this information “on-line” in order to carry out a complex task (49). In primates, the dlPFC has been proposed as the central neural substrate of WM (50). Neuroimaging studies using PET and fMRI have confirmed the importance of the dlPFC, but also have implicated additional brain regions, such as the inferior parietal lobule and cerebellum (51, 52). In a recent <sup>1</sup>H fMRS study with a single-voxel placement in left dlPFC, a significant 2.7% increase in glutamate was observed during a standard 2-back WM task compared to a continuous visual crosshair fixation in healthy young adults (Table 1) (40). The elevation in dlPFC glutamate observed with a temporal resolution of 32 s is consistent with the engagement of that region in WM processing that has been revealed by task-based BOLD fMRI studies. However, increased glutamate was more pronounced during the first-half compared to the second-half of the 64 s block. This suggests a temporal variation in the dlPFC engagement during WM task. This temporal effect has not been reported in fMRI studies using the N-back WM paradigm and warrants further investigation to determine whether the disengagement over time is related to WM proficiency. In all, the observed temporal dynamics of WM-related modulation of dlPFC glutamate provides a solid basis for new means of evaluating the effects of cognitive intervention, pharmacological therapies, or manipulation of the physiological (e.g., stress-provoking) conditions.

### Learning and Memory—Hippocampus

Glutamate plays a key role in learning and memory *via* its activity in the frontal and hippocampal circuits. The hippocampus is particularly rich in glutamatergic neurons, and memory

consolidation in the hippocampus depends on synaptic plasticity mediated by glutamatergic N-methyl-D-aspartate (NMDA) receptors (53, 54). In addition, firing rate of hippocampal neurons is associated with acquisition of new associative memories (55). Therefore, it is plausible that memory processing would be linked to increased modulation of hippocampal glutamate, presumably driven by increased activity at NMDA receptors. This hypothesis was tested by Stanley et al. (36). During performance of an associative learning task with object–location pairs, healthy adults displayed, as expected, unique temporal dynamics of glutamate modulation in the right hippocampus (**Table 1**). In this <sup>1</sup>H fMRS application with a 54 s temporal resolution, the epochs of memory consolidation and retrieval were clearly differentiated by the temporal pattern of glutamate modulation. Moreover, the temporal dynamics of glutamate modulation were associated with learning proficiency: fast learners demonstrated up to 11% increase in glutamate during the early trials, whereas a significant but smaller and later increase of 8% was observed in slow learners. These results are in accord with the notion of altered glutamatergic neuroplasticity as the central mediator of learning and memory. The observed link between memory performance and glutamatergic system activity is particularly important given the proposed role of glutamatergic dysfunction as the core phenomenon in cognitive aging, age-related neurodegenerative disorders such as Alzheimer's disease (AD), and severe psychiatric conditions such as schizophrenia. Structural changes in the hippocampus and its subfields, especially CA1, which is enriched in glutamatergic neurons, have been observed in the course of cognitive aging and AD (56–59). Although the mechanisms of these changes remain unclear, regional gray matter shrinkage observed on MRI is likely to reflect reduction of neuropil, to which dendritic arborization and dendritic spines contribute a significant volume fraction (60). Dendritic spine density is highly plastic and is driven by changes in Ca<sup>2+</sup> flux modulated by glutamatergic activity (61). It is plausible to assume that impairment in glutamate modulation may eventually result in reduced dendritic plasticity and contribute to regional neuropil shrinkage. Therefore, impairment of task-related glutamatergic modulation may provide a very early marker for impending cognitive dysfunction and a valuable instrument of monitoring response to interventions that are aimed at mitigating the targeted cognitive declines.

## Cognitive Control—ACC

The ACC plays a key role in multiple higher cognitive processes including monitoring and evaluating conflict in information processing (62, 63). The Stroop task, which requires naming the color of displayed words when the name of the color matches the color of the displayed word (congruent trials) and when the color does not match the color of the displayed word (incongruent trials), is commonly used to assess conflict-monitoring engagement. BOLD fMRI studies using the Stroop task have consistently shown increased activation in the dorsal ACC related to trials of high conflict and with low top-down control (64). Based on this premise, Taylor et al. (65) investigated whether the Stroop task can induce a change in glutamate in the dorsal ACC of healthy adults using <sup>1</sup>H fMRS at 7 T (**Table 1**). Compared to the rest condition, a 2.6% increase in glutamate was reported

during the Stroop task, which included a mixture of congruent and incongruent conditions as well as trials with words only (no color) and color only (no words). However, differences in dorsal ACC glutamate modulation between trial conditions within the Stroop were not reported.

In another study using the similar Stroop task with <sup>1</sup>H fMRS at 7 T, Taylor et al. (66) extended the investigation to individuals with major depressive disorder (MDD) and schizophrenia. The observation of increased glutamate level in the dorsal ACC during the Stroop task compared to rest was replicated in healthy adults. However, no significant change in glutamate was observed in individuals with schizophrenia, while participants with MDD demonstrated decreased glutamate in the dorsal ACC during the task compared to rest. The non-significant change in glutamate with task in the participants with schizophrenia appears consistent with decreased BOLD fMRI activation during Stroop in schizophrenia (67). Interestingly, the lower glutamate in the dorsal ACC during Stroop in MDD may reflect a shift in the E/I balance toward decreased excitability that is potentially driven by an increase in the inhibitory drive (see **Figure 1** and below for further discussion).

## Visuospatial Cognition—Parietal and Posterior Cingulate Cortices

Tasks involving the visuospatial attention and memory system were recently investigated using <sup>1</sup>H fMRS at 3 T (**Table 1**). In healthy individuals, a non-significant modulation of glutamate was observed in the parietal–occipital cortex during a visuospatial attention task compared to the control condition (68). In another study, no significant task-related glutamate modulation was observed in the parietal–posterior cingulate cortex of healthy adults, patients with AD and individuals with amnestic mild cognitive impairment who performed a face-name associative memory task compared to the rest control condition (69). In both studies, details on the variability of the glutamate measurements were omitted and, therefore, it remains unclear whether the method afforded detection of a task-related change in glutamate of the order of 10% or less. It may be possible that the selected tasks were not at the level of difficulty that produced significant variations in glutamate level or that dynamics of glutamate are inherently weaker in the examined locations compared to the hippocampus and prefrontal cortex. Also, the lack of specific behavioral constraints during the rest condition might have increased variability in glutamate within brain areas that show BOLD fMRI activation under rest. Therefore, rest, under these circumstances, may represent a nonspecific, yet, not truly task-free condition and thus a suboptimal choice as a control comparison. These remain among multiple questions to be addressed in the further development of the method.

## BIOLOGICAL SIGNIFICANCE OF CHARACTERIZING GLUTAMATE MODULATION

The observed dynamic changes in glutamate levels during perceptual, motor, and cognitive tasks may open a new window into

neural bases of normal and abnormal cognition and behavior. To accomplish that goal, the apparent brain changes in this key neurotransmitter must be linked to cellular and molecular processes that occur in the brain.

Neural activity generated in response to physiological stimuli triggers changes in many complex neurovascular and neuro-metabolic processes, including increased cerebral blood flow, glycolysis ( $\text{CMR}_{\text{Glc}}$ ), and oxidative metabolism ( $\text{CMR}_{\text{O}_2}$ ), as well as synthesis of neurotransmitters (4, 5, 70–72)—all of which depend on significant increase in energy consumption. The temporal and spatial characteristics of these processes are not fully understood (4). Most notably, there is a mismatch (i.e., ~44 vs ~30%, respectively) between glucose utilization (non-oxidative  $\text{CMR}_{\text{Glc}}$ ) and oxygen consumption ( $\text{CMR}_{\text{O}_2}$ ) in response to physiological stimuli (73, 74). Fox et al. (75) were the first to report this mismatch, which sparked the interest and focus of early <sup>1</sup>H fMRS studies from the 1990s, as noted above (17–19, 21). However, more recent high-field <sup>1</sup>H fMRS studies provided compelling evidence that the mismatch of  $\Delta\text{CMR}_{\text{Glc}} > \Delta\text{CMR}_{\text{O}_2}$  is short-lived. It is necessary only for facilitating the transition to a new metabolic steady state following the onset of a physiological stimulus. It is this transitional change that is believed to be reflected by the dynamic changes of glutamate observed on <sup>1</sup>H fMRS (35, 44, 71).

This transition between metabolic steady states is primarily driven by oxidative metabolism (71) is consistent with recalibration of excitatory and inhibitory activity balance in local circuits, and establishing an E/I equilibrium that underpins a new functional state of the brain (Figure 1) (4, 6, 7). At the synaptic level, following the release of glutamate, excess of the neurotransmitter is taken up by surrounding astrocytes and is subsequently converted, predominantly to glutamine, with the help of glutamine synthetase. Glutamine is then released and taken up by the presynaptic neuron where it is converted into glutamate by mitochondrial glutaminase, to complete the glutamate–glutamine cycle (76). A near 1:1 relationship between neuronal glucose oxidation and the glutamate–glutamine cycling (70, 77, 78) implies that the metabolic and neurotransmitter pools of glutamate, as typically viewed in the <sup>1</sup>H MRS literature (79, 80), are tightly coupled and hence, indistinguishable by <sup>1</sup>H MRS (70). Moreover, in astrocytes, the oxidative pathway regulates the glutamate turnover (synthesis and degradation) and the high-energy phosphate, adenosine triphosphate, can be generated to supply the demand of increased synthesis without the need of glycolysis (81). This association between increased excitatory synaptic transmission and increased synthesis of exogenous glutamate provides a cellular basis for meaningful interpretation of glutamate measures obtained from <sup>1</sup>H fMRS.

Translating this relationship to the macro-circuit level implies that glutamate levels and changes therein that are observed in a single-voxel by <sup>1</sup>H fMRS reflect the net cortical output driven by the excitation and inhibition balance on local circuits. The implication is that a net increase in synaptic excitability is reflected at the cortical (macro-circuit) level as a relative increase in glutamate, which is observed on the signal produced by <sup>1</sup>H fMRS (Figure 1) (6, 7). Notably, an opposite shift in the E/I balance on local circuits increases the inhibitory drive and consequently,

decreases the net excitability, which is reflected in a relatively lower glutamate level registered on <sup>1</sup>H fMRS. The salient point of this interpretation is that <sup>1</sup>H fMRS is not simply indicating an “ON” or “OFF” brain response to stimulation but can reflect a stimulus-induced change in glutamate that reflects new metabolic steady states driven by relative shifts in the E/I equilibrium (Figure 1). Because cellular glutamate changes are tightly linked to synaptic plasticity (82), the apparent glutamate alterations observed on a macro level are likely to reflect experience-related plasticity as well. The implications of using <sup>1</sup>H fMRS as a proxy of cellular process that are unobservable *in vivo* are far reaching. Further development and refinement of the method bodes well for the fields, in which the role of glutamate in core phenomena of behavior, cognition, and psychopathology has been established through the use of animal models (83). Fulfillment of these promises, however, hinges on resolving several key issues in methodology and interpretation.

## THE PROS AND CONS OF <sup>1</sup>H fMRS

The key advantage of <sup>1</sup>H fMRS over the staple of cognitive neuroscience, BOLD-based fMRI, is that task-related changes in glutamate can be traced directly to established metabolic processes, and are not mediated by neurovascular effects. This relative directness of the method bypasses neurovascular mediators that may be affected by significant alterations of the vascular system and impairment of its regulation. Moreover, <sup>1</sup>H fMRS is a quantitative method that can measure not only the magnitude of change in glutamate but its basal “non-task-active” steady-state level, which is not the case for fMRI. This makes the method particularly suitable for studying the neural basis of cognitive declines in older adults and persons with age-related neurodegenerative disorders, in whom vascular risk factors are highly prevalent and cognitively relevant (56). This relative directness of <sup>1</sup>H fMRS is a feature that may significantly advance the understanding of brain dynamics underlying normal and abnormal cognition. To fulfill this promise, several key issues need to be addressed.

One unresolved concern is that as several groups have pointed out, there is evidence of a BOLD  $T_2^*$  effect on the spectral peaks including glutamate during task compared to the control condition. This  $T_2^*$  contribution narrows spectral linewidths by about 0.2–0.3 Hz in the visual cortex at 4 T, 0.5 Hz in the visual cortex at 7 T, and 0.25 Hz in the motor cortex at 7 T on task-related spectra (35, 41, 43, 44, 84, 85). This BOLD-linked confound, however, is yet to be reported at 3 T. In theory, the spectral fitting method such as LCModel (86) should account for changes in the spectral linewidth without influencing the accuracy of the metabolite quantification. Nonetheless, Mangia et al. (85) reported a non-significant reduction in glutamate levels with increasing spectral linewidth, which potentially suggests a bias on LCModel fitting. As a result, applying a linewidth broadening to spectra acquired during task to ensure linewidths are matched across all spectra has become a common practice as part of the post-processing for 7 T <sup>1</sup>H fMRS studies (35, 41, 43, 44, 85).

The magnitude of task-related change in glutamate levels vary considerably across the extant reports (Table 1), from as low as 2% up to 18%, and the reasons for such variability are

unclear. This wide range may reflect multiple methodological variations among studies including sample size, acquisition protocol, and the differential accuracy and precision between field strengths (e.g., 3 vs. 7 T). Also, the participants' characteristics and properties of the task may play a role in adding variability to the measured magnitude of the observed change. In most extant studies, the comparison condition was either a pseudo-rest state (i.e., passive state with no specific instructions), routine motor activity, or visual fixation on a stimulus without specific task-related instructions. The purpose of the control condition is to assess a steady state level of glutamate to be contrasted with those that are associated with task activity. For example, in the <sup>1</sup>H fMRS study of the hippocampus by Stanley et al. (36), the control condition paradigm included a cued finger to thumb tapping task due to its strong attention and motor processing, without any learning or memory components. Likewise, the dlPFC <sup>1</sup>H fMRS study by Woodcock et al. (40) incorporated a visual fixation crosshair condition as the baseline control condition, again, to minimize any potential dlPFC engagement during the control condition. Moreover, Lynn et al. (87) demonstrated differences in steady-state levels of glutamate as well as variability of glutamate in the left dlPFC across different conditions where the primary functional specialization of the dlPFC was not associated to these conditions (e.g., relaxed with eyes closed, visual fixation crosshair, visual flashing checkerboard, and motor finger tapping). The visual fixation crosshair condition demonstrated the lowest and less variable glutamate over the acquisition period compared to the relaxed eyes closed condition. The latter is consistent with studies reporting greater variability in glutamate during rest epochs compared to task (44, 88). Also, the steady-state glutamate level was significantly higher during the visual flashing checkerboard compared to the visual fixation crosshair condition. This is surprising considering that the left dlPFC is not the primary brain area for visual stimuli but is involved in multiple cognitive operations including deployment and maintenance of attention (89–92). We surmise that substantial variability in glutamate levels over time occurs during conditions in which behavior is poorly constrained (e.g., pseudo-resting state), and that better-defined and constrained non-cognitive control tasks such as visual fixation or finger tapping, are a better choice for baseline condition for frontal areas of interest. This hypothesis merits further empirical testing.

To make an *in vivo* method truly useful in investigating task-related changes it is imperative to establish high reliability and temporal stability of task-related glutamate measures. No such evidence is currently available for <sup>1</sup>H fMRS, and reliability studies are urgently needed.

Because cognitive activity occurs in a wide range of time windows and calls for multiple interacting brain circuits, not every task may be equally suitable for investigation with <sup>1</sup>H fMRS. Investigation of task properties and relevant brain locations that maximize the validity of <sup>1</sup>H fMRS findings is necessary for optimization of the <sup>1</sup>H fMRS application to investigating complex cognitive and psychiatric phenomena. Of critical importance is leveraging <sup>1</sup>H fMRS animal studies that can use more sensitive methods that are available for human

studies and are, therefore, critically important for validation of the method (93–96). It is important, however, to apply these methods not only with precision and degree of invasive control that are available in animal models but also with parameters that are equivalent to those that are suitable for humans. Such *translational harmonization* of methods is critically important in the understanding of task-related glutamate changes observed in human subjects.

Finally, <sup>1</sup>H fMRS is still a project in progress. The one aspect of the method that significantly improved over the years is the temporal resolution of acquiring the glutamate signal, which has been brought well under a minute (40). The advantage of high temporal resolution is the possibility of investigating temporal course of glutamate change within relatively short-lived stages of cognitive processing (96), and gauging the course of modulation within a task block (36, 40). However, it may take ~1–2 min for glutamate to reach its maximum level following stimulus onset (35, 41, 43). This may reflect the time needed for the synaptic reorganization process, shifting the E/I balance in the local circuits, and establishing the new steady state of glutamate. On the other hand, a relatively rapid change in glutamate within the dlPFC during the WM task has been reported. Glutamate surge was greater during the first half of each 64 s block than the second one (40). Thus, examining the patterns of glutamate modulation as a function of various time scales is as important as refining temporal resolution of the method.

## CONCLUSION

<sup>1</sup>H fMRS is an exciting and promising technique that can offer important insights into the neurochemicals underpinnings of cognition and their temporal dimensions. In this review, we summarize preliminary but compelling evidence demonstrating the ability of <sup>1</sup>H fMRS to detect changes in glutamate during various perceptual, motor, and cognitive tasks. Moreover, the method can detect changes in glutamate modulation that are induced by manipulations that affect cognitive performance. It is highly plausible that these 2–18% task-related changes in glutamate reflect transitions to new metabolic steady states driven by relative shifts in the E/I equilibrium through synaptic plasticity. Within this conceptual framework, <sup>1</sup>H fMRS provides a sensitive tool for investigating the neural basis of cognitive operations that are directly relevant to specific deficits in psychiatric disorders or neurodegenerative diseases associated with advanced age.

## AUTHOR CONTRIBUTIONS

Both authors contributed to the writing of the manuscript.

## FUNDING

This work was supported by NIMH grant R01 MH111177 (PI: JS) and NIA grant R01 011230 (PI: NR) as well as by the Lycaki-Young Funds from the State of Michigan.

## REFERENCES

- Kassem MS, Lagopoulos J, Stait-Gardner T, Price WS, Chohan TW, Arnold JC, et al. Stress-induced grey matter loss determined by MRI is primarily due to loss of dendrites and their synapses. *Mol Neurobiol* (2013) 47:645–61. doi:10.1007/s12035-012-8365-7
- Attwell D, Laughlin SB. An energy budget for signaling in the grey matter of the brain. *J Cereb Blood Flow Metab* (2001) 21:1133–45. doi:10.1097/00004647-200110000-00001
- Somogyi P, Tamás G, Luján R, Buhl EH. Salient features of synaptic organisation in the cerebral cortex. *Brain Res Brain Res Rev* (1998) 26:113–35. doi:10.1016/S0165-0173(97)00061-1
- Isaacson JS, Scanziani M. How inhibition shapes cortical activity. *Neuron* (2011) 72:231–43. doi:10.1016/j.neuron.2011.09.027
- Lauritzen M, Mathiesen C, Schaefer K, Thomsen KJ. Neuronal inhibition and excitation, and the dichotomic control of brain hemodynamic and oxygen responses. *Neuroimage* (2012) 62:1040–50. doi:10.1016/j.neuroimage.2012.01.040
- Maffei A. Fifty shades of inhibition. *Curr Opin Neurobiol* (2017) 43:43–7. doi:10.1016/j.conb.2016.12.003
- Tatti R, Haley MS, Swanson OK, Tselha T, Maffei A. Neurophysiology and regulation of the balance between excitation and inhibition in neocortical circuits. *Biol Psychiatry* (2017) 81:821–31. doi:10.1016/j.biopsych.2016.09.017
- Marsman A, van den Heuvel MP, Klomp DW, Kahn RS, Luijten PR, Hulshoff Pol HE. Glutamate in schizophrenia: a focused review and meta-analysis of <sup>1</sup>H-MRS studies. *Schizophr Bull* (2013) 39:120–9. doi:10.1093/schbul/sbr069
- Lewis DA. Inhibitory neurons in human cortical circuits: substrate for cognitive dysfunction in schizophrenia. *Curr Opin Neurobiol* (2014) 26:22–6. doi:10.1016/j.conb.2013.11.003
- Murrough JW, Abdallah CG, Mathew SJ. Targeting glutamate signalling in depression: progress and prospects. *Nat Rev Drug Discov* (2017) 16:472–86. doi:10.1038/nrd.2017.16
- Pereira JB, Valls-Pedret C, Ros E, Palacios E, Falcon C, Bargallo N, et al. Regional vulnerability of hippocampal subfields to aging measured by structural and diffusion MRI. *Hippocampus* (2014) 24:403–14. doi:10.1002/hipo.22234
- Dickstein DL, Weaver CM, Luebke JI, Hof PR. Dendritic spine changes associated with normal aging. *Neuroscience* (2013) 251:21–32. doi:10.1016/j.neuroscience.2012.09.077
- Backman L, Lindenberger U, Li SC, Nyberg L. Linking cognitive aging to alterations in dopamine neurotransmitter functioning: recent data and future avenues. *Neurosci Biobehav Rev* (2010) 34:670–7. doi:10.1016/j.neubiorev.2009.12.008
- Grace AA. Disruption of cortical-limbic interaction as a substrate for comorbidity. *Neurotox Res* (2006) 10:93–101. doi:10.1007/BF03033238
- Stanley JA. In vivo magnetic resonance spectroscopy and its application to neuropsychiatric disorders. *Can J Psychiatry* (2002) 47:315–26. doi:10.1177/070674370204700402
- Duncan NW, Wiebking C, Northoff G. Associations of regional GABA and glutamate with intrinsic and extrinsic neural activity in humans – a review of multimodal imaging studies. *Neurosci Biobehav Rev* (2014) 47:36–52. doi:10.1016/j.neubiorev.2014.07.016
- Prichard J, Rothman D, Novotny E, Petroff O, Kuwabara T, Avison M, et al. Lactate rise detected by <sup>1</sup>H NMR in human visual cortex during physiologic stimulation. *Proc Natl Acad Sci U S A* (1991) 88:5829–31. doi:10.1073/pnas.88.13.5829
- Merboldt KD, Bruhn H, Hänicke W, Michaelis T, Frahm J. Decrease of glucose in the human visual cortex during photic stimulation. *Magn Reson Med* (1992) 25:187–94. doi:10.1002/mrm.1910250119
- Sappey-Marinier D, Calabrese G, Fein G, Hugg JW, Biggins C, Weiner MW. Effect of photic stimulation on human visual cortex lactate and phosphates using <sup>1</sup>H and <sup>31</sup>P magnetic resonance spectroscopy. *J Cereb Blood Flow Metab* (1992) 12:584–92. doi:10.1038/jcbfm.1992.82
- Stanley JA, Bartha R, Drost DJ, Williamson PC. Comparison of metabolite levels due to long and short motor cortex activation using <sup>1</sup>H MR spectroscopy. *Proceedings of the 2nd Annual Meeting of the Society of Magnetic Resonance*. Berkeley, CA: SMR (1994). 678 p.
- Frahm J, Krüger G, Merboldt KD, Kleinschmidt A. Dynamic uncoupling and recoupling of perfusion and oxidative metabolism during focal brain activation in man. *Magn Reson Med* (1996) 35:143–8. doi:10.1002/mrm.1910350202
- Tkac I, Andersen P, Adriany G, Merkle H, Ugurbil K, Gruetter R. In vivo <sup>1</sup>H NMR spectroscopy of the human brain at 7 T. *Magn Reson Med* (2001) 46:451–6. doi:10.1002/mrm.1213
- Yang S, Hu J, Kou Z, Yang Y. Spectral simplification for resolved glutamate and glutamine measurement using a standard STEAM sequence with optimized timing parameters at 3, 4, 4.7, 7, and 9.4T. *Magn Reson Med* (2008) 59:236–44. doi:10.1002/mrm.21463
- Pradhan S, Bonekamp S, Gillen JS, Rowland LM, Wittenburg SA, Edden RAE, et al. Comparison of single voxel brain MRS AT 3T and 7T using 32-channel head coils. *Magn Reson Imaging* (2015) 33:1013–8. doi:10.1016/j.mri.2015.06.003
- Kreis R. Issues of spectral quality in clinical <sup>1</sup>H-magnetic resonance spectroscopy and a gallery of artifacts. *NMR Biomed* (2004) 17:361–81. doi:10.1002/nbm.891
- Garwood M, DelaBarre L. The return of the frequency sweep: designing adiabatic pulses for contemporary NMR. *J Magn Reson* (2001) 153:155–77. doi:10.1006/jmre.2001.2340
- Le Roux P, Gilles RJ, McKinnon GC, Carlier PG. Optimized outer volume suppression for single-shot fast spin-echo cardiac imaging. *J Magn Reson Imaging* (1998) 8:1022–32. doi:10.1002/jmri.1880080505
- Scheenen TWJ, Klomp DWJ, Wijnen JP, Heerschap A. Short echo time <sup>1</sup>H-MRSI of the human brain at 3T with minimal chemical shift displacement errors using adiabatic refocusing pulses. *Magn Reson Med* (2008) 59:1–6. doi:10.1002/mrm.21302
- Mlynárik V, Gambarota G, Frenkel H, Gruetter R. Localized short-echo-time proton MR spectroscopy with full signal-intensity acquisition. *Magn Reson Med* (2006) 56:965–70. doi:10.1002/mrm.21043
- Tkáč I, Starcuk Z, Choi IY, Gruetter R. In vivo <sup>1</sup>H NMR spectroscopy of rat brain at 1 ms echo time. *Magn Reson Med* (1999) 41:649–56. doi:10.1002/(SICI)1522-2594(199904)41:4<649::AID-MRM2>3.0.CO;2-G
- Frahm J, Bruhn H, Gyngell ML, Merboldt KD, Hänicke W, Sauter R. Localized high-resolution proton NMR spectroscopy using stimulated echoes: initial applications to human brain in vivo. *Magn Reson Med* (1989) 9:79–93. doi:10.1002/mrm.1910090110
- Tkáč I, Gruetter R. Methodology of <sup>1</sup>H NMR spectroscopy of the human brain at very high magnetic fields. *Appl Magn Reson* (2005) 29:139–57. doi:10.1007/BF03166960
- Gruetter R, Tkáč I. Field mapping without reference scan using asymmetric echo-planar techniques. *Magn Reson Med* (2000) 43:319–23. doi:10.1002/(SICI)1522-2594(200002)43:2<319::AID-MRM22>3.0.CO;2-1
- Gruetter R. Automatic, localized in vivo adjustment of all first- and second-order shim coils. *Magn Reson Med* (1993) 29:804–11. doi:10.1002/mrm.1910290613
- Schaller B, Xin L, O'Brien K, Magill AW, Gruetter R. Are glutamate and lactate increases ubiquitous to physiological activation? A <sup>1</sup>H functional MR spectroscopy study during motor activation in human brain at 7Tesla. *Neuroimage* (2014) 93(Pt 1):138–45. doi:10.1016/j.neuroimage.2014.02.016
- Stanley JA, Burgess A, Khatib D, Ramaseshan K, Arshad M, Wu H, et al. Functional dynamics of hippocampal glutamate during associative learning assessed with in vivo <sup>1</sup>H functional magnetic resonance spectroscopy. *Neuroimage* (2017) 153:189–97. doi:10.1016/j.neuroimage.2017.03.051
- Duarte JMN, Lei H, Mlynárik V, Gruetter R. The neurochemical profile quantified by in vivo <sup>1</sup>H NMR spectroscopy. *Neuroimage* (2012) 61:342–62. doi:10.1016/j.neuroimage.2011.12.038
- Dou W, Speck O, Benner T, Kaufmann J, Li M, Zhong K, et al. Automatic voxel positioning for MRS at 7 T. *MAGMA* (2015) 28:259–70. doi:10.1007/s10334-014-0469-9
- Bai X, Harris AD, Gong T, Puts NAJ, Wang G, Schär M, et al. Voxel placement precision for GABA-edited magnetic resonance spectroscopy. *Open J Radiol* (2017) 07:35–44. doi:10.4236/ojrad.2017.71004
- Woodcock EA, Anand C, Khatib D, Diwadkar VA, Stanley JA. Working memory modulates glutamate levels in the prefrontal cortex during <sup>1</sup>H fMRS. *Front Psychiatry* (2018) 9:66. doi:10.3389/fpsyg.2018.00066
- Mangia S, Tkáč I, Gruetter R, Van De Moortele PF, Maraviglia B, Ugurbil K. Sustained neuronal activation raises oxidative metabolism to a new steady-state

- level: evidence from <sup>1</sup>H NMR spectroscopy in the human visual cortex. *J Cereb Blood Flow Metab* (2007) 27:1055–63. doi:10.1038/sj.jcbfm.9600401
42. Lin Y, Stephenson MC, Xin L, Napolitano A, Morris PG. Investigating the metabolic changes due to visual stimulation using functional proton magnetic resonance spectroscopy at 7 T. *J Cereb Blood Flow Metab* (2012) 32:1484–95. doi:10.1038/jcbfm.2012.33
  43. Schaller B, Mekler R, Xin L, Kunz N, Gruetter R. Net increase of lactate and glutamate concentration in activated human visual cortex detected with magnetic resonance spectroscopy at 7 tesla. *J Neurosci Res* (2013) 91:1076–83. doi:10.1002/jnr.23194
  44. Bednářík P, Tkac I, Giove F, Dinuzzo M, Deelchand DK, Emir UE, et al. Neurochemical and BOLD responses during neuronal activation measured in the human visual cortex at 7 Tesla. *J Cereb Blood Flow Metab* (2015) 35:601–10. doi:10.1038/jcbfm.2014.233
  45. Apšvalka D, Gadie A, Clemence M, Mullins PG. Event-related dynamics of glutamate and BOLD effects measured using functional magnetic resonance spectroscopy (fMRS) at 3T in a repetition suppression paradigm. *Neuroimage* (2015) 118:292–300. doi:10.1016/j.neuroimage.2015.06.015
  46. Asemi A, Ramaseshan K, Burgess A, Diwadkar VA, Bressler SL. Dorsal anterior cingulate cortex modulates supplementary motor area in coordinated unimanual motor behavior. *Front Hum Neurosci* (2015) 9:309. doi:10.3389/fnhum.2015.00309
  47. Mullins PG, Rowland LM, Jung RE, Sibbitt WL. A novel technique to study the brains response to pain: proton magnetic resonance spectroscopy. *Neuroimage* (2005) 26:642–6. doi:10.1016/j.neuroimage.2005.02.001
  48. Gussew A, Rzanny R, Erdtel M, Scholle HC, Kaiser WA, Mentzel HJ, et al. Time-resolved functional <sup>1</sup>H MR spectroscopic detection of glutamate concentration changes in the brain during acute heat pain stimulation. *Neuroimage* (2010) 49:1895–902. doi:10.1016/j.neuroimage.2009.09.007
  49. Baddeley A. Working memory. *Curr Biol* (2010) 20:R136–40. doi:10.1016/j.cub.2009.12.014
  50. Goldman-Rakic PS. Cellular basis of working memory. *Neuron* (1995) 14:477–85. doi:10.1016/0896-6273(95)90304-6
  51. Nyberg L, Cabeza R. Brain imaging of memory. In: Tulving E, editor. *The Oxford Handbook of Memory*. Oxford: Oxford University Press (2000). p. 501–19.
  52. Owen AM, Mcmillan KM, Laird AR, Bullmore E. N-back working memory paradigm: a meta-analysis of normative functional neuroimaging studies. *Hum Brain Mapp* (2005) 25:46–59. doi:10.1002/hbm.20131
  53. Bliss TV, Collingridge GL. A synaptic model of memory: long-term potentiation in the hippocampus. *Nature* (1993) 361:31–9. doi:10.1038/361031a0
  54. Day M, Langston R, Morris RGM. Glutamate-receptor-mediated encoding and retrieval of paired-associate learning. *Nature* (2003) 424:205–9. doi:10.1038/nature01769
  55. Suzuki WA. Making new memories: the role of the hippocampus in new associative learning. *Ann N Y Acad Sci* (2007) 1097:1–11. doi:10.1196/annals.1379.007
  56. Raz N, Rodriguez KM. Differential aging of the brain: patterns, cognitive correlates and modifiers. *Neurosci Biobehav Rev* (2006) 30:730–48. doi:10.1016/j.neubiorev.2006.07.001
  57. Mueller SG, Weiner MW. Selective effect of age, Apo e4, and Alzheimer's disease on hippocampal subfields. *Hippocampus* (2009) 19:558–64. doi:10.1002/hipo.20614
  58. Small SA, Schobel SA, Buxton RB, Witter MP, Barnes CA. A pathophysiological framework of hippocampal dysfunction in ageing and disease. *Nat Rev Neurosci* (2011) 12:585–601. doi:10.1038/nrn3085
  59. Raz N, Daugherty AM, Bender AR, Dahle CL, Land S. Volume of the hippocampal subfields in healthy adults: differential associations with age and a pro-inflammatory genetic variant. *Brain Struct Funct* (2015) 220:2663–74. doi:10.1007/s00429-014-0817-6
  60. Kassem LA, Gamal El-Din MM, Yassin NA. Mechanisms of vincristine-induced neurotoxicity: possible reversal by erythropoietin. *Drug Discov Ther* (2011) 5:136–43. doi:10.5582/ddt.2011.v5.3.136
  61. Maiti P, Manna J, Ilavazhagan G, Rossignol J, Dunbar GL. Molecular regulation of dendritic spine dynamics and their potential impact on synaptic plasticity and neurological diseases. *Neurosci Biobehav Rev* (2015) 59:208–37. doi:10.1016/j.neubiorev.2015.09.020
  62. MacLeod CM, MacDonald PA. Interdimensional interference in the Stroop effect: uncovering the cognitive and neural anatomy of attention. *Trends Cogn Sci* (2000) 4:383–91. doi:10.1016/S1364-6613(00)01530-8
  63. Barch DM, Braver TS, Akbudak E, Conturo T, Ollinger J, Snyder A. Anterior cingulate cortex and response conflict: effects of response modality and processing domain. *Cereb Cortex* (2001) 11:837–48. doi:10.1093/cercor/11.9.837
  64. Botvinick MM, Cohen JD, Carter CS. Conflict monitoring and anterior cingulate cortex: an update. *Trends Cogn Sci* (2004) 8:539–46. doi:10.1016/j.tics.2004.10.003
  65. Taylor R, Schaefer B, Densmore M, Neufeld RWJ, Rajakumar N, Williamson PC, et al. Increased glutamate levels observed upon functional activation in the anterior cingulate cortex using the Stroop Task and functional spectroscopy. *Neuroreport* (2015) 26:107–12. doi:10.1097/WNR.0000000000000309
  66. Taylor R, Neufeld RW, Schaefer B, Densmore M, Rajakumar N, Osuch EA, et al. Functional magnetic resonance spectroscopy of glutamate in schizophrenia and major depressive disorder: anterior cingulate activity during a color-word Stroop task. *NPJ Schizophr* (2015) 1:15028. doi:10.1038/njpschz.2015.28
  67. Minzenberg MJ, Laird AR, Thelen S, Carter CS, Glahn DC. Meta-analysis of 41 functional neuroimaging studies of executive function in schizophrenia. *Arch Gen Psychiatry* (2009) 66:811–22. doi:10.1001/archgenpsychiatry.2009.91
  68. Lindner M, Bell T, Iqbal S, Mullins PG, Christakou A. In vivo functional neurochemistry of human cortical cholinergic function during visuospatial attention. *PLoS One* (2017) 12:e0171338. doi:10.1371/journal.pone.0171338
  69. Jahng G-H, Oh J, Lee D-W, Kim H-G, Rhee HY, Shin W, et al. Glutamine and glutamate complex, as measured by functional magnetic resonance spectroscopy, alters during face-name association task in patients with mild cognitive impairment and Alzheimers disease. *J Alzheimers Dis* (2016) 52:145–59. doi:10.3233/JAD-150877
  70. Rothman DL, Behar KL, Hyder F, Shulman RG. In vivo NMR studies of the glutamate neurotransmitter flux and neuroenergetics: implications for brain function. *Annu Rev Physiol* (2003) 65:401–27. doi:10.1146/annurev.physiol.65.092101.142131
  71. Mangia S, Giove F, Dinuzzo M. Metabolic pathways and activity-dependent modulation of glutamate concentration in the human brain. *Neurochem Res* (2012) 37:2554–61. doi:10.1007/s11064-012-0848-4
  72. Lanz B, Gruetter R, Duarte JM. Metabolic flux and compartmentation analysis in the brain in vivo. *Front Endocrinol (Lausanne)* (2013) 4:156.
  73. Dienel GA. Fueling and imaging brain activation. *ASN Neuro* (2012) 4:267–321. doi:10.1042/AN20120021
  74. Mergenthaler P, Lindauer U, Dienel GA, Meisel A. Sugar for the brain: the role of glucose in physiological and pathological brain function. *Trends Neurosci* (2013) 36:587–97. doi:10.1016/j.tins.2013.07.001
  75. Fox PT, Raichle ME, Mintun MA, Dence C. Nonoxidative glucose consumption during focal physiologic neural activity. *Science* (1988) 241:462–4. doi:10.1126/science.3260686
  76. Magistretti PJ. Neuron-glia metabolic coupling and plasticity. *J Exp Biol* (2006) 209:2304–11. doi:10.1242/jeb.02208
  77. Sibson NR, Dhankhar A, Mason GF, Rothman DL, Behar KL, Shulman RG. Stoichiometric coupling of brain glucose metabolism and glutamatergic neuronal activity. *Proc Natl Acad Sci U S A* (1998) 95:316–21. doi:10.1073/pnas.95.1.316
  78. Shen J, Petersen KE, Behar KL, Brown P, Nixon TW, Mason GF, et al. Determination of the rate of the glutamate/glutamine cycle in the human brain by *in vivo* <sup>13</sup>C NMR. *Proc Natl Acad Sci U S A* (1999) 96:8235–40. doi:10.1073/pnas.96.14.8235
  79. Berg CJVD, Garfinkel D. A stimulation study of brain compartments. Metabolism of glutamate and related substances in mouse brain. *Biochem J* (1971) 123:211–8. doi:10.1042/bj1230211
  80. Erecinska M, Silver IA. Metabolism and role of glutamate in mammalian brain. *Prog Neurobiol* (1990) 35:245–96. doi:10.1016/0301-0082(90)90013-7
  81. McKenna MC. Glutamate pays its own way in astrocytes. *Front Endocrinol (Lausanne)* (2013) 4:191. doi:10.3389/fendo.2013.00191
  82. McEwen BS, Morrison JH. The brain on stress: vulnerability and plasticity of the prefrontal cortex over the life course. *Neuron* (2013) 79:16–29. doi:10.1016/j.neuron.2013.06.028
  83. Thomas EH, Bozoglu K, Rossell SL, Gurvich C. The influence of the glutamatergic system on cognition in schizophrenia: a systematic review. *Neurosci Biobehav Rev* (2017) 77:369–87. doi:10.1016/j.neubiorev.2017.04.005

84. Zhu XH, Chen W. Observed BOLD effects on cerebral metabolite resonances in human visual cortex during visual stimulation: a functional (<sup>1</sup>H) MRS study at 4 T. *Magn Reson Med* (2001) 46:841–7. doi:10.1002/mrm.1267
85. Mangia S, Tkác I, Gruetter R, Van De Moortele PF, Giove F, Maraviglia B, et al. Sensitivity of single-voxel <sup>1</sup>H-MRS in investigating the metabolism of the activated human visual cortex at 7 T. *Magn Reson Imaging* (2006) 24:343–8. doi:10.1016/j.mri.2005.12.023
86. Provencher SW. Estimation of metabolite concentrations from localized in vivo proton NMR spectra. *Magn Reson Med* (1993) 30:672–9. doi:10.1002/mrm.1910300604
87. Lynn J, Woodcock EA, Anand C, Khatib D, Stanley JA. Differences in steady-state glutamate levels and variability between ‘non-task-active’ control conditions: evidence from <sup>1</sup>H fMRS of the prefrontal cortex. *Neuroimage* (2018) 172:554–61. doi:10.1016/j.neuroimage.2018.01.069
88. Ip IB, Berrington A, Hess AT, Parker AJ, Emir UE, Bridge H. Combined fMRI-MRS acquires simultaneous glutamate and BOLD-fMRI signals in the human brain. *Neuroimage* (2017) 155:113–9. doi:10.1016/j.neuroimage.2017.04.030
89. Fox MD, Snyder AZ, Vincent JL, Corbetta M, Van Essen DC, Raichle ME. The human brain is intrinsically organized into dynamic, anticorrelated functional networks. *Proc Natl Acad Sci USA* (2005) 102:9673–8. doi:10.1073/pnas.0504136102
90. Damoiseaux JS, Rombouts SA, Barkhof F, Scheltens P, Stam CJ, Smith SM, et al. Consistent resting-state networks across healthy subjects. *Proc Natl Acad Sci U S A* (2006) 103:13848–53. doi:10.1073/pnas.0601417103
91. Cole MW, Schneider W. The cognitive control network: integrated cortical regions with dissociable functions. *Neuroimage* (2007) 37:343–60. doi:10.1016/j.neuroimage.2007.03.071
92. Banich MT. Executive function: the search for an integrated account. *Curr Dir Psychol Sci* (2009) 18:89–94. doi:10.1111/j.1467-8721.2009.01615.x
93. Xu S, Yang J, Li CQ, Zhu W, Shen J. Metabolic alterations in focally activated primary somatosensory cortex of alpha-chloralose-anesthetized rats measured by <sup>1</sup>H MRS at 11.7 T. *Neuroimage* (2005) 28:401–9. doi:10.1016/j.neuroimage.2005.06.016
94. Iltis I, Koski DM, Eberly LE, Nelson CD, Deelchand DK, Valette J, et al. Neurochemical changes in the rat prefrontal cortex following acute phenylcyclidine treatment: an in vivo localized (<sup>1</sup>H) MRS study. *NMR Biomed* (2009) 22:737–44. doi:10.1002/nbm.1385
95. Just N, Sonnay S. Investigating the role of glutamate and GABA in the modulation of transthalamic activity: a combined fMRI-fMRS study. *Front Physiol* (2017) 8:30. doi:10.3389/fphys.2017.00030
96. Sonnay S, Duarte JMN, Just N. Lactate and glutamate dynamics during prolonged stimulation of the rat barrel cortex suggest adaptation of cerebral glucose and oxygen metabolism. *Neuroscience* (2017) 346:337–48. doi:10.1016/j.neuroscience.2017.01.034

**Conflict of Interest Statement:** The authors declare that the research was conducted in the absence of any commercial or financial relationships that could be construed as a potential conflict of interest.

Copyright © 2018 Stanley and Raz. This is an open-access article distributed under the terms of the Creative Commons Attribution License (CC BY). The use, distribution or reproduction in other forums is permitted, provided the original author(s) and the copyright owner are credited and that the original publication in this journal is cited, in accordance with accepted academic practice. No use, distribution or reproduction is permitted which does not comply with these terms.



# Intelligence and Brain Efficiency: Investigating the Association between Working Memory Performance, Glutamate, and GABA

Anouk Marsman<sup>1\*</sup>, René C. W. Mandl<sup>1</sup>, Dennis W. J. Klomp<sup>2</sup>, Wiepke Cahn<sup>1</sup>, René S. Kahn<sup>1</sup>, Peter R. Luijten<sup>2</sup> and Hilleke E. Hulshoff Pol<sup>1</sup>

<sup>1</sup>Brain Center Rudolf Magnus, Department of Psychiatry, University Medical Center Utrecht, Utrecht, Netherlands,

<sup>2</sup>Department of Radiology, University Medical Center Utrecht, Utrecht, Netherlands

## OPEN ACCESS

**Edited by:**

Paul Croarkin,  
Mayo Clinic,  
United States

**Reviewed by:**

Ernest Pedapati,  
Cincinnati Children's Hospital  
Medical Center, United States

Frank P. MacMaster,  
University of Calgary, Canada

**\*Correspondence:**

Anouk Marsman  
anoukm@drcmr.dk

**Specialty section:**

This article was submitted to  
Neuroimaging and Stimulation,  
a section of the journal  
*Frontiers in Psychiatry*

**Received:** 31 May 2017

**Accepted:** 07 August 2017

**Published:** 15 September 2017

**Citation:**

Marsman A, Mandl RCW, Klomp DWJ, Cahn W, Kahn RS, Luijten PR and Hulshoff Pol HE (2017) Intelligence and Brain Efficiency: Investigating the Association between Working Memory Performance, Glutamate, and GABA. *Front. Psychiatry* 8:154. doi: 10.3389/fpsy.2017.00154

Intelligence is a measure of general cognitive functioning capturing a wide variety of different cognitive functions. It has been hypothesized that the brain works to minimize the resources allocated toward higher cognitive functioning. Thus, for the intelligent brain, it may be that not simply more is better, but rather, more efficient is better. Energy metabolism supports both inhibitory and excitatory neurotransmission processes. Indeed, in glutamatergic and GABAergic neurons, the primary energetic costs are associated with neurotransmission. We tested the hypothesis that minimizing resources through the excitation–inhibition balance encompassing gamma-aminobutyric acid (GABA) and glutamate may be beneficial to general cognitive functioning using 7 T <sup>1</sup>H-MRS in 23 healthy individuals (male/female = 16/7, 27.7 ± 5.3 years). We find that a higher working memory index is significantly correlated with a lower GABA to glutamate ratio in the frontal cortex and with a lower glutamate level in the occipital cortex. Thus, it seems that working memory performance is associated with the excitation–inhibition balance in the brain.

**Keywords:** <sup>1</sup>H-MRS, 7 T, gamma-aminobutyric acid, glutamate, intelligence

## INTRODUCTION

Intelligence is a measure of general cognitive functioning capturing a wide variety of different cognitive functions (1). Intelligence has long been (albeit modestly) associated with brain size (2–4). More recently, intellectual functioning has been implicated in brain functioning (5) and in the efficiency of the functional (6) and structural brain network (7). Regional structural differences in relationship to intelligence have been demonstrated in several studies in healthy individuals (2, 3, 8) and in individuals with local brain lesions (9). However, it is not known how the human brain handles complex cognitive tasks while being such an expensive organ to operate, utilizing some 20% of all oxygen taken in and 25% of all glucose produced while representing only about 2% of the body's weight (10, 11). Indeed, it has been hypothesized that the brain works to minimize the resources allocated toward higher cognitive functioning (12). Thus, for the intelligent brain, it

may be that not simply more is better, but rather more *efficient* is better.

Glutamate (Glu) and gamma-aminobutyric acid (GABA) are the major excitatory and inhibitory neurotransmitters in the central nervous system. In both glutamatergic and GABAergic neurons, the primary energetic costs are associated with neurotransmission, and the energetic needs of these neurons dominate the cerebral cortex energy requirements (13, 14). In the resting awake state, 80% of energy used by the brain supports events associated with neuronal firing and cycling of GABA and glutamate, and in the actively awake individual, the change in energy (and its coupled activity) induced by stimulation during task performance is very small in comparison to its baseline value (15). Thus, minimizing resources through the inhibition-excitation balance encompassing GABA and glutamate may be beneficial to general cognitive functioning. While general intellectual functioning has been related to brain neurochemistry in several studies, measuring largely positive associations with the brain metabolite *N*-acetyl aspartate (NAA) (16, 17), a marker of neuronal integrity (18, 19), these measures do not provide information on the inhibition-excitation balance. To obtain such information, one needs to reliably measure both glutamate and GABA levels, which is not an easy task using MR scanners operating at conventional magnetic field strengths.

Proton magnetic resonance spectroscopy (<sup>1</sup>H-MRS) at a field strength of 7 T has an increased sensitivity and spectral resolution. For instance, at 7 T, it is now possible to adequately separate the glutamate and glutamine signals resulting in a higher accuracy of glutamate measurement (20). Despite the increased sensitivity, measurement of GABA is not straightforward because of its low concentration compared to other brain metabolites and its obscured signal due to overlapping signals of higher intensity. To overcome this problem, spectral editing techniques can be applied to isolate the GABA signal (21). Using these methods, we were able to show that higher cognitive functioning was associated with lower GABA levels in the prefrontal cortex in patients with schizophrenia (22).

We explored possible associations between the excitation-inhibition balance in the brain and intelligence in the prefrontal cortex and in the occipital cortex. For this purpose, we measured GABA and glutamate levels using <sup>1</sup>H-MRS at a magnetic field strength of 7 T in healthy adults. While a whole brain approach would be ideal for studying intelligence, it is currently not feasible to measure GABA and glutamate reliably at a whole brain level using MRS. Therefore, we chose the prefrontal and occipital cortex because the prefrontal cortex has long been found to be important to general cognitive functioning and because the occipital cortex could be considered as a control area. This selection of areas has limitations. Indeed, the frontal lobes are often considered the primary focus of human intelligence (23, 24). However, the parieto-frontal integration theory for intelligence (25–27), an association with the whole brain network with intelligence (6), and association of intelligence level with cortical thickness change in many brain areas, including prefrontal and occipital cortices (28) suggest that many different parts of the brain may be involved in intelligence. Moreover, the occipital cortex was also involved in earlier studies [e.g., Ref. (23)]. We

hypothesized that the prefrontal cortex is essential for intelligence and thus expect an association with GABA and glutamate and intelligence level in this brain area and not in the occipital cortex in this exploratory study.

## MATERIALS AND METHODS

### Subjects

A total of 23 healthy individuals (16 males/7 females) participated in the study. Participants had no major psychiatric or neurological history, no history of drug or alcohol abuse, and no first-degree relatives with psychiatric or neurological disorders. The study was approved by the Medical Ethics Committee of the University Medical Center Utrecht, The Netherlands, and performed according to the directives of the Declaration of Helsinki (amendment of Seoul, 2008). Participants provided written informed consent prior to the examination. Mean (SD) age was 27.7 (5.3) years, and average completed years of education was 14.1 ± 2.1 years.

### Cognitive Assessment

All participants underwent a general cognitive assessment using the full Wechsler Adult Intelligence Scale (WAIS-III-NL) (29). The total intelligence quotient (TIQ) as well as the verbal (VIQ) and performance (PIQ) intelligence quotients, the perceptual reasoning index (PRI), verbal comprehension index (VCI), and the working memory index (WMI) were measured.

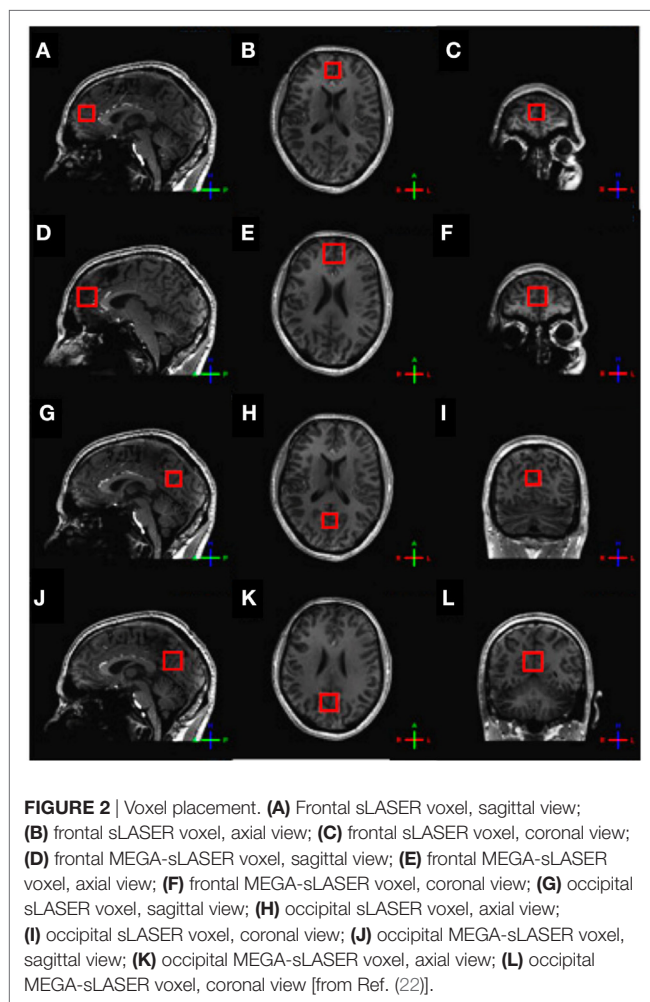
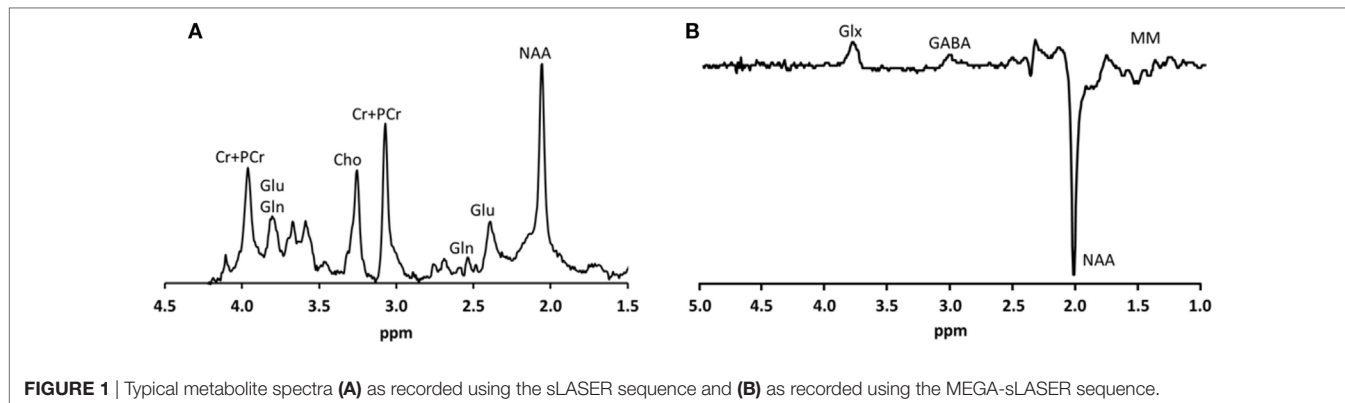
### MR Acquisition

All investigations were performed on a 7 T whole body MR scanner (Philips, Cleveland, OH, USA). A birdcage transmit head coil was used in dual transmit driven by 2 × 4 kW amplifiers, in combination with a 32-channel receive coil (both Nova Medical, Inc., Burlington, MA, USA).

For anatomical reference and gray and white matter tissue classification, a T<sub>1</sub>-weighted magnetization prepared rapid gradient echo sequence was obtained (450 slices, slice thickness = 0.8 mm, TR = 7 ms, TE = 3 ms, flip angle = 8°, FOV = 250 mm × 200 mm × 180 mm, 312 × 312 acquisition matrix, SENSE factor 2.7, scan duration = 408 s).

For the assessment of glutamate, <sup>1</sup>H-MRS experiments were conducted using a sLASER sequence (semi-localized by adiabatic selective refocusing; TE = 28 ms, 32 averages, TR = 5 s) (Figure 1A). Voxels (2 cm × 2 cm × 2 cm) were located in the medial prefrontal and medial occipital lobe (Figure 2). Non-water-suppressed spectra were obtained for quantification (carrier frequency was set to the chemical shift of H<sub>2</sub>O, acquisition time = 10 s).

GABA-edited <sup>1</sup>H-MRS experiments were conducted using a MEGA-sLASER sequence (TE = 74 ms, 64 averages, TR = 4 s) (Figure 1B) (31). Voxels (2.5 cm × 2.5 cm × 2.5 cm) were located in the medial frontal and medial occipital region (Figure 2). Prior to the MRS exams, second order B<sub>0</sub> shimming was applied using the FASTERMAP algorithm at the voxel of interest (30, 32). Second, at this location, a high B<sub>1</sub> field was generated to minimize chemical shift displacement artifacts (33). The



highest possible  $B_1$  field was generated by optimizing the phase of both transmit channels to locally assure constructive  $B_1$  interferences (34).

## Spectral Fitting and Quantification

Retrospective phase and frequency alignment was performed on all data sets of each measurement (35). Fitting of the sLASER spectra was performed with LCModel-based software

implemented in Matlab (36), which uses *a priori* knowledge of the spectral components to fit metabolite resonances (37). The following 16 metabolites and a measured macromolecular baseline (38) were fitted to the spectra: acetate, aspartate, choline (Cho), phosphorylcholine, glycerophosphorylcholine, phosphorylethanolamine, creatine (Cr), phosphocreatine (PCr), NAA, *N*-acetyl aspartyl glutamate, GABA, Glu, glutamine (Gln), glutathione (GSH), myo-inositol (mIns), and taurine (Tau). Glutamate levels were estimated using the water signal as an internal reference and calculated as follows:

$$[\text{met}] = \left( \frac{\frac{\text{signal}_{\text{met}}}{\text{signal}_{\text{water}}} * (\text{volGM} * [\text{water}_{\text{GM}}] + \text{volWM} * [\text{water}_{\text{WM}}] + \text{volCSF} * [\text{water}_{\text{pure}}])}{\text{volGM} + \text{volWM}} \right)$$

where  $[\text{met}]$  is the metabolite concentration,  $\text{signal}_{\text{met}}$  is the fitted signal intensity of the metabolite, accounting for the number of protons, and  $\text{signal}_{\text{water}}$  is the fitted signal intensity of water, accounting for the number of protons;  $\text{volGM}$ ,  $\text{volWM}$ , and  $\text{volCSF}$  are, respectively, the gray matter fraction, white matter fraction, and cerebrospinal fluid (CSF) fraction in the voxel; and  $[\text{water}_{\text{GM}}]$ ,  $[\text{water}_{\text{WM}}]$ , and  $[\text{water}_{\text{pure}}]$  are, respectively, the water concentration in gray matter, white matter, or CSF. For determining the contribution of gray matter, white matter, and CSF of each voxel, the software package SPM8 was used to segment the  $T_1$ -weighted image. In the  $T_1$ -weighted image, the position of the  $^1\text{H}$ -MRS voxel was determined, after which the amount of gray matter, white matter, and CSF in the  $^1\text{H}$ -MRS voxel was computed. To account for differences in transverse relaxation between water and metabolites, a correction was applied based on reported  $T_2$  values at 7 T of 47 ms on average for water and 107 ms assumed for the metabolites (39). Statistical analysis of the gray and white matter fractions in the frontal and occipital MEGA-sLASER (GABA/Cr) and sLASER (glutamate) revealed correlations  $>0.95$  for both gray and white matter fractions in the two voxels.

Fitting of the MEGA-sLASER spectra was performed by frequency-domain fitting of the GABA and creatine resonances to a Lorentzian line-shape function in Matlab. GABA levels were expressed as the ratios of their peak areas relative to the peak areas of the creatine resonance (GABA/Cr).

## Statistical Analysis

Statistical analyses were performed using SPSS 21.0 (2012, Chicago, IL, USA). Data were controlled for their normality of the distributions. No transformations for correction were needed. To evaluate differences in metabolite concentrations and gray and white matter fractions between the frontal and occipital areas, paired *t*-tests were done. To evaluate associations between brain metabolite levels with general intelligence measures, partial correlation coefficients were done with corrections for age, sex, and for gray and white matter fractions (40). The partial correlation between IQ and metabolite levels was defined as the correlation between the residuals of IQ and metabolite levels resulting from the linear regressions of IQ and metabolite levels with the controlling variables, i.e., age, sex, and gray and white matter fractions of the sLASER and/or MEGA-sLASER voxels. To correct for multiple comparisons, while taking the considerable dependency among intelligence quotient measures and the exploratory nature of the study into account, we restricted the significance level of the correlations to  $p \leq 0.01$ .

## RESULTS

### Intelligence Measures

The mean (SD) of the TIQ was 108 (13), the verbal intelligence quotient (VIQ) was 109 (12), the performance intelligence quotient (PIQ) was 107 (14), the VCI was 111 (13), the PRI was 108 (15), and the WMI was 105 (12) (Table 1).

### Metabolite Concentrations in the Frontal and Occipital Areas

Because of poor spectral quality as established by a Cramér-Rao lower bound of more than 20% and visual inspection, some data were excluded from the study. Frontal MRS results are based on 18 subjects and occipital MRS results are based on 17 subjects. Frontal GABA-edited MRS results are based on 19 subjects

and occipital GABA-edited MRS results are also based on 19 subjects.

Paired *t*-tests for differences in metabolite concentrations and gray and white matter fractions between the frontal and occipital areas revealed no significant differences except for a higher white matter fraction in the occipital sLASER voxel, but this finding did not survive the analysis after correction for age and sex (Table 1).

### Brain Metabolites, Gray and White Matter Fractions, and Intelligence

A higher WMI was significantly correlated with a lower GABA/Glu ratio (GABA/Cr to Glu/Cr ratio) in the frontal cortex [ $r(7) = -0.80, p = 0.01$ ] and not significantly in the occipital cortex [ $r(7) = 0.68, p = 0.04$ ] (Table 2; Figure 3).

A higher WMI was not significantly correlated with the frontal GABA/Cr ratio [ $r(10) = -0.05, p = \text{ns}$ ], frontal glutamate concentration [ $r(10) = -0.53, p = 0.076$ ], and occipital GABA/Cr ratio [ $r(9) = 0.42, p = 0.19$ ]. A higher WMI was significantly associated with a lower occipital glutamate concentration [ $r(10) = -0.79, p < 0.004$ ] (Table 2; Figure 4).

No significant associations were found for TIQ, Verbal intelligence quotient, performance intelligence quotient, VCI, and PRI with any of the metabolites in the frontal and occipital cortices. All correlations with metabolites were corrected for age, sex, and gray and white matter fractions.

### Brain Metabolites, Age, and Sex

There were no other significant associations between metabolite levels in the prefrontal and occipital cortices with age. These correlations were corrected for sex, and gray and white matter fractions. There were no significant associations between metabolite levels in the prefrontal and occipital cortices with sex.

### Correlations among Metabolites

Following correction for age, sex, gray and white matter fractions, in the occipital cortex, a significant negative correlation

**TABLE 1 |** Intelligence and brain metabolites in healthy individuals.<sup>a</sup>

Intelligence	(Sub) test score	Mean (SD)	Min	Max
	Total IQ	108 (13)	82	131
	Verbal IQ	109 (12)	82	128
	Performance IQ	107 (14)	78	127
	Verbal comprehension index	111 (13)	91	132
	Perceptual reasoning index	108 (15)	79	129
	Working memory index	105 (12)	86	124
' <sup>1</sup> H-MRS sequence	Metabolite	Prefrontal [mean (SD)]	Occipital [mean (SD)]	Paired <i>t</i> -test
MEGA-sLASER	GABA/Cr ratio	0.14 (0.03)	0.13 (0.03)	ns
	Gray matter (%)	68.1 (11.3)	68.0 (11.9)	ns
	White matter (%)	24.0 (11.8)	27.7 (13.2)	ns
sLASER	Glutamate (mM)	8.65 (1.14)	8.48 (1.26)	ns
	Gray matter (%)	71.4 (14.3)	70.1 (12.7)	ns
	White matter (%)	19.5 (15.6)	25.2 (14.6)	$p < 0.05^b$

<sup>a</sup>Uncorrected data based on two separate <sup>1</sup>H-MRS measurements and *T<sub>1</sub>*-weighted volume measurements performed in two brain areas (medial prefrontal and medial occipital).

For assessment of GABA/Cr ratios, a MEGA-sLASER sequence was performed and successfully completed in 19 individuals in the medial prefrontal cortex and in 18 individuals in the medial occipital cortex. A sLASER sequence was performed for assessment of glutamate and successfully completed in 18 individuals in the medial prefrontal cortex and in 17 individuals in the medial occipital cortex. Volume data are based on 21 individuals except for the occipital MEGA-sLASER voxel volumes, which are based on 18 individuals.

<sup>b</sup>Following corrections for age and sex, this difference was no longer significant.

was found between GABA/Cr ratio and glutamate concentration [ $r(7) = -0.85, p < 0.01$ ].

Higher GABA/Cr ratios in the prefrontal cortex were significantly correlated with lower glutamate concentrations [ $r(7) = -0.89, p < 0.01$ ] in the occipital cortex (**Figure 5**).

## DISCUSSION

To our knowledge, this study presents the first proton magnetic resonance spectroscopy measurements of GABA and glutamate levels *in vivo* at a magnetic field strength of 7 T associated with level of intelligence. The main finding is that a higher WMI is associated with a significantly lower GABA/Glu ratio in the

frontal cortex. However, in contrast to what was expected, we also find a significantly lower glutamate concentration in the occipital cortex. This may suggest that the excitation–inhibition balance in the frontal cortex, and perhaps to a lesser extent in the occipital cortex, is associated with working memory. Working memory refers to the ability to actively hold information on-line over brief periods of time (41). Working memory is one of the factors marking intelligence and has been closely related to general intelligence, although the extent of overlap is point of discussion (42). Moreover, working memory has been positively associated with gray and white matter volume, and with white matter tracts, and these associations are under genetic control (3, 43). Interestingly, based on studies in animals, it has been found that a successful working memory performance requires an exquisite balance of the excitatory and inhibitory circuitry in the prefrontal cortex that includes glutamate and GABA (41). Neurons in the prefrontal cortex have been shown to fire persistently during the maintenance phase of working memory tasks for which a balance between inhibitory and excitatory neurons are thought to be required. Supportive evidence for such a system during activation in the human brain was found in a study where a lower resting-state GABA level was associated with higher amplitude of the BOLD fMRI response to a simple visual stimulus in the visual cortex (44) [for review, see Ref. (45)]. Other negative associations were found between resting-state GABA level with visual orientation discrimination performance in the occipital cortex (46), and in the supplementary motor area with tactile discrimination performance (47, 48), which also support associations between GABA levels in the human cortex with cognitive functioning. Here, we show, by using  $^1\text{H}$ -MRS at 7 T, that lower frontal resting-state GABA/Glu ratios and lower occipital glutamate concentrations may lead to a higher working memory performance in healthy adults, possibly through a more efficient inhibition–excitation balance.

**TABLE 2 |** Brain metabolites and intelligence.<sup>a</sup>

Metabolites	Cognition					
	TIQ	VIQ	PIQ	VCI	PRI	WMI
<b>Prefrontal</b>						
GABA/Cr	0.31	0.28	0.30	0.25	0.37	-0.05
Glutamate	-0.01	-0.25	0.26	0.01	0.28	-0.53
GABA/Glu	-0.51	-0.67	-0.19	-0.41	-0.13	<b>-0.80**</b>
<b>Occipital</b>						
GABA/Cr	0.03	0.09	-0.08	0.04	-0.18	0.42
Glutamate	-0.19	-0.27	-0.07	-0.17	-0.10	<b>-0.79**</b>
GABA/Glu	0.14	0.22	-0.06	0.05	-0.19	<b>0.68*</b>

Bold font indicates significant correlations.

<sup>a</sup>Pearson correlations, corrected for age, sex, and for local gray matter and white matter fractions.

\*\* $p \leq 0.01$ .

\* $p \leq 0.05$ .

TIQ, total intelligence quotient; VIQ, verbal intelligence quotient; PIQ, performance intelligence quotient; VCI, verbal comprehension index; PRI, perceptual reasoning index; WMI, working memory index.

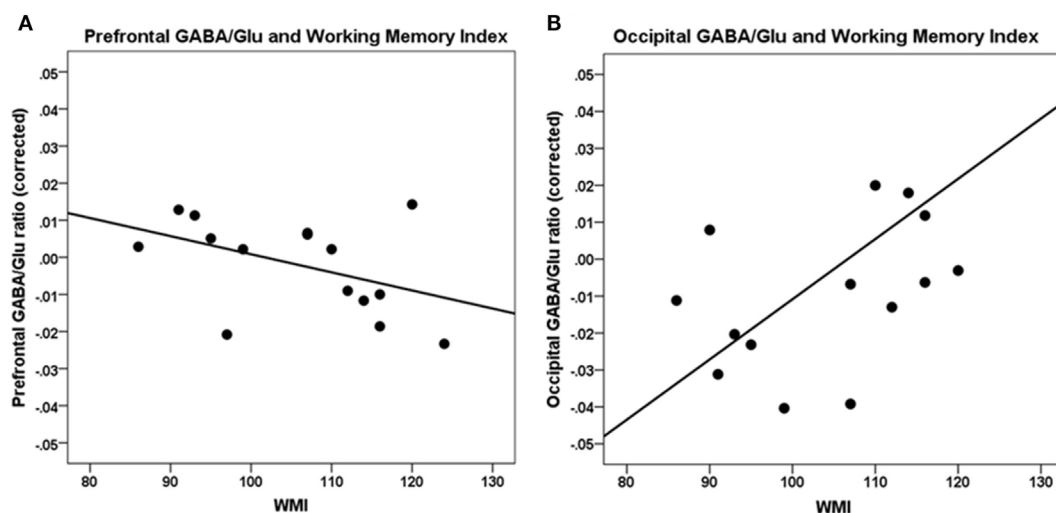


**FIGURE 3 |** Correlations between working memory index (WMI) and GABA/Glu ratio. **(A)** Prefrontal GABA/Glu ratios are significantly correlated with WMI [ $r(7) = -0.80, p = 0.01$ ]. **(B)** Occipital GABA/Glu ratios are not significantly correlated with WMI. Data are presented corrected for gray and white matter fractions, age, and sex.

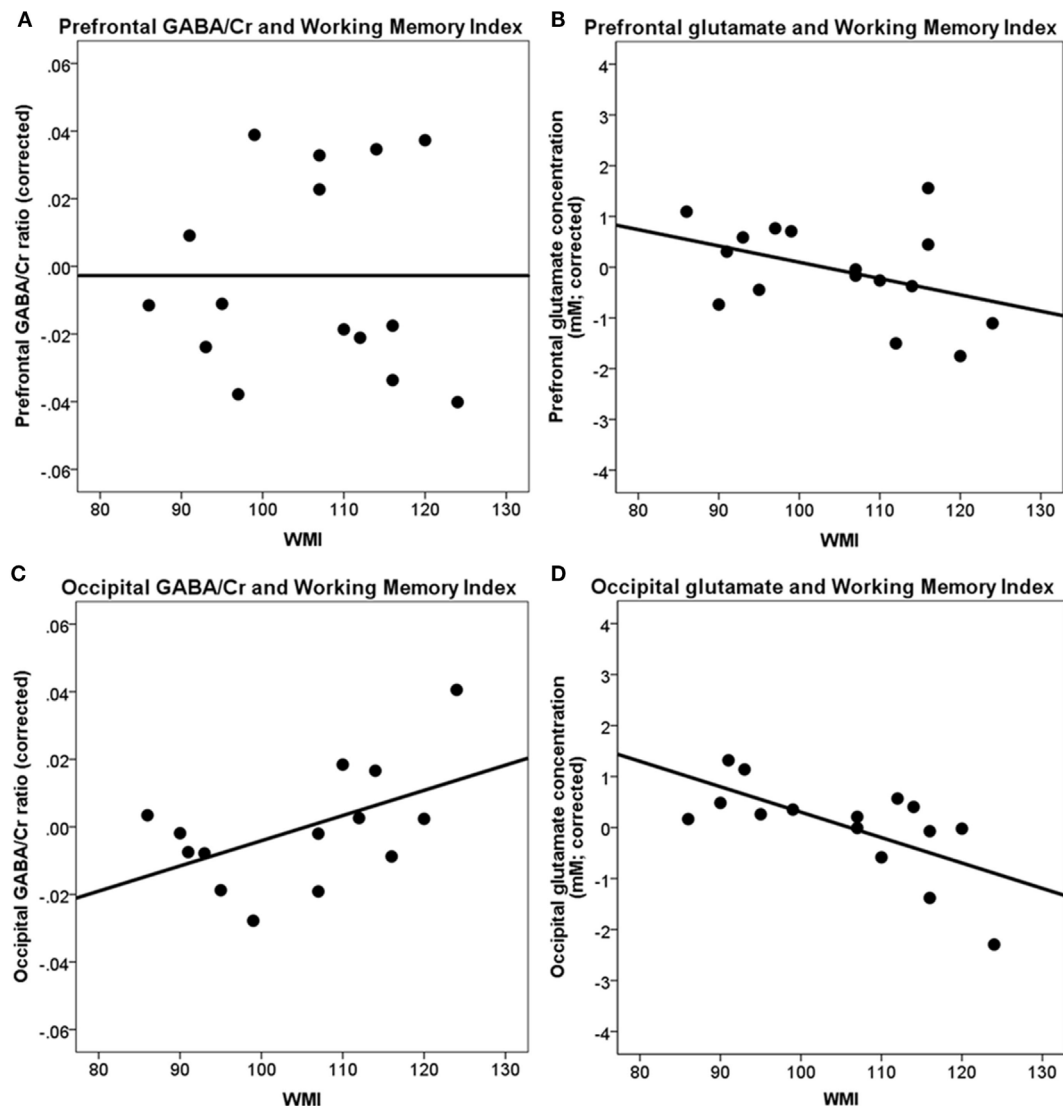


**FIGURE 4** | Correlations between prefrontal and occipital GABA/Cr and glutamate with working memory index (WMI). **(A)** Prefrontal GABA/Cr ratios are not significantly correlated with WMI; **(B)** prefrontal glutamate concentrations are not significantly correlated with WMI; **(C)** occipital GABA/Cr ratios are not significantly correlated with WMI; **(D)** occipital glutamate concentrations are significantly correlated with WMI [ $r(10) = -0.79, p < 0.004$ ]. Data are presented corrected for gray and white matter fractions, age, and sex.

Our measurements of brain metabolites were done in the frontal and occipital cortices using sLASER and MEGA-sLASER at 7 T. We could thus measure to which extend the metabolites were correlated within individuals. The most prominent association was found between levels of glutamate and GABA/Cr ratio in the occipital cortex, with higher levels of glutamate being associated with lower levels of GABA/Cr ( $-0.85$ ). Interestingly, a significant negative correlation between GABA/Cr in the occipital cortex and glutamate level in the prefrontal cortex was also found, thus suggesting a possible differential and maybe connected resting state association between these two anatomically distant brain regions.

This study has some limitations to take into account. One, with MRS, one cannot distinguish intracellular and extracellular

metabolite levels. Two, because of its low concentration, a large voxel size is needed to reliably and time-efficiently measure GABA. Hence, the voxel contained both gray and white matter. Three, the stringent correction for multiple comparisons was not possible due to the relatively limited number of participants that were included in the study. We chose for a more lenient approach to allow for the exploration of the association between these metabolite levels and intellectual functioning. Future studies with larger number of participants may allow for a more stringent correction for the multiple comparisons to confirm the stability of these findings.

Future studies using instance modern network analyses (49) may reveal how such connections between metabolite levels act. Such studies may reveal to which extent the associations between

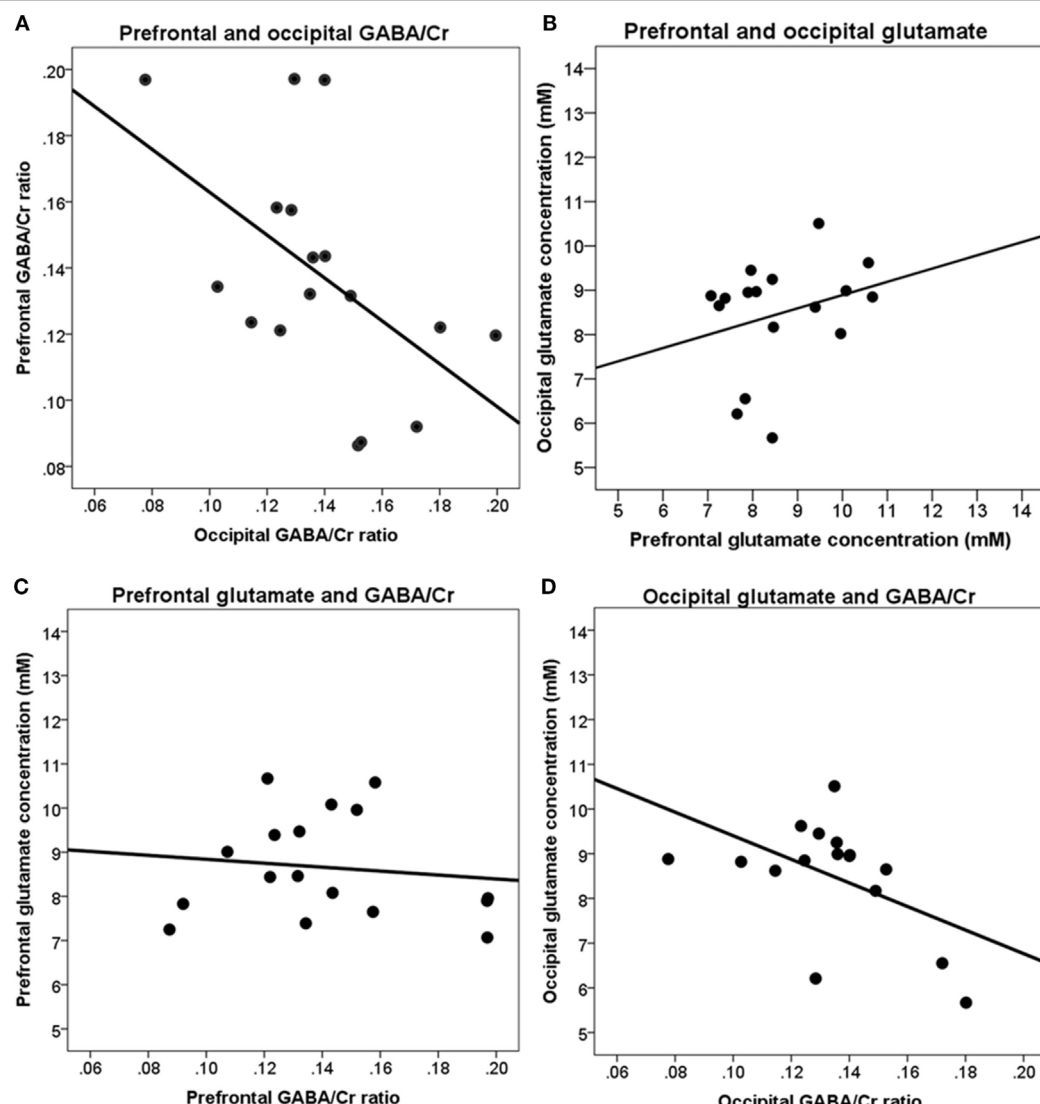


**FIGURE 5 |** Correlations between brain metabolites in the prefrontal and occipital cortices. **(A)** Prefrontal and occipital GABA/Cr ratios are not significantly correlated; **(B)** prefrontal and occipital glutamate concentrations are not significantly correlated; **(C)** prefrontal GABA/Cr ratios and glutamate concentrations are not significantly correlated; **(D)** occipital GABA/Cr ratios and glutamate concentrations are significantly correlated [ $r(7) = -0.85, p < 0.01$ ]. Data are presented uncorrected for gray and white matter fractions, age, and sex.

intelligence and brain metabolites are linked to local glucose levels and BOLD fMRI effects as well as to network efficiency of these nodes with the rest of the brain. There is evidence that the metabolic costs of a brain area (i.e., a node in a network) are proportional to the number of (mathematical) paths it has to connect with other nodes, and that the metabolic costs of a path are proportional to the physical distance it spans between nodes (50). Interestingly, Brodmann areas with a high glycolytic index were also found to be hub areas (i.e., have a high centrality rank); including Brodmann areas 32 and 33 (51), which are anatomically overlapping with the medial prefrontal voxel location of our current study. A functional neural network study revealed that a higher intelligence was associated with more efficient brain

network (6), and thus possibly with a more efficient use of local brain metabolism including GABA and glutamate. Indeed, associations between GABA, glutamate, BOLD signal (52, 53), and functional connectivity (54) have been reported. A recent study found that the frontal GABA/Glx ratio (Glx is the sum of the glutamate and glutamine signals) is related to oscillatory modulations during a working memory task, showing that a low GABA/Glx ratio is needed for efficient inhibition of irrelevant neural activity in precise task performance (55). Changes in GABA and glutamate levels have been found in patients with schizophrenia, a disorder, which is known to affect cognitive functioning (22, 30, 56). Recent evidence supports the involvement of glutamate and GABA in working memory performance in schizophrenia (57).

In conclusion, we found that working memory performance is associated with the excitation–inhibition balance in the brain.

## ETHICS STATEMENT

This study was carried out in accordance with the recommendations of the institutional ethics board (METC) with written informed consent from all subjects. All subjects gave written informed consent in accordance with the Declaration of Helsinki. The protocol was approved by the institutional ethics board (METC).

## REFERENCES

- Deary IJ. Intelligence. *Annu Rev Psychol* (2012) 63:453–82. doi:10.1146/annurev-psych-120710-100353
- Thompson PM, Cannon TD, Narr KL, van ET, Poutanen VP, Huttunen M, et al. Genetic influences on brain structure. *Nat Neurosci* (2001) 4:1253–8. doi:10.1038/nn758
- Posthuma D, de Geus EJ, Baare WF, Hulshoff Pol HE, Kahn RS, Boomsma DI. The association between brain volume and intelligence is of genetic origin. *Nat Neurosci* (2002) 5:83–4. doi:10.1038/nn0202-83
- Toga AW, Thompson PM. Genetics of brain structure and intelligence. *Annu Rev Neurosci* (2005) 28:1–23. doi:10.1146/annurev.neuro.28.061604.135655
- Song M, Zhou Y, Li J, Liu Y, Tian L, Yu C, et al. Brain spontaneous functional connectivity and intelligence. *Neuroimage* (2008) 41:1168–76. doi:10.1016/j.neuroimage.2008.02.036
- van den Heuvel MP, Stam CJ, Kahn RS, Hulshoff Pol HE. Efficiency of functional brain networks and intellectual performance. *J Neurosci* (2009) 29:7619–24. doi:10.1523/JNEUROSCI.1443-09.2009
- Chiang MC, Barysheva M, Shattuck DW, Lee AD, Madsen SK, Avedissian C, et al. Genetics of brain fiber architecture and intellectual performance. *J Neurosci* (2009) 29:2212–24. doi:10.1523/JNEUROSCI.4184-08.2009
- Hulshoff Pol HE, Schnack HG, Posthuma D, Mandl RC, Baaré WFC, Van Oel CJ, et al. Genetic contributions to human brain morphology and intelligence. *J Neurosci* (2006) 26:10235–42. doi:10.1523/JNEUROSCI.1312-06.2006
- Glascher J, Tranel D, Paul LK, Rudrauf D, Rorden C, Hornaday A, et al. Lesion mapping of cognitive abilities linked to intelligence. *Neuron* (2009) 61:681–91. doi:10.1016/j.neuron.2009.01.026
- Clarke DD, Sokoloff L. Circulation and energy metabolism of the brain. In: Siegel GJ, Agranoff BW, Albers RW, Fisher SK, Uhler MD, editors. *Basic Neurochemistry: Molecular, Cellular and Medical Aspects*. Philadelphia: Lippincott-Raven (1999). p. 637–70.
- Raichle ME, Gusnard DA. Appraising the brain's energy budget. *Proc Natl Acad Sci U S A* (2002) 99:10237–9. doi:10.1073/pnas.172399499
- Jung RE, Haier RJ. The Parieto-Frontal Integration Theory (P-FIT) of intelligence: converging neuroimaging evidence. *Behav Brain Sci* (2007) 30:135–54. doi:10.1017/S0140525X07001185
- Patel AB, De Graaf RA, Mason GF, Rothman DL, Shulman RG, Behar KL. The contribution of GABA to glutamate/glutamine cycling and energy metabolism in the rat cortex *in vivo*. *Proc Natl Acad Sci U S A* (2005) 102:5588–93. doi:10.1073/pnas.0501703102
- Rothman DL, Behar KL, Hyder F, Shulman RG. In vivo NMR studies of the glutamate neurotransmitter flux and neuroenergetics: implications for brain function. *Annu Rev Physiol* (2003) 65:401–27. doi:10.1146/annurev.physiol.65.092101.142131
- Shulman RG, Rothman DL, Behar KL, Hyder F. Energetic basis of brain activity: implications for neuroimaging. *Trends Neurosci* (2004) 27:489–95. doi:10.1016/j.tins.2004.06.005
- Jung RE, Gasparovic C, Chavez RS, Caprihan A, Barrow R, Yeo RA. Imaging intelligence with proton magnetic resonance spectroscopy. *Intelligence* (2009) 37:192–8. doi:10.1016/j.intell.2008.10.009
- Ross AJ, Sachdev PS. Magnetic resonance spectroscopy in cognitive research. *Brain Res Brain Res Rev* (2004) 44:83–102. doi:10.1016/j.brainresrev.2003.11.001
- Barker PB. N-acetyl aspartate – a neuronal marker? *Ann Neurol* (2001) 49:423–4. doi:10.1002/ana.90
- Moffett JR, Ross B, Arun P, Madhavarao CN, Namboodiri AM. N-Acetylaspartate in the CNS: from neurodiagnostics to neurobiology. *Prog Neurobiol* (2007) 81:89–131. doi:10.1016/j.pneurobio.2006.12.003
- Tkac I, Andersen P, Adriany G, Merkle H, Ugurbil K, Gruetter R. In vivo 1H NMR spectroscopy of the human brain at 7T. *Magn Reson Med* (2001) 46:451–6. doi:10.1002/mrm.1213
- Puts NA, Edden RA. In vivo magnetic resonance spectroscopy of GABA: a methodological review. *Prog Nucl Magn Reson Spectrosc* (2012) 60:29–41. doi:10.1016/j.pnmrs.2011.06.001
- Marsman A, Mandl RCW, Klomp DWJ, Bohlken MM, Boer VO, Andreychenko A, et al. GABA and glutamate in schizophrenia: a 7T 1H-MRS study. *Neuroimage Clin* (2014) 6:398–407. doi:10.1016/j.nicl.2014.10.005
- Duncan J, Seitz RJ, Kolodny J, Bor D, Herzog H, Ahmed A, et al. A neural basis for general intelligence. *Science* (2000) 289:457–60. doi:10.1126/science.289.5478.457
- Gray JR, Chabris CF, Braver TS. Neural mechanisms of general fluid intelligence. *Nat Neurosci* (2003) 6(3):316–22. doi:10.1038/nn1014
- Vakhitov AA, Ryman SG, Flores RA, Jung RE. Functional brain networks contributing to the parieto-frontal integration theory of Intelligence. *Neuroimage* (2014) 103:349–54. doi:10.1016/j.neuroimage.2014.09.055
- Haier RJ, Siegel BV, Nuechterlein KH, Hazlett E, Wu JC, Paek J, et al. Cortical glucose metabolic rate correlates of abstract reasoning and attention studied with positron emission tomography. *Intelligence* (1988) 12:199–217. doi:10.1016/0160-2896(88)90016-5
- Barbey AK, Colom R, Solomon J, Krueger F, Forbes C, Grafman J. An integrative architecture for general intelligence and executive function revealed by lesion mapping. *Brain* (2012) 135:1154–64. doi:10.1093/brain/aws021
- Schnack HG, van Haren NE, Brouwer RM, Evans A, Durston S, Boomsma DI, et al. Changes in thickness and surface area of the human cortex and their relationship with intelligence. *Cereb Cortex* (2015) 25(6):1608–17. doi:10.1093/cercor/bht357
- Wechsler D. *Wechsler Adult Intelligence Scale (WAIS-III). Dutch Version*. Lisse, The Netherlands: Swets & Zeitlinger (1997).
- Gruetter R, Boesch C. Fast, non-iterative shimming on spatially localized signals: in vivo analysis of the magnetic field along axes. *J Magn Reson* (1992) 96:323–34.
- Andreychenko A, Boer VO, Arteaga de Castro CS, Luijten PR, Klomp DW. Efficient spectral editing at 7 T: GABA detection with MEGA-sLASER. *Magn Reson Med* (2012) 68(4):1018–25. doi:10.1002/mrm.24131
- Gruetter R. Automatic, localized in vivo adjustment of all first- and second-order shim coils. *Magn Reson Med* (1993) 29:804–11. doi:10.1002/mrm.1910290613

## AUTHOR CONTRIBUTIONS

AM was involved in the design of the study, data acquisition, data analysis, and writing of the manuscript. RM and HH were involved in the design of the study, data analysis, and writing of the manuscript. DK, WC, RK, and PL were involved in the design of the study and revising the manuscript.

## ACKNOWLEDGMENTS

This research was funded by the Netherlands Organisation for Scientific Research (NWO) VIDI Grant 917-46-370 (to HP); Utrecht University High Potential Grant (to HP).

33. Versluis MJ, Kan HE, van Buchem MA, Webb AG. Improved signal to noise in proton spectroscopy of the human calf muscle at 7 T using localized B1 calibration. *Magn Reson Med* (2010) 63:207–11. doi:10.1002/mrm.22195
34. Boer VO, van Lier AL, Hoogduin JM, Wijnen JP, Luijten PR, Klomp DW. 7-T (1) H MRS with adiabatic refocusing at short TE using radiofrequency focusing with a dual-channel volume transmit coil. *NMR Biomed* (2011) 24:1038–46. doi:10.1002/nbm.1641
35. Waddell KW, Avison MJ, Joers JM, Gore JC. A practical guide to robust detection of GABA in human brain by J-difference spectroscopy at 3 T using a standard volume coil. *Magn Reson Imaging* (2007) 25:1032–8. doi:10.1016/j.mri.2006.11.026
36. De Graaf RA. NMR Processing Software for Spectroscopy, Imaging and Spectroscopic Imaging (1999) [Computer Software].
37. Govindaraju V, Young K, Maudsley AA. Proton NMR chemical shifts and coupling constants for brain metabolites. *NMR Biomed* (2000) 13:129–53. doi:10.1002/1099-1492(200005)13:3<129::AID-NBM619>3.3.CO;2-M
38. Behar KL, Rothman DL, Spencer DD, Petroff OA. Analysis of macromolecule resonances in 1H NMR spectra of human brain. *Magn Reson Med* (1994) 32:294–302. doi:10.1002/mrm.1910320304
39. Marjanska M, Auerbach EJ, Valabregue R, Van de Moortele PF, Adriany G, Garwood M. Localized 1H NMR spectroscopy in different regions of human brain in vivo at 7 T: T2 relaxation times and concentrations of cerebral metabolites. *NMR Biomed* (2012) 25:332–9. doi:10.1002/nbm.1754
40. Morrison DF. *Multivariate Statistical Methods*. New York: McGraw-Hill (1976).
41. Goldman-Rakic PS. Cellular basis of working memory. *Neuron* (1995) 14:477–85. doi:10.1016/0896-6273(95)90304-6
42. Ackerman PL, Beier ME, Boyle MO. Working memory and intelligence: the same or different constructs? *Psychol Bull* (2005) 131:30–60. doi:10.1037/0033-2909.131.1.30
43. Karlsgodt KH, Kochunov P, Winkler AM, Laird AR, Almasy L, Duggirala R, et al. A multimodal assessment of the genetic control over working memory. *J Neurosci* (2010) 30:8197–202. doi:10.1523/JNEUROSCI.0359-10.2010
44. Muthukumaraswamy SD, Evans CJ, Edden RA, Wise RG, Singh KD. Individual variability in the shape and amplitude of the BOLD-HRF correlates with endogenous GABAergic inhibition. *Hum Brain Mapp* (2012) 33:455–65. doi:10.1002/hbm.21223
45. Karlsgodt KH, Bachman P, Winkler AM, Bearden CE, Glahn DC. Genetic influence on the working memory circuitry: behavior, structure, function and extensions to illness. *Behav Brain Res* (2011) 225:610–22. doi:10.1016/j.bbr.2011.08.016
46. Edden RA, Muthukumaraswamy SD, Freeman TC, Singh KD. Orientation discrimination performance is predicted by GABA concentration and gamma oscillation frequency in human primary visual cortex. *J Neurosci* (2009) 29:15721–6. doi:10.1523/JNEUROSCI.4426-09.2009
47. Boy F, Evans CJ, Edden RA, Singh KD, Husain M, Sumner P. Individual differences in subconscious motor control predicted by GABA concentration in SMA. *Curr Biol* (2010) 20:1779–85. doi:10.1016/j.cub.2010.09.003
48. Puts NA, Edden RA, Evans CJ, McGlone F, McGonigle DJ. Regionally specific human GABA concentration correlates with tactile discrimination thresholds. *J Neurosci* (2011) 31:16556–60. doi:10.1523/JNEUROSCI.4489-11.2011
49. Sporns O. *Networks of the Brain*. Cambridge: The MIT Press (2011).
50. Bullmore E, Sporns O. The economy of brain network organization. *Nat Rev Neurosci* (2012) 13:336–49. doi:10.1038/nrn3214
51. Vaishnavi SN, Vlassenko AG, Rundle MM, Snyder AZ, Mintun MA, Raichle ME. Regional aerobic glycolysis in the human brain. *Proc Natl Acad Sci U S A* (2010) 107:17757–62. doi:10.1073/pnas.1010459107
52. Northoff G, Walter M, Schulte RF, BEck J, Dyak U, Henning A, et al. GABA concentrations in the human anterior cingulate cortex predict negative BOLD responses in fMRI. *Nat Neurosci* (2007) 10:1515–7. doi:10.1038/nn2001
53. Enzi B, Duncan NW, Kaufmann J, Tempelmann C, Wiebking C, Northoff G. Glutamate modulates resting state activity in the perigenual anterior cingulate cortex – a combined fMRI-MRS study. *Neuroscience* (2012) 227:102–9. doi:10.1016/j.neuroscience.2012.09.039
54. Kapogiannis D, Reiter DA, Willette AA, Mattson MP. Posteromedial cortex glutamate and GABA predict intrinsic functional connectivity of the default mode network. *Neuroimage* (2013) 64:112–9. doi:10.1016/j.neuroimage.2012.09.029
55. Takei Y, Fujihara K, Tagawa M, Hironaga N, Near J, Kasagi M, et al. The inhibition/excitation ratio related to task-induced oscillatory modulations during a working memory task: a multimodal-imaging study using MEG and MRS. *Neuroimage* (2016) 128:302–15. doi:10.1016/j.neuroimage.2015.12.057
56. Marsman A, Boer VO, Luijten PR, Hulshoff Pol HE, Klomp DWJ, Mandl RCW. Detection of glutamate alterations in the human brain using 1H-MRS: comparison of STEAM and sLASER at 7T. *Front Psychiatry* (2017) 8:60. doi:10.3389/fpsyg.2017.00060
57. Rowland LM, Summerfelt A, Wijtenburg SA, Du X, Chiappelli JJ, Krishna N, et al. Frontal glutamate and gamma-aminobutyric acid levels and their associations with mismatch negativity and digit sequencing task performance in schizophrenia. *JAMA Psychiatry* (2016) 73(2):166–74. doi:10.1001/jamapsychiatry.2015.2680

**Conflict of Interest Statement:** The authors declare that the research was conducted in the absence of any commercial or financial relationships that could be construed as a potential conflict of interest.

Copyright © 2017 Marsman, Mandl, Klomp, Cahn, Kahn, Luijten and Hulshoff Pol. This is an open-access article distributed under the terms of the Creative Commons Attribution License (CC BY). The use, distribution or reproduction in other forums is permitted, provided the original author(s) or licensor are credited and that the original publication in this journal is cited, in accordance with accepted academic practice. No use, distribution or reproduction is permitted which does not comply with these terms.



# Risk-Conferring Glutamatergic Genes and Brain Glutamate Plus Glutamine in Schizophrenia

Juan R. Bustillo<sup>1,2,3\*</sup>, Veena Patel<sup>4</sup>, Thomas Jones<sup>1,2</sup>, Rex Jung<sup>5</sup>, Nattida Payaknait<sup>1,2</sup>, Clifford Qualls<sup>6</sup>, Jose M. Canive<sup>1,2,3,7</sup>, Jingyu Liu<sup>4,8</sup>, Nora Irma Perrone-Bizzozero<sup>1,2,3</sup>, Vince D. Calhoun<sup>1,2,3,4,8</sup>, Jessica A. Turner<sup>4,9</sup> and Charles Gasparovic<sup>4</sup>

<sup>1</sup>Department of Psychiatry, University of New Mexico, Albuquerque, NM, United States, <sup>2</sup>Department of Behavioral Sciences, University of New Mexico, Albuquerque, NM, United States, <sup>3</sup>Department of Neurosciences, University of New Mexico, Albuquerque, NM, United States, <sup>4</sup>Mind Research Network, Albuquerque, NM, United States, <sup>5</sup>Department of Neurosurgery, University of New Mexico, Albuquerque, NM, United States, <sup>6</sup>Department of Mathematics and Statistics, University of New Mexico, Albuquerque, NM, United States, <sup>7</sup>The New Mexico VA Health Care System, Albuquerque, NM, United States, <sup>8</sup>Department of Electrical Engineering, University of New Mexico, Albuquerque, NM, United States, <sup>9</sup>Department of Psychology, Georgia State University, Atlanta, GA, United States

## OPEN ACCESS

### Edited by:

Anouk Marsman,  
Copenhagen University  
Hospital Hvidovre, Denmark

### Reviewed by:

Gabriele Ende,  
Central Institute of Mental Health,  
Germany

Philip R. Corlett,  
Yale University, United States

### \*Correspondence:

Juan R. Bustillo  
jbustillo@salud.unm.edu

### Specialty section:

This article was submitted to  
Neuroimaging and Stimulation,  
a section of the journal  
Frontiers in Psychiatry

Received: 30 January 2017

Accepted: 24 April 2017

Published: 12 June 2017

### Citation:

Bustillo JR, Patel V, Jones T, Jung R, Payaknait N, Qualls C, Canive JM, Liu J, Perrone-Bizzozero NI, Calhoun VD, Turner JA and Gasparovic C (2017) Risk-Conferring Glutamatergic Genes and Brain Glutamate Plus Glutamine in Schizophrenia. *Front. Psychiatry* 8:79.  
doi: 10.3389/fpsy.2017.00079

**Background:** The proton magnetic resonance spectroscopy (<sup>1</sup>H-MRS) signals from glutamate (or the combined glutamate and glutamine signal—Glx) have been found to be greater in various brain regions in people with schizophrenia. Recently, the Psychiatric Genetics Consortium reported that several common single-nucleotide polymorphisms (SNPs) in glutamate-related genes confer increased risk of schizophrenia. Here, we examined the relationship between presence of these risk polymorphisms and brain Glx levels in schizophrenia.

**Methods:** <sup>1</sup>H-MRS imaging data from an axial, supraventricular tissue slab were acquired in 56 schizophrenia patients and 67 healthy subjects. Glx was measured in gray matter (GM) and white matter (WM) regions. The genetic data included six polymorphisms genotyped across an Illumina 5M SNP array. Only three of six glutamate as well as calcium-related SNPs were available for examination. These included three glutamate-related polymorphisms (rs10520163 in CLCN3, rs12704290 in GRM3, and rs12325245 in SLC38A7), and three calcium signaling polymorphisms (rs1339227 in RIMS1, rs7893279 in CACNB2, and rs2007044 in CACNA1C). Summary risk scores for the three glutamate and the three calcium polymorphisms were calculated.

**Results:** Glx levels in GM positively correlated with glutamate-related genetic risk score but only in younger ( $\leq 36$  years) schizophrenia patients ( $p = 0.01$ ). Glx levels did not correlate with calcium risk scores. Glx was higher in the schizophrenia group compared to levels in controls in GM and WM regardless of age ( $p < 0.001$ ).

**Conclusion:** Elevations in brain Glx are in part, related to common allelic variants of glutamate-related genes known to increase the risk for schizophrenia. Since the glutamate risk scores did not differ between groups, some other genetic or environmental factors likely interact with the variability in glutamate-related risk SNPs to contribute to an increase in brain Glx early in the illness.

**Keywords:** glutamate, genetics, single-nucleotide polymorphisms, spectroscopy, schizophrenia

## INTRODUCTION

Higher brain glutamate, glutamine, or glutamate plus glutamine (Glx) measured with proton magnetic resonance spectroscopy ( $^1\text{H}$ -MRS) have been reported in schizophrenia, more consistently in subcortical regions (1). Though striatal elevations decrease with antipsychotic treatment (2), higher levels are reported in subjects at-risk for psychosis, as well as in never-medicated and chronic schizophrenia groups (1). This suggests that the elevations persist in medicated patients, although perhaps to a less severe extent and may be a trait variable (1). Consistent with this, in the largest sample to date (schizophrenia = 104, healthy control = 97), we reported higher Glx in medial frontal and parietal cortical regions, in clinically stable medicated schizophrenia patients (3). The *N*-methyl-d-aspartate receptor hypofunction model is a potential mechanism to account for increased glutamate metabolites in schizophrenia. It postulates dysfunction of these receptors in gamma-amino-butyric acid interneurons. Presumably, this results in disinhibition of pyramidal neurons and a paradoxical increase in presynaptic glutamate release across multiple cortical and subcortical fields. Though several genes have been proposed (4), the mechanisms accounting for increased glutamate in schizophrenia remain unknown.

Two studies have examined specific relationships of putative schizophrenia-related genes and brain glutamate levels in patients with the illness, with negative findings (5, 6). Recently, the Psychiatric Genetics Consortium [PGC (7)], the most comprehensive genome-wide association study to date, reported that 6 of 108 loci found to confer risk for schizophrenia involve genes clearly implicated in brain glutamate function (several other identified loci are likely to affect glutamate metabolism and synaptic function indirectly). However, there have been no investigations examining the impact of polymorphisms in these genes on brain glutamate concentrations in people with schizophrenia.

In the present study, we examined the relationships between three of the six glutamate-related risk-conferring single-nucleotide polymorphisms (SNPs) identified by the PGC and brain glutamate levels in schizophrenia and healthy control subjects (the other three SNPs could not be measured with the platform used). To evaluate the specificity of the relationship, we also examined correlations with calcium signaling SNPs also found to confer risk for schizophrenia by the PGC. A subgroup of subjects from our recent  $^1\text{H}$ -MRS study (3) for whom a saliva sample for genomics was collected was included. Because these common SNPs alleles clearly confer risk for the illness, are in genes directly involved in brain glutamate function (7), and Glx is abnormally increased in schizophrenia (1, 3), we hypothesized that schizophrenia subjects with a higher score of risk-conferring glutamate-related SNPs would have higher Glx brain levels. Because we previously reported increased Glx in both gray matter (GM) and white matter (WM) of medial frontal and parietal regions in schizophrenia subjects (3), we examined both tissue types without specific predictions.

## MATERIALS AND METHODS

### Subjects

Patients with schizophrenia were recruited from the University of New Mexico Hospitals and the Albuquerque Veterans Affairs

Medical Center. Inclusion criteria were (1) DSM IV TR diagnosis of schizophrenia made through consensus by two research psychiatrists using the information from a structured interview (SCID DSM IV TR, Patient Version), medical records, and family informants and (2) clinically stable on the same antipsychotic medications for at least 4 weeks. Exclusion criteria were (1) diagnosis of neurological disorder, (2) current substance use disorder (except for nicotine), (3) metallic implants, (4) claustrophobia, and (5) other than Caucasian ancestry. Healthy controls were additionally excluded for any of the following: (1) any current DSM IV TR axis I disorder [determined with SCID DSM IV TR Non-Patient Version; (except current nicotine) or any past history of a disorder (except for substance use)] and (2) a first degree relative with a psychotic disorder. The local internal review board approved the study. Subjects provided written informed consent and were paid for their participation.

### Clinical Assessments

Patients were assessed for psychopathology with the Positive and Negative Syndrome Scale (8), the Simpson Angus Scale [SAS (9)] for parkinsonism, the Barnes Akathisia Rating Scale (10), and the Abnormal Involuntary Movement Scale (11). Assessments were completed within 1 week of scanning.

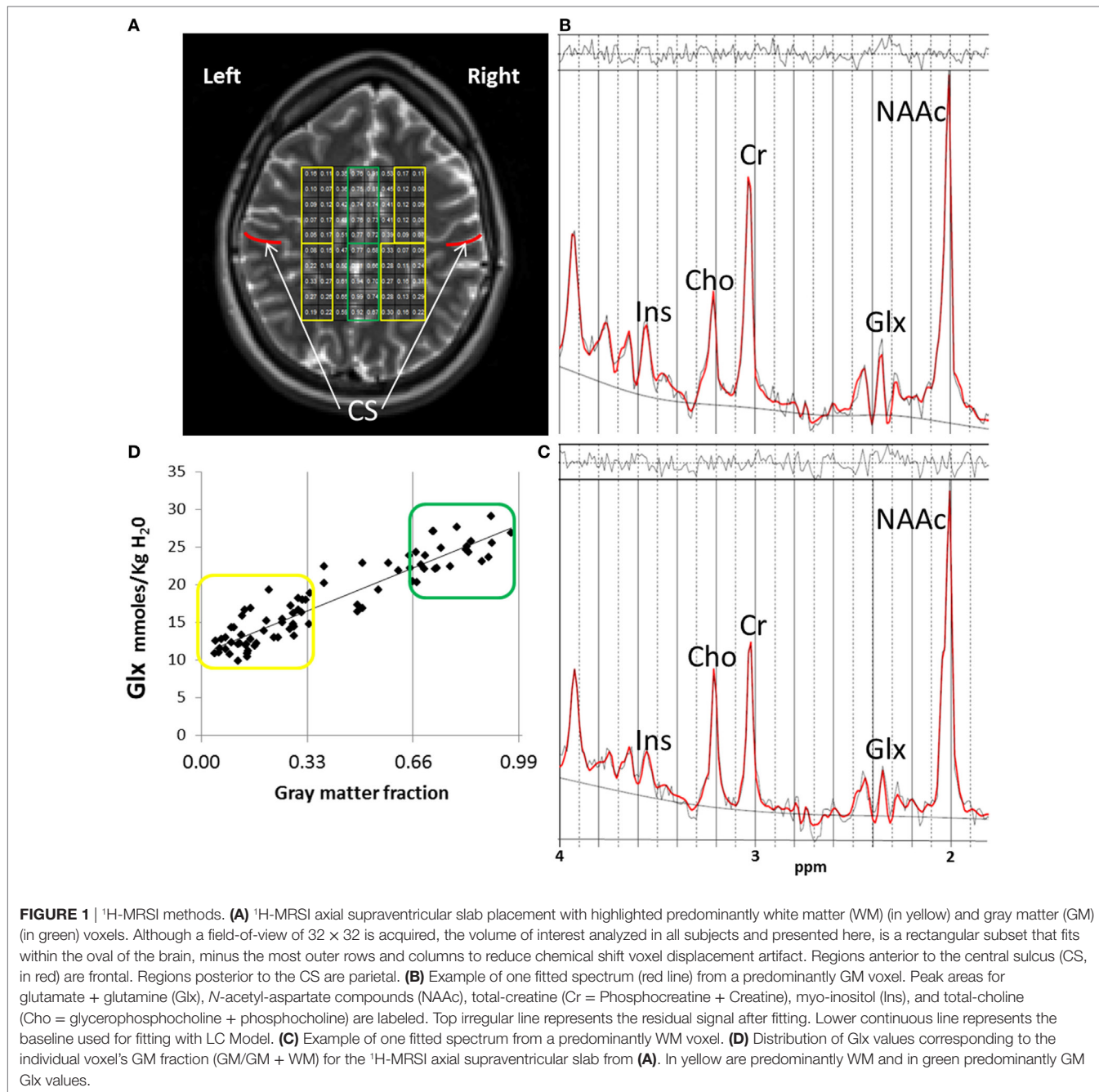
### Magnetic Resonance Studies

#### Acquisition

Scanning was performed on a 3-T scanner (VB-17; 12 channel head-coil). Subjects were told to try to remain awake during the acquisition but no task was implemented. T1-weighted images were collected with 3D-MPRAGE for voxel tissue segmentation (TR/TE/TI 1,500/3.87/700 ms, flip angle 10°, field-of-view = 256 mm × 256 mm, 1-mm thick slice).  $^1\text{H}$ -MRS imaging was performed with a phase-encoded version of a point-resolved spectroscopy sequence, to allow the simultaneous acquisition of multiple voxels as described previously (12). Acquisitions were obtained both with and without water presaturation. The following parameters were used: TE = 40 ms, TR = 1,500 ms, slice thickness = 15 mm, FOV = 220 mm × 220 mm, circular *k*-space sampling (radius = 12), Cartesian *k*-space size = 32 × 32 after zero filling, *k*-space Hamming filter with 50% width and number of averages = 1, total scan time = 582 s. The nominal voxel size was 0.71 cm<sup>3</sup> but the effective voxel volume is estimated to be 2.4 cm<sup>3</sup>, taking into account the *k*-space sampling and filtering. The  $^1\text{H}$ -MRSI volume of interest was prescribed from an axial T<sub>2</sub>-weighted image to lie immediately above the lateral ventricles and parallel to the anterior-posterior commissure axis, and included portions of the cingulate gyrus and the medial frontal and parietal lobes (Figure 1A). To minimize the chemical shift artifact, the transmitter was set to the frequency of the NAA methyl-peak during the acquisition of the metabolite spectra and to the frequency of the water-peak during the acquisition of the unsuppressed water spectra.

#### Spectral Fitting

Data were automatically preprocessed and fitted using LC Model [Version 6.1 (13)] with a simulated basis-set for the sequence parameters which included the following metabolites: alanine,



aspartate, creatine, phosphocreatine, gamma-amino-butyric acid, glutamine, glutamate, glycerophosphocholine, phosphocholine, myo-inositol, lactate,  $N$ -acetyl-aspartate,  $N$ -acetyl-aspartylglutamate, scyllo-inositol, and guanidine. Lipids and macromolecule contributions were fitted using the default simulated intensities of LC Model, which included soft constraints for peak position and line width and prior probabilities of the ratios of macromolecule and lipid peaks. Spectra were fitted in the range between 1.8 and 4.2 ppm and scaled to the non-suppressed water intensity (12). The SD of the fit of the Glx signals, provided by LC Model (related to the Cramer–Rao lower bounds and a measure

of the confidence of the fit) was used to exclude data with low confidence. Only data with an LC Model SD  $\leq 20\%$  were further analyzed (13) (**Figures 1B,C**).

#### Partial-Volume–Relaxation Correction

The Glx results from LC Model were corrected as described previously and are reported in units of molality (moles/kg tissue water) (14). Briefly, the Glx signals were corrected for partial-volume and relaxation effects using GM, WM, and cerebrospinal fluid (CSF) maps from segmented T1-weighted images with SPM5. Water densities and relaxation times in each tissue or CSF compartment

were obtained from the literature, for this correction (14). Our group has previously documented the test-retest reliability of these methods (12). As previously discussed (3), voxels were further classified based on their GM fraction as [100 × GM/(GM + WM) as “predominantly” GM (>66%) or “predominantly” WM < 34%; **Figure 1D**]. Finally, because glutamate and glutamine concentrations vary depending on tissue type and most voxels contained various proportions of GM and WM (15), we also used the GM fraction of each voxel as a covariate in the statistical analyzes (see below).

## Genetics

### SNP Selection and Analyzes

Our aim was to study the six SNPs identified in the PGC (7) involved in glutamatergic function and the six SNPs involved in calcium signaling (**Table 1**). The genetic data originated from each subject's saliva samples processed via 5M Illumina HumanOmni5-Quad SNP array (Illumina, www.illumina.com) and we used Illumina Genome Studio Genotyping Module to optimize call rates. Genome wide scan data from each participant underwent quality assurance testing before inclusion in the analysis. Requirements per SNP included a minor allele frequency greater than 5%, Hardy-Weinberg equilibrium ( $p < 10^{-6}$ ), and data for over 90% of participants in the sample. Three individuals missing over 10% of the total SNPs found in the platform were excluded. Only three of the glutamate-related and three of the calcium signaling SNPs were available for 125 subjects.

### Imputation

Any missing genotypes at the six loci of interest were selectively imputed via IMPUTE2 software (v2.3.1) and the 1000 Genomes Phase 3 reference dataset. SNPs rs12704290, rs12325245, and rs1339227 were imputed for all subjects. SNP rs2007044 was imputed for 1 subject. Imputed SNPs demonstrated a 0.9 or greater imputation probability estimate.

### Adjustment

For each subject, the number of risk alleles (1 for homozygous non-risk, 2 for heterozygous, and 3 for homozygous risk) was multiplied by the odds ratio (OD) for schizophrenia from the PGC (12) at each SNP. In order to examine the potential effect of ethnicity, we used PLINK to calculate 10 multidimensional scaling (MDS) factors (equivalent to principal components) from the subjects' SNP array data. The top principal components are generally associated with population structure, in other words ethnicity information. The top MDS factors were entered into the relevant PROC-MIXED model.

### Summary Scores

Each SNP OD-adjusted risk value was summed to a total risk score (range 3–9) for glutamate-related SNPs and for calcium signaling SNPs. The direction of effect on Glx brain levels of a risk allele is unknown. However, as proof of concept, the total risk score approach supports the testing of the hypothesis that a higher risk score would positively correlate with the more abnormal (higher) Glx levels in schizophrenia [reported in the literature (1, 3)].

### Statistical Analysis

We examined whether the relationships between brain Glx and glutamate-related and calcium signaling genetic risk scores differed across schizophrenia and healthy controls. Because Glx brain levels differ by tissue type and age (15), and there are progressive tissue changes in schizophrenia (16), these variables (age and voxel tissue composition) must be considered in the analyzes. PROC-MIXED (SAS version-9) uses all available data, accounts for correlation between repeated measurements in the same subject (i.e., Glx in many voxels), and can handle missing data more appropriately than other methods (17). Hence, we implemented four repeated-measures PROC-MIXED analyzes: glutamate-related risk score and Glx in GM (1) and in WM (2); as well as calcium signaling risk score and Glx in GM (3) and in

**TABLE 1 |** Genotype distribution of the available glutamate-related and calcium signaling risk single-nucleotide polymorphisms (SNPs) from the PGC study in schizophrenia and healthy control subjects.

Schizophrenia PGC			Genotype distribution (current sample)							
Gene	SNP	Rank (of 108)	Available	Homozygous non-risk		Heterozygous		Homozygous risk		
				HC	Sz	HC	Sz	HC	Sz	
Glutamate	GRM3 (7q21.12)	rs12704290	48	Yes	0.0	0.02	0.13	0.1	0.86	0.88
	CLCN3 (4q.33)	rs10520163	59	Yes	0.16	0.29	0.59	0.55	0.23	0.16
	SLC38A7 (16q21)	rs12325245	98	Yes	0.84	0.83	0.16	0.14	0.0	0.03
	GRIN2A (16p13.2)	rs9922678	90	No	—	—	—	—	—	—
	GRIA1 (5q33.2)	rs79212538	79	No	—	—	—	—	—	—
	SRR (17p13.3)	rs4523957	47	No	—	—	—	—	—	—
Calcium	CACNA1C (12)	rs2007044	4	Yes	0.52	0.45	0.31	0.40	0.16	0.16
	CACNB2 (10)	rs7893279	20	Yes	0.21	0.22	0.16	0.17	0.63	0.60
	RIMS1 (6q12-13)	rs1339227	108	Yes	0.05	0.07	0.27	0.24	0.69	0.69
	CACNA1 (22q13.1)	Chr22_39987017_D	41	No	—	—	—	—	—	—
	NRG (11)	rs55661361	24	No	—	—	—	—	—	—
	ATP2A2 (12)	rs4766428	58	No	—	—	—	—	—	—

PGC is Psychiatric Genetics Consortium (7); HC is healthy control group ( $n = 67$ ); Sz is schizophrenia group ( $n = 58$ ).

WM (4) ( $p = 0.05/4$ , Bonferroni-corrected  $p = 0.0125$ ). Each of these omnibus tests included *Glx* concentration in all selected voxels as the repeated-measures dependent variable, with the following independent variables: *risk score* as the within-subject factor, *diagnostic-group* (schizophrenia, healthy control) as the between-group factor and age as a covariate. In order to facilitate the visualization (by plotting data) of the hypothesized correlations between *Glx* concentrations (continuous) and risk scores (continuous), age was dichotomized into *age-group* for the model; we chose a median split of  $\leq 36$  years as a neutral cutoff (results did not differ with age dichotomization of  $< 30$  or  $> 45$ ).

As in our previous  $^1\text{H}$ -MRS imaging study (3), we followed a hierarchical, systematic approach to statistical analyzes. To address type-1 errors, only the highest order significant interactions involving *diagnostic-group* and *risk score* (the relevant variables of interest) are presented in the *Results* and followed-up with PROC-MIXED *post hoc* tests; this protects the *post hoc* tests for type-I errors (18, 19). In order to control for effects of *diagnostic-group* differences in spectral fitting [e.g., bias in metabolite values due to worse quality in the ill group as previously reported (3)], we used the Cramer–Rao lower bounds (CRLB = SD/concentration  $\times 100$ ). The CRLB (not the SD reported by LC Model) should be used to account for group differences in spectral quality, since CRLB is independent of concentration (personal communication, Provencher, creator of LC Model). Hence, if the groups differed in CRLBs, GM fraction, relevant demographic or substance use characteristics, these were entered into the model as additional covariates. The potential confound of antipsychotic medication was examined by adding the drug dosage as standardized olanzapine equivalents (20) to the appropriate model in the schizophrenia group. Likewise, the effects of various symptom severity and neurological side-effects measures were examined in each relevant model. All tests were two-tailed and we used Satterthwaite's correction for unequal variances.

## RESULTS

### Demographics, Substance Use History, and Quality of Spectral Fitting

Fifty-eight schizophrenia and 67 healthy controls were studied. There were no significant differences between the groups in: age, gender, Hispanic ethnicity, socioeconomic status (SES) of the subject, or SES of the family of origin, smoking status, vascular risk factors, or history of opiate or sedative use disorders (Table 2). Schizophrenia subjects had more frequent lifetime histories of alcohol ( $p = 0.006$ ), cannabis ( $p < 0.001$ ), cocaine ( $p = 0.02$ ), hallucinogens ( $p = 0.004$ ), and stimulant use disorders ( $p = 0.05$ ). Also, the schizophrenia group had slightly, but significantly, higher CRLB for *Glx* ( $\text{Glx}_{\text{CRLB}}$ ) in GM ( $F_{1,123} = 53.3$ ,  $p < 0.001$ ) and WM ( $F_{1,123} = 36.9$ ,  $p < 0.001$ ). However, schizophrenia and controls did not differ in GM fractions for GM ( $p = 0.11$ ) or for WM ( $p = 0.15$ ). As expected, CSF proportion across voxels was higher in the schizophrenia than the control group ( $p < 0.001$ ). This difference was addressed by the partial-volume correction method (14).

**TABLE 2 |** Demographic, clinical, and spectral quality characteristics of the subjects.

	Schizophrenia (n = 58)	Healthy controls (n = 67)
Age, years	38 ± 14	36 ± 12
Gender (male/female)	46/12	49/18
Hispanic (yes/no)	19/37	24/43
Socioeconomic status (SES)	4.5 ± 1.6	4.3 ± 1.5
Parental SES	4.1 ± 1.7	3.9 ± 1.5
Smoker (yes/no)	13/42	18/49
Vascular risk score <sup>a</sup>	2.0 ± 1.8	2.3 ± 1.8
History of alcohol use disorder (yes/no)	18/36	7/54*
History of cannabis use disorder (yes/no)	15/39	1/60*
History of hallucinogen use disorder (yes/no)	4/50	0/61*
History of stimulant use disorder (yes/no)	7/47	0/61*
History of cocaine use disorder (yes/no)	5/49	0/61*
History of opiate use disorder (yes/no)	3/51	0/61
History of sedative use disorder (yes/no)	2/52	0/61
Current smoker (yes/no)	13/42	18/49
$\text{Glx}_{\text{CRLB}}^{\text{b}}$ gray matter (GM)	3.8 ± 0.8	3.6 ± 0.7*
$\text{Glx}_{\text{CRLB}}$ white matter (WM)	2.6 ± 0.6	2.5 ± 0.4*
GM fraction GM	0.819 ± 0.1	0.813 ± 0.1
GM fraction WM	0.150 ± 0.08	0.146 ± 0.08
Cerebrospinal fluid per voxel	0.085 ± 0.1	0.073 ± 0.09*
Age onset psychosis	20.9 ± 8.4	N/A
Positive symptoms	14.8 ± 5.2	N/A
Negative symptoms	14.6 ± 4.0	N/A
Tardive dyskinesia	4.2 ± 3.6	N/A
Parkinsonism	9.5 ± 2.0	N/A
Akathisia	0.2 ± 0.5	N/A
Antipsychotic dose in mgs <sup>c</sup>	14.8 ± 12.5	N/A

\* $p < 0.05$ .

<sup>a</sup>Vascular risk score, 0–4 (score of 1 each for cardiac illness, hypertension, dyslipidemia, and diabetes).

<sup>b</sup>CRLB is Cramer–Rao lower bounds (CRLB = SD × metabolite concentration/100).

<sup>c</sup>Glx is glutamate + glutamine.

<sup>d</sup>In olanzapine equivalents (20).

± is for SD.

### Glx and Glutamate-Related Risk Scores Gray Matter

Glx was positively correlated with glutamate risk score but only in the younger schizophrenia group (*diagnostic-group* × *age-group* × *risk-score*:  $F_{1,117} = 6.8$ ,  $p = 0.01$ ; Figure 2). This three-way interaction remained after adjusting for  $\text{Glx}_{\text{CRLB}}$  (actually became more robust,  $F_{1,117} = 10.5$ ,  $p = 0.001$ ), as well as after controlling for histories of alcohol, cannabis, cocaine, stimulant, and hallucinogen use ( $p$ 's between 0.002 and 0.003). Also the three-way interaction remained after adding the top 3, 4, or 5 MDS factors to address potential effects of ethnicity ( $p$ 's between 0.02 and 0.008). *Post hoc* PROC-MIXED confirmed that among the younger *age-group*, the relationships between Glx and *risk-score* differed between the schizophrenia and control groups ( $F_{1,59} = 9.9$ ,  $p = 0.003$ ). However, among the older *age-group*, these correlations did not differ between schizophrenia and control groups ( $F_{1,58} = 0.55$ ,  $p = 0.46$ ). Still, when examining the whole schizophrenia group, the associations between Glx and risk score differed between the younger and the older *age-groups* ( $F_{1,54} = 5.9$ ,  $p = 0.02$ ). Finally, in a test randomizing the dependent variable (Glx) 1,000 times, the observed (6.8) or higher  $F$  values occurred in 2 of the 1,000

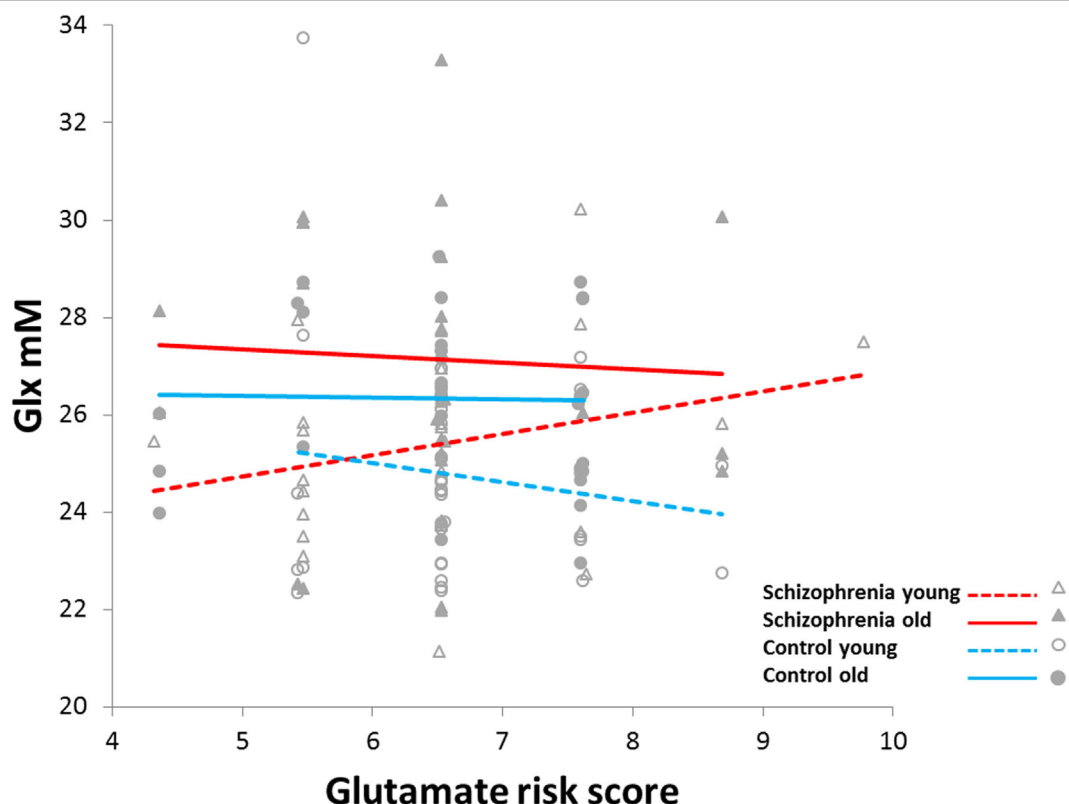


**FIGURE 2 |** Increased slope of glutamine plus glutamate (Glx) concentration versus glutamate-related risk score in younger schizophrenia (<36 years) compared to younger controls, older schizophrenia ( $\geq 36$  years), and older controls ( $F_{1,117} = 6.8, p = 0.01$ ).

permutations ( $p = 0.002$ ). This provides further support that the above findings are unlikely to be the result of chance variations.

The differences in relationships between Glx and genetic score among the younger and older schizophrenia *age-groups* remained when accounting for age of onset of psychosis ( $p = 0.04$ ), positive ( $p = 0.04$ ) and depressive symptoms ( $p = 0.03$ ), antipsychotic dose ( $p = 0.01$ ) and severity of tardive dyskinesia ( $p = 0.007$ ), parkinsonism ( $p = 0.02$ ), and akathisia ( $p = 0.02$ ). However, the differences became a trend when adjusting for negative symptoms score ( $F_{1,52} = 3.5, p = 0.07$ ). Finally, severity of negative symptoms did not differ between younger ( $14.9 \pm 4.3$ ) and older ( $14.2 \pm 3.8$ ) schizophrenia patients ( $p = 0.5$ ).

### White Matter

A significant *diagnostic-group*  $\times$  *age-group*  $\times$  *risk-score* interaction ( $F_{1,117} = 7.7, p = 0.007$ ), disappeared when adjusting for Glx<sub>CRLB</sub> ( $F_{1,117} = 0.2, p = 0.65$ ). There were no other significant interactions or main effects involving *diagnostic-group*; see Supplementary Material for full statistical model.

### Glx and Calcium Signaling Risk Scores

#### Gray Matter

The only significant effect involving diagnosis was the *diagnostic-group*  $\times$  *risk-score* interaction ( $F_{1,119} = 5.0, p = 0.03$ ). However, significance disappeared when adjusting for Glx<sub>CRLB</sub> ( $F_{1,119} = 0.05, p = 0.82$ ).

### White Matter

A significant *diagnostic-group*  $\times$  *age-group*  $\times$  *risk-score* interaction ( $F_{1,117} = 8.4, p = 0.005$ ), disappeared when adjusting for Glx<sub>CRLB</sub> ( $F_{1,117} = 0.2, p = 0.63$ ).

### Group Differences for Genetic Risk Scores and Glx Levels

Not surprisingly in this small sample, genetic *risk-scores* did not differ between the schizophrenia and the healthy controls for glutamate ( $t_{123} = 1.02, p = 0.31$ ) or for calcium-related ( $t_{123} = 0.02, p = 0.98$ ) SNPs. Glx was higher in the schizophrenia compared to the control group, adjusting for age or tissue type ( $F_{1,122} = 26.5, p < 0.001$ ); however, this is not a new finding but merely a statement that the subgroup examined in this report behaves similar to the full sample from the original study (3) in terms of Glx levels.

### DISCUSSION

We found that among younger subjects with schizophrenia, scores in glutamate-related risk-conferring SNPs positively correlated with Glx levels in GM. In older schizophrenia patients, as in the healthy controls regardless of age, there was no such relationship. This pattern of relationships was not found for *risk-scores* in neuronal calcium signaling SNPs and was not accounted by variance in antipsychotic dose or other common confounds, such as prior

substance use histories or the quality of spectral fitting. Finally, Glx levels were higher in the schizophrenia group but the genetic risks scores did not differ from the healthy controls.

Only two other studies have examined the relationship between a glutamate-related gene and *in vivo* brain glutamate in schizophrenia. Ongur et al. (5) reported that a haplotype of four SNPs within the glutaminase 1 (GLS1) gene was positively associated with the glutamine/glutamate ratio (Gln/Glu) in the parieto-occipital cortex. The sample included a combination of subjects with schizophrenia, bipolar disorder, and healthy controls but there was no difference in the haplotype score versus Gln/Glu correlation across the groups. Gruber et al. (6) found that methionine homozygous carriers for the val66met SNP (*rs6265*) of the brain-derived neurotrophic factor (BDNF) gene had lower hippocampal glutamate in a combined group of schizophrenia, bipolar disorder, and healthy controls. Again, there were no differences in the associations across groups. However, the PGC did not rank any SNPs in GLS1 or BDNF into the top 108 schizophrenia risk loci (7).

What do these findings tell us about the pathophysiology of schizophrenia? The positive correlation between glutamate-related genes and GM Glx in the younger schizophrenia group is somewhat specific (i.e., not seen with the calcium signaling genes). *GRM3* codes for a glutamate receptor predominantly expressed in astrocytes (21); *CLCN3* is a voltage-gated chloride channel critical for glutamate reuptake in synaptic vesicles of neurons (22); and *SLC38A7* encodes a sodium-coupled L-glutamine transporter expressed in neurons (23). In addition, <sup>1</sup>H-MRS visible Glx includes metabolic and neurotransmitter glutamate pools, as well as glutamine, and most glutamine is the product of synaptic glutamate re-uptaked by glial cells (24). Hence, variability in specific common SNPs in these genes, known to confer risk for schizophrenia, can be plausibly related to abnormally increased levels of Glx in GM, though elucidation of the specific mechanisms will require additional experimental approaches. However, the normal range in glutamate *risk-scores* found in our schizophrenia sample is not sufficient to account for increases in Glx. Hence, some other factors, genetic and/or environmental, must interact with the glutamate genetic risk to increase glutamatergic cortical levels during the early course of the illness. Likewise, this relationship is not apparent in older schizophrenia subjects, with similar glutamate risks scores, also suggests that other factors affect Glx concentration in schizophrenia. Epigenetic factors, like differential methylation of glutamate risk genes during the course of illness, could potentially affect Glx brain levels. In support of this possibility, our recent MRI/genetic/epigenetic preliminary data showed that variation in methylation of PGC gene loci is more robustly related to GM concentration reductions in schizophrenia than the variability in the risk-conferring SNPs themselves (25). Alternatively, other non-specific factors like aging or disease duration may increase Glx levels and obscure a relationship with risk scores in the older subjects.

This study had several strengths, including the assessment of many GM and WM voxels with standardized metrics of quality of spectral fits. As in our recent report (3), controlling for group differences in CRLB can have major effects on the results. However, some limitations must be acknowledged. First, the sample size is

small, and replication is necessary. We are not currently aware of a similar <sup>1</sup>H-MRS imaging database of supraventricular Glx in schizophrenia with broad SNP characterization for a replication. However, ours is the first proof-of-principle study documenting an association between risk-conferring glutamate-related SNPs and Glx brain levels in schizophrenia. With greater standardization of <sup>1</sup>H-MRS protocols, future larger studies would be able to clearly document the extent of specific genetic contributions to glutamatergic dysfunction. Second, glutamate was not resolved from glutamine in this study, and Glx levels do not reflect the rate of glutamatergic metabolism, which would be a more functionally relevant measure. Glutamate and glutamine are present in all brain cell types, so <sup>1</sup>H-MRS measurements combine several functional compartments. Hence, interpretation of Glx brain differences is not straight forward. <sup>13</sup>C-MRS, though technically demanding and yet to be widely applied in large human samples, could in future studies assess more directly glutamate and glutamine metabolic cycling and their relationship to glutamate-related risk genes in schizophrenia. Third, Glx measurements were acquired without controlling for cognitive state, which can affect glutamate levels (26). Fourth, schizophrenia subjects were treated with antipsychotic medications, agents known to affect brain glutamate levels (2). However, adjustment for antipsychotic dosage within the schizophrenia group, did not cancel the difference in correlations between *risk-score* and Glx concentrations across the younger and older *age-groups*. Fourth, only three of the six glutamate and three of the six calcium-related SNPs from PGC were examined due to limited coverage of the Illumina SNP array used. Hence, a complete assessment of the six risk-conferring SNPs could yield different results. Furthermore, it is possible that other risk genes involved in a metabolic pathway that feeds into glutamatergic neurotransmission may also be related to Glx brain concentrations. Fifth, the cortical regions studied were not found to have increased Glx in a recent meta-analysis (1). However, the meta-analysis was published before our recent study, which has by far the largest sample [ $N = 201$  (3)]; still the supplemental data of the meta-analysis showed a small effect size (0.12) for Glx greater in Sz than controls in medial frontal cortex, consistent with our results. Sixth, our criteria for excluding subjects with missing SNP data (>10% of the total SNPs) may be somewhat liberal. Finally, the schizophrenia group had a greater past history of several substance use disorders that could affect Glx levels (27). However, controlling for this history did not eliminate the main findings.

In summary we report in younger schizophrenia patients, a positive relationship between GM Glx levels, with a combined score for glutamate-related SNPs found to confer risk for the illness. This relationship is somewhat specific, as it is not present in WM (which also had increased Glx in schizophrenia), or for calcium signaling SNPs (which also confer risk for schizophrenia). The overall findings suggest that though variance in some common SNPs may indeed contribute to the increased cortical glutamate levels in schizophrenia, other genetic and/or environmental mechanisms must also be involved early in the disease. Future studies very early in the illness with greater Glx brain coverage and examining epigenetic factors that modulate the impact of specific risk-conferring SNPs may shed further light

on the underlying neurobiology of glutamatergic dysfunction in schizophrenia. Also, modulators of presynaptic glutamate release may be particularly effective for patient subgroups early in the illness and which have dysregulation of central nervous system glutamatergic tone (28).

## ETHICS STATEMENT

This study was carried out in accordance with the recommendations of UNM-HSC Human Research Review Committee with written informed consent from all subjects. All subjects gave written informed consent in accordance with the Declaration of Helsinki. The protocol was approved by the Human Research Review Committee.

## AUTHOR CONTRIBUTIONS

JB: design, data collection and analyses, and writing of the manuscript. VP, NP, TJ, RJ, CQ, NP-B, JL, JC, JT, VC, and CG: data analyses and writing of the manuscript.

## REFERENCES

- Merritt K, Egerton A, Kempton MJ, Taylor MJ, McGuire PK. Nature of glutamate alterations in schizophrenia: a meta-analysis of proton magnetic resonance spectroscopy studies. *JAMA Psychiatry* (2016) 73(7):665–74. doi:10.1001/jamapsychiatry.2016.0442
- de la Fuente-Sandoval C, Leon-Ortiz P, Azcarraga M, Stephano S, Favila R, Diaz-Galvis L, et al. Glutamate levels in the associative striatum before and after 4 weeks of antipsychotic treatment in first-episode psychosis: a longitudinal proton magnetic resonance spectroscopy study. *JAMA Psychiatry* (2013) 70(10):1057–66. doi:10.1001/jamapsychiatry.2013.289
- Bustillo JR, Jones T, Chen H, Lemke N, Abbott C, Qualls C, et al. Glutamatergic and neuronal dysfunction in gray and white matter: a spectroscopic imaging study in large schizophrenia sample. *Schizophr Bull* (2016) 43(3):611–9. doi:10.1093/schbul/sbw122
- Harrison PJ, Weinberger DR. Schizophrenia genes, gene expression, and neuropathology: on the matter of their convergence. *Mol Psychiatry* (2005) 10(1):40–68; image 5. doi:10.1038/sj.mp.4001558
- Ongur D, Haddad S, Prescott AP, Jensen JE, Siburian R, Cohen BM, et al. Relationship between genetic variation in the glutaminase gene GLS1 and brain glutamine/glutamate ratio measured in vivo. *Biol Psychiatry* (2011) 70(2):169–74. doi:10.1016/j.biopsych.2011.01.033
- Gruber O, Hasan A, Scherk H, Wobrock T, Schneider-Axmann T, Ekawardhani S, et al. Association of the brain-derived neurotrophic factor val66met polymorphism with magnetic resonance spectroscopic markers in the human hippocampus: in vivo evidence for effects on the glutamate system. *Eur Arch Psychiatry Clin Neurosci* (2012) 262(1):23–31. doi:10.1007/s00406-011-0214-6
- Schizophrenia Working Group of the Psychiatric Genomics Consortium. Biological insights from 108 schizophrenia-associated genetic loci. *Nature* (2014) 511(7510):421–7. doi:10.1038/nature13595
- Kay SR, Fiszbein A, Opler LA. The Positive and Negative Syndrome Scale (PANSS) for schizophrenia. *Schizophr Bull* (1987) 13(2):261–76. doi:10.1093/schbul/13.2.261
- Simpson GM, Angus JW. A rating scale for extrapyramidal side effects. *Acta Psychiatr Scand Suppl* (1970) 212:11–9. doi:10.1111/j.1600-0447.1970.tb02066.x
- Barnes TR. A rating scale for drug-induced akathisia. *Br J Psychiatry* (1989) 154:672–6. doi:10.1192/bjp.154.5.672
- Schooler NR, Kane JM. Research diagnoses for tardive dyskinesia. *Arch Gen Psychiatry* (1982) 39(4):486–7. doi:10.1001/archpsyc.1982.04290040080014
- Gasparovic C, Bedrick EJ, Mayer AR, Yeo RA, Chen H, Damaraju E, et al. Test-retest reliability and reproducibility of short-echo-time spectroscopic imaging of human brain at 3T. *Magn Reson Med* (2011) 66(2):324–32. doi:10.1002/mrm.22858
- Provencher SW. Automatic quantitation of localized in vivo 1H spectra with LCModel. *NMR Biomed* (2001) 14(4):260–4. doi:10.1002/nbm.698
- Gasparovic C, Song T, Devier D, Bockholt HJ, Caprihan A, Mullins PG, et al. Use of tissue water as a concentration reference for proton spectroscopic imaging. *Magn Reson Med* (2006) 55(6):1219–26. doi:10.1002/mrm.20901
- Maudsley AA, Domenig C, Govind V, Darkazanli A, Studholme C, Arheart K, et al. Mapping of brain metabolite distributions by volumetric proton MR spectroscopic imaging (MRSI). *Magn Reson Med* (2009) 61(3):548–59. doi:10.1002/mrm.21875
- Olabi B, Ellison-Wright I, McIntosh AM, Wood SJ, Bullmore E, Lawrie SM. Are there progressive brain changes in schizophrenia? A meta-analysis of structural magnetic resonance imaging studies. *Biol Psychiatry* (2011) 70(1):88–96. doi:10.1016/j.biopsych.2011.01.032
- Gueorguieva R, Krystal JH. Move over ANOVA: progress in analyzing repeated-measures data and its reflection in papers published in the archives of general psychiatry. *Arch Gen Psychiatry* (2004) 61(3):310–7. doi:10.1001/archpsyc.61.3.310
- Day B. *Statistical Methods in Cancer Research Volume I – The Analysis of Case-Control Studies*. Lyon: IARC Publications (1980). 196 p.
- Koopman L. *An Introduction to Contemporary Statistics*. Kent: PWS-Kent Publishers (1981).
- Gardner DM, Murphy AL, O'Donnell H, Centorrino F, Baldessarini RJ. International consensus study of antipsychotic dosing. *Am J Psychiatry* (2010) 167(6):686–93. doi:10.1176/appi.ajp.2009.09060802
- Sun W, McConnell E, Pare JF, Xu Q, Chen M, Peng W, et al. Glutamate-dependent neuroglial calcium signaling differs between young and adult brain. *Science* (2013) 339(6116):197–200. doi:10.1126/science.1226740
- Stobrawa SM, Breiderhoff T, Takamori S, Engel D, Schweizer M, Zdebik AA, et al. Disruption of ClC-3, a chloride channel expressed on synaptic vesicles, leads to a loss of the hippocampus. *Neuron* (2001) 29(1):185–96. doi:10.1016/S0896-6273(01)00189-1
- Hagggrund MG, Sreedharan S, Nilsson VC, Shaik JH, Almkvist IM, Backlin S, et al. Identification of SLC38A7 (SNAT7) protein as a glutamine transporter expressed in neurons. *J Biol Chem* (2011) 286(23):20500–11. doi:10.1074/jbc.M110.162404
- Rae CD. A guide to the metabolic pathways and function of metabolites observed in human brain 1H magnetic resonance spectra. *Neurochem Res* (2014) 39(1):1–36. doi:10.1007/s11064-013-1199-5
- Lin DLJ, Chen J, Sui J, Du Y, Calhoun VD. Exploration of genetic and epigenetic effects on brain gray matter density in schizophrenia. *12th International Imaging Genetics Conference*. Irvine (2016).

## ACKNOWLEDGMENTS

The authors are grateful to Nicholas Lemke and Patrick Gallegos, employees of the UNM Department of Psychiatry and Behavioral Sciences and to Diana South and Cathy Smith, MRN employees, for their contributions with data collection.

## FUNDING

This study was supported by NIMH R01MH084898 to JB, NIMH 2R01MH065304 and VACSR&D IIR-04-212-3 to JC and 1P20RR021938/P20GM103472 and 1R01EB006841 to VC and DHHS/NIH/NCRR 3 UL1 RR031977-02S2.

## SUPPLEMENTARY MATERIAL

The Supplementary Material for this article can be found online at <http://journal.frontiersin.org/article/10.3389/fpsy.2017.00079/full#supplementary-material>.

26. Apsvalka D, Gadic A, Clemence M, Mullins PG. Event-related dynamics of glutamate and BOLD effects measured using functional magnetic resonance spectroscopy (fMRS) at 3T in a repetition suppression paradigm. *Neuroimage* (2015) 118:292–300. doi:10.1016/j.neuroimage.2015.06.015
27. Prisciandaro JJ, Schacht JP, Prescott AP, Renshaw PE, Brown TR, Anton RF. Associations between recent heavy drinking and dorsal anterior cingulate N-acetylaspartate and glutamate concentrations in non-treatment-seeking individuals with alcohol dependence. *Alcohol Clin Exp Res* (2016) 40(3):491–6. doi:10.1111/acer.12977
28. Kinon BJ, Millen BA, Zhang L, McKinzie DL. Exploratory analysis for a targeted patient population responsive to the metabotropic glutamate 2/3 receptor agonist pomaglumetad methionil in schizophrenia. *Biol Psychiatry* (2015) 78(11):754–62. doi:10.1016/j.biopsych.2015.03.016

**Conflict of Interest Statement:** JB received honoraria for advisory board consulting from Otsuka America Pharmaceutical Inc. in 2013. VP, TJ, RJ, NP, CQ, JC, JL, NP-B, VC, JT, and CG reported no biomedical financial interests or potential conflicts of interest.

Copyright © 2017 Bustillo, Patel, Jones, Jung, Payaknait, Qualls, Canive, Liu, Perrone-Bizzozero, Calhoun, Turner and Gasparovic. This is an open-access article distributed under the terms of the Creative Commons Attribution License (CC BY). The use, distribution or reproduction in other forums is permitted, provided the original author(s) or licensor are credited and that the original publication in this journal is cited, in accordance with accepted academic practice. No use, distribution or reproduction is permitted which does not comply with these terms.



# Effects of Antipsychotic Administration on Brain Glutamate in Schizophrenia: A Systematic Review of Longitudinal $^1\text{H}$ -MRS Studies

Alice Egerton<sup>1\*</sup>, Akarmi Bhachu<sup>1</sup>, Kate Merritt<sup>1</sup>, Grant McQueen<sup>1</sup>, Agata Szulc<sup>2</sup> and Philip McGuire<sup>1</sup>

<sup>1</sup> Department of Psychosis Studies, King's College London, Institute of Psychiatry, Psychology and Neuroscience, London, UK, <sup>2</sup> Department of Psychiatry, Medical University of Warsaw, Warsaw, Poland

## OPEN ACCESS

### Edited by:

Paul Croarkin,  
Mayo Clinic, USA

### Reviewed by:

Milan Scheidegger,  
ETH Zurich, Switzerland  
Meredith A. Reid,  
Auburn University, USA

### \*Correspondence:

Alice Egerton  
alice.egerton@kcl.ac.uk

### Specialty section:

This article was submitted  
to Neuroimaging and Stimulation,  
a section of the journal  
*Frontiers in Psychiatry*

Received: 31 January 2017

Accepted: 10 April 2017

Published: 28 April 2017

### Citation:

Egerton A, Bhachu A, Merritt K, McQueen G, Szulc A and McGuire P (2017) Effects of Antipsychotic Administration on Brain Glutamate in Schizophrenia: A Systematic Review of Longitudinal  $^1\text{H}$ -MRS Studies. *Front. Psychiatry* 8:66.  
doi: 10.3389/fpsy.2017.00066

Schizophrenia is associated with brain glutamate dysfunction, but it is currently unclear whether antipsychotic administration can reduce the extent of glutamatergic abnormality. We conducted a systematic review of proton magnetic resonance spectroscopy ( $^1\text{H}$ -MRS) studies examining the effects of antipsychotic treatment on brain glutamate levels in schizophrenia. The Medline database was searched to identify relevant articles published until December 2016. Inclusion required that studies examined longitudinal changes in brain glutamate metabolites in patients with schizophrenia before and after initiation of first antipsychotic treatment or a switch in antipsychotic treatment. The searches identified eight eligible articles, with baseline and follow-up measures in a total of 168 patients. The majority of articles reported a numerical reduction in brain glutamate metabolites with antipsychotic treatment, and the estimated overall mean reduction of 6.5% in Glx (the combined signal from glutamate and glutamine) across brain regions. Significant reductions in glutamate metabolites in at least one brain region were reported in four of the eight studies, and none of the studies reported a significant glutamatergic increase after antipsychotic administration. Relationships between the degree of change in glutamate and the degree of improvement in symptoms have been inconsistent but may provide limited evidence that antipsychotic response may be associated with lower glutamate levels before treatment and a greater extent of glutamatergic reduction during treatment. Further longitudinal, prospective studies of glutamate and antipsychotic response are required to confirm these findings.

**Keywords:** schizophrenia, magnetic resonance spectroscopy, glutamates, antipsychotics, treatment response

## INTRODUCTION

Animal, postmortem, and genetic studies indicate that schizophrenia is associated with abnormalities in glutamatergic neurotransmission (1), but it is unclear whether antipsychotic treatment may impact on glutamate dysfunction in patients. Our recent meta-analysis suggests that schizophrenia is associated with a general elevation in glutamate metabolites, with some variation observed across brain regions and patient subgroups (2). Elevations in frontal cortical or hippocampal glutamate may lead to secondary elevations in striatal dopamine release, characteristic of schizophrenia (3–6).

Observations of glutamate dysfunction prior to illness onset (7–9), and in patients who are antipsychotic naïve or who have received minimal antipsychotic treatment (10, 11), suggest that glutamatergic dysregulation is a pathological feature of schizophrenia, rather than an effect of antipsychotic exposure. However, it is unknown whether antipsychotic treatment can reduce, or indeed worsen, glutamatergic abnormalities. Potentially, modulation of glutamatergic transmission with antipsychotic treatment could occur *via* downstream effects of D2 antagonism and/or *via* interactions at other receptor subtypes. Alternatively, if current antipsychotics do not adequately address glutamatergic dysfunction, this would support the suggestion that adjunctive treatment with glutamatergic agents may have additional therapeutic benefit.

The idea that antipsychotics may modulate glutamatergic neurotransmission is supported by experimental animal studies showing a reduction in frontal cortical glutamate following administration of some, but not all antipsychotics (12–19). In rodents, decreases in frontal glutamate have been observed using *ex vivo* proton nuclear magnetic resonance (<sup>1</sup>H-NMR) following administration of clozapine and olanzapine, but not haloperidol, risperidone, or aripiprazole (12). *In vivo* microdialysis studies in rodents have demonstrated reductions in pharmacologically induced elevations in frontal glutamate by risperidone, paliperidone, clozapine, aripiprazole, olanzapine, and haloperidol (13–19). However, a lack of significant effects of haloperidol on resting or stimulated glutamate metabolites in the rat brain have also been reported (19–22), and when antipsychotics are administered in the absence of pharmacologically stimulated glutamate release, antipsychotic-induced glutamate elevations may also be observed (23, 24). Together, these studies may suggest that antipsychotic glutamate-modulatory effects may be dependent on the animal model or glutamatergic assay, as well as the level of basal glutamatergic tone. Differential effects of antipsychotics may also be mediated by differing receptor binding profiles, and it has been suggested that downregulation of 5HT<sub>2A</sub> receptors by antipsychotics with high 5HT<sub>2A</sub> affinity may be important in reducing glutamatergic signaling (15, 16).

In man, brain glutamate levels can be measured *in vivo* using proton magnetic resonance spectroscopy (<sup>1</sup>H-MRS), usually within a specific *a priori* brain region of interest. Depending on the achieved resolution, <sup>1</sup>H-MRS can provide concentration estimates for glutamate and glutamine or, at lower field strengths, the combined glutamate plus glutamine signal, which is termed Glx. The idea that antipsychotics may reduce glutamate elevation in schizophrenia is supported by a cross-sectional study that detected an elevation in Glx in non-medicated, but not in medicated schizophrenia (25). In our recent meta-analysis, meta-regression showed no significant relationship between regional glutamate, glutamine, or Glx and mean chlorpromazine equivalent antipsychotic dose (2). Nonetheless, longitudinal studies examining glutamate metabolites before and after antipsychotic treatment are required to address this question directly. Several such studies have now been published and the purpose of this article is to provide systematic review of their findings.

As a second objective, we also review the relationships between glutamate and symptomatic response in longitudinal studies of

antipsychotic treatment. Cross-sectional <sup>1</sup>H-MRS studies show that glutamate metabolite levels differ between patients who have or have not responded well to antipsychotic treatment (26–29). This may suggest that glutamate level may predict the degree to which symptoms are likely to respond to antipsychotic administration, or that symptom reduction occurs in parallel with antipsychotic glutamatergic modulation. We, therefore, appraised the evidence from longitudinal studies for the value of glutamate levels in predicting or monitoring antipsychotic response.

## METHODS

### Study Selection

The review was conducted in accordance with PRISMA guidelines (30). The Medline electronic database was searched to identify journal articles published until 19 December 2016, using the following freeform and MeSH search terms: (“GLUTAMATE” OR “GLX”) AND (“SPECTROSCOPY” OR “MRS”) AND (“ANTIPSYCHOTIC”) AND (“SCHIZOPHRENIA” OR “PSYCHOSIS”). Reference lists of the returned articles were hand searched for further relevant publications.

Inclusion required that articles were published in peer-reviewed journals in English or English translation. Inclusion also required that studies reported <sup>1</sup>H-MRS glutamate, glutamine, or Glx before and after either first initiation of antipsychotic medication or initiation of a change in antipsychotic administration. Inclusion was limited to investigations performed in patients with first episode psychosis, schizophrenia, or schizoaffective disorder. Where separate articles reported overlapping datasets, the article reporting the largest dataset was included. Where articles reported glutamate measures over multiple time-points, the glutamate measure at longest time-point was included to provide maximal time for any antipsychotic effects to emerge.

Returned articles were initially screened for inclusion through reading of article titles and abstracts. Full text was then screened for articles potentially meeting the inclusion criteria. Two authors independently performed the searches and identified articles for inclusion (Akarmi Bhachu and Alice Egerton).

### Data Extraction

For qualitative comparison of antipsychotic-induced change in glutamate metabolites across studies, the percentage difference in glutamatergic metabolite level over the antipsychotic treatment period was extracted from each article. This was calculated as the percentage mean difference (PMD), where PMD = [(mean glutamate metabolite level after treatment – mean glutamate metabolite level before treatment)/mean glutamate metabolite level before treatment] × 100. Where these values were not reported (31, 32), they were extracted from figures using WebPlotDigitizer (<http://arohatgi.info/WebPlotDigitizer>). Extracted data also included the reported statistical significance of the change in glutamatergic metabolite over the antipsychotic treatment period, the demographic and clinical characteristics of the sample, the antipsychotic/s prescribed and the duration of treatment, and the brain region investigated.

## RESULTS

The initial search identified 51 articles, of which 40 were excluded at the title and abstract screening stage. At the full-text screening, one study was excluded as it was not available in English (33). Analysis of the sample reported in Ref. (34) was subsequently extended (35). One article (36) was excluded as it reported a sub-sample of participants included in a larger cohort and longer term follow-up (31). This resulted in final inclusion of eight original articles (10, 31, 32, 34, 37–40).

## Methodological Characteristics

The methodological characteristics of the included articles are provided in **Table 1**. Eight articles provided glutamate measures at baseline and after antipsychotic administration in a total of 168 patients. The sample sizes completing to  $^1\text{H}$ -MRS follow-up ranged from 7 to 42 patients. Three studies recruited patients with first episode psychosis who were antipsychotic naïve or had received minimal antipsychotic exposure (10, 31, 37). A further study in first episode psychosis did not describe antipsychotic exposure prior to baseline glutamatergic measurement (39). Two studies in chronic schizophrenia included washout periods of at least 7 days prior to baseline glutamate measurement and antipsychotic re-initiation (34, 40). One study in chronic schizophrenia investigated the change in glutamate measures following a switch from conventional antipsychotic treatment to olanzapine and did not include a washout period (38). The final study did not specify stage of illness, but included only patients who were antipsychotic naïve or antipsychotic-free for a minimum of 6 months (32).

The majority of studies examined glutamatergic change in samples including patients on a variety of typical and atypical antipsychotic drugs, administered as standard clinical care (10, 31, 32, 34, 39) (**Table 1**). The remaining three studies investigated specific antipsychotic compounds, with one study investigating olanzapine (38) and two studies investigating risperidone (37, 40). The antipsychotic treatment period ranged from 1 to 80 months.

Four studies acquired glutamate measures at a field strength of 1.5-T and, therefore, reported glutamate primarily as the combined Glx signal (32, 34, 38, 40). Two studies were performed at 3-T, one of which reported Glx (39) and one of which reported both glutamate and Glx (37). The remaining two studies, performed at 4-T, reported glutamate, glutamine (10, 31), and Glx (31).

Glutamatergic measures were reported as water-scaled values in ratio to voxel creatine (Cr) (32, 34, 38–40) or corrected for voxel cerebrospinal fluid (CSF) content (10, 31, 37). Brain regions investigated included the frontal cortex (seven studies), thalamus (four studies), temporal cortex (two studies), basal ganglia or striatum (two studies), parieto–occipital cortex (one study), and cerebellum (one study) (**Table 2**).

## Effect of Antipsychotic Treatment on Brain Glutamate Levels

Across brain regions, the PMD in Glx after antipsychotic treatment ranged from a 12.5% increase (38) to a 27% decrease (39). In the majority of observations (10 out of 15), there was a numerical reduction in Glx, with an overall mean decrease of 6.5% (**Figure 1**). The PMD in Glx could not be calculated from the information available in one article (10). A decrease in Glx of 6.5% ( $\pm 11\%$ ) can be estimated to be associated with an effect size of approximately  $d_z = 0.6$ . Accordingly, this translates to a within-subjects' sample size of 24 patients to observe a significant change in Glx over antipsychotic treatment, at 80% power and  $\alpha = 0.05$ , two-tailed.

Four of the eight included studies reported statistically significant glutamatergic reductions over antipsychotic treatment in at least one brain region investigated (31, 34, 37, 39). Specifically, significant reductions in Glx occurred in the thalamus over 80 months of mixed antipsychotic administration (31), in the left temporal lobe over 2 months of mixed antipsychotic administration (34), and in the frontal lobe over 6 months of mixed antipsychotic administration (39), and in glutamate in right striatum over 1 month of risperidone administration (37). Additionally, Choe et al. (32) also reported a reduction in prefrontal cortical Glx over 1–6 months antipsychotic treatment in 29/34 patients but did not report the statistical outcome associated with this finding. Extraction and analysis of data from the figure provided in the article found a significant reduction in frontal cortical Glx [mean  $\pm$  SD Glx at baseline:  $0.95 \pm 0.30$ ; follow-up:  $0.75 \pm 0.31$ ; paired samples *t*-test:  $t(29) = 3.06$ ;  $P = 0.005$ ]. There were no reports of significant increases in glutamate metabolites with antipsychotic treatment. Three of the eight studies did not report significant effects of antipsychotic treatment on glutamate measures in any brain area across the patient sample (10, 38, 40).

**TABLE 1 | Methodological characteristics of studies investigating the effects of antipsychotics on brain glutamate measures.**

Reference	N	Age	Illness stage	DOI	AP regime	AP	Pre-baseline AP	Months
(32)	34	NR	NR	NR	NR	Hal; Tfpz; Pzd; Clz	Naïve or >6 months w/o	1–6
(38)	14	NR	SZ	NR	Fixed	OI	Conventional AP, no w/o	2
(40)	14	$32 \pm 7$	SZ	$9 \pm 6$	Fixed	Ri	>7 days	2
(10)	7	$27 \pm 9$	FEP	$0.6 \pm 0.8$	Flexible	Qu, Ri, Ar, Hal	Lifetime exposure <3 weeks	12
(31)	17	$25 \pm 7$	FEP	$1.8 \pm 2$	Flexible	Hal, Zpx, Ri, Ol, Qu, Zip; Clz	Naïve	80
(34)	42	$32 \pm 6$	SZ	$0.2 \pm 0.5$	Flexible	Ri, Ol, Clz, Pz, Cpz, Ppz	w/o >7 days	1.4–2.1
(39)	16	$31 \pm 12$	FEP	NR	Flexible	Ri, Olz, Ar, Qu	NR	6
(37)	24	$27 \pm 8$	FEP	$0.4 \pm 0.5$	Fixed	Ri	Naïve	1

Age, mean  $\pm$  SD years; AP, antipsychotic; DOI, mean  $\pm$  SD duration of illness in years; FEP, first episode psychosis; N, number of patients completing the follow-up assessment; NR, not reported; SZ, schizophrenia; w/o, washout period; Ar, aripiprazole; Clz, clozapine; Hal, haloperidol; Ol, olanzapine; Ppz, perphenazine; Pz, perazine; Pzd, pimozide; Qu, quetiapine; Ri, risperidone; Tfpz, trifluoperazine; Zip, ziprasidone; Zpx, zuclopentixol.

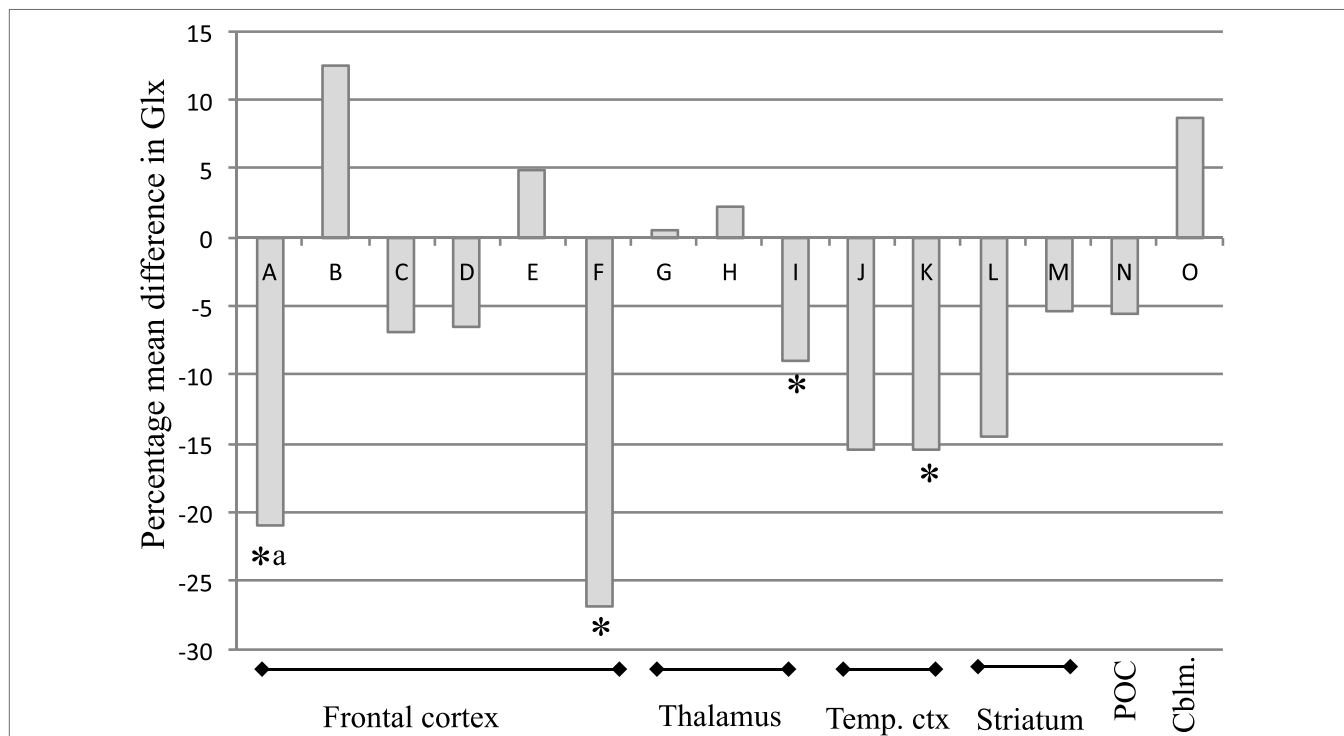
**TABLE 2 | Results of studies investigating the effects of antipsychotics on brain glutamate measures and relationships with symptoms.**

Reference	Voxel location	Field strength (T)	Glutamate measure	PMD	Relationships with symptom change
(32)	FC	1.5	Glx/Cr	-21 <sup>a,b</sup>	Positive correlation between $\Delta$ Glx and $\Delta$ BPRS score
(38)	R. ACC L. ACC	1.5	Glx/Cr	+12	NS correlation between $\Delta$ Glx and $\Delta$ SANS total score. Sig. increase in Glx in responders (+46%) compared to non-responders (-21%)
(40)	L. FC L. TC L. Thal	1.5	Glx/Cr	-7 -16 0.5	NS correlation between $\Delta$ Glx and $\Delta$ PANSS
(10)	ACC L. FWM L. Thal	4	Glu; Gln; /CSF	NA	
(31)	L. ACC L. Thal	4	Glx; Glu; Gln; /CSF Glx; Glu; Gln; /CSF	5, 5, 4 -9 <sup>a</sup> , -1, -16	Positive correlation between $\Delta$ Glx in L. Thal and Life Skills Profile Rating Scale score at follow-up
(34)	L. FC L. TC L. Thal	1.5	Glx/Cr	-6 -15 <sup>a</sup> 2	NS correlation between $\Delta$ Glx in temporal lobe and $\Delta$ PANSS
(39)	FC L. BG POC	3	Glx/Cr	-27 <sup>a</sup> -14 -5	NS correlations between $\Delta$ Glx and $\Delta$ PANSS
(37)	R. Striatum Cblm	3	Glx; Glu; /CSF Glx; Glu; /CSF	-5; -7 <sup>a</sup> +9; +3	Negative correlation between both $\Delta$ Glx and $\Delta$ Glu in R. striatum and $\Delta$ PANSS general score

ACC, anterior cingulate cortex; BG, basal ganglia; BPRS, Brief Psychiatric Rating Scale; Cblm, cerebellum; Cr, scaled to voxel creatine; CSF, corrected for voxel cerebrospinal fluid content;  $\Delta$ , change; L, left; FC, frontal cortex; FWM, frontal white matter; Gln, glutamine; Glu, glutamate; Glx, glutamate plus glutamine; NA, not available; NS, non-significant; PANSS, positive and negative syndrome scale for schizophrenia; PMD, percentage mean difference; POC, parieto-occipital cortex; R, right; SANS, scale for assessment of negative symptoms; TC, temporal cortex; Thal, thalamus.

<sup>a</sup>Reported as significant finding.

<sup>b</sup>Significance calculated from figure in article.

**FIGURE 1 | Percentage mean difference (PMD) in Glx in individual studies of Glx at baseline and after antipsychotic administration in schizophrenia.**

PMD was calculated as [(mean Glx level at after treatment – mean Glx level before treatment)/mean Glx level before treatment]  $\times$  100. Abbreviations: Glx, combined signal from glutamate and glutamine; Temp. ctx, temporal cortex; POC, parieto-occipital cortex; Cblm, cerebellum. Letters relate to articles as follows: A (32) B (38) C (40) D (34) E (31) F (39) G (40) H (34) I (31) J (40) K (34) L (39) M (37) N (39) O (37). \*Reported as significant finding; <sup>a</sup>Significance calculated from figure in article.

## Relationships between Change in Glutamate and Symptom Reduction on Antipsychotic Administration

The included studies reported mixed findings regarding associations between the degree of change in glutamate and the degree of symptomatic reduction with antipsychotic treatment (**Table 2**). Significant positive associations were reported for change in frontal Glx and change in the total score on the Brief Psychiatric Rating Scale (BPRS) (32), and for change in striatal glutamate and Glx and change in Positive and Negative Syndrome Scale (PANSS) general symptom score (37). One study reported a positive correlation between the change in thalamic Glx over 80 months antipsychotic treatment and Life Skills Profile Rating Scale Score at 80 months (31). These observations suggest that a greater degree of glutamate reduction is associated with a greater degree of symptomatic improvement during antipsychotic treatment. However, four of the eight included studies reported no significant correlations between changes in glutamate metabolite levels and changes in symptom severity (34, 38–40). While one of these studies found no significant correlation between change in glutamate and change in the Scale for Assessment of Negative Symptoms (SANS) total score on olanzapine administration (38), a secondary analysis dividing the group into responders and non-responders based on the change in SANS total score found a 46% Glx increase in responders, compared to a 21% Glx decrease in non-responders, and a significant difference between these groups (38). This is broadly inconsistent with the reports of positive associations between glutamate reduction and symptom reduction (32, 37).

None of the studies included in the review examined whether glutamate measures before antipsychotic treatment predicted the degree of subsequent symptomatic response to antipsychotic administration. However, a separate article (35) presenting additional analysis of data presented in a previous article (34) found that frontal Glx at baseline was significantly lower in subsequent responders than non-responders.

## DISCUSSION

The main finding of this review is that the majority of studies reported a numerical reduction in glutamate metabolites following antipsychotic treatment in schizophrenia, with half of the reviewed studies finding significant reductions in at least one brain region. In contrast, no significant increases in glutamate metabolites were reported. Schizophrenia is associated with a general increase in glutamate metabolites, which varies with region and with illness stage (2). This review provides some suggestion that antipsychotics may reduce glutamatergic elevations in schizophrenia but indicates that this effect may be relatively small or limited to subgroups of patients.

The mean change in Glx over antipsychotic treatment was estimated from the available data as a decrease in the range of 6.5% across regions, which would require a within-subjects' sample size of 24 patients to achieve 80% power. Only three of the eight available studies had sample sizes of 24 or more patients (32, 34, 37) and the three studies with the smallest sample sizes (10, 38, 40) were the studies that did not find significant effects of

antipsychotics on glutamatergic measures, suggesting that they may have been underpowered. Two of these smaller studies (38, 40) also differed in that they recruited patients with long antipsychotic medication histories, which may have also limited the ability to observe further glutamatergic reduction.

Our estimates of percentage reduction in glutamatergic metabolites following antipsychotic treatment in schizophrenia and the associated sample size calculations are limited by the availability of relatively few published studies. These studies have also investigated different brain regions, and glutamate dysfunction in schizophrenia may vary by region as well as by illness stage (2). In some cases, it was also necessary to extract values from published figures, which is less accurate than using reported values, and measures included both creatine-scaled or voxel CSF corrected data. As further studies become available, estimates of the percentage reduction can be updated and formal meta-analyses of effect sizes can be performed including inspection of potential influences such as regional specificity, patient subgroups, and duration of antipsychotic treatment. General limitations of <sup>1</sup>H-MRS include the estimation of the total concentrations of glutamate metabolites in the voxel, rather than imaging of glutamate involved in neurotransmission specifically, and inability to resolve glutamate from glutamine at lower field strengths and thereby interpretation of the combined Glx signal. Advanced methodological approaches, such as <sup>1</sup>H-MRS at high field strengths or <sup>13</sup>C-MRS to inspect glutamate cycling may address some of these issues in future studies.

Reductions in glutamate metabolites following antipsychotic treatment would be consistent with the cross-sectional report of elevated prefrontal cortical Glx in non-antipsychotic medicated but not antipsychotic-medicated schizophrenia (25). While the mechanism by which antipsychotics might reduce glutamate is not yet clear, rodent studies also find reductions in basal or stimulated glutamate following administration of some antipsychotics (12–19), which may relate to the 5HT<sub>2A</sub> antagonist activity of atypical agents (16, 41, 42). Atypical antipsychotics may also indirectly modulate glutamate release by modifying glutamatergic receptor activity or density (43–45). The majority of patients included in the reviewed studies were prescribed atypical antipsychotics, which may, therefore, have increased the potential to observe glutamatergic reductions. Future studies could specifically compare the ability of D2-selective antipsychotics to antipsychotics with marked 5HT<sub>2A</sub> affinity to modulate glutamate in schizophrenia.

The timescales over which antipsychotic effects on glutamatergic measures have been evaluated range from 4 weeks (37) to 7 years (31). It might be predicted that longer durations of antipsychotic treatment may be associated with progressive glutamate reductions. Across the included studies, there was not suggestion of this, for example significant decreases in frontal Glx were observed after administration of antipsychotics for 1–6 months (32, 39), but not 12 or 80 months (10, 31). Individual studies that included repeated glutamatergic measurement also do not evidence progressive glutamatergic reduction (10, 31). This may suggest that antipsychotic effects on glutamatergic systems are most apparent within the initial stages of treatment, which could be explored in future studies. A further consideration for longitudinal assessment of glutamatergic measures in schizophrenia

is the potential interacting effects of other confounds, such as disease progression, aging effects, or volumetric changes. The study of longest duration detected correlations between the reductions in thalamic glutamine and gray matter loss in the superior temporal gyrus over 30 months (36), and gray matter loss in frontal, parietal, temporal, and limbic regions over 7 years (31), possibly reflecting excitotoxic processes.

The second aim of this article was to review the potential relationships between glutamate and the degree of antipsychotic response in longitudinal studies. Our review only identified one study prospectively examining the relationship between baseline glutamate and subsequent response, which reported higher baseline Glx/Cr across voxels in the frontal and temporal lobes and thalamus in subsequent antipsychotic non-responders than responders (35). Two studies also reported correlations between the extent of glutamatergic reduction and the extent of symptomatic improvement over the antipsychotic treatment period (32, 37). These findings are consistent with observations of higher frontal glutamate levels in some (26, 27, 46), but not all (29), cross-sectional studies comparing treatment-responsive and non-responsive schizophrenia, and of higher striatal Glx/Cr in treatment resistant compared to treatment-responsive patients (29). The observation that glutamate levels may predict antipsychotic response (35) is also supported by recent pharmacogenomic findings that single nucleotide polymorphisms in genes encoding glutamatergic proteins associate with response to risperidone in

first episode psychosis (47). In contrast, the conflicting result of an increase in frontal Glx/Cr in olanzapine responders compared to non-responders was reported in one study (38), and several studies reported no correlations between glutamatergic change and symptomatic improvement (34, 38–40). The idea that antipsychotic administration is less effective in reducing glutamate and improving symptoms in patients with the highest levels of glutamate before treatment could be further explored through re-analysis of existing longitudinal <sup>1</sup>H-MRS studies, and investigated in future longitudinal studies potentially combining glutamate <sup>1</sup>H-MRS with glutamate genetic approaches.

## AUTHOR CONTRIBUTIONS

AE and AB performed the literature searches and data extraction. KM and GM checked data for accuracy. All authors contributed to interpretation of the data and the final draft of the manuscript.

## FUNDING

This study was supported by a grant from the Medical Research Council, UK to Dr. Egerton (MR/L003988/1). This study presents independent research funded in part by the National Institute for Health Research (NIHR) Biomedical Research Centre at South London and Maudsley National Health Service (NHS) Foundation Trust and King's College London.

## REFERENCES

- Javitt DC. Glutamatergic theories of schizophrenia. *Isr J Psychiatry Relat Sci* (2010) 47:4–16.
- Merritt K, Egerton A, Kempton MJ, Taylor MJ, McGuire PK. Nature of glutamate alterations in schizophrenia: a meta-analysis of proton magnetic resonance spectroscopy studies. *JAMA Psychiatry* (2016) 73:665–74. doi:10.1001/jamapsychiatry.2016.0442
- Laruelle M, Kegeles LS, Abi-Dargham A. Glutamate, dopamine, and schizophrenia: from pathophysiology to treatment. *Ann N Y Acad Sci* (2003) 1003:138–58. doi:10.1196/annals.1300.063
- Carlsson A. Neurocircuits and neurotransmitter interactions in schizophrenia. *Int Clin Psychopharmacol* (1995) 10(Suppl 3):21–8. doi:10.1097/00004850-199509003-00004
- Lisman JE, Coyle JT, Green RW, Javitt DC, Benes FM, Heckers S, et al. Circuit-based framework for understanding neurotransmitter and risk gene interactions in schizophrenia. *Trends Neurosci* (2008) 31:234–42. doi:10.1016/j.tins.2008.02.005
- Stone JM, Morrison PD, Pilowsky LS. Glutamate and dopamine dysregulation in schizophrenia – a synthesis and selective review. *J Psychopharmacol* (2007) 21:440–52. doi:10.1177/0269881106073126
- Stone JM, Day F, Tsagarakis H, Valli I, McLean MA, Lythgoe DJ, et al. Glutamate dysfunction in people with prodromal symptoms of psychosis: relationship to gray matter volume. *Biol Psychiatry* (2009) 66:533–9. doi:10.1016/j.biopsych.2009.05.006
- Egerton A, Stone JM, Chaddock CA, Barker GJ, Bonoldi I, Howard RM, et al. Relationship between brain glutamate levels and clinical outcome in individuals at ultra high risk of psychosis. *Neuropsychopharmacology* (2014) 39:2891–9. doi:10.1038/npp.2014.143
- de la Fuente-Sandoval C, Leon-Ortiz P, Favila R, Stephano S, Mamo D, Ramirez-Bermudez J, et al. Higher levels of glutamate in the associative-striatum of subjects with prodromal symptoms of schizophrenia and patients with first-episode psychosis. *Neuropsychopharmacology* (2011) 36:1781–91. doi:10.1038/npp.2011.65
- Bustillo JR, Rowland LM, Mullins P, Jung R, Chen H, Qualls C, et al. (1) H-MRS at 4 Tesla in minimally treated early schizophrenia. *Mol Psychiatry* (2010) 15:629–36. doi:10.1038/mp.2009.121
- Theberge J, Bartha R, Drost DJ, Menon RS, Malla A, Takhar J, et al. Glutamate and glutamine measured with 4.0 T proton MRS in never-treated patients with schizophrenia and healthy volunteers. *Am J Psychiatry* (2002) 159:1944–6. doi:10.1176/appi.ajp.159.11.1944
- McLoughlin GA, Ma D, Tsang TM, Jones DN, Cilia J, Hill MD, et al. Analyzing the effects of psychotropic drugs on metabolite profiles in rat brain using <sup>1</sup>H NMR spectroscopy. *J Proteome Res* (2009) 8:1943–52. doi:10.1021/pr800892u
- Roenker NL, Gudelsky G, Ahlbrand R, Bronson SL, Kern JR, Waterman H, et al. Effect of paliperidone and risperidone on extracellular glutamate in the prefrontal cortex of rats exposed to prenatal immune activation or MK-801. *Neurosci Lett* (2011) 500:167–71. doi:10.1016/j.neulet.2011.06.011
- Abekawa T, Ito K, Nakagawa S, Nakato Y, Koyama T. Effects of aripiprazole and haloperidol on progression to schizophrenia-like behavioural abnormalities and apoptosis in rodents. *Schizophr Res* (2011) 125:77–87. doi:10.1016/j.schres.2010.08.011
- Abekawa T, Ito K, Koyama T. Different effects of a single and repeated administration of clozapine on phencyclidine-induced hyperlocomotion and glutamate releases in the rat medial prefrontal cortex at short- and long-term withdrawal from this antipsychotic. *Naunyn Schmiedebergs Arch Pharmacol* (2007) 375:261–71. doi:10.1007/s00210-007-0154-x
- Lopez-Gil X, Artigas F, Adell A. Role of different monoamine receptors controlling MK-801-induced release of serotonin and glutamate in the medial prefrontal cortex: relevance for antipsychotic action. *Int J Neuropsychopharmacol* (2009) 12:487–99. doi:10.1017/S1461145708009267
- Lopez-Gil X, Babot Z, Amargos-Bosch M, Sunol C, Artigas F, Adell A. Clozapine and haloperidol differently suppress the MK-801-increased glutamatergic and serotonergic transmission in the medial prefrontal cortex of the rat. *Neuropsychopharmacology* (2007) 32:2087–97. doi:10.1038/sj.npp.1301356
- Amitai N, Kuczenski R, Behrens MM, Markou A. Repeated phencyclidine administration alters glutamate release and decreases GABA markers in the

- prefrontal cortex of rats. *Neuropharmacology* (2012) 62:1422–31. doi:10.1016/j.neuropharm.2011.01.008
19. Carli M, Calcagno E, Mainolfi P, Mainini E, Invernizzi RW. Effects of aripiprazole, olanzapine, and haloperidol in a model of cognitive deficit of schizophrenia in rats: relationship with glutamate release in the medial prefrontal cortex. *Psychopharmacology (Berl)* (2011) 214:639–52. doi:10.1007/s00213-010-2065-7
  20. Bustillo J, Barrow R, Paz R, Tang J, Seraji-Bozorgzad N, Moore GJ, et al. Long-term treatment of rats with haloperidol: lack of an effect on brain N-acetyl aspartate levels. *Neuropsychopharmacology* (2006) 31:751–6. doi:10.1038/sj.npp.1300874
  21. Lindquist DM, Dunn RS, Cecil KM. Long term antipsychotic treatment does not alter metabolite concentrations in rat striatum: an *in vivo* magnetic resonance spectroscopy study. *Schizophr Res* (2011) 128:83–90. doi:10.1016/j.schres.2011.02.019
  22. Huang M, Panos JJ, Kwon S, Oyamada Y, Rajagopal L, Meltzer HY. Comparative effect of flurasidone and blonanserin on cortical glutamate, dopamine, and acetylcholine efflux: role of relative serotonin (5-HT)2A and DA D2 antagonism and 5-HT1A partial agonism. *J Neurochem* (2014) 128:938–49. doi:10.1111/jnc.12512
  23. Yamamura S, Ohoyama K, Hamaguchi T, Kashimoto K, Nakagawa M, Kanehara S, et al. Effects of quetiapine on monoamine, GABA, and glutamate release in rat prefrontal cortex. *Psychopharmacology (Berl)* (2009) 206:243–58. doi:10.1007/s00213-009-1601-9
  24. Tanahashi S, Yamamura S, Nakagawa M, Motomura E, Okada M. Clozapine, but not haloperidol, enhances glial D-serine and L-glutamate release in rat frontal cortex and primary cultured astrocytes. *Br J Pharmacol* (2012) 165:1543–55. doi:10.1111/j.1476-5381.2011.01638.x
  25. Kegeles LS, Mao X, Stanford AD, Girgis R, Ojeil N, Xu X, et al. Elevated prefrontal cortex gamma-aminobutyric acid and glutamate-glutamine levels in schizophrenia measured *in vivo* with proton magnetic resonance spectroscopy. *Arch Gen Psychiatry* (2012) 69:449–59. doi:10.1001/archgenpsychiatry.2011.1519
  26. Egerton A, Brugger S, Raffin M, Barker GJ, Lythgoe DJ, McGuire PK, et al. Anterior cingulate glutamate levels related to clinical status following treatment in first-episode schizophrenia. *Neuropsychopharmacology* (2012) 37:2515–21. doi:10.1038/npp.2012.113
  27. Demjaha A, Egerton A, Murray RM, Kapur S, Howes OD, Stone JM, et al. Antipsychotic treatment resistance in schizophrenia associated with elevated glutamate levels but normal dopamine function. *Biol Psychiatry* (2013) 75:e11–3. doi:10.1016/j.biopsych.2013.06.011
  28. Mouschlianitis E, Bloomfield MA, Law V, Beck K, Selvaraj S, Rasquinha N, et al. Treatment-resistant schizophrenia patients show elevated anterior cingulate cortex glutamate compared to treatment-responsive. *Schizophr Bull* (2016) 42:744–52. doi:10.1093/schbul/sbv151
  29. Goldstein ME, Anderson VM, Pillai A, Kydd RR, Russell BR. Glutamatergic neurometabolites in clozapine-responsive and -resistant schizophrenia. *Int J Neuropsychopharmacol* (2015) 18:pyu117. doi:10.1093/ijnp/ypyu117
  30. Moher D, Liberati A, Tetzlaff J, Altman DG, Group P. Preferred reporting items for systematic reviews and meta-analyses: the PRISMA statement. *J Clin Epidemiol* (2009) 62:1006–12. doi:10.1016/j.jclinepi.2009.06.005
  31. Aoyama N, Theberge J, Drost DJ, Manchanda R, Northcott S, Neufeld RW, et al. Grey matter and social functioning correlates of glutamatergic metabolic loss in schizophrenia. *Br J Psychiatry* (2011) 198:448–56. doi:10.1192/bj.psy.2011.079608
  32. Choe BY, Suh TS, Shinn KS, Lee CW, Lee C, Paik IH. Observation of metabolic changes in chronic schizophrenia after neuroleptic treatment by *in vivo* hydrogen magnetic resonance spectroscopy. *Invest Radiol* (1996) 31:345–52. doi:10.1097/00004424-199606000-00006
  33. de la Fuente-Sandoval C, Favila R, Alvarado P, Leon-Ortiz P, Diaz-Galvis L, Amezcuia C, et al. [Glutamate increase in the associative striatum in schizophrenia: a longitudinal magnetic resonance spectroscopy preliminary study]. *Gac Med Mex* (2009) 145:109–13.
  34. Szulc A, Galinska B, Tarasow E, Waszkiewicz N, Konarzewska B, Poplawska R, et al. Proton magnetic resonance spectroscopy study of brain metabolite changes after antipsychotic treatment. *Pharmacopsychiatry* (2011) 44:148–57. doi:10.1055/s-0031-1279739
  35. Szulc A, Konarzewska B, Galinska-Skok B, Lazarczyk J, Waszkiewicz N, Tarasow E, et al. Proton magnetic resonance spectroscopy measures related to short-term symptomatic outcome in chronic schizophrenia. *Neurosci Lett* (2013) 547:37–41. doi:10.1016/j.neulet.2013.04.051
  36. Theberge J, Williamson KE, Aoyama N, Drost DJ, Manchanda R, Malla AK, et al. Longitudinal grey-matter and glutamatergic losses in first-episode schizophrenia. *Br J Psychiatry* (2007) 191:325–34. doi:10.1192/bjp.bp.106.033670
  37. de la Fuente-Sandoval C, Leon-Ortiz P, Azcarraga M, Stephano S, Favila R, Diaz-Galvis L, et al. Glutamate levels in the associative striatum before and after 4 weeks of antipsychotic treatment in first-episode psychosis: a longitudinal proton magnetic resonance spectroscopy study. *JAMA Psychiatry* (2013) 70:1057–66. doi:10.1001/jamapsychiatry.2013.289
  38. Goff DC, Hennen J, Lyoo IK, Tsai G, Wald LL, Evins AE, et al. Modulation of brain and serum glutamatergic concentrations following a switch from conventional neuroleptics to olanzapine. *Biol Psychiatry* (2002) 51:493–7. doi:10.1016/S0006-3223(01)01321-X
  39. Goto N, Yoshimura R, Kakeda S, Nishimura J, Moriya J, Hayashi K, et al. Six-month treatment with atypical antipsychotic drugs decreased frontal-lobe levels of glutamate plus glutamine in early-stage first-episode schizophrenia. *Neuropsychiatr Dis Treat* (2012) 8:119–22. doi:10.2147/NDT.S25582
  40. Szulc A, Galinska B, Tarasow E, Dzienis W, Kubas B, Konarzewska B, et al. The effect of risperidone on metabolite measures in the frontal lobe, temporal lobe, and thalamus in schizophrenic patients. A proton magnetic resonance spectroscopy (1H MRS). *Pharmacopsychiatry* (2005) 38:214–9. doi:10.1055/s-2005-873156
  41. Ceglia I, Carli M, Baviera M, Renoldi G, Calcagno E, Invernizzi RW. The 5-HT receptor antagonist M100,907 prevents extracellular glutamate rising in response to NMDA receptor blockade in the mPFC. *J Neurochem* (2004) 91:189–99. doi:10.1111/j.1471-4159.2004.02704.x
  42. Moghaddam B, Adams BW. Reversal of phencyclidine effects by a group II metabotropic glutamate receptor agonist in rats. *Science* (1998) 281:1349–52. doi:10.1126/science.281.5381.1349
  43. Eastwood SL, Porter RH, Harrison PJ. The effect of chronic haloperidol treatment on glutamate receptor subunit (GluR1, GluR2, KA1, KA2, NR1) mRNAs and glutamate binding protein mRNA in rat forebrain. *Neurosci Lett* (1996) 212:163–6. doi:10.1016/0304-3940(96)12801-9
  44. Laruelle M, Frankle WG, Narendran R, Kegeles LS, Abi-Dargham A. Mechanism of action of antipsychotic drugs: from dopamine D(2) receptor antagonism to glutamate NMDA facilitation. *Clin Ther* (2005) 27(Suppl A):S16–24. doi:10.1016/j.clinthera.2005.07.017
  45. Molteni R, Calabrese F, Racagni G, Fumagalli F, Riva MA. Antipsychotic drug actions on gene modulation and signaling mechanisms. *Pharmacol Ther* (2009) 124:74–85. doi:10.1016/j.pharmthera.2009.06.001
  46. Mouschlianitis ED, Bloomfield MA, Law V, Beck K, Selvaraj S, Rasquinham R, et al. Treatment resistant schizophrenia patients show anterior cingulate cortex glutamate increase compared to treatment responsive patients. *Schizophr Bull* (2016) 42(3):744–52. doi:10.1093/schbul/sbv151
  47. Stevenson JM, Reilly JL, Harris MS, Patel SR, Weiden PJ, Prasad KM, et al. Antipsychotic pharmacogenomics in first episode psychosis: a role for glutamate genes. *Transl Psychiatry* (2016) 6:e739. doi:10.1038/tp.2016.10

**Disclaimer:** The views expressed are those of the authors and do not necessarily represent those of the NHS, NIHR, or Department of Health.

**Conflict of Interest Statement:** The authors declare that the research was conducted in the absence of any commercial or financial relationships that could be construed as a potential conflict of interest.

Copyright © 2017 Egerton, Bhachu, Merritt, McQueen, Szulc and McGuire. This is an open-access article distributed under the terms of the Creative Commons Attribution License (CC BY). The use, distribution or reproduction in other forums is permitted, provided the original author(s) or licensor are credited and that the original publication in this journal is cited, in accordance with accepted academic practice. No use, distribution or reproduction is permitted which does not comply with these terms.



# Glutamate Levels and Resting Cerebral Blood Flow in Anterior Cingulate Cortex Are Associated at Rest and Immediately Following Infusion of S-Ketamine in Healthy Volunteers

Kirsten Borup Bojesen<sup>1,2\*</sup>, Kasper Aagaard Andersen<sup>1,2,3</sup>, Sophie Nordahl Rasmussen<sup>1,2,3</sup>, Lone Baandrup<sup>1</sup>, Line Malmer Madsen<sup>4</sup>, Birte Yding Glenthøj<sup>1,2</sup>, Egill Rostrup<sup>3</sup> and Brian Villumsen Broberg<sup>1</sup>

<sup>1</sup>Centre for Neuropsychiatric Schizophrenia Research (CNSR), Centre for Clinical Intervention and Neuropsychiatric Schizophrenia Research (CINS), Mental Health Centre Glostrup, University of Copenhagen, Glostrup, Denmark, <sup>2</sup>Department of Clinical Medicine, Faculty of Health and Medical Sciences, University of Copenhagen, Copenhagen, Denmark, <sup>3</sup>Functional Imaging Unit, Department of Clinical Physiology and Nuclear Medicine, Rigshospitalet Glostrup, University of Copenhagen, Copenhagen, Denmark, <sup>4</sup>Department of Anaesthesia, Glostrup Hospital, University of Copenhagen, Glostrup, Denmark

## OPEN ACCESS

### Edited by:

Hilleke Hulshoff Pol,  
Utrecht University, Netherlands

### Reviewed by:

Martin Walter,  
Universität Tübingen, Germany  
Mitul Ashok Mehta,  
King's College London, United  
Kingdom

### \*Correspondence:

Kirsten Borup Bojesen  
kirsten.borup.bojesen@regionh.dk

### Specialty section:

This article was submitted to  
Neuroimaging and Stimulation,  
a section of the journal  
*Frontiers in Psychiatry*

Received: 29 August 2017

Accepted: 19 January 2018

Published: 06 February 2018

### Citation:

Bojesen KB, Andersen KA,  
Rasmussen SN, Baandrup L,  
Madsen LM, Glenthøj BY, Rostrup E  
and Broberg BV (2018) Glutamate  
Levels and Resting Cerebral Blood  
Flow in Anterior Cingulate Cortex Are  
Associated at Rest and Immediately  
Following Infusion of S-Ketamine in  
Healthy Volunteers.

Front. Psychiatry 9:22.  
doi: 10.3389/fpsy.2018.00022

Progressive loss of brain tissue is seen in some patients with schizophrenia and might be caused by increased levels of glutamate and resting cerebral blood flow (rCBF) alterations. Animal studies suggest that the normalisation of glutamate levels decreases rCBF and prevents structural changes in hippocampus. However, the relationship between glutamate and rCBF in anterior cingulate cortex (ACC) of humans has not been studied in the absence of antipsychotics and illness chronicity. Ketamine is a noncompetitive N-methyl-D-aspartate receptor antagonist that transiently induces schizophrenia-like symptoms and neurobiological disturbances in healthy volunteers (HVs). Here, we used S-ketamine challenge to assess if glutamate levels were associated with rCBF in ACC in 25 male HVs. Second, we explored if S-ketamine changed the neural activity as reflected by rCBF alterations in thalamus (Thal) and accumbens that are connected with ACC. Glutamatergic metabolites were measured in ACC with magnetic resonance (MR) spectroscopy and whole-brain rCBF with pseudo-continuous arterial spin labelling on a 3-T MR scanner before, during, and after infusion of S-ketamine (total dose 0.375 mg/kg). In ACC, glutamate levels were associated with rCBF before ( $p < 0.05$ ) and immediately following S-ketamine infusion ( $p = 0.03$ ), but not during and after. S-Ketamine increased rCBF in ACC ( $p < 0.001$ ) but not the levels of glutamate ( $p = 0.96$ ). In subcortical regions, S-ketamine altered rCBF in left Thal ( $p = 0.03$ ). Our results suggest that glutamate levels in ACC are associated with rCBF at rest and in the initial phase of an increase. Furthermore, S-ketamine challenge transiently induces abnormal activation of ACC and left Thal that both are implicated in the pathophysiology of schizophrenia. Future longitudinal studies should investigate if increased glutamate and rCBF are related to the progressive loss of brain tissue in initially first-episode patients.

**Keywords:** glutamate, magnetic resonance spectroscopy, cerebral blood flow, pseudo-continuous arterial spin labelling, ketamine, schizophrenia, structural brain changes

## INTRODUCTION

Schizophrenia is a devastating disease with a progressive loss of brain tissue in a subgroup of patients (1). The cause of the loss is currently unknown, but persistently high levels of the neurotransmitter glutamate and alterations of resting cerebral blood flow (rCBF) might be implicated. The loss of brain tissue is among others seen in the temporal and frontal regions (1–5) comprising the anterior cingulate cortex (ACC) and hippocampus that both might be implicated in the pathophysiology of schizophrenia (6–9). Interestingly, increased brain glutamate in rodents has been linked to structural changes in ACC and hippocampus (10, 11). In addition, preclinical studies suggest that glutamate is a key regulator of rCBF (12). However, studies investigating the association between glutamate, rCBF, and structural changes in patients with schizophrenia are sparse and have mainly focused on the hippocampus. In hippocampus of unmedicated patients, a negative association between glutamatergic metabolites and brain volume has been found (13), and in prodromal patients, a correlation between cerebral blood volume and structural brain changes in patients that later transitioned to psychosis was observed (11). Interestingly, a rodent study found that the normalisation of increased brain glutamate in hippocampus was able to both normalize rCBF and prevent structural changes (11). This suggests that glutamate-modulating agents might be neuroprotective, at least in hippocampus. However, the association between glutamate, rCBF, and structural changes has not been explored in ACC and nearby prefrontal areas where increased glutamatergic metabolites are found in some studies of early schizophrenia (14–16), and the loss of brain tissue is seen both early and later in the illness (1–5). Only one study has examined the association between glutamate and rCBF in ACC of medicated patients (17). This study found a positive correlation between rCBF in white matter (WM) and levels of glutamate in a large group of patients, but interpretation was limited by treatment with antipsychotics and a broad age range since both factors affect glutamate (18, 19) and rCBF (20). The confounding effects of antipsychotics and illness duration can be avoided by recruiting first-episode, antipsychotic-naïve or minimally treated patients, but glutamate and rCBF have only been studied separately in this patient group. Glutamatergic metabolites in ACC or nearby medial prefrontal cortex (mPFC) are either increased (14–16), decreased (21), or similar (22) compared to healthy volunteers (HVs). Likewise, rCBF studies have found increased (23, 24), decreased (25), and unchanged (26, 27) levels in the prefrontal cortex of antipsychotic-naïve schizophrenia. Although speculative, these findings might reflect that a subgroup of patients is characterized by both increased glutamatergic activity and enhanced rCBF. This could very well be the subgroup, where progressive loss of brain tissue is found later in the illness (1). In sum, studies investigating the association between glutamate and rCBF in ACC of antipsychotic-naïve schizophrenia are warranted given that the normalisation of these disturbances could prevent structural changes in hippocampus. Early prevention of progressive loss of brain tissue in the course of schizophrenia is clinically relevant because structural changes have been associated with poorer functional outcome (28).

Pharmacological models of schizophrenia are an alternative approach to study brain abnormalities not confounded by antipsychotics and illness duration. Ketamine is a noncompetitive N-Methyl-D-Aspartate receptor antagonist that transiently induces schizophrenia-like symptoms when administered to HV (29, 30). Ketamine also increases glutamate in the prefrontal cortex of rats (31) and glutamate, glutamine (gln), or gln/glutamate in ACC of HVs in some (32–34), but not all studies (35). Ketamine also enhances rCBF in ACC and other prefrontal areas in HV (36–39). The sub-anesthetic doses used correspond to doses used to treat depressive disorder (40), and ketamine challenge is generally considered safe.

The primary aim of this study was to investigate if glutamate and rCBF in ACC were associated before, during, and after the infusion of a sub-anesthetic dose of S-ketamine administered to HVs. Because abnormal thalamocortical interactions might underlie schizophrenia (41) and lead to striatal, dopaminergic disturbances (8, 42–44), we also examined rCBF alterations during S-ketamine infusion in the accumbens and thalamus (Thal) that are connected with ACC (45).

## PARTICIPANTS AND METHODS

The study was a noncontrolled pre-post intervention design where 25 nonsmoking, right-handed healthy male volunteers aged 21–31 years received constant i.v. infusion of S-ketamine (Pfizer) during magnetic resonance imaging (MRI) scanning. The dosing regimen was 0.25 mg/kg for 20 min and thereafter 0.125 mg/kg for 20 min to keep blood levels stable. S-Ketamine was used since the racemic form (mixture of S- and R-ketamine) is not available in Denmark.

Levels of glutamate in ACC and whole-brain rCBF were obtained before, during, and after S-ketamine infusion as shown in **Figure 1**.

Exclusion criteria were current or previous psychiatric illness tested with Schedules for Clinical Assessment in Neuropsychiatry (46), drug and alcohol abuse as reported by self-report and confirmed with urine testing (Rapid Response, Jepsen HealthCare, Tune, DK), psychiatric disease in first-degree relatives, past or present physical illness, the use of nicotine substitutes, the previous use of ketamine; or the use of benzodiazepines, antipsychotics, anticonvulsants, or antidepressant (as e.g., sleeping medication) within the past 2 months. The study was approved by the Committee on Biomedical Research Ethics for the Capital Region of Denmark (H-4-2014-033), and all participants provided written informed consent after the study procedures were fully explained.

Psychotomimetic effects were assessed with the Positive and Negative Syndrome Scale (PANSS) (47) and the effect on mood with the Positive and Negative Affect Schedule (PANAS) (48) by trained raters before and after S-ketamine infusion. For assessments after infusion, participants were asked about their experiences during infusion while being on the scanner.

## Magnetic Resonance Acquisitions

Data were acquired using a 3-T Philips Achieva system (Philips Healthcare, Eindhoven, Netherlands) equipped with a

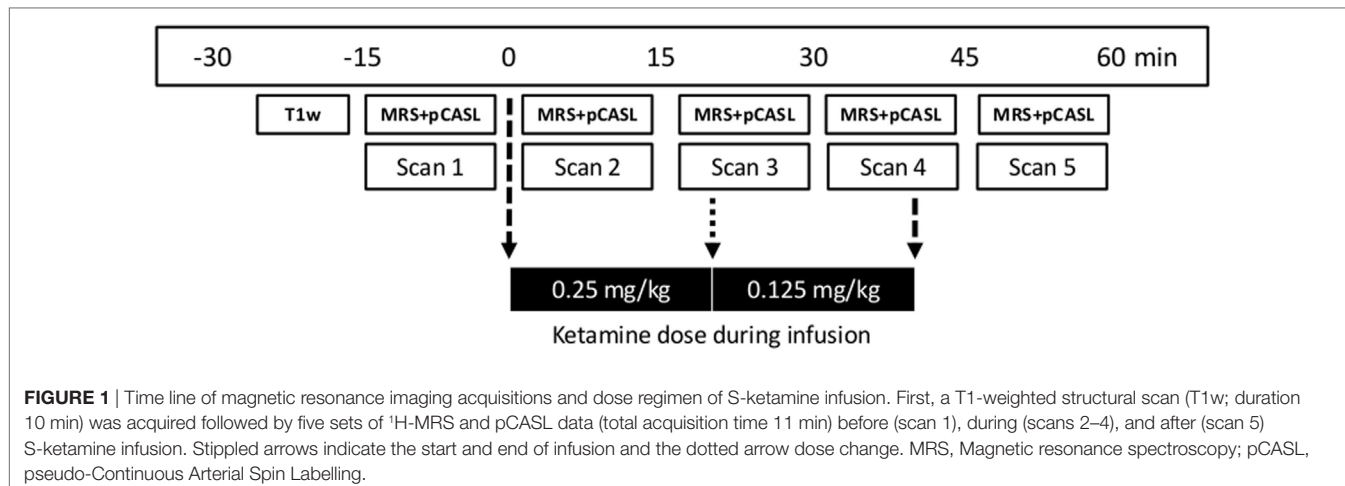


**FIGURE 1 |** Time line of magnetic resonance imaging acquisitions and dose regimen of S-ketamine infusion. First, a T1-weighted structural scan (T1w; duration 10 min) was acquired followed by five sets of  $^1\text{H}$ -MRS and pCASL data (total acquisition time 11 min) before (scan 1), during (scans 2–4), and after (scan 5) S-ketamine infusion. Stippled arrows indicate the start and end of infusion and the dotted arrow dose change. MRS, Magnetic resonance spectroscopy; pCASL, pseudo-Continuous Arterial Spin Labelling.

32-channel head coil (*In vivo*, Orlando, FL, USA). A whole-brain three-dimensional high-resolution T1-weighted structural scan (TR 10 ms, TE 4.6 ms, flip angle =  $8^\circ$ , and voxel size =  $0.79 \text{ mm} \times 0.79 \text{ mm} \times 0.80 \text{ mm}$ ) was obtained for grey matter (GM) and white matter (WM) WM tissue classification and anatomical reference. A forehead strap was placed to minimize head motion. One participant moved approximately 2 mm, all others <0.7 mm.

Proton magnetic resonance spectroscopy ( $^1\text{H}$ -MRS) and unsuppressed water reference spectra were obtained with frequency-stabilised point-resolved spectroscopy (TE 30 ms, TR 3,000 ms, 128 averages with MOIST water suppression). A  $2.0 \text{ cm} \times 2.0 \text{ cm} \times 2.0 \text{ cm}$  voxel was prescribed in ACC (Brodmann areas 24 and 32) by drawing a line through the extremities of corpus callosum, placing the point of the voxel at the intersection and aligning to corpus callosum as shown in **Figure 2C**. Similar acquired acquisitions have revealed good test-retest reliability for glutamate with a percentage coefficient of variation <7% (unpublished data). Acquisition time was 7 min.

A pseudo-Continuous Arterial Spin Labelling (pCASL) sequence was used to assess rCBF as described elsewhere (49). The sequence consisted of 30 pairs of perfusion weighted and control scans (dual echo EPI; 16 slices of 5 mm with an in-plane resolution of  $3.55 \text{ mm} \times 3.55 \text{ mm}$ ; SENSE factor 2.3; TR = 4,100 ms; TE = 12 ms, 28.5 ms at a post-labelling delay of 1,600 ms; labelling duration 1,650 ms; background inversion pulses at 1,663 and 2,850 ms after the start of labelling). M0 scan: TR/TE = 10 s/9 ms. Acquisition time was 4 min.

## $^1\text{H}$ -MRS Analysis

Proton magnetic resonance spectroscopy spectra were analysed with LCModel version 6.3-1 J (50) within the spectral range of 0.2 and 4.0 ppm using water scaling to estimate the concentration of neurometabolites from a standard basis set comprising alanine, aspartate, creatine (Cr), phosphocreatine (PCr), GABA, glucose, gln, glutamate, glycerophosphocholine (GPC), phosphocholine (PCh), glutathione, *myo*-inositol (Ins), lactate, N-acetyl aspartate (NAA), NAA glutamate, *scyllo*-Ins, and taurine. Spectra quality was evaluated by visual inspection, and individual

neurometabolites with Cramer-Rao Lower bound (CRLB) >20% were excluded. The percentage of GM and WM in the  $^1\text{H}$ -MRS voxel was estimated and used to calculate institutional units of glutamate (glu<sub>IU</sub>), glx (glx<sub>IU</sub>), and gln<sub>IU</sub> corrected for cerebrospinal fluid contamination as described in the Supplementary Material. Glu<sub>IU</sub> was used as the primary outcome, and glx<sub>IU</sub> and gln<sub>IU</sub> were analysed as the secondary outcomes to allow comparison with other studies. In exploratory analyses, glutamate, glx, and gln scaled to Cr (Cr + PCr) were analysed.

## pCASL Analysis

Calculation of rCBF was done using the FSL software package ([https://fsl.fmrib.ox.ac.uk/fsl/downloads\\_registration](https://fsl.fmrib.ox.ac.uk/fsl/downloads_registration)). First, the “Brain extraction Tool” was used to remove non-brain tissue from a T1-weighted image. Second, the pCASL data obtained before, during, and after ketamine infusion were co-registered with the skull-stripped T1-weighted image, and, lastly, the T1-weighted image was nonlinearly co-registered to Montreal Neurological Institute (MNI) space and the combined transformation was applied to the rCBF maps.

The effects of S-ketamine on rCBF were investigated with both voxel-based and region of interest (ROI) analyses. Voxel-based analysis identified areas with the most significant increase of rCBF using an analysis of variance (ANOVA) model and permutation-based statistical inference. We further used threshold-free cluster enhancement to account for spatial dependencies. The statistical maps were thresholded at  $p < 0.05$  and corrected for multiple comparisons (FWE correction). ROI analyses were performed in two defined cortical areas with the first corresponding to the position of the MRS voxel in ACC and the second to the region with most significant voxel-based changes of rCBF, and in the subcortical regions provided by the MNI atlas from FSL (left and right Thal, caudate, accumbens, and putamen). The rCBF was calculated as both absolute values in mL/100 g/min and as normalised values by dividing each voxel with the global mean for each subject to reduce inter-subject variation caused by a difference in global rCBF. Normalised rCBF was used as the primary outcome to enhance the sensitivity to regional changes, but absolute rCBF values are reported as well.

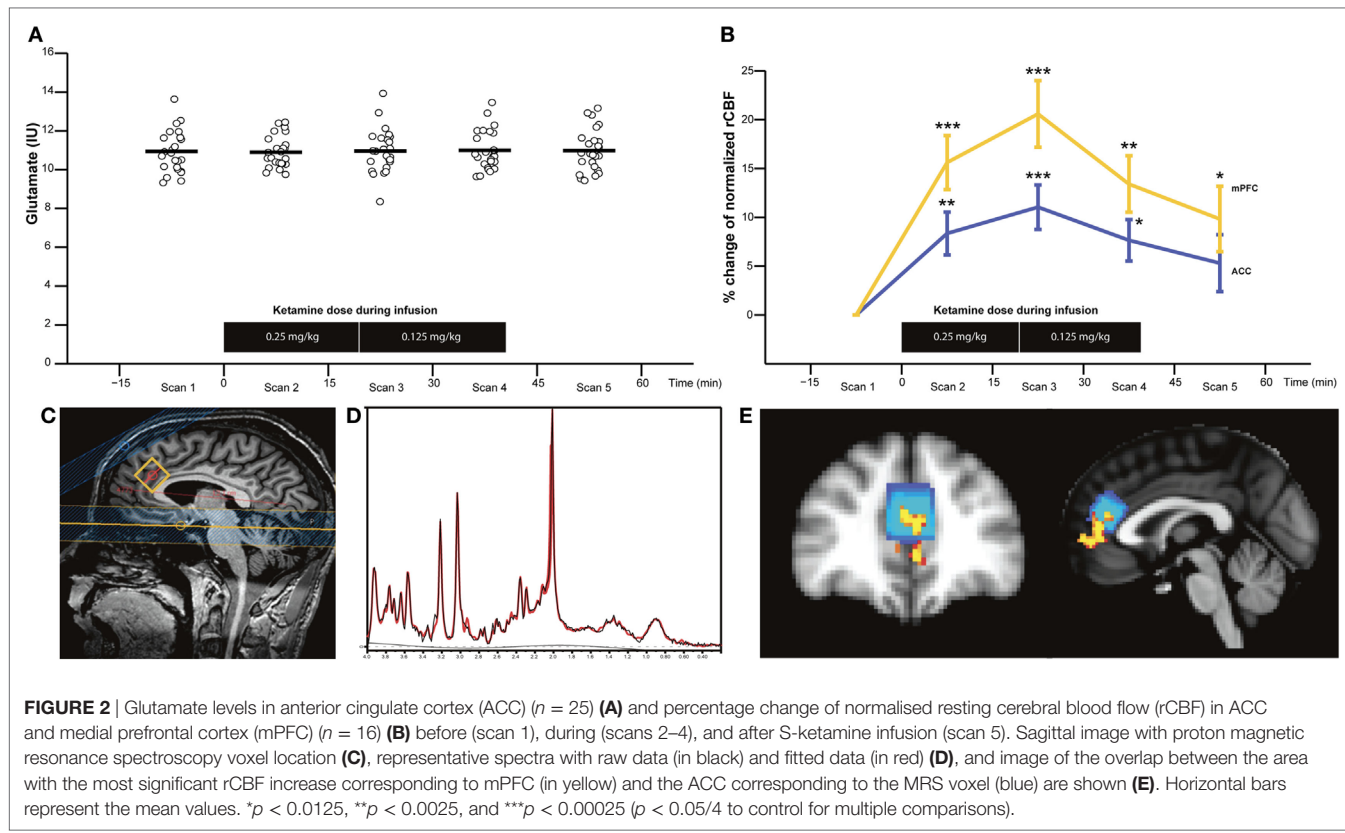


**FIGURE 2 |** Glutamate levels in anterior cingulate cortex (ACC) ( $n = 25$ ) (A) and percentage change of normalised resting cerebral blood flow (rCBF) in ACC and medial prefrontal cortex (mPFC) ( $n = 16$ ) (B) before (scan 1), during (scans 2–4), and after S-ketamine infusion (scan 5). Sagittal image with proton magnetic resonance spectroscopy voxel location (C), representative spectra with raw data (in black) and fitted data (in red) (D), and image of the overlap between the area with the most significant rCBF increase corresponding to mPFC (in yellow) and the ACC corresponding to the MRS voxel (blue) are shown (E). Horizontal bars represent the mean values. \* $p < 0.0125$ , \*\* $p < 0.0025$ , and \*\*\* $p < 0.000025$  ( $p < 0.05/4$  to control for multiple comparisons).

## Statistics

The primary hypothesis that levels of glutamate (independent variable) would be associated with normalised rCBF in ACC (dependent variable) during each of the five scans was tested with five separate linear regression models with a significance level set to  $p < 0.05$  for this *a priori* hypothesis.

The main effect of S-ketamine on levels of glutamatergic metabolites and rCBF was evaluated separately using a one-way repeated measures ANOVA (rmANOVA) with statistical significance defined as  $p < 0.05$  for the main effects and  $p < 0.0125$  for *post hoc* *t*-tests (separate *t*-tests Bonferroni corrected with  $p/4$  scans during S-ketamine infusion). Multivariate tests of the main effect are reported if the assumption of sphericity was violated. No outliers were identified according to Cook distance criterion (51).

PANSS (total, positive, negative, and general subscores) and PANAS (positive- and negative-affect scores) before and after ketamine infusion were analysed using Wilcoxon signed rank test. Correlations between mental state effect changes induced by S-ketamine and levels of glutamate or normalised rCBF in the ACC voxel were tested with Spearman's rho and corrected for multiple comparisons (Bonferroni). Statistical analyses were performed in SAS version 7.1 (SAS institute, Cary, NC, USA).

## RESULTS

### Mental State Changes and Laboratory Results with S-Ketamine

The mental state changes with S-ketamine and demographic variables of participants are summarized in Table 1. S-Ketamine

significantly increased PANSS total, and all subscores with items P2 (disorganized thinking) and P3 (hallucinations) being most prominently affected with an increase of 104 and 184%, respectively. Furthermore, S-ketamine significantly decreased positive affect. The negative affect increased but not to a significant extent.

Serum levels of S-ketamine obtained from four HVs after scan 5 as test samples were  $140.5 \pm 27.0$  ng/mL.

### Glutamatergic Metabolites before, during, and after S-Ketamine

No spectra were excluded after visual inspection, and the quality was good as shown in a representative spectrum in Figure 2D. CRLB values were <9% for glutamate and glx, but 23 gln-values were excluded due to CRLB >20%. Full-width half-maximum, signal-to-noise ratio, and CRLB for glutamate, NAA, myo-Ins, and choline did not differ during the five MRS acquisitions, but CRLB for glx, gln, and PCr + Cr did as summarized in Table S1 in Supplementary Material.

*Glutamate (glu<sub>IU</sub>), glutamine (glx<sub>IU</sub>), glutamine (gln<sub>IU</sub>), and other neurometabolites:* There were no significant main effects of time for glu<sub>IU</sub> [ $F(4, 96) = 0.13$ ,  $p = 0.962$ ] (Figure 2A), glx<sub>IU</sub> [ $F(4, 96) = 1.07$ ,  $p = 0.374$ ], gln<sub>IU</sub> [ $F(4, 36) = 0.64$ ,  $p = 0.635$ ], or other neurometabolites such as NAA, Cr + PCr, choline (GPC + PCh), and myo-Ins. The mean values of metabolites are provided in Table S2 in Supplementary Material. The inclusion of glutamate, glx, or gln scaled to Cr in the rmANOVA did not change the results. Lastly, no main effect of time was found for glu<sub>IU</sub>, glx<sub>IU</sub>, and gln<sub>IU</sub> in the subgroup of HV, which also had a pCASL scan ( $n = 16$ ). In sum, S-ketamine

infusion did not appear to affect glutamatergic metabolites in the ACC voxel.

## rCBF before, during, and after S-Ketamine

pseudo-Continuous Arterial Spin Labelling data were only usable for 16 subjects due to technical challenges.

### Voxel-Based Analysis

Voxel-based analysis of the absolute rCBF (mL/100 g/min) revealed that the most significant increase of rCBF during scan

**TABLE 1** | Demographic characteristics and psychotomimetic effects with S-ketamine.

Characteristic		Means
N (males only)		25
Age, years $\pm$ SD		25.4 $\pm$ 3.3
BMI, kg/m <sup>2</sup> $\pm$ SD		23.5 $\pm$ 2.0
Years of education $\pm$ SD		14 $\pm$ 2
PANSS total $\pm$ SEM	Pre	32.0 $\pm$ 0.5
	Post	38.4 $\pm$ 1.2***
PANSS positive $\pm$ SEM	Pre	7.5 $\pm$ 0.3
	Post	10.8 $\pm$ 0.4**
PANSS negative $\pm$ SEM	Pre	7.5 $\pm$ 0.1
	Post	8.5 $\pm$ 0.5**
PANSS general $\pm$ SEM	Pre	17.0 $\pm$ 0.3
	Post	19.2 $\pm$ 0.7**
Positive affect $\pm$ SEM	Pre	30.7 $\pm$ 1.2
	Post	23.5 $\pm$ 1.5***
Negative affect $\pm$ SEM	Pre	11.8 $\pm$ 0.4
	Post	13.3 $\pm$ 0.7

BMI, body mass index; PANSS, Positive and Negative Syndrome Scale.

\*\* $p < 0.01$ .

\*\*\* $p < 0.001$ .

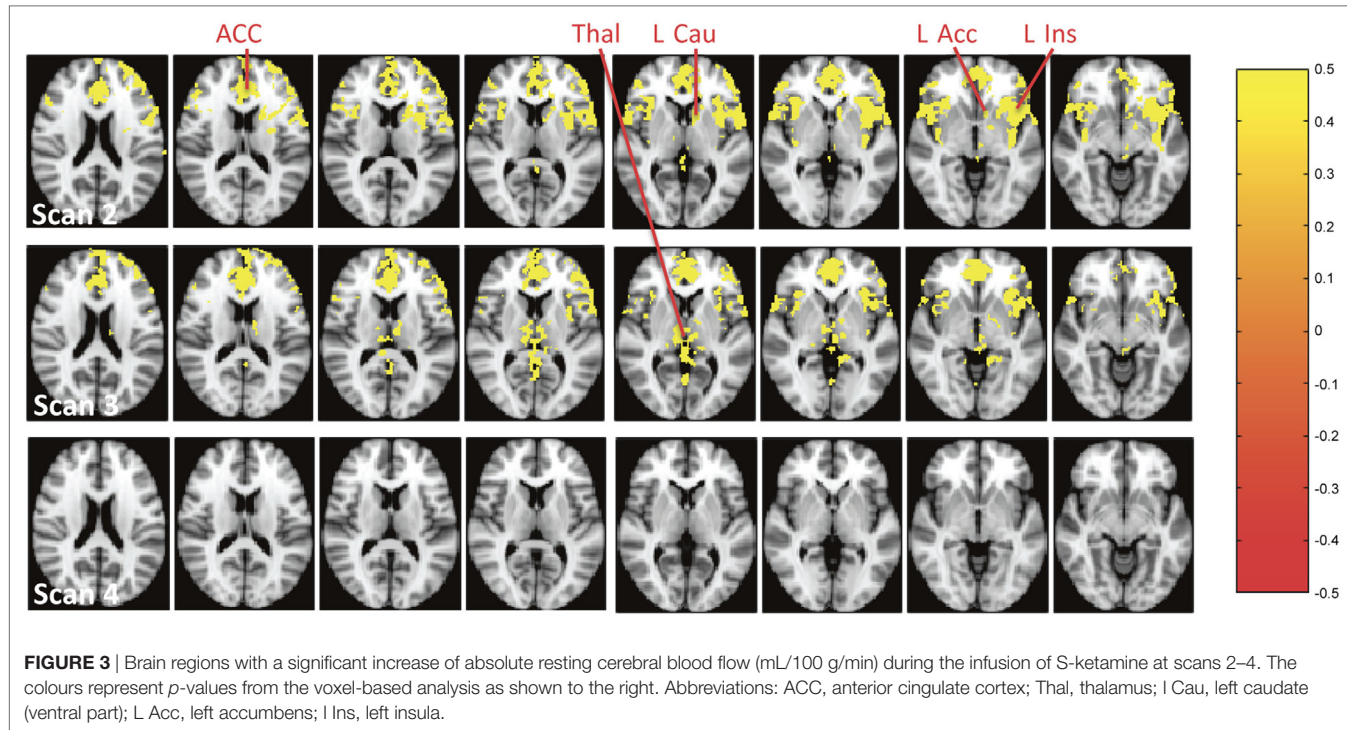
2 was in mPFC/ACC, insula, left accumbens (L Acc), and left ventral caudate (Figure 3, scan 2), and during scan 3 in left and right Thal (Figure 3, scan 3).

After normalizing rCBF, the most significant increase was seen in Brodmann area 32 (MNI coordinates  $x = 45, y = 83, z = 45$ ) that corresponds to mPFC and partly overlaps with the MRS voxel in ACC (Figure 2E).

### ROI Analyses of Absolute and Normalised rCBF Changes

The rMANOVA of ROIs revealed a significant main effect of time for absolute rCBF (mL/100 g/min) in the two defined cortical ROIs mPFC ( $F(4, 60) = 29.6, p < 0.0001$ ) and the ACC voxel (denoted ACC hereinafter) ( $F(4, 60) = 13.44, p = 0.0002$ ) with *post hoc* tests revealing a significant increase in mPFC during scan 2 ( $26 \pm 3\%, p < 0.0001$ ), scan 3 ( $30 \pm 4\%, p < 0.0001$ ), scan 4 ( $21 \pm 5\%, p = 0.0014$ ), and at trend level that did not survive correction for multiple comparisons during scan 5 ( $12 \pm 4\%, p = 0.025$ ), and in ACC during scan 2 ( $18 \pm 3\%, p < 0.0001$ ), scan 3 ( $20 \pm 3\%, p = 0.0001$ ), and scan 4 ( $15 \pm 4\%, p = 0.006$ ), but not during scan 5 ( $7 \pm 4\%, p = 0.11$ ). Absolute values in mL/100 g/min for the five scans are reported in Table S3 in Supplementary Material. In the subcortical ROIs, a significant main effect of time was seen in left and right Thal, left caudate (L Cau), and L Acc, although the *post hoc* tests only were significant during scan 2 for L Cau and L Acc as reported in Table S4 in Supplementary Material.

After normalizing rCBF, the main effect of S-ketamine remained significant in mPFC ( $F(4, 60) = 15.06, p < 0.0001$ ), ACC ( $F(4, 60) = 5.45, p = 0.0008$ ), and left Thal ( $F(4, 12) = 4.08, p = 0.026$ ). *Post hoc* tests revealed a significant increase in mPFC and ACC during scans 2–4, and additionally in mPFC during



scan 5 (**Figure 2B**). In left Thal, normalised rCBF appeared to decrease during scan 2; however, the *post hoc* tests were insignificant. No main effect of time was seen in right Thal, 1 Cau, right caudate, right accumbens, left putamen, and right putamen. Statistics and percentage increase compared to preinfusion (scan 1) of normalised rCBF values for cortical and subcortical ROIs are provided in Tables S5 and S6 in Supplementary Material, respectively.

In sum, S-ketamine infusion affected mPFC/ACC and left Thal after correction for the effect of global blood flow (normalisation).

## Relationship between Levels of Glutamate and Normalised rCBF in ACC before, during, and after S-Ketamine

Higher levels of  $\text{glu}_{\text{IU}}$  were significantly associated with higher values of normalised rCBF in ACC prior to S-ketamine infusion during scan 1 ( $b = 0.05$ ,  $t = 2.19$ ,  $p = 0.046$ ) and immediately following infusion during scan 2 ( $b = 0.07$ ,  $t = 2.41$ ,  $p = 0.03$ , **Figure 4**), but not to a significant extent during scan 3 ( $b = 0.04$ ,  $t = 1.64$ ,  $p = 0.12$ ), scan 4 ( $b = 0.01$ ,  $t = 0.45$ ,  $p = 0.66$ ), or scan 5 ( $b = 0.02$ ,  $t = 0.62$ ,  $p = 0.55$ ). When adjusting for age, similar results were observed, although only borderline significant during scan 1 (scan 1:  $p = 0.05$ ; scan 2:  $p < 0.05$ ; scan 3:  $p = 0.15$ ; scan 4:  $p = 0.60$ ; scan 5:  $p = 0.56$ ).

$\text{Glx}_{\text{IU}}$  was associated with normalised rCBF in ACC prior to S-ketamine infusion at a trend level that did not survive correction for multiple comparison ( $p < 0.05/2 = 0.025$ ) during scan 1 ( $b = 0.03$ ,  $t = 2.29$ ,  $p = 0.038$ ), and significantly during scan 2 ( $b = 0.06$ ,  $t = 3.85$ ,  $p = 0.002$ ) but not during scans 3, 4, or 5 ( $p > 0.05$ ). Similar results were obtained when adjusting for age (scan 1:  $p = 0.035$ ; scan 2:  $p = 0.002$ ; scans 3–5:  $p > 0.05$ ).

No association was found between  $\text{gln}_{\text{IU}}$  and normalised rCBF in ACC, neither when adjusting for age. Also, there was no main effect of age for any of the metabolites, and all the  $\text{glu}_{\text{IU}}/\text{gln}_{\text{IU}}$   $\times$  age interactions were insignificant and removed from the analyses.

## Relationship between Changes in Mental State with S-Ketamine, Levels of Glutamate, and Normalised rCBF in mPFC

Neither glutamate in ACC nor normalised rCBF in mPFC during S-ketamine infusion (scans 2–4) correlated with changes in PANSS total, positive, negative, and general or positive and negative affect to a significant extent.

## Physiological Data

Ketamine infusion did not significantly affect blood pressure (systolic) or heart rate.

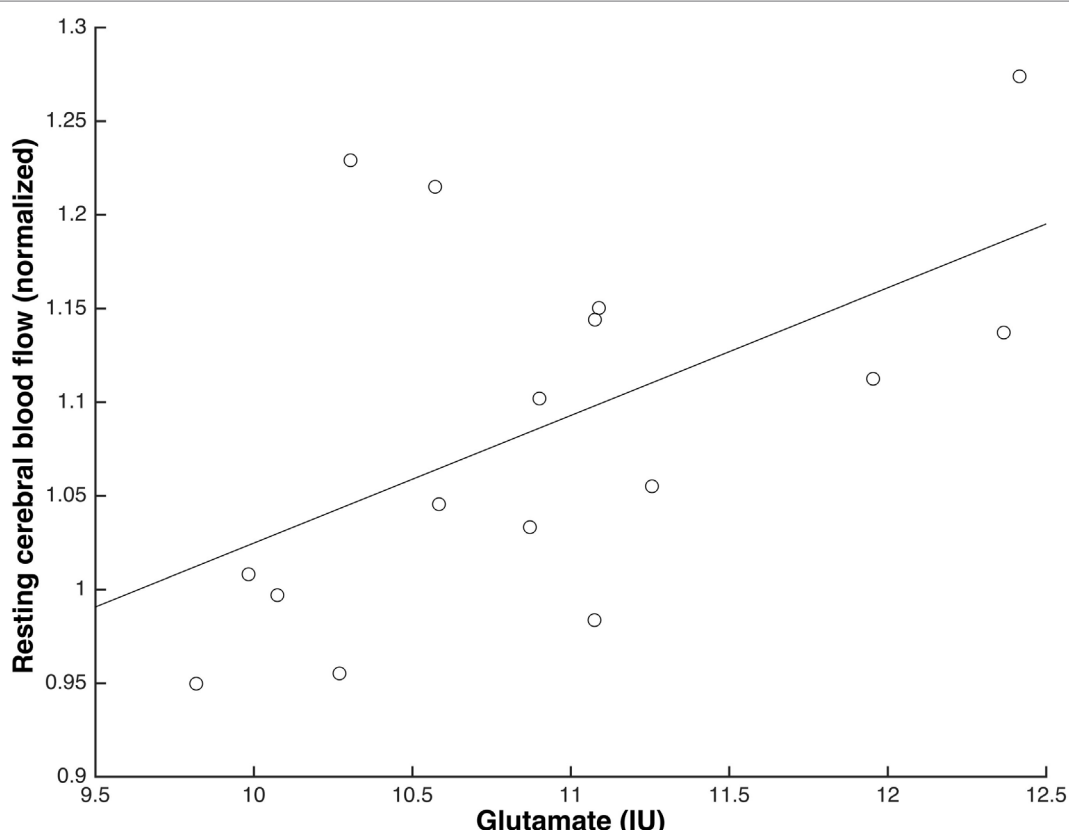


**FIGURE 4** | Glutamate levels and normalised resting cerebral blood flow (rCBF) in anterior cingulate cortex were positively associated immediately following S-ketamine infusion (scan 2) ( $N = 16$ ;  $b = 0.07$ ,  $t = 2.41$ ,  $p = 0.03$ ).

## DISCUSSION

The primary finding of this study was that levels of glutamate were positively associated with normalised rCBF in ACC before and immediately following the infusion of S-ketamine in HV. In addition, S-ketamine transiently induced abnormal neural activation as measured by altered normalised rCBF in mPFC, ACC, and left Thal. However, levels of glutamate in ACC were not affected during S-ketamine infusion.

The results support that glutamate levels and rCBF are associated in ACC as also seen in a recent study of medicated patients with schizophrenia (17), a rodent study of hippocampus (11), and preclinical studies (12). Importantly, this association was independent of antipsychotic exposure and psychiatric illness chronicity.

In terms of clinical relevance, a rodent study revealed that the normalisation of increased glutamate and enhanced rCBF could prevent structural changes in hippocampus (11). Given that glutamate and rCBF were associated in ACC in our study, it is likely that glutamate-modulating agents also might be neuroprotective in this area as well when given to schizophrenia patients with increased glutamate levels. The progressive loss of brain tissue in schizophrenia is only seen in a subgroup of patients (1), and we speculate if increased glutamatergic activity and enhanced rCBF characterize the subgroup of patients who experience structural changes later in the illness. Thus, future studies should aim at investigating if increased glutamate in ACC and enhanced rCBF in first-episode patients predict the progressive loss of brain tissue.

The association between glutamate levels and normalised rCBF in the ACC was only seen before (scan 1) and immediately following (scan 2), but not during (scans 3 and 4) or after (scan 5) S-ketamine infusion, which can indicate that glutamate mainly regulates rCBF during an increase in HVs, whereas other factors might be involved during the maintenance and decrease of enhanced rCBF. In preclinical studies, glutamatergic neurotransmission plays a key role in the regulation of cerebral blood flow by activating N-Methyl-D-Aspartate receptors on neurons and metabotropic glutamate receptors on astrocytes (12). The subsequent rise in intracellular  $\text{Ca}^{2+}$  leads to the release of intracellular-vasodilating messengers but can also cause blood vessel constriction (12). The outcome of intracellular  $\text{Ca}^{2+}$  rise is influenced by preexisting vessel tone and the  $\text{O}_2$  concentration, in that dilation occurs with physiological  $\text{O}_2$  concentrations and constriction with supraphysiological  $\text{O}_2$  concentrations (12, 52). Although speculative, our findings might imply that S-ketamine initially induces vasodilation, but that this effect diminishes or ceases after some time due to persistently increased  $\text{O}_2$  and enhanced vessel tone.

Levels of glutamate as measured with  $^1\text{H}$ -MRS in ACC were unaffected during the infusion of S-ketamine. This is in agreement with one previous study (35) but in contrast with two others (32, 33). Several factors might explain this finding. First, the  $^1\text{H}$ -MRS voxel in ACC was placed a bit dorsal from mPFC where the most significant increase of rCBF was seen (Figure 2E). Although the ACC voxel and mPFC overlap, the increase of glutamate levels in ACC might not have been sufficient to be detected with  $^1\text{H}$ -MRS.

Second, our dose regimen of S-ketamine might have been too high. We administered pure S-ketamine in a dosing regimen corresponding to previous studies where the racemic form was used (50% R- and 50% S-ketamine) (32, 33, 35), but it seems likely that the dose of pure S-ketamine and the racemic form does not correspond to 1:1 since R-ketamine restricts the clearance of the S-enantiomer (53). In addition, racemic ketamine mainly increases extracellular cortical glutamate at low doses in rats (31), and it is notable that the two  $^1\text{H}$ -MRS studies that found increased levels of glutamate (33) or gln (32) used a lower dose of racemic ketamine than in the present study and the other study where glutamate was unaffected (35). Third, one of the MRS ketamine studies found increased gln but not glutamate (32). Gln reflects glutamate released by the synapse and taken up by astrocytes only (54), whereas glutamate reflects other metabolic processes as well (55). Therefore, minor changes of the glutamate level in the synaptic cleft can be blurred by the glutamate contained in presynaptic vesicles and astrocytes. However, gln is challenging to accurately quantify at field strengths below 4 T due to overlapping resonance frequencies with glutamate. Lastly, a ketamine-induced increase of glutamatergic metabolites might be easier to detect in pathological conditions like depression, where resting glutamate is decreased (56).

S-Ketamine significantly affected rCBF in several areas. The voxel-based analysis revealed that the most significant increase of both absolute (mL/100 g/min) and normalised rCBFs was in ACC and the overlapping mPFC (Figures 2B,E), which is in line with previous PET (36, 37) and MRI studies (39), administering racemic ketamine to HVs. This confirms that the main effect of S-ketamine also is mediated through ACC/mPFC. The rCBF enhancements are most likely induced by the S-enantiomer, since the administration of pure R-ketamine seems to decrease rCBF in HVs (57).

Our second aim was to explore if S-ketamine transiently induced the abnormal neural activation of the accumbens and Thal as reflected by rCBF alterations since these areas are connected with ACC (45) and implicated in the pathophysiology of schizophrenia (8, 42–44). Absolute rCBF was significantly increased in L Acc and left ventral caudate (left ventral striatum) and Thal (Figure 3, scan 2). However, only the effect in ACC/mPFC remained significant in the voxel-based analyses when rCBF was normalised. In the ROI analyses, a significant increase of absolute rCBF was also seen in ACC, mPFC, left and right Thal, L Acc, and L Cau (Tables S3 and S4 in Supplementary Material) but only remained significant in ACC, mPFC, and left Thal after normalizing rCBF (Tables S5 and S6 in Supplementary Material). In left Thal, S-ketamine seemed to decrease normalised rCBF during scan 2, although not to a significant extent. This decrease might reflect a feedback mechanism due to the increased activity of ACC and mPFC. In sum, S-ketamine mainly seems to affect ACC/mPFC and left Thal, although accumbens might be activated to a minor extent. This is in accord with a ketamine study of rats that found mainly increased cortical glutamate and only to a minor extent increased striatal dopamine (31), and a SPECT study of HVs where striatal dopamine was unaffected by ketamine (58). Taken together, it seems that ketamine challenge only affects striatal dopaminergic activity to a minor extent. This

is a limitation if ketamine challenge is used as a pharmacological model of schizophrenia where increased striatal dopaminergic activity is one of the best validated findings (59). Interestingly, the SPECT study found that striatal dopaminergic activity in HV was enhanced more by administering both amphetamine and ketamine than amphetamine alone (58). It is possible that this combined administration mimics the neurobiology of schizophrenia better.

S-Ketamine transiently induced schizophrenia-like symptoms as measured with PANSS and thereby replicated previous findings (29, 30). PANSS positive increased by three points, which in general is considered clinically relevant if the impact of novel treatments is to be tested during S-ketamine challenge (30). The effect of S-ketamine on mood was measured with PANAS (48) since ketamine has an antidepressant effect as well (40). In contrast to this, we found that S-ketamine significantly decreased positive affect, which might reflect the negative symptoms induced by S-ketamine in this and other studies (29, 30). In addition, a recent study of mice indicates that only the R-enantiomer has an antidepressant effect (60).

Previous PET studies have reported a positive correlation between enhanced rCBF in the ACC and schizophrenia-like symptoms, mainly psychosis (36–38). By contrast, we did not find any significant correlations between the maximal rCBF increase in mPFC and the mental state effects induced by S-ketamine. Interestingly, this is in line with another recent pCASL ketamine challenge study (39). Several factors might influence the inconsistency between studies. First, the use of PET versus MR can impact findings. Second, different dosing regimens were used, and the psychotomimetic effects of ketamine are dose-dependent (30). Third, S- and R-ketamine induce differential psychopathology (57) and differences can be ascribed to the use of racemic versus S-ketamine. Moreover, different rating scales were used. Lastly, our data might have lacked power since pCASL data only were available for 16 subjects out of 25.

The study has several limitations that should be mentioned. First, we did not include a placebo group and cannot rule out that levels of glutamate increased preinfusion due to expectation of S-ketamine administration. Second, we did not include any scales to assess the dissociation effect of S-ketamine. Lastly, only 16 of the subjects had a useable pCASL scan, and some analyses might be underpowered.

In conclusion, our findings support the notion that glutamate levels in ACC are associated with rCBF in male HVs at rest and during the initial phase of an increase, and that S-ketamine transiently induces psychotomimetic effects and alters the activation of the ACC/mPFC and left Thal, resembling important aspects of schizophrenia. Future S-ketamine challenge studies can be improved by including a placebo group, placing the <sup>1</sup>H-MRS voxel more ventral, and optimising the dose regimen of S-ketamine for measures of glutamatergic metabolites. Furthermore, studies investigating the association between prefrontal glutamate,

rCBF, and progressive loss of brain tissue in initially first-episode patients with schizophrenia are warranted.

## ETHICS STATEMENT

This study was carried out in accordance with the recommendations of “guidelines for research with legally competent adults, Danish National Committee on Biomedical Research Ethics” with written informed consent from all subjects. All subjects gave written informed consent in accordance with the Declaration of Helsinki. The protocol was approved by the “Committee on Biomedical Research Ethics for the Capital Region of Denmark (H-4-2014-033).”

## AUTHOR CONTRIBUTIONS

All authors made substantial contributions to all of the following: (1) the conception and design of the study, or acquisition of data, or analysis and interpretation of data, (2) drafting the article or revising it critically for important intellectual content, (3) final approval of the version to be submitted, and (4) all authors agree to be accountable for all aspects of the work. Specifically, KB, KA, LB, ER, LM, BB, and BG designed the study; KA, SN, and BB collected the data; and KB, KA, SN, BB, and ER analysed the data. KB, KA, and BB drafted the manuscript.

## ACKNOWLEDGMENTS

We thank Mr. Mikkel Erlang for assistance with the production of the figures and Mrs. Anne B. Jensen for assistance with proofreading of the manuscript.

## FUNDING

Funding for this study was provided by an independent grant from the Lundbeck Foundation (R155-2013-16337) to Lundbeck Foundation Centre of Excellence for Clinical Intervention and Neuropsychiatric Schizophrenia Research (CINS) and grants from the Faculty of Health and Medical Sciences, University of Copenhagen (KB); Danish counsel for independent research (KA); Danish psychiatric society (SR); and Mental Health Services, capital region of Denmark (LB). The funding sources had no further role in study design; in the collection, analysis, and interpretation of data; in the writing of the report; and in the decision to submit the paper for publication.

## SUPPLEMENTARY MATERIAL

The Supplementary Material for this article can be found online at <http://www.frontiersin.org/articles/10.3389/fpsyg.2018.00022/full#supplementary-material>.

## REFERENCES

1. Andreasen NC, Nopoulos P, Magnotta V, Pierson R, Ziebell S, Ho BC. Progressive brain change in schizophrenia: a prospective longitudinal study of

first-episode schizophrenia. *Biol Psychiatry* (2011) 70(7):672–9. doi:10.1016/j.biopsych.2011.05.017

2. Bora E, Fornito A, Radua J, Walterfang M, Seal M, Wood SJ, et al. Neuro-anatomical abnormalities in schizophrenia: a multimodal voxelwise meta-

- analysis and meta-regression analysis. *Schizophr Res* (2011) 127(1–3):46–57. doi:10.1016/j.schres.2010.12.020
3. Chan RC, Di X, McAlonan GM, Gong QY. Brain anatomical abnormalities in high-risk individuals, first-episode, and chronic schizophrenia: an activation likelihood estimation meta-analysis of illness progression. *Schizophr Bull* (2011) 37(1):177–88. doi:10.1093/schbul/sbp073
  4. Ellison-Wright I, Glahn DC, Laird AR, Thelen SM, Bullmore E. The anatomy of first-episode and chronic schizophrenia: an anatomical likelihood estimation meta-analysis. *Am J Psychiatry* (2008) 165(8):1015–23. doi:10.1176/appi.ajp.2008.07101562
  5. Glahn DC, Laird AR, Ellison-Wright I, Thelen SM, Robinson JL, Lancaster JL, et al. Meta-analysis of gray matter anomalies in schizophrenia: application of anatomic likelihood estimation and network analysis. *Biol Psychiatry* (2008) 64(9):774–81. doi:10.1016/j.biopsych.2008.03.031
  6. Williamson P. Early models of the final common pathway 2: basal ganglia – thalamocortical circuits. In: Williamson P, editor. *Mind, Brain, and Schizophrenia*. New York: OUP Oxford (2005). p. 143–54.
  7. Williamson PC, Allman JM. A framework for interpreting functional networks in schizophrenia. *Front Hum Neurosci* (2012) 6:184. doi:10.3389/fnhum.2012.00184
  8. Grace AA. Gating of information flow within the limbic system and the pathophysiology of schizophrenia. *Brain Res Brain Res Rev* (2000) 31(2–3):330–41. doi:10.1016/S0165-0173(99)00049-1
  9. Lodge DJ, Grace AA. Aberrant hippocampal activity underlies the dopamine dysregulation in an animal model of schizophrenia. *J Neurosci* (2007) 27(42):11424–30. doi:10.1523/JNEUROSCI.2847-07.2007
  10. Olney JW, Farber NB. Glutamate receptor dysfunction and schizophrenia. *Arch Gen Psychiatry* (1995) 52(12):998–1007. doi:10.1001/archpsyc.1995.03950240016004
  11. Schobel SA, Chaudhury NH, Khan UA, Paniagua B, Styner MA, Asllani I, et al. Imaging patients with psychosis and a mouse model establishes a spreading pattern of hippocampal dysfunction and implicates glutamate as a driver. *Neuron* (2013) 78(1):81–93. doi:10.1016/j.neuron.2013.02.011
  12. Attwell D, Buchan AM, Charpak S, Lauritzen M, Macvicar BA, Newman EA. Glial and neuronal control of brain blood flow. *Nature* (2010) 468(7321):232–43. doi:10.1038/nature09613
  13. Kraguljac NV, White DM, Reid MA, Lahti AC. Increased hippocampal glutamate and volumetric deficits in unmedicated patients with schizophrenia. *JAMA Psychiatry* (2013) 70(12):1294–302. doi:10.1001/jamapsychiatry.2013.2437
  14. Théberge J, Bartha R, Drost DJ, Menon RS, Malla A, Takhar J, et al. Glutamate and glutamine measured with 4.0 T proton MRS in never-treated patients with schizophrenia and healthy volunteers. *Am J Psychiatry* (2002) 159(11):1944–6. doi:10.1176/appi.ajp.159.11.1944
  15. Kegeles LS, Mao X, Stanford AD, Girgis R, Ojeil N, Xu X, et al. Elevated prefrontal cortex gamma-aminobutyric acid and glutamate-glutamine levels in schizophrenia measured *in vivo* with proton magnetic resonance spectroscopy. *Arch Gen Psychiatry* (2012) 69(5):449–59. doi:10.1001/archgenpsychiatry.2011.1519
  16. Bustillo JR, Rowland LM, Mullins P, Jung R, Chen H, Qualls C, et al. 1H-MRS at 4 Tesla in minimally treated early schizophrenia. *Mol Psychiatry* (2010) 15(6):629–36. doi:10.1038/mp.2009.121
  17. Wijtenburg SA, Wright SN, Korenic SA, Gaston FE, Ndubuizu N, Chiappelli J, et al. Altered glutamate and regional cerebral blood flow levels in schizophrenia: a 1H-MRS and pCASL study. *Neuropsychopharmacology* (2017) 42(2):562–71. doi:10.1038/npp.2016.172
  18. de la Fuente-Sandoval C, León-Ortiz P, Azcárraga M, Stephano S, Favila R, Díaz-Galvis L, et al. Glutamate levels in the associative striatum before and after 4 weeks of antipsychotic treatment in first-episode psychosis a longitudinal proton magnetic resonance spectroscopy study. *JAMA Psychiatry* (2013) 70(10):1057–66. doi:10.1001/jamapsychiatry.2013.289
  19. Marsman A, van den Heuvel MP, Klomp DW, Kahn RS, Luijten PR, Hulshoff Pol HE. Glutamate in schizophrenia: a focused review and meta-analysis of (1)H-MRS studies. *Schizophr Bull* (2013) 39(1):120–9. doi:10.1093/schbul/sbr069
  20. Goozee R, Handley R, Kempton MJ, Dazzan P. A systematic review and meta-analysis of the effects of antipsychotic medications on regional cerebral blood flow (rCBF) in schizophrenia: association with response to treatment. *Neurosci Biobehav Rev* (2014) 43:118–36. doi:10.1016/j.neubiorev.2014.03.014
  21. Wang J, Tang Y, Zhang T, Cui H, Xu L, Zeng B, et al. Reduced gamma-aminobutyric acid and glutamate+glutamine levels in drug-naïve patients with first-episode schizophrenia but not in those at ultrahigh risk. *Neural Plast* (2016) 2016:3915703. doi:10.1155/2016/3915703
  22. Aoyama N, Théberge J, Drost DJ, Manchanda R, Northcott S, Neufeld RW, et al. Grey matter and social functioning correlates of glutamatergic metabolic loss in schizophrenia. *Br J Psychiatry* (2011) 198(6):448–56. doi:10.1192/bj.p.110.079608
  23. Catafau AM, Parellada E, Lomeña FJ, Bernardo M, Pavía J, Ros D, et al. Prefrontal and temporal blood flow in schizophrenia: resting and activation technetium-99m-HMPAO SPECT patterns in young neuroleptic-naïve patients with acute disease. *J Nucl Med* (1994) 35(6):935–41.
  24. Parellada E, Catafau AM, Bernardo M, Lomena F, Gonzalez-Monclus E, Setoain J. Prefrontal dysfunction in young acute neuroleptic-naïve schizophrenic patients: a resting and activation SPECT study. *Psychiatry Res* (1994) 55(3):131–9. doi:10.1016/0925-4927(94)90021-3
  25. Andreasen NC, O'Leary DS, Flaum M, Nopoulos P, Watkins GL, Boles Ponto LL, et al. Hypofrontality in schizophrenia: distributed dysfunctional circuits in neuroleptic-naïve patients. *Lancet* (1997) 349(9067):1730–4. doi:10.1016/S0140-6736(96)08258-X
  26. Vita A, Bressi S, Perani D, Invernizzi G, Giobbio GM, Dieci M, et al. High-resolution SPECT study of regional cerebral blood flow in drug-free and drug-naïve schizophrenic patients. *Am J Psychiatry* (1995) 152(6):876–82. doi:10.1176/ajp.152.6.876
  27. Early TS, Reiman EM, Raichle ME, Spitznagel EL. Left globus pallidus abnormality in never-medicated patients with schizophrenia. *Proc Natl Acad Sci U S A* (1987) 84(2):561–3. doi:10.1073/pnas.84.2.561
  28. Cahn W, van Haren NE, Hulshoff Pol HE, Schnack HG, Caspers E, Laponder DA, et al. Brain volume changes in the first year of illness and 5-year outcome of schizophrenia. *Br J Psychiatry* (2006) 189:381–2. doi:10.1192/bj.p.105.015701
  29. Krystal JH, Karper LP, Seibyl JP, Freeman GK, Delaney R, Bremner JD, et al. Subanesthetic effects of the noncompetitive NMDA antagonist, ketamine, in humans. Psychotomimetic, perceptual, cognitive, and neuroendocrine responses. *Arch Gen Psychiatry* (1994) 51(3):199–214. doi:10.1001/archpsyc.1994.03950030035004
  30. Kleinloog D, Uit den Boogaard A, Dahan A, Mooren R, Klaassen E, Stevens J, et al. Optimizing the glutamatergic challenge model for psychosis, using S+-ketamine to induce psychomimetic symptoms in healthy volunteers. *J Psychopharmacol* (2015) 29(4):401–13. doi:10.1177/0269881115570082
  31. Moghaddam B, Adams B, Verma A, Daly D. Activation of glutamatergic neurotransmission by ketamine: a novel step in the pathway from NMDA receptor blockade to dopaminergic and cognitive disruptions associated with the prefrontal cortex. *J Neurosci* (1997) 17(8):2921–7.
  32. Rowland LM, Bustillo JR, Mullins PG, Jung RE, Lenroot R, Landgraf E, et al. Effects of ketamine on anterior cingulate glutamate metabolism in healthy humans: a 4-T proton MRS study. *Am J Psychiatry* (2005) 162(2):394–6. doi:10.1176/appi.ajp.162.2.394
  33. Stone JM, Dietrich C, Edden R, Mehta MA, De Simoni S, Reed LJ, et al. Ketamine effects on brain GABA and glutamate levels with 1H-MRS: relationship to ketamine-induced psychopathology. *Mol Psychiatry* (2012) 17(7):664–5. doi:10.1038/mp.2011.171
  34. Li M, Demenescu LR, Colic L, Metzger CD, Heinze HJ, Steiner J, et al. Temporal dynamics of antidepressant ketamine effects on glutamine cycling follow regional fingerprints of AMPA and NMDA receptor densities. *Neuropsychopharmacology* (2017) 42(6):1201–9. doi:10.1038/npp.2016.184
  35. Taylor MJ, Tiangga ER, Mhuircheartaigh RN, Cowen PJ. Lack of effect of ketamine on cortical glutamate and glutamine in healthy volunteers: a proton magnetic resonance spectroscopy study. *J Psychopharmacol* (2012) 26(5):733–7. doi:10.1177/026988111405359
  36. Breier A, Malhotra AK, Pinals DA, Weisenfeld NI, Pickar D. Association of ketamine-induced psychosis with focal activation of the prefrontal cortex in healthy volunteers. *Am J Psychiatry* (1997) 154(6):805–11. doi:10.1176/ajp.154.6.805
  37. Vollenweider FX, Leenders KL, Scharfetter C, Antonini A, Maguire P, Missimer J, et al. Metabolic hyperfrontality and psychopathology in the ketamine model

- of psychosis using positron emission tomography (PET) and [18F]fluorodeoxyglucose (FDG). *Eur Neuropsychopharmacol* (1997) 7(1):9–24. doi:10.1016/S0924-977X(96)00039-9
38. Holcomb HH, Lahti AC, Medoff DR, Cullen T, Tamminga CA. Effects of non-competitive NMDA receptor blockade on anterior cingulate cerebral blood flow in volunteers with schizophrenia. *Neuropsychopharmacology* (2005) 30(12):2275–82. doi:10.1038/sj.npp.1300824
39. Pollak TA, De Simoni S, Barimani B, Zelaya FO, Stone JM, Mehta MA. Phenomenologically distinct psychotomimetic effects of ketamine are associated with cerebral blood flow changes in functionally relevant cerebral foci: a continuous arterial spin labelling study. *Psychopharmacology (Berl)* (2015) 232(24):4515–24. doi:10.1007/s00213-015-4078-8
40. Fond G, Loundou A, Rabu C, Macgregor A, Lançon C, Brittner M, et al. Ketamine administration in depressive disorders: a systematic review and meta-analysis. *Psychopharmacology (Berl)* (2014) 231(18):3663–76. doi:10.1007/s00213-014-3664-5
41. Pratt J, Dawson N, Morris BJ, Grent-t-Jong T, Roux F, Uhlhaas PJ. Thalamocortical communication, glutamatergic neurotransmission and neural oscillations: a unique window into the origins of ScZ? *Schizophr Res* (2016) 180:4–12. doi:10.1016/j.schres.2016.05.013
42. Carlsson A. The neurochemical circuitry of schizophrenia. *Pharmacopsychiatry* (2006) 39(Suppl 1):S10–4. doi:10.1055/s-2006-931483
43. Glenthøj BY, Hemmingsen R. Dopaminergic sensitization: implications for the pathogenesis of schizophrenia. *Prog Neuropsychopharmacol Biol Psychiatry* (1997) 21(1):23–46. doi:10.1016/S0278-5846(96)00158-3
44. Grace AA. Phasic versus tonic dopamine release and the modulation of dopamine system responsiveness: a hypothesis for the etiology of schizophrenia. *Neuroscience* (1991) 41(1):1–24. doi:10.1016/0306-4522(91)90196-U
45. Alexander GE, Crutcher MD, DeLong MR. Basal ganglia-thalamocortical circuits: parallel substrates for motor, oculomotor, “prefrontal” and “limbic” functions. *Prog Brain Res* (1990) 85:119–46. doi:10.1016/S0079-6123(08)62678-3
46. Wing JK, Babor T, Brugha T, Burke J, Cooper JE, Giel R, et al. SCAN. Schedules for clinical assessment in neuropsychiatry. *Arch Gen Psychiatry* (1990) 47(6):589–93. doi:10.1001/archpsyc.1990.01810180089012
47. Kay SR, Fiszbein A, Opler LA. The positive and negative syndrome scale (PANSS) for schizophrenia. *Schizophr Bull* (1987) 13(2):261–76. doi:10.1093/schbul/13.2.261
48. Watson D, Clark LA, Tellegen A. Development and validation of brief measures of positive and negative affect: the PANAS scales. *J Pers Soc Psychol* (1988) 54(6):1063–70. doi:10.1037/0022-3514.54.6.1063
49. Dai W, Garcia D, de Bazelaire C, Alsop DC. Continuous flow-driven inversion for arterial spin labeling using pulsed radio frequency and gradient fields. *Magn Reson Med* (2008) 60(6):1488–97. doi:10.1002/mrm.21790
50. Provencher SW. Estimation of metabolite concentrations from localized *in vivo* proton NMR spectra. *Magn Reson Med* (1993) 30(6):672–9. doi:10.1002/mrm.1910300604
51. Cook RWS. *Residuals and Influence in Regression*. New York, NY: Chapman & Hall (1982).
52. Gordon GR, Choi HB, Rungta RL, Ellis-Davies GC, MacVicar BA. Brain metabolism dictates the polarity of astrocyte control over arterioles. *Nature* (2008) 456(7223):745–9. doi:10.1038/nature07525
53. Ihmsen H, Geisslinger G, Schuttler J. Stereoselective pharmacokinetics of ketamine: R(-)-ketamine inhibits the elimination of S(+)-ketamine. *Clin Pharmacol Ther* (2001) 70(5):431–8. doi:10.1016/S0009-9236(01)06321-4
54. Sibson NR, Mason GF, Shen J, Cline GW, Herskovits AZ, Wall JE, et al. *In vivo* (13)C NMR measurement of neurotransmitter glutamate cycling, anaplerosis and TCA cycle flux in rat brain during. *J Neurochem* (2001) 76(4):975–89. doi:10.1046/j.1471-4159.2001.00074.x
55. Rothman DL, De Feyter HM, de Graaf RA, Mason GF, Behar KL. 13C MRS studies of neuroenergetics and neurotransmitter cycling in humans. *NMR Biomed* (2011) 24(8):943–57. doi:10.1002/nbm.1772
56. Milak MS, Proper CJ, Mulhern ST, Parter AL, Kegeles LS, Ogden RT, et al. A pilot *in vivo* proton magnetic resonance spectroscopy study of amino acid neurotransmitter response to ketamine treatment of major depressive disorder. *Mol Psychiatry* (2016) 21(3):320–7. doi:10.1038/mp.2015.83
57. Vollenweider FX, Leenders KL, Oye I, Hell D, Angst J. Differential psychopathology and patterns of cerebral glucose utilisation produced by (S)- and (R)-ketamine in healthy volunteers using positron emission tomography (PET). *Eur Neuropsychopharmacol* (1997) 7(1):25–38. doi:10.1016/S0924-977X(96)00042-9
58. Kegeles LS, Abi-Dargham A, Zea-Ponce Y, Rodenhiser-Hill J, Mann JJ, Van Heertum RL, et al. Modulation of amphetamine-induced striatal dopamine release by ketamine in humans: implications for schizophrenia. *Biol Psychiatry* (2000) 48(7):627–40. doi:10.1016/S0006-3223(00)00976-8
59. Howes OD, Kapur S. The dopamine hypothesis of schizophrenia: version III – the final common pathway. *Schizophr Bull* (2009) 35(3):549–62. doi:10.1093/schbul/sbp006
60. Zanos P, Moaddel R, Morris PJ, Georgiou P, Fischell J, Elmer GI, et al. NMDAR inhibition-independent antidepressant actions of ketamine metabolites. *Nature* (2016) 533(7604):481–6. doi:10.1038/nature17998

**Conflict of Interest Statement:** BG is the leader of a Lundbeck Foundation Centre of Excellence for Clinical Intervention and Neuropsychiatric Schizophrenia Research (CINS), which is partially financed by two independent grants from the Lundbeck Foundation (R25-A2701 and R155-2013-16337), and partially financed by the Mental Health Services in the Capital Region of Denmark, the University of Copenhagen, and other foundations. All grants are the property of the Mental Health Services in the Capital Region of Denmark and administrated by them. KB, KA, SR, LM, ER, and BB declare no potential conflict of interest.

Copyright © 2018 Bojesen, Andersen, Rasmussen, Baandrup, Madsen, Glenthøj, Rostrup and Broberg. This is an open-access article distributed under the terms of the Creative Commons Attribution License (CC BY). The use, distribution or reproduction in other forums is permitted, provided the original author(s) and the copyright owner are credited and that the original publication in this journal is cited, in accordance with accepted academic practice. No use, distribution or reproduction is permitted which does not comply with these terms.



# GABAergic Mechanisms in Schizophrenia: Linking Postmortem and *In Vivo* Studies

Jeroen C. de Jonge<sup>1</sup>, Christiaan H. Vinkers<sup>1</sup>, Hilleke E. Hulshoff Pol<sup>1</sup>  
and Anouk Marsman<sup>1,2\*</sup>

<sup>1</sup>Brain Center Rudolf Magnus, Department of Psychiatry, University Medical Center Utrecht, Utrecht, Netherlands,

<sup>2</sup>Danish Research Centre for Magnetic Resonance, Copenhagen University Hospital Hvidovre, Hvidovre, Denmark

## OPEN ACCESS

### Edited by:

André Schmidt,  
King's College London,  
United Kingdom

### Reviewed by:

Florenzo Conti,  
Università Politecnica  
delle Marche, Italy  
Fei Du,  
Harvard Medical School,  
United States

### \*Correspondence:

Anouk Marsman  
anoukm@drcmr.dk

### Specialty section:

This article was submitted to  
Neuroimaging and Stimulation,  
a section of the journal  
*Frontiers in Psychiatry*

Received: 31 March 2017

Accepted: 22 June 2017

Published: 11 August 2017

### Citation:

De Jonge JC, Vinkers CH, Hulshoff Pol HE and Marsman A (2017) GABAergic Mechanisms in Schizophrenia: Linking Postmortem and *In Vivo* Studies. *Front. Psychiatry* 8:118.  
doi: 10.3389/fpsy.2017.00118

Schizophrenia is a psychiatric disorder characterized by hallucinations, delusions, disorganized thinking, and impairments in cognitive functioning. Evidence from postmortem studies suggests that alterations in cortical  $\gamma$ -aminobutyric acid (GABAergic) neurons contribute to the clinical features of schizophrenia. *In vivo* measurement of brain GABA levels using magnetic resonance spectroscopy (MRS) offers the possibility to provide more insight into the relationship between problems in GABAergic neurotransmission and clinical symptoms of schizophrenia patients. This study reviews and links alterations in the GABA system in postmortem studies, animal models, and human studies in schizophrenia. Converging evidence implicates alterations in both presynaptic and postsynaptic components of GABAergic neurotransmission in schizophrenia, and GABA may thus play an important role in the pathophysiology of schizophrenia. MRS studies can provide direct insight into the GABAergic mechanisms underlying the development of schizophrenia as well as changes during its course.

**Keywords:** GABA, schizophrenia, magnetic resonance spectroscopy, postmortem studies, *in vivo* studies

## BACKGROUND

Schizophrenia is a severe chronic psychiatric disorder characterized by hallucinations, delusions, disorganized thinking, and impairments in cognitive functioning, affecting approximately 1% of the population. Several lines of evidence suggest that abnormalities of specific cortical inhibitory neurons and its neurotransmitter  $\gamma$ -aminobutyric acid (GABA) could play an important role in the pathophysiology of schizophrenia (1). The current evidence on GABAergic abnormalities in schizophrenia is mostly based on postmortem studies and has not yet provided a conclusive answer about GABAergic alterations and activity in schizophrenia. *In vivo* measurements of GABA in schizophrenia may reveal additional insights. The aim of this study is to review the findings of postmortem and animal studies on different components of GABAergic neurotransmission and *in vivo* magnetic resonance spectroscopy (MRS) findings on GABA levels in the brains of patients with schizophrenia. To collect relevant literature, a PubMed search was performed using the following terms: ((schizophrenia [tiab] OR schizophrenic\* [tiab]) AND (glutamate decarboxylase [tiab] OR glutamic acid decarboxylase [tiab] OR GAD [tiab] OR GAD67 [tiab] OR GAD65 [tiab] OR GABA [tiab] OR gamma-aminobutyric acid [tiab] OR glutamate [tiab] OR glutameric [tiab] OR gene expression [tiab])).

## NEUROBIOLOGY OF GABA

### Presynaptic GABA Synthesis and Release

GABA is synthesized by decarboxylation of glutamate by glutamic acid decarboxylase (GAD) (Figure 1) (2). Based on its molecular weight, it is possible to distinguish two isotypes, the 65 kDa isotype GAD65 and the 67 kDa isotype GAD67, which are involved in different aspects of GABAergic neurotransmission (3). GAD65 is responsible for rapid synthesis of GABA during periods of high synaptic demand; it is predominantly located on axon terminals and synaptic vesicle membranes and is thus primarily associated with packaging and release of GABA (4–7). GAD67 is responsible for basal GABA levels (4, 5) and the majority (80–90%) of GABA synthesis (8); it is located in the cytosol and is thus primarily associated with GABA synthesis and non-vesicular release (6, 7).

After synthesis in the presynaptic terminal, GABA is packaged into vesicles by the vesicular GABA transporter (VGAT), which is embedded in the vesicular membrane (9). A presynaptic action potential can induce a  $\text{Ca}^{2+}$ -mediated fusion of the vesicle membrane and the presynaptic neuron membrane, which leads to release of GABA into the synaptic cleft. Alternatively, after strong depolarization or altered ion homeostasis, specific GABA transporters (GAT) may reverse their direction resulting in non-vesicular release of GABA (9, 10).

### Postsynaptic GABA Receptors

After release into the synaptic cleft, GABA exerts its inhibitory activity by binding to two types of receptors, such as  $\text{GABA}_A$  and  $\text{GABA}_B$  receptors.  $\text{GABA}_A$  receptors are ligand-gated  $\text{Cl}^-$  channels and produce most of the physiological actions of GABA (11).  $\text{GABA}_A$  receptors have a pentameric subunit structure derived from different gene families and include  $\alpha$ ,  $\beta$ ,  $\gamma$ ,  $\delta$ ,  $\epsilon$ ,  $\pi$ , and  $\theta$  subunits. Some of these subunits have several isoforms ( $\alpha 1–6$ ,  $\beta 1–3$ , and  $\gamma 1–3$ ) (12). In most cases, the pentamers of subunits include a pair of  $\alpha$  subunits and a pair of  $\beta$  subunits in combination with a fifth subunit ( $\gamma$  or  $\delta$ ) (13).

### GABA Transport

The synaptic activity of GABA is terminated when GABA is taken up by GAT that are embedded in the membranes of neurons and astrocytes (10). In humans, four types of GAT can be distinguished, GAT-1 to 3 and the betaine GABA transporter (BGT-1). GAT-1 is widely expressed in the brain, predominantly in presynaptic GABA neurons, and is thus primarily responsible for GABA reuptake (9, 10). GAT-3 is primarily responsible for GABA uptake into local astrocytes (14). In contrast to GAT-1 and GAT-3, GAT-2 and BGT-1 play a very limited role in GABAergic neurotransmission (10).

When GABA is taken up by neurons, it can either be repacked into vesicles or it can be degraded to succinic semialdehyde

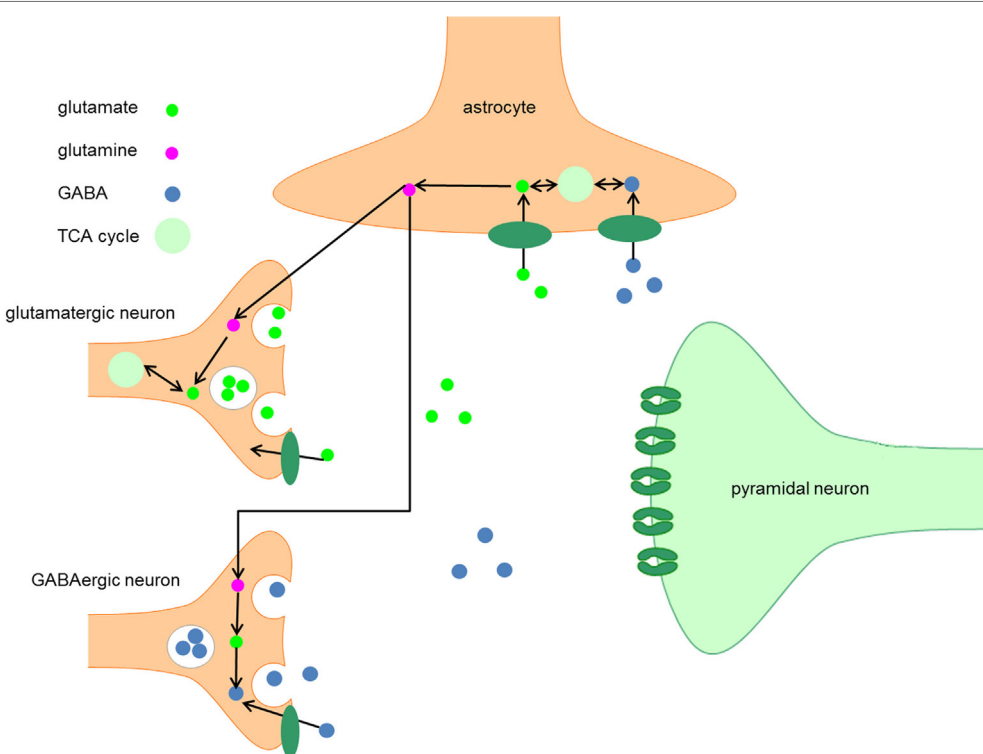


**FIGURE 1 |** Metabolism of GABA. After synthesis in the presynaptic terminal of GABA neurons, GABA is packaged into vesicles by the vesicular GABA transporter, which is embedded in the vesicular membrane. The synaptic activity of GABA is terminated when GABA is taken up by GABA transporters embedded in the plasma membranes of neurons and astrocytes. When GABA is taken up by neurons, it can be either repacked in vesicles for neurotransmission or it can be degraded by the enzyme GABA transaminase to succinic semialdehyde (SSA). After conversion of SSA to succinate, it enters the TCA cycle and is subsequently converted into glutamate. The following conversion of glutamate to GABA by GAD65 and GAD67 completes the GABA cycle.

(SSA) by the enzyme GABA transaminase. After conversion of SSA to succinate, the latter enters the TCA cycle and is subsequently converted into glutamate (10, 15). The following conversion of glutamate to GABA by GAD65 or GAD67 completes the GABA cycle (**Figure 1**).

## ALTERED GABAergic NEUROTRANSMISSION IN SCHIZOPHRENIA

### GAD67 in Schizophrenia

One of the most consistent postmortem findings in schizophrenia is a reduction of mRNA encoding for GAD67 in the dorsolateral prefrontal cortex (DLPFC) in layers 1 through 5 (3–5, 16–29), which results in a reduction of GAD67 protein levels although this has been less extensively studied (**Table 1**) (4, 30, 31). Since the majority of studies reported unaltered or increased neuronal density, it is unlikely that the reduction of GAD67 mRNA can be attributed to a decrease in the number of neurons in schizophrenia (16, 27, 32, 33). Rather, the density of neurons expressing a detectable level of GAD67 mRNA is decreased (27); expression of GAD67 mRNA is decreased below a detectable level in 25–35% of GABAergic neurons, while the remaining neurons have GAD67 mRNA levels similar to controls (27, 29). It has therefore been suggested that impaired GAD67 gene expression is limited to a certain subset of GABAergic neurons (27, 31). This subset could concern the chandelier, double bouquet, or wide-arbor neurons, which can be distinguished by the presence of specific calcium-binding proteins (**Box 1**) (1).

The subset that is affected in schizophrenia appears to include parvalbumin-containing GABAergic neurons. In schizophrenia, parvalbumin mRNA expression is reduced in prefrontal cortex (PFC) layers 3 and 4, but not layers 2, 5, or 6 (5, 27, 29, 51). The overall expression of parvalbumin mRNA is decreased whereas the density of neurons expressing detectable levels of parvalbumin is unaltered (5, 52, 53), implying that the reduction of parvalbumin mRNA is not accompanied by a loss of parvalbumin-containing neurons. The reduced parvalbumin mRNA expression is associated with the decreased density of GAD67 mRNA-positive GABAergic neurons. 50% of the parvalbumin-positive neurons lack detectable amounts of GAD67 mRNA (5), whereas calretinin mRNA (which is expressed by a different subset of neurons—see **Box 1**) expression and the density of calretinin-positive neurons remain unchanged in schizophrenia (5, 54). These findings imply that the reduced GAD67 mRNA expression may be selective for the parvalbumin-containing subgroup of GABA neurons in the PFC (5). Recent evidence suggests that GAD67 protein levels are unaltered in the chandelier neurons, suggesting that other parvalbumin-containing neurons, such as the basket cells, are involved (31).

The observed alterations regarding parvalbumin are not likely to be caused by exposure to antipsychotic medication. Long-term exposure to haloperidol and benzotropine did not lead to an altered expression of parvalbumin mRNA (5). Furthermore, transcript levels for parvalbumin were reduced to the same extent in the DLPFC of medication-naïve patients compared to patients

**TABLE 1 |** Postmortem studies on glutamic acid decarboxylase (GAD) in schizophrenia.

Reference	Brain region	Findings	Comments
Akbarian et al. (16)	Dorsolateral prefrontal cortex (DLPFC) (BA9)	GAD67 mRNA ↓	
Impagnatiello et al. (34)	Superior temporal gyrus (STG) (BA22)	GAD67 protein ↓	
Benes et al. (35)	Anterior cingulate cortex (ACC) (BA24)	GAD65-IR terminals =	
	DLPFC (BA9)		
Guidotti et al. (30)	DLPFC (BA9)	GAD67 mRNA ↓	Schizophrenia and bipolar disorder
		GAD67 protein ↓	
Mirnics et al. (24)	DLPFC (BA9)	GAD67 mRNA ↓	
Volk et al. (27)	DLPFC (BA9)	GAD67 mRNA ↓	
Hakak et al. (36)	DLPFC (BA46)	GAD 67 mRNA ↑	Elderly patients
		GAD65 mRNA ↑	
Knable et al. (23)	DLPFC (BA9)	GAD67 mRNA ↓	
Hashimoto et al. (5)	DLPFC (BA9)	GAD67 mRNA ↓	
Dracheva et al. (37)	DLPFC (BA46)	GAD67 mRNA ↑	Elderly patients
	Primary visual cortex (VC) (BA17)	GAD65 mRNA ↑	
Woo et al. (28)	ACC (BA24)	GAD67 mRNA ↓	Schizophrenia and bipolar disorder
Hashimoto et al. (19)	DLPFC (BA9)	GAD67 mRNA ↓	
Fatemi et al. (38)	Cerebellar cortex	GAD67 protein ↓	Schizophrenia, bipolar disorder, and major depression
		GAD65 protein ↓	
Veldic et al. (25)	DLPFC (BA9)	GAD67 mRNA ↓	Schizophrenia and bipolar disorder
Straub et al. (39)	DLPFC	GAD67 mRNA ↓	
		GAD67 protein =	
Veldic et al. (26)	DLPFC (BA9)	GAD67 mRNA ↓	
Woo et al. (29)	DLPFC (BA9)	GAD67 mRNA ↓	
Hashimoto et al. (20)	DLPFC (BA9)	GAD67 mRNA ↓	
Hashimoto et al. (21)	ACC (BA24)	GAD67 mRNA ↓	
	Primary motor cortex		
	Primary VC		

(Continued)

**TABLE 1 |** Continued

Reference	Brain region	Findings	Comments
Thompson et al. (3)	ACC (BA24)	GAD67 mRNA ↓	Schizophrenia, bipolar disorder, and major depression
	Orbital frontal cortex (OFC) (BA45)	(OFC, caudate, nucleus accumbens)	
	STG (BA22)		
	Caudate		
	Putamen		
	Nucleus accumbens		
	Medial dorsal thalamus		
Duncan et al. (17)	Anterior thalamus		
	DLPFC (BA9/46)	GAD67 mRNA ↓	
Curley et al. (4)	DLPFC	GAD67 mRNA ↓	
		GAD67 protein ↓	
Kimoto et al. (22)	DLPFC (BA9)	GAD67 mRNA ↓	
Glausier et al. (40)	DLPFC (BA9)	GAD65 mRNA =	
Rocco et al. (31)	DLPFC (BA9)	GAD67 protein unaltered in chandelier neurons	

**BOX 1 |** Subsets of GABAergic neurons.

Based on molecular, morphological, and physiological features, it is possible to distinguish different subsets of cortical GABA neurons, with the double bouquet, basket, and chandelier cells being the most abundant cortical GABAergic interneuron subsets (1, 18). The subpopulations have different influences on the regulation of information processing in the dorsolateral prefrontal cortex (DLPFC), partly because the axons of the GABAergic interneurons synapse at different locations on the pyramidal neuron (1, 41, 42). Furthermore, it is possible to identify certain morphological and functional subgroups of GABA neurons which contain different calcium-binding proteins (43–45).

*Chandelier neurons* synapse at axon initial segments (AIS) of pyramidal neurons and therefore provide inhibitory inputs to the AIS. These synaptic connections are formed in such a way that vertical arrays, so-called “cartridges,” are formed (1, 46). Furthermore, these neurons contain the calcium-binding protein parvalbumin (5, 47).

*Basket or wide-arbor neurons* synapse at cell bodies and proximal dendrites of pyramidal neurons. Similar to chandelier neurons, basket cells in the prefrontal cortex contain the protein *parvalbumin* (43).

*Double bouquet neurons* contain the calcium-binding protein *calbindin* and target the distal dendrites of pyramidal neurons (1, 48).

A third calcium-binding protein, *calretinin*, is expressed by approximately 50% GABAergic neurons, mainly *double bouquet cells*, in the DLPFC (43).

Since the parvalbumin-containing chandelier and basket neurons synapse at the AIS and soma, respectively, they provide a much stronger inhibitory regulation of the pyramidal neurons as compared to double bouquet cells, which synapse at the distal dendrites (49, 50). Given the heterogeneity in synaptic targets and specific features of the different subclasses of GABAergic neurons, altered interactions between different GABAergic neurons and pyramidal neurons may influence neuronal activity and hence functional output in different manners.

receiving antipsychotic medication (20). Animal studies have shown that treatment with dopamine D2-receptor antagonists influences the expression of GAD67 mRNA in the basal ganglia

**TABLE 2 |** Postmortem studies on GABA transporters (GAT)-1 in schizophrenia.

Reference	Brain region	Findings
Woo et al. (65)	Dorsolateral prefrontal cortex (DLPFC) (BA9)	GAT-1-IR cartridges of chandelier neurons ↓
Pierris et al. (66)	DLPFC (BA46)	GAT-1-IR cartridges of chandelier neurons ↓
Ohnuma et al. (64)	DLPFC (BA9/10)	GAT-1 mRNA ↓
Volk et al. (59)	DLPFC (BA9)	GAT-1 mRNA ↓
Konopaske et al. (62)	Auditory association area (BA42)	GAT-1-IR cartridges of chandelier neurons =
Hashimoto et al. (20)	DLPFC (BA9)	GAT-1 mRNA ↓
Hashimoto et al. (21)	DLPFC (BA9) Anterior cingulate cortex (BA24) Primary visual cortex Primary motor cortex	GAT-1 mRNA ↓

(BG) (55–58) but not in the PFC; however, D2-receptor density in the PFC is much lower than in the BG (20, 27).

## GAT-1 in Schizophrenia

The transporter protein GAT-1 is present in the presynaptic neuron and is responsible for the synaptic reuptake of GABA (19, 59). It plays a role in both tonic and phasic GABA-mediated inhibition (60, 61). GAT-1 terminates the synaptic activity of GABA and regulates the duration and efficacy of synaptic GABAergic transmission (62); therefore, reduced GAT-1 levels suggest increased availability of GABA in the synapse (63). Several studies found reduced mRNA levels encoding for the GAT-1 protein in schizophrenia. GAT-1 mRNA levels are decreased in GABAergic neurons in the DLPFC (Table 2) (20, 21, 59, 62, 64). Together with the diminished expression of GAD67 mRNA, it is unclear whether this results in a net increase or decrease of the inhibitory tone on pyramidal cells (63). Moreover, GAT-1 mRNA expression is reduced below detectable levels in a subset of GABAergic neurons and relatively unaltered in the majority of the GABAergic neurons (59). The affected subset appears to include parvalbumin-containing neurons (1, 59). The reduction of GAT-1 mRNA expression is limited to layers 2 through 5, the same layers in which parvalbumin-containing neurons are found (59, 65).

The subset of GABAergic neurons where reduced GAT-1 mRNA levels are detected is possibly the subset of chandelier neurons (see Box 1). A marker of chandelier neurons is their GAT-1 immunoreactivity; the density of GAT-1 immunoreactive cartridges is decreased in schizophrenia, while markers of other axon terminal populations remain unchanged (65, 66). The lower density of GAT-1 immunoreactive cartridges implies decreased GAT-1 protein, which is associated with decreased GAT-1 mRNA levels. Putting together these findings, reduced GAT-1 mRNA levels may therefore account for the decreased density of GAT-1 immunoreactive axon cartridges in chandelier neurons (59). The reduction of GAT-1 immunoreactive cartridges cannot be attributed to a reduction of chandelier neurons, since the density of GABAergic neurons [identified by parvalbumin (52, 53) and VGAT (67)] is unchanged. Thus concluding, the density of

chandelier neurons containing GAT-1 protein in the DLPFC in patients with schizophrenia was reduced whereas the density of parvalbumin-containing neurons remains unaltered. This finding suggests that the reduced levels of GAT-1 mRNA are limited to the chandelier neurons (29, 65).

Long-term exposure to therapeutic blood levels of haloperidol in monkeys did not result in changes in the expression of GAT-1 mRNA or the expression of GAT-1 protein (65, 66, 68), nor did effects of alcohol abuse or benzodiazepine use explain the findings (20, 21).

## Postsynaptic GABA Receptors in Schizophrenia

GABA<sub>A</sub> receptors are ligand-gated chloride ion channels and produce most of the physiological actions of GABA (11). GABA<sub>A</sub> receptors have a pentameric subunit structure and the subunits are derived from different gene families encoding for different subunits including  $\alpha$ 1–6,  $\beta$ 1–3,  $\gamma$ 1–3,  $\delta$ ,  $\epsilon$ ,  $\pi$ , and  $\theta$  (12). The pentamers of subunits include in most cases a pair of  $\alpha$  subunits and a pair of  $\beta$  subunits in combination with a fifth subunit ( $\gamma$  or  $\delta$ ) (13). Early studies demonstrated increased binding of muscimol, a selective GABA<sub>A</sub> receptor agonist, in pyramidal neuronal cell bodies in patients with schizophrenia (69–71); however, muscimol can bind to all types of GABA<sub>A</sub> receptor subunits. Recent advancements in technology have enabled investigation of deficits of individual GABA<sub>A</sub> receptor subunits (72).

Subunits of the  $\alpha$ -type can be characterized by their subcellular localization within the central nervous system. Over 95% of the GABAergic synapses on the axon initial segment (AIS) of pyramidal neurons contain the  $\alpha$ 2 subunit, while only 15% of cortical GABA receptors contain the  $\alpha$ 2 subunit (73, 74). It appears that this subunit is characterized by high affinity, fast activation, and slow deactivation (75). Given its anatomical position and functional features, the GABA<sub>A</sub>  $\alpha$ 2 subunit serves as a major source for inhibitory tone on pyramidal neurons (46). Parvalbumin-containing neurons, which appear to exhibit a reduced expression of GAT-1 and GAD67 mRNA in schizophrenia, target the AIS of pyramidal neurons. Indeed, it has been demonstrated that in schizophrenia, the GABA<sub>A</sub>  $\alpha$ 2-receptor subunit is upregulated in the AIS of pyramidal neurons (46, 69, 76). This increase in  $\alpha$ 2 subunit density may occur in response to reduced extracellular GABA concentrations due to diminished GABA synthesis (1, 46). Furthermore, GAT-1 immunoreactive cartridges and the density of  $\alpha$ 2 subunits at the postsynapse of pyramidal neurons demonstrate an inverse correlation, which implies that GABA<sub>A</sub>  $\alpha$ 2 subunits are upregulated at the AIS of pyramidal neurons and GAT-1 is downregulated to provide a synergistic compensation for the diminished GABAergic activity (46). In contrast to GAD67 mRNA and GAT-1 mRNA, mRNA expression levels of postsynaptic GABA<sub>A</sub>  $\alpha$ 2-receptor subunits seem to be unaltered (16, 17). Reductions of  $\alpha$ 2-receptor subunits are exclusively found at the AIS synapses; the lack of upregulation of  $\alpha$ 2 subunit mRNA might be explained by the fact that inhibitory synapses at the AIS of pyramidal neurons make up less than 10% of the total number of inhibitory synapses of the pyramidal neuron (16, 77).

mRNA levels of the GABA<sub>A</sub>  $\alpha$ 1,  $\gamma$ 2,  $\alpha$ 4,  $\alpha$ 5, and  $\delta$  receptor subunits are suggested to be downregulated in the DLPFC of patients with schizophrenia (Table 3) (20, 21, 47, 78–80). However, two studies reported an increase of  $\alpha$ 1 subunit mRNA expression (34, 64), one study revealed an increase of  $\alpha$ 5 subunit mRNA (34), one study observed an increase of the GABA<sub>A</sub> receptor  $\alpha$ 1 subunit protein (72), and one study demonstrated no change of the  $\alpha$ 4 receptor subunit (80). In contrast to the  $\alpha$ 2 subunit localized at the AIS of pyramidal neurons, GABA<sub>A</sub> receptors containing the  $\alpha$ 1,

**TABLE 3 |** Postmortem studies on postsynaptic GABA receptors in schizophrenia.

Reference	Brain region	Findings
Hanada et al. (71)	Dorsolateral prefrontal cortex (DLPFC) (BA9) Caudate	GABA <sub>A</sub> receptor binding ↑
Benes et al. (76)	Anterior cingulate cortex (ACC)	GABA <sub>A</sub> receptor binding ↑
Akbarian et al. (16)	DLPFC (BA9)	GABA <sub>A</sub> $\alpha$ 1–5 receptor subunit mRNA = GABA <sub>A</sub> $\gamma$ 2-receptor subunit mRNA =
Benes et al. (69)	DLPFC (BA10)	GABA <sub>A</sub> receptor binding ↑
Huntsman et al. (79)	DLPFC (BA9)	GABA <sub>A</sub> receptor $\gamma$ 2 subunit mRNA ↓
Impagnatiello et al. (34)	DLPFC (BA9)	GABA <sub>A</sub> receptor $\alpha$ 1 subunit mRNA ↑ GABA <sub>A</sub> receptor $\alpha$ 5 subunit mRNA ↑
Dean et al. (70)	DLPFC (BA9)	GABA <sub>A</sub> receptor binding ↑
Ohnuma et al. (64)	DLPFC (BA9) BA10	GABA <sub>A</sub> receptor $\alpha$ 1 subunit mRNA ↑
Mirnics et al. (24)	DLPFC (BA9)	GABA <sub>A</sub> receptor $\beta$ 1, $\gamma$ 2/3, $\pi$ subunit mRNA ↓
Ishikawa et al. (72)	DLPFC (BA9)	GABA <sub>A</sub> receptor $\alpha$ 1, $\beta$ 2/3 subunit ↑
Ishikawa et al. (83)	DLPFC (BA9)	GABA <sub>A</sub> receptor 1 protein ↓
Vawter et al. (47)	DLPFC (BA9 + BA46)	GABA <sub>A</sub> receptor $\delta$ subunit mRNA ↓
Volk et al. (46)	Prefrontal cortex	GABA <sub>A</sub> receptor $\alpha$ 2 subunit protein ↑
Hashimoto et al. (20)	DLPFC (BA9)	GABA <sub>A</sub> receptor $\alpha$ 1/4, $\beta$ 3, $\gamma$ 2, $\delta$ subunit mRNA ↓
Hashimoto et al. (21)	DLPFC (BA9) ACC (BA24) Primary visual and motor cortices	GABA <sub>A</sub> receptor $\alpha$ 1, $\delta$ subunit mRNA ↓
Maldonado-Avilés et al. (80)	DLPFC (BA9)	GABA <sub>A</sub> receptor $\delta$ subunit mRNA ↓ GABA <sub>A</sub> receptor $\alpha$ 4 subunit mRNA =
Duncan et al. (17)	DLPFC (BA9/BA46)	GABA <sub>A</sub> receptor $\alpha$ 5 subunit mRNA ↓ GABA <sub>A</sub> receptor $\alpha$ 1/2 subunit mRNA =
Beneyto et al. (78)	DLPFC	GABA <sub>A</sub> receptor $\alpha$ 2 subunit mRNA ↑ GABA <sub>A</sub> receptor $\alpha$ 1/5, $\beta$ 2 subunit mRNA ↓ GABA <sub>A</sub> receptor $\alpha$ 3, $\beta$ 1, $\beta$ 3 =

$\alpha 5$ ,  $\gamma 2$ , and  $\delta$  (often co-expressed by  $\alpha 4$ ) subunits are predominantly localized in the dendrites of pyramidal neurons (73, 81, 82). The observed alterations in the postsynaptic GABA<sub>A</sub> receptors do not seem to be a consequence of an increased number of neurons, because the majority of studies have reported no change or an increase in neuron density (27, 32, 33, 51).

Animal studies in which rats were exposed to benzodiazepines did not reveal changes in the expression level of  $\alpha 2$  subunit mRNA or protein levels and long-term exposure to haloperidol or olanzapine did not result in altered  $\alpha 1$ ,  $\alpha 2$ ,  $\alpha 5$ ,  $\beta 2$ , or  $\delta$  subunit mRNA levels (20, 78, 84). Postmortem studies show that  $\alpha 1$  and  $\delta$  subunits are reduced to the same extent in the DLPFC of patients who were not taking antipsychotic medication at the time of death, which is unlikely to be driven by the effects of alcohol abuse or benzodiazepine use (20, 21). (For an overview of pre- and postsynaptic GABAergic alterations, see **Figure 2**.)

## Widespread GABAergic Alterations in Schizophrenia

There is sufficient histological–pathological evidence to link impairments in GABAergic neurotransmission in other cortical regions than the DLPFC to pathologies and cognitive dysfunctions observed in schizophrenia (63).

Similar to the DLPFC, the anterior cingulate cortex (ACC), primary visual cortex (VC), and primary motor cortex are characterized by the same deficits in GABAergic gene expression as seen in the DLPFC, including selective involvement of parvalbumin-containing subsets of GABA neurons. The largest

declines were reported for the levels of mRNA encoding for parvalbumin (21). These brain areas also exhibit a decrease of GAD67 mRNA, GAD65 mRNA, GAT-1 mRNA, and GABA<sub>A</sub> receptor  $\alpha 1$  and  $\delta$  subunits (1, 21, 28). Calretinin levels remained unchanged (21). GABA-related transcript expression is suggested to be decreased to the same extent in all aforementioned brain regions, so there possibly is no preferential involvement of the DLPFC (21). The reduced expression of GABA<sub>A</sub> receptor  $\alpha 1$  and  $\delta$  subunits in these cortical areas also imply that reduced phasic and tonic inhibition, respectively, might be a feature shared by multiple cortical regions.

Furthermore, in addition to the ACC, primary VC, and primary motor cortex which demonstrated similar GABAergic expression deficits as the DLPFC, the orbital frontal cortex (OFC), superior temporal gyrus (STG), striatum, and thalamus show a diminished GAD67 mRNA expression as well (3). In addition, the STG and auditory gyri demonstrated reduced GAT-1 protein levels (34). Reduction in GABAergic activity in the OFC could lead to disturbances related to emotional and cognitive functioning and may therefore underlie symptoms regarding social withdrawal and apathetic behavior (85). In addition, abnormalities in the STG could contribute to deficit auditory processing and auditory hallucinations (3). These findings imply that the aberrations seen in the DLPFC may not be due to alterations in DLPFC circuitry only, but that the altered transcript levels appear to be the consequence of a common upstream mechanism that operates across multiple cortical areas.

## Integration of Postmortem Findings on GABAergic Neurotransmission

A possible integrative model for the alterations in GABA neurotransmission is that a subset of prefrontal GABA neurons is affected in schizophrenia. In contrast to the reduced GAD67 and the consequent attenuation of inhibitory GABAergic neurotransmission, the reduction of GAT-1 mRNA expression tends to increase the synaptic activity of GABA (63). In addition, GABA<sub>A</sub> receptors are upregulated in postsynaptic pyramidal neurons, which suggests a compensatory increase in response to the decreased extracellular GABA concentrations (46, 70, 76). However, based on postmortem studies, it is not possible to identify the initial deficit in the pathological chain and, therefore, two scenarios are possible (see **Figure 2**).

The most likely scenario is an overall reduced GABAergic activity in schizophrenia. This implies that the initial step in this specific pathologic process is the presynaptic reduction of GABA synthesis, followed by a secondary, compensatory reduction of reuptake by means of GAT-1 and by compensatory upregulation of postsynaptic GABA receptors (1, 18, 86). This synergistic attempt, to improve the GABAergic neurotransmission at the synapse of the pyramidal neuron AIS, serves to compensate for the initial deficit in synthesis of GABA. Consistent with the theory that the reduction of synthesis is the first step in the pathological chain, mice lacking the GAT-1 gene do not develop diminished levels of GAD67 mRNA. This indicates that the reduction of GAD67 is the initial event (87). Furthermore, GABA hypofunction due to decreased synthesis reflected by the diminished levels of GAD67 mRNA was imitated in rats by means of pharmacological

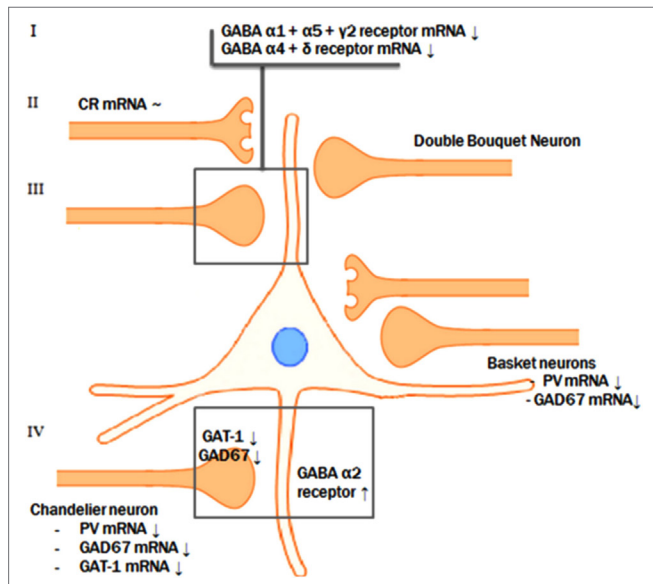


**FIGURE 2 |** Pre- and postsynaptic GABAergic alterations. The reductions of GAD67 mRNA, parvalbumin mRNA, and GAT-1 mRNA levels in the parvalbumin-containing chandelier neurons seem to result in a compensatory postsynaptic upregulation of  $\alpha 2$ -receptor at the axon initial segment of the pyramidal neuron. Presynaptic alterations in neurons targeting the dendritic domain of the pyramid neuron might also be accompanied by abnormalities of the postsynaptic GABA  $\alpha 1$ ,  $\alpha 5$ , and  $\gamma 2$  and the extrasynaptic  $\alpha 4$  and  $\delta$  receptor subunits.

blockade of prefrontal GABA<sub>A</sub> receptors. This resulted in impaired working memory performance, a cognitive function characteristically disturbed in patients with schizophrenia (88, 89). However, it is still controversial whether the compensatory mechanisms are sufficient to overcome the decreased GABA synthesis. In other words, it is unknown if the net effect of the diminished presynaptic synthesis on the one hand and the decreased reuptake increased postsynaptic reception on the other hand result in an increase or decrease of the inhibitory tone on pyramidal cells by GABAergic neurons (63). In conclusion, the most likely scenario is that reduced presynaptic GABA production results in a reduced reuptake of GABA and in upregulated postsynaptic GABA receptors in schizophrenia.

Alternatively, an excessive increase of GABAergic activity due to both primary diminished reuptake and upregulated postsynaptic receptors may also be an initial step in the pathological process followed by secondary compensatory downregulation of GAD67 mRNA in chandelier neurons due to the excessive GABAergic activity. Furthermore, the effects of pharmaceuticals involved in GABAergic neurotransmission seem to be in line with the hypothesis of excess GABAergic activity. For example, lorazepam, a positive allosteric modulator of GABAergic neurotransmission, results in a deterioration of working memory aberrations while flumazenil, a partial inverse agonist, leads to improvement of the working memory deficits (63). Thus, according to this scenario, excessive GABAergic activity could be the result of an initial postsynaptic upregulation of the GABA<sub>A</sub> receptor and downregulation of the presynaptic GABA reuptake transporters as a first step in the pathological chain (63).

Finally, the aberrations seen in the DLPFC may not be due to alterations in DLPFC circuitry, but instead reflect transcript levels that are a consequence of a common upstream mechanism that operates across multiple cortical areas in schizophrenia.

In conclusion, the most likely scenario involves reduced GABA concentrations due to a compromised production of GABA reflected by the diminished concentration of GAD67 mRNA. However, due to the observation that presynaptic GAT-1 is reduced and postsynaptic receptors are upregulated, postmortem studies do not provide a conclusive answer about the net GABAergic concentrations and activity. Therefore, *in vivo* studies could provide additional insights into GABA levels in clinical states contributing to a more definitive formulation about the pathological cascade and GABAergic alterations in schizophrenia.

## IN VIVO MRS OF GABA IN SCHIZOPHRENIA

GABA can be measured *in vivo* using proton MRS (<sup>1</sup>H-MRS). MRS provides a means to non-invasively identify and quantify metabolites in tissue and can be carried out with an MR scanner. MRS makes use of the magnetic properties of nuclei, e.g., the proton (<sup>1</sup>H). Because the magnetic properties of a nucleus are influenced by its chemical environment, it is possible to identify signals from different molecules within the MR spectrum. However, measurement of GABA with <sup>1</sup>H-MRS is challenging since its low concentration results in a relatively small signal which is overlapped by more intense signals from more abundant

metabolites. It is possible to separate the GABA signal from other, more intense signals with spectral editing techniques. With spectral editing the magnetic properties of a specific molecule are used to improve detection of that molecule.

Based on presynaptic and postsynaptic GABAergic alterations in postmortem studies, it is possible to identify numerous brain areas such as the ACC, primary VC, primary motor cortex, OFC, BG, STG, thalamus, but especially the DLPFC in which it is expected to measure altered GABAergic concentrations by <sup>1</sup>H-MRS. As mentioned before, postmortem studies do not provide a conclusive answer about the net GABAergic concentrations and activity. Therefore, <sup>1</sup>H-MRS could provide additional insights, contributing to a more definitive formulation about the pathological cascade and GABAergic alterations in schizophrenia. However, up until now MRS studies on GABA in schizophrenia are rather scarce and only cross-sectional. Moreover, the current literature is inconsistent regarding the measured GABA levels in different brain regions of patients with schizophrenia. Currently, seven studies reported GABA reductions (90–96), six studies reported unchanged GABA levels (90, 92–94, 97, 98), and two studies reported increased levels (Table 4) (97, 99). Since GABA levels may differ in early (90, 91, 93, 94) and chronic schizophrenia (91, 93, 94, 98, 99), brain levels might also be dependent on the stage of the disease. Recent meta-analysis showed no changes in GABA levels in patients with schizophrenia in any given brain region, however, when averaging GABA levels across all measured brain regions per study, GABA appeared to be lower in patients compared to healthy controls (100).

The fluctuating and inconsistent findings of the few MRS studies that have been published so far in schizophrenia could be explained by several factors such as small and heterogeneous sample sizes, low magnetic field strengths resulting in a less robust measurement of GABA, methodological limitations leading to relatively large voxel volumes and marginal adjustments with regard to gray and white matter differences (Table 4) (15). Moreover, most studies measured GABA referenced to creatine and although this is a common approach, fluctuations in creatine concentrations could be, to a certain extent, responsible for the observed GABAergic findings. However, the most prominent limitation compromises the undetermined role of antipsychotic medication use with regard to GABA levels measured by <sup>1</sup>H-MRS.

## GABA AND ANTIPSYCHOTIC MEDICATION

In 38 chronic schizophrenia patients, higher GABA concentrations were found in the left BG in patients using typical antipsychotics as compared to patients using atypical antipsychotics (82). Furthermore, a positive correlation was reported between GABA concentration in the left BG and anticholinergic medication (98). It is thus possible that antipsychotic medication influences GABA concentrations and different types of medications could have differing effects (98).

However, in patients diagnosed with schizophrenia and using antipsychotic medication at baseline, the use of atypical antipsychotics did not have any effects on GABA concentrations in the left BG, frontal lobe, and parieto-occipital lobe during a follow-up

**TABLE 4 |** *In vivo* magnetic resonance spectroscopy studies of GABA in schizophrenia.

Reference	Findings			Antipsychotic medication, % of patients			Comments
	Early SZ	Chronic SZ	Mixed population	Early SZ	Chronic SZ	Mixed population	
Goto et al. (90)	ACC: baseline = 6M = baseline–6M = BG: baseline ↓ 6M ↓ baseline–6M = POC: baseline = 6M = baseline–6M =			Atypical 100% (risperidone, olanzapine, aripiprazole, quetiapine)			Patients were examined at baseline and after 6 months of antipsychotic treatment
Ongur et al. (99)		ACC ↑ POC ↑			Unknown 100%		1 early SZ patient (0.5%)
Tayoshi et al. (98)	ACC =				Typical ± atypical 42%		
	BG =				Atypical only 58%		
Yoon et al. (96)		VC ↓				Typical 8% Atypical 54% Unmedicated 38%	
Kegeles et al. (97)		MPFC: unmed. ↑ med. = unmed.–med. = DLPFC: unmed. = med. = unmed.–med. =		Atypical 100%	Typical 20%		
					Atypical 80%		
Kelemen et al. (91)	VC: baseline ↓ 6M ↓			Typical 11% Atypical 89%			Patients were examined at baseline and after 6 months of antipsychotic treatment
Marsman et al. (92)		PFC ↓ POC =			Atypical 100%		Min.–max. disease duration: 1–213 months
Rowland et al. (93)	ACC =  CSO =	ACC ↓ ACC early-chronic = CSO = CSO early-chronic =		Atypical 100%	Typical 20% Atypical 80%		
Rowland et al. (94)	ACC =	ACC ↓  ACC early-chronic ↓		Typical 3.5% Atypical 86% Typical + atypical 3.5% Unmedicated 7%	Typical 13% Atypical 58% Typical + atypical 19% Unmedicated 10%		
Wang et al. (95)	PFC ↓			Drug naïve 100%			All first-episode SZ

ACC, anterior cingulate cortex; BG, basal ganglia; POC, parieto-occipital lobe; PFC, prefrontal cortex; MPFC, medial prefrontal cortex; DLPFC, dorsolateral prefrontal cortex; CSO, centrum semiovale; VC, visual cortex.

period of 6 months (90). At baseline, the concentration of GABA in the left BG in these first-episode patients was decreased (81), but this reduction was not reversed after 6 months of treatment with antipsychotic medication (84). Interestingly, clinical condition, assessed by PANSS scores, did improve during this time period. This suggests that medication use has no profound effect on GABA concentrations in patients with schizophrenia although

there does occur a clinical improvement (90, 101). However, it is also possible that the medication regimen prevented further progressive reduction of GABA concentrations in these patients. Studying patients not taking antipsychotic medication may provide valuable additional insights regarding this matter. A recent study addressed this topic and evaluated GABA concentration in 16 unmedicated patients, consisting of 9 medication-naïve patients

and 7 patients with no antipsychotic medication use 14 days prior to the investigation. This study observed higher GABA concentrations in never- and unmedicated patients compared to medicated patients (97). This implies that medication use might lead to a normalization of GABA concentrations (97). However, as mentioned before, medicated patients did not show any alterations regarding GABA concentrations after 6 months of antipsychotic therapy (90). Possibly, patients that were minimally treated at baseline differed from those that were medication naïve (90, 101), and the normalization of GABA concentrations due to antipsychotic treatment takes place at the beginning of the treatment. To formulate a conclusive answer, future studies are required, which assess both within-subject medication and medication-naïve study designs. In conclusion, many factors contribute to the inconsistency in literature and future studies need to take these factors into account to reconcile the fluctuating findings.

## GABA AND COGNITION

The observed changes in GABAergic neurotransmission may have functional significance (96). GABA measurement in the VC revealed reduced concentrations, and this decrease was positively correlated with orientation-specific surround suppression (OSSS) (96). OSSS is a behavioral measure of visual inhibition, and it is believed that this process relies on GABAergic neurotransmission in the VC (85). Furthermore, poorer performance on attention tests was correlated with decreased GABA concentrations in patients with schizophrenia (93). These observations are consistent with the GABA deficit hypothesis, which states that reduced GABAergic neurotransmission results in cognitive deficits, and imply that MRS is able to measure the pool of cortical GABA that has a direct relationship with GABA-mediated functions (15). Since the GABAergic expression deficits exhibit a widespread cortical involvement, it is likely that such aberrations generalize to other cortical areas (21, 96).

On the other hand, recent research showed a negative association between level of cognitive functioning and GABA level in the PFC in schizophrenia patients (92). Together with the finding that GABA levels are reduced in schizophrenia and albeit the finding that intelligence levels are lower in patients compared to matched healthy controls (102), this may imply that the GABA deficit hypothesis mainly applies to patients with lower intelligence (92). Alternatively, patients with higher intelligence may have better treatment compliance, possibly resulting in lower GABA levels (92).

## INTEGRATING POSTMORTEM AND *IN VIVO* GABA FINDINGS IN SCHIZOPHRENIA

The reported elevation of GABA levels in the MPFC by <sup>1</sup>H-MRS in unmedicated patients seems to be inconsistent with the results of postmortem studies, which exhibit an impaired GABA synthesis of parvalbumin-containing subclasses of GABA neurons reflected by diminished GAD67 mRNA levels (97). This discrepancy could be explained by the extensive exposure of

the postmortem brain samples to antipsychotic medication in predominantly chronically ill patients (18). Furthermore, the observed elevated GABA levels in the MPFC might also be an overcompensation of other subclasses of GABA neurons (97). The NMDA-receptor hypofunction hypothesis puts forward that an intrinsic deficit of GABA neurons, including impaired GABA synthesis, results in disinhibition of pyramidal neurons. The deficit regulation of pyramidal neurons by GABAergic neurotransmission leads to glutamate elevations (48, 103). Therefore, the remaining unimpaired subclasses (subclasses other than the parvalbumin-containing subclass) could be stimulated by the increased glutameric activity, and this could serve as a compensation for the diminished synthesis in the parvalbumin-containing subclass (97).

Recent advantages in ultrahigh-field MR techniques allow for a more robust assessment of GABA levels, and future studies must point out whether *in vivo* measurement of GABA corresponds with the observed GABA deficiencies in postmortem tissues and whether the GABAergic deficits occur in a pan-cortical manner. Moreover, future studies might point out if GABA concentrations predict functional outcome and if alterations in GABA concentrations relate to therapy response. It is clear that GABA measurement by *in vivo* MR spectroscopy could be of great value, but it is also evident that further work is needed to provide additional information on the validation of MR spectroscopy of GABA in schizophrenia.

## CONCLUSION

Converging evidence implicates alterations in both presynaptic and postsynaptic components of GABA neurotransmission to fulfill an important role in the pathophysiology of schizophrenia. Multiple research sites using *in situ* hybridization, DNA microarray, or real-time quantitative PCR have consistently found reduced levels of GAD67 mRNA or a reduced density of neurons positive for GAD67 mRNA in the DLPFC as one of the most consistent findings with regard to pathological changes in schizophrenia. This decrease is the consequence of a reduction of GAD67 mRNA in a subset of GABA neurons. The affected neurons appear to include the parvalbumin-containing neurons. Parvalbumin-positive cells in the DLPFC include chandelier cells, targeting the upregulated  $\alpha$ 2-receptor subunit at the AIS of the pyramidal neuron. Furthermore, since GAD67 mRNA expression deficits were also observed in layers without parvalbumin expression, other subclasses may contribute to the observed GABAergic gene expression deficits as well. Furthermore, since other brain regions demonstrated similar GABAergic gene expression deficits as the DLPFC, disturbances in GABAergic neurotransmission could be the consequence of a common upstream effect. Therefore, identifying a common pathophysiology might give rise to new pharmacological opportunities in the treatment of schizophrenia. Measurement of GABA levels *in vivo* by means of MRS offers the possibility to approach the illness from a unique perspective and provides additional insights in the relationship between deficit components of GABA neurotransmission and GABA-mediated inhibitory activity. However, the current literature is inconsistent regarding the measured GABA levels in different brain regions

of patients with schizophrenia. Future MRS studies using GABA editing are required to give us a better understanding of the pathophysiology of schizophrenia in different stages of the disease. Particularly GABA-editing at ultrahigh-field strengths will be beneficial for detection of the relatively small GABA signal, because of the increased sensitivity, resolution, and signal-to-noise ratio, allowing for an accurate and time-efficient assessment of GABA levels.

## REFERENCES

- Lewis DA, Hashimoto T, Volk DW. Cortical inhibitory neurons and schizophrenia. *Nat Rev Neurosci* (2005) 6(4):312–24. doi:10.1038/nrn1648
- Petroff OA. GABA and glutamate in the human brain. *Neuroscientist* (2002) 8(6):562–73. doi:10.1177/107385402238515
- Thompson M, Weickert CS, Wyatt E, Webster MJ. Decreased glutamic acid decarboxylase(67) mRNA expression in multiple brain areas of patients with schizophrenia and mood disorders. *J Psychiatr Res* (2009) 43(11):970–7. doi:10.1016/j.jpsychires.2009.02.005
- Curley AA, Arion D, Volk DW, Asafu-Adjei JK, Sampson AR, Fish KN, et al. Cortical deficits of glutamic acid decarboxylase 67 expression in schizophrenia: clinical, protein, and cell type-specific features. *Am J Psychiatry* (2011) 168(9):921–9. doi:10.1176/appi.ajp.2011.11010052
- Hashimoto T, Volk DW, Eggan SM, Mirnics K, Pierri JN, Sun Z, et al. Gene expression deficits in a subclass of GABA neurons in the prefrontal cortex of subjects with schizophrenia. *J Neurosci* (2003) 23(15):6315–26.
- Soghomian JJ, Martin DL. Two isoforms of glutamate decarboxylase: why? *Trends Pharmacol Sci* (1998) 19(12):500–5. doi:10.1016/S0165-6147(98)01270-X
- Tian N, Petersen C, Kash S, Baekkeskov S, Copenhagen D, Nicoll R. The role of the synthetic enzyme GAD65 in the control of neuronal gamma-aminobutyric acid release. *Proc Natl Acad Sci U S A* (1999) 96(22):12911–6. doi:10.1073/pnas.96.22.12911
- Asada H, Kawamura Y, Maruyama K, Kume H, Ding R, Ji FY, et al. Mice lacking the 65 kDa isoform of glutamic acid decarboxylase (GAD65) maintain normal levels of GAD67 and GABA in their brains but are susceptible to seizures. *Biochem Biophys Res Commun* (1996) 229(3):891–5. doi:10.1006/bbrc.1996.1898
- Roth FC, Draguhn A. GABA metabolism and transport: effects on synaptic efficacy. *Neural Plast* (2012) 2012:805830. doi:10.1155/2012/805830
- Rowley NM, Madsen KK, Schousboe A, Steve WH. Glutamate and GABA synthesis, release, transport and metabolism as targets for seizure control. *Neurochem Int* (2012) 61(4):546–58. doi:10.1016/j.neuint.2012.02.013
- Sieghart W, Fuchs K, Tretter V, Ebert V, Jechlinger M, Höger H, et al. Structure and subunit composition of GABA(A) receptors. *Neurochem Int* (1999) 34(5):379–85. doi:10.1016/S0197-0186(99)00045-5
- Mangan PS, Sun C, Carpenter M, Goodkin HP, Sieghart W, Kapur J. Cultured hippocampal pyramidal neurons express two kinds of GABA(A) receptors. *Mol Pharmacol* (2005) 67(3):775–88. doi:10.1124/mol.104.007385
- Mohler H. GABA(A) receptor diversity and pharmacology. *Cell Tissue Res* (2006) 326(2):505–16. doi:10.1007/s00441-006-0284-3
- Roettger VR, Amara SG. GABA and glutamate transporters: therapeutic and etiologic implications for epilepsy. *Adv Neurol* (1999) 79:551–60.
- Maddock RJ, Buonocore MH. MR spectroscopic studies of the brain in psychiatric disorders. *Curr Top Behav Neurosci* (2012) 11:199–251. doi:10.1007/7854\_2011\_197
- Akbarian S, Kim JJ, Potkin SG, Hagman JO, Tafazzoli A, Bunney WE Jr, et al. Gene expression for glutamic acid decarboxylase is reduced without loss of neurons in prefrontal cortex of schizophrenics. *Arch Gen Psychiatry* (1995) 52(4):258–66. doi:10.1001/archpsyc.1995.03950160008002
- Duncan CE, Webster MJ, Rothmond DA, Bahn S, Elashoff M, Shannon WC. Prefrontal GABA(A) receptor alpha-subunit expression in normal postnatal human development and schizophrenia. *J Psychiatr Res* (2010) 44(10):673–81. doi:10.1016/j.jpsychires.2009.12.007
- Guidotti A, Auta J, Davis JM, Dong E, Grayson DR, Veldic M, et al. GABAergic dysfunction in schizophrenia: new treatment strategies on the horizon. *Psychopharmacology (Berl)* (2005) 180(2):191–205. doi:10.1007/s00213-005-2212-8
- Hashimoto T, Bergen SE, Nguyen QL, Xu B, Monteggia LM, Pierri JN, et al. Relationship of brain-derived neurotrophic factor and its receptor TrkB to altered inhibitory prefrontal circuitry in schizophrenia. *J Neurosci* (2005) 25(2):372–83. doi:10.1523/JNEUROSCI.4035-04.2005
- Hashimoto T, Arion D, Unger T, Maldonado-Avilés JG, Morris HM, Volk DW, et al. Alterations in GABA-related transcriptome in the dorsolateral prefrontal cortex of subjects with schizophrenia. *Mol Psychiatry* (2008) 13(2):147–61. doi:10.1038/sj.mp.4002011
- Hashimoto T, Bazmi HH, Mirnics K, Wu Q, Sampson AR, Lewis DA. Conserved regional patterns of GABA-related transcript expression in the neocortex of subjects with schizophrenia. *Am J Psychiatry* (2008) 165(4):479–89. doi:10.1176/appi.ajp.2007.07081223
- Kimoto S, Bazmi HH, Lewis DA. Lower expression of glutamic acid decarboxylase 67 in the prefrontal cortex in schizophrenia: contribution of altered regulation by Zif268. *Am J Psychiatry* (2014) 171(9):969–78. doi:10.1176/appi.ajp.2014.14010004
- Knable MB, Barci BM, Bartko JJ, Webster MJ, Torrey EF. Molecular abnormalities in the major psychiatric illnesses: classification and regression tree (CRT) analysis of post-mortem prefrontal markers. *Mol Psychiatry* (2002) 7(4):392–404. doi:10.1038/sj.mp.4001034
- Mirnics K, Middleton FA, Marquez A, Lewis DA, Levitt P. Molecular characterization of schizophrenia viewed by microarray analysis of gene expression in prefrontal cortex. *Neuron* (2000) 28(1):53–67. doi:10.1016/S0896-6273(00)00085-4
- Veldic M, Guidotti A, Maloku E, Davis JM, Costa E. In psychosis, cortical interneurons overexpress DNA-methyltransferase 1. *Proc Natl Acad Sci U S A* (2005) 102(6):2152–7. doi:10.1073/pnas.0409665102
- Veldic M, Kadriu B, Maloku E, Agis-Balboa RC, Guidotti A, Davis JM, et al. Epigenetic mechanisms expressed in basal ganglia GABAergic neurons differentiate schizophrenia from bipolar disorder. *Schizophr Res* (2007) 91(1–3):51–61. doi:10.1016/j.schres.2006.11.029
- Volk DW, Austin MC, Pierri JN, Sampson AR, Lewis DA. Decreased glutamic acid decarboxylase67 messenger RNA expression in a subset of prefrontal cortical gamma-aminobutyric acid neurons in subjects with schizophrenia. *Arch Gen Psychiatry* (2000) 57(3):237–45. doi:10.1001/archpsyc.57.3.237
- Woo TU, Walsh JP, Benes FM. Density of glutamic acid decarboxylase 67 messenger RNA-containing neurons that express the N-methyl-D-aspartate receptor subunit NR2A in the anterior cingulate cortex in schizophrenia and bipolar disorder. *Arch Gen Psychiatry* (2004) 61(7):649–57. doi:10.1001/archpsyc.61.7.649
- Woo TU, Kim AM, Viscidi E. Disease-specific alterations in glutamatergic neurotransmission on inhibitory interneurons in the prefrontal cortex in schizophrenia. *Brain Res* (2008) 1218:267–77. doi:10.1016/j.brainres.2008.03.092
- Guidotti A, Auta J, Davis JM, Di-Giorgi-Gerevini V, Dwivedi Y, Grayson DR, et al. Decrease in reelin and glutamic acid decarboxylase67 (GAD67) expression in schizophrenia and bipolar disorder: a postmortem brain study. *Arch Gen Psychiatry* (2000) 57(11):1061–9. doi:10.1001/archpsyc.57.11.1061
- Rocco BR, Lewis DA, Fish KN. Markedly lower glutamic acid decarboxylase 67 protein levels in a subset of boutons in schizophrenia. *Biol Psychiatry* (2016) 79(12):1006–15. doi:10.1016/j.biopsych.2015.07.022
- Benes FM, McSparron J, Bird ED, SanGiovanni JP, Vincent SL. Deficits in small interneurons in prefrontal and cingulate cortices of schizophrenic

## AUTHOR CONTRIBUTIONS

JJ contributed to the design of the study, performed literature research, and wrote and prepared the manuscript. CV contributed to the writing of the manuscript. HH contributed to the design of the study and the writing of the manuscript. AM contributed to the design of the study and supervised and contributed to the literature research, writing, and preparation of the manuscript.

- and schizoaffective patients. *Arch Gen Psychiatry* (1991) 48(11):996–1001. doi:10.1001/archpsyc.1991.01810350036005
33. Daviss SR, Lewis DA. Local circuit neurons of the prefrontal cortex in schizophrenia: selective increase in the density of calbindin-immunoreactive neurons. *Psychiatry Res* (1995) 59(1–2):81–96. doi:10.1016/0165-1781(95)02720-3
  34. Impagnatiello F, Guidotti AR, Pesold C, Dwivedi Y, Caruncho H, Pisu MG, et al. A decrease of reelin expression as a putative vulnerability factor in schizophrenia. *Proc Natl Acad Sci USA* (1998) 95(26):15718–23. doi:10.1073/pnas.95.26.15718
  35. Benes FM, Todtenkopf MS, Logiotatos P, Williams M. Glutamate decarboxylase(65)-immunoreactive terminals in cingulate and prefrontal cortices of schizophrenic and bipolar brain. *J Chem Neuroanat* (2000) 20(3–4):259–69. doi:10.1016/S0891-0618(00)00105-8
  36. Hakak Y, Walker JR, Li C, Wong WH, Davis KL, Buxbaum JD, et al. Genome-wide expression analysis reveals dysregulation of myelination-related genes in chronic schizophrenia. *Proc Natl Acad Sci U S A* (2001) 98(8):4746–51. doi:10.1073/pnas.081071198
  37. Dracheva S, Elhakem SL, McGurk SR, Davis KL, Haroutunian V. GAD67 and GAD65 mRNA and protein expression in cerebrocortical regions of elderly patients with schizophrenia. *J Neurosci Res* (2004) 76(4):581–92. doi:10.1002/jnr.20122
  38. Fatemi SH, Stary JM, Earle JA, Araghi-Niknam M, Eagan E. GABAergic dysfunction in schizophrenia and mood disorders as reflected by decreased levels of glutamic acid decarboxylase 65 and 67 kDa and Reelin proteins in cerebellum. *Schizophr Res* (2005) 72(2–3):109–22. doi:10.1016/j.schres.2004.02.017
  39. Straub RE, Lipska BK, Egan MF, Goldberg TE, Callicott JH, Mayhew MB, et al. Allelic variation in GAD1 (GAD67) is associated with schizophrenia and influences cortical function and gene expression. *Mol Psychiatry* (2007) 12(9):854–69. doi:10.1038/sj.mp.4001988
  40. Glausier JR, Fish KN, Lewis DA. Altered parvalbumin basket cell inputs in the dorsolateral prefrontal cortex of schizophrenia subjects. *Mol Psychiatry* (2014) 19(1):30–6. doi:10.1038/mp.2013.152
  41. McBain CJ, Fisahn A. Interneurons unbound. *Nat Rev Neurosci* (2001) 2(1):11–23. doi:10.1038/35049047
  42. Markram H, Toledo-Rodriguez M, Wang Y, Gupta A, Silberberg G, Wu C. Interneurons of the neocortical inhibitory system. *Nat Rev Neurosci* (2004) 5(10):793–807. doi:10.1038/nrn1519
  43. Conde F, Lund JS, Jacobowitz DM, Baimbridge KG, Lewis DA. Local circuit neurons immunoreactive for calretinin, calbindin D-28k or parvalbumin in monkey prefrontal cortex: distribution and morphology. *J Comp Neurol* (1994) 341(1):95–116. doi:10.1002/cne.903410109
  44. Gabbott PL, Bacon SJ. Local circuit neurons in the medial prefrontal cortex (areas 24a,b,c, 25 and 32) in the monkey: I. Cell morphology and morphometrics. *J Comp Neurol* (1996) 364(4):567–608. doi:10.1002/(SICI)1096-9861(19960122)364:4<567::AID-CNE1>3.3.CO;2-K
  45. Kawaguchi Y, Kubota Y. GABAergic cell subtypes and their synaptic connections in rat frontal cortex. *Cereb Cortex* (1997) 7(6):476–86. doi:10.1093/cercor/7.6.476
  46. Volk DW, Pierri JN, Fritschy JM, Auh S, Sampson AR, Lewis DA. Reciprocal alterations in pre- and postsynaptic inhibitory markers at chandelier cell inputs to pyramidal neurons in schizophrenia. *Cereb Cortex* (2002) 12(10):1063–70. doi:10.1093/cercor/12.10.1063
  47. Vawter MP, Crook JM, Hyde TM, Kleinman JE, Weinberger DR, Becker KG, et al. Microarray analysis of gene expression in the prefrontal cortex in schizophrenia: a preliminary study. *Schizophr Res* (2002) 58(1):11–20. doi:10.1016/S0920-9964(01)00377-2
  48. Lewis DA, Moghaddam B. Cognitive dysfunction in schizophrenia: convergence of gamma-aminobutyric acid and glutamate alterations. *Arch Neurol* (2006) 63(10):1372–6. doi:10.1001/archneur.63.10.1372
  49. Cobb SR, Buhl EH, Halasy K, Paulsen O, Somogyi P. Synchronization of neuronal activity in hippocampus by individual GABAergic interneurons. *Nature* (1995) 378(6552):75–8. doi:10.1038/378075a0
  50. Pouille F, Scanziani M. Enforcement of temporal fidelity in pyramidal cells by somatic feed-forward inhibition. *Science* (2001) 293(5532):1159–63. doi:10.1126/science.1060342
  51. Akbarian S, Huang HS. Molecular and cellular mechanisms of altered GAD1/GAD67 expression in schizophrenia and related disorders. *Brain Res Rev* (2006) 52(2):293–304. doi:10.1016/j.brainresrev.2006.04.001
  52. Beasley CL, Zhang ZJ, Patten I, Reynolds GP. Selective deficits in prefrontal cortical GABAergic neurons in schizophrenia defined by the presence of calcium-binding proteins. *Biol Psychiatry* (2002) 52(7):708–15. doi:10.1016/S0006-3223(02)01360-4
  53. Woo TU, Miller JL, Lewis DA. Schizophrenia and the parvalbumin-containing class of cortical local circuit neurons. *Am J Psychiatry* (1997) 154(7):1013–5. doi:10.1176/ajp.154.7.1013
  54. Cotter D, Landau S, Beasley C, Stevenson R, Chana G, MacMillan L, et al. The density and spatial distribution of GABAergic neurons, labelled using calcium binding proteins, in the anterior cingulate cortex in major depressive disorder, bipolar disorder, and schizophrenia. *Biol Psychiatry* (2002) 51(5):377–86. doi:10.1016/S0006-3223(01)01243-4
  55. Chen JF, Weiss B. Irreversible blockade of D2 dopamine receptors by fluphenazine-N-mustard increases glutamic acid decarboxylase mRNA in rat striatum. *Neurosci Lett* (1993) 150(2):215–8. doi:10.1016/0304-3940(93)90539-W
  56. Delfs JM, Anegawa NJ, Chesselet MF. Glutamate decarboxylase messenger RNA in rat pallidum: comparison of the effects of haloperidol, clozapine and combined haloperidol-scopolamine treatments. *Neuroscience* (1995) 66(1):67–80. doi:10.1016/0306-4522(94)00572-M
  57. Delfs JM, Ellison GD, Mercugliano M, Chesselet MF. Expression of glutamic acid decarboxylase mRNA in striatum and pallidum in an animal model of tardive dyskinesia. *Exp Neurol* (1995) 133(2):175–88. doi:10.1006/exnr.1995.1020
  58. Jolkonen J, Jenner P, Marsden CD. GABAergic modulation of striatal peptide expression in rats and the alterations induced by dopamine antagonist treatment. *Neurosci Lett* (1994) 180(2):273–6. doi:10.1016/0304-3940(94)90537-1
  59. Volk D, Austin M, Pierri J, Sampson A, Lewis DA. GABA transporter-1 mRNA in the prefrontal cortex in schizophrenia: decreased expression in a subset of neurons. *Am J Psychiatry* (2001) 158(2):256–65. doi:10.1176/appi.ajp.158.2.256
  60. Bragina L, Marchionni I, Omrani A, Cozzi A, Pellegrini-Giampietro DE, Cherubini E, et al. GAT-1 regulates both tonic and phasic GABA<sub>A</sub> receptor-mediated inhibition in the cerebral cortex. *J Neurochem* (2008) 105:1781–93. doi:10.1111/j.1471-4159.2008.05273.x
  61. Melone M, Ciappelloni S, Conti F. A quantitative analysis of cellular and synaptic localization of GAT-1 and GAT-3 in rat neocortex. *Brain Struct Funct* (2015) 220:885–97. doi:10.1007/s00429-013-0690-8
  62. Konopaske GT, Sweet RA, Wu Q, Sampson A, Lewis DA. Regional specificity of chandelier neuron axon terminal alterations in schizophrenia. *Neuroscience* (2006) 138(1):189–96. doi:10.1016/j.neuroscience.2005.10.070
  63. Menzies L, Ooi C, Kamath S, Suckling J, McKenna P, Fletcher P, et al. Effects of gamma-aminobutyric acid-modulating drugs on working memory and brain function in patients with schizophrenia. *Arch Gen Psychiatry* (2007) 64(2):156–67. doi:10.1001/archpsyc.64.2.156
  64. Ohnuma T, Augood SJ, Arai H, McKenna PJ, Emson PC. Measurement of GABAergic parameters in the prefrontal cortex in schizophrenia: focus on GABA content, GABA(A) receptor alpha-1 subunit messenger RNA and human GABA transporter-1 (HGAT-1) messenger RNA expression. *Neuroscience* (1999) 93(2):441–8. doi:10.1016/S0306-4522(99)00189-X
  65. Woo TU, Whitehead RE, Melchitzky DS, Lewis DA. A subclass of prefrontal gamma-aminobutyric acid axon terminals are selectively altered in schizophrenia. *Proc Natl Acad Sci U S A* (1998) 95(9):5341–6. doi:10.1073/pnas.95.9.5341
  66. Pierri JN, Chaudry AS, Woo TU, Lewis DA. Alterations in chandelier neuron axon terminals in the prefrontal cortex of schizophrenic subjects. *Am J Psychiatry* (1999) 156(11):1709–19.
  67. Rocco BR, DeDionisio AM, Lewis DA, Fish KN. Alterations in a unique class of cortical chandelier cell axon cartridges in schizophrenia. *Biol Psychiatry* (2017) 82(1):40–8. doi:10.1016/j.biopsych.2016.09.018
  68. Volk DW, Lewis DA. Impaired prefrontal inhibition in schizophrenia: relevance for cognitive dysfunction. *Physiol Behav* (2002) 77(4–5):501–5. doi:10.1016/S0031-9384(02)00936-8
  69. Benes FM, Vincent SL, Marie A, Khan Y. Up-regulation of GABA(A) receptor binding on neurons of the prefrontal cortex in schizophrenic subjects. *Neuroscience* (1996) 75(4):1021–31. doi:10.1016/0306-4522(96)00328-4
  70. Dean B, Hussain T, Hayes W, Scarr E, Kitsoulis S, Hill C, et al. Changes in serotonin2A and GABA(A) receptors in schizophrenia: studies on the

- human dorsolateral prefrontal cortex. *J Neurochem* (1999) 72(4):1593–9. doi:10.1046/j.1471-4159.1999.721593.x
71. Hanada S, Mita T, Nishino N, Tanaka C. [3H]muscimol binding sites increased in autopsied brains of chronic schizophrenics. *Life Sci* (1987) 40(3):259–66. doi:10.1016/0024-3205(87)90341-9
  72. Ishikawa M, Mizukami K, Iwakiri M, Hidaka S, Asada T. Immunohistochemical and immunoblot study of GABA(A) alpha1 and beta2/3 subunits in the prefrontal cortex of subjects with schizophrenia and bipolar disorder. *Neurosci Res* (2004) 50(1):77–84. doi:10.1016/j.neures.2004.06.006
  73. Fritschy JM, Mohler H. GABAA-receptor heterogeneity in the adult rat brain: differential regional and cellular distribution of seven major subunits. *J Comp Neurol* (1995) 359(1):154–94. doi:10.1002/cne.903590111
  74. Nusser Z, Sieghart W, Benke D, Fritschy JM, Somogyi P. Differential synaptic localization of two major gamma-aminobutyric acid type A receptor alpha subunits on hippocampal pyramidal cells. *Proc Natl Acad Sci U S A* (1996) 93(21):11939–44. doi:10.1073/pnas.93.21.11939
  75. Lavoie AM, Tingey JJ, Harrison NL, Pritchett DB, Twyman RE. Activation and deactivation rates of recombinant GABA(A) receptor channels are dependent on alpha-subunit isoform. *Biophys J* (1997) 73(5):2518–26. doi:10.1016/S0006-3495(97)78280-8
  76. Benes FM, Sorensen I, Vincent SL, Bird ED, Sathi M. Increased density of glutamate-immunoreactive vertical processes in superficial laminae in cingulate cortex of schizophrenic brain. *Cereb Cortex* (1992) 2(6):503–12. doi:10.1093/cercor/2.6.503
  77. Gonzalez-Burgos G, Fish KN, Lewis DA. GABA neuron alterations, cortical circuit dysfunction and cognitive deficits in schizophrenia. *Neural Plast* (2011) 2011:723184. doi:10.1155/2011/723184
  78. Benyamin M, Abbott A, Hashimoto T, Lewis DA. Lamina-specific alterations in cortical GABA(A) receptor subunit expression in schizophrenia. *Cereb Cortex* (2011) 21(5):999–1011. doi:10.1093/cercor/bhq169
  79. Huntsman MM, Tran BV, Potkin SG, Bunney WE Jr, Jones EG. Altered ratios of alternatively spliced long and short gamma2 subunit mRNAs of the gamma-amino butyrate type A receptor in prefrontal cortex of schizophrenics. *Proc Natl Acad Sci U S A* (1998) 95(25):15066–71. doi:10.1073/pnas.95.25.15066
  80. Maldonado-Avilés JG, Curley AA, Hashimoto T, Morrow AL, Ramsey AJ, O'Donnell P, et al. Altered markers of tonic inhibition in the dorsolateral prefrontal cortex of subjects with schizophrenia. *Am J Psychiatry* (2009) 166(4):450–9. doi:10.1176/appi.ajp.2008.08101484
  81. Ali AB, Thomson AM. Synaptic alpha 5 subunit-containing GABAA receptors mediate IPSPs elicited by dendrite-preferring cells in rat neocortex. *Cereb Cortex* (2008) 18(6):1260–71. doi:10.1093/cercor/bhm160
  82. Hendry SH, Huntsman MM, Vinuela A, Mohler H, de Blas AL, Jones EG. GABAA receptor subunit immunoreactivity in primate visual cortex: distribution in macaques and humans and regulation by visual input in adulthood. *J Neurosci* (1994) 14(4):2383–401.
  83. Ishikawa M, Mizukami K, Iwakiri M, Asada T. Immunohistochemical and immunoblot analysis of gamma-aminobutyric acid B receptor in the prefrontal cortex of subjects with schizophrenia and bipolar disorder. *Neurosci Lett* (2005) 383(3):272–7. doi:10.1016/j.neulet.2005.04.025
  84. Chen S, Huang X, Zeng XJ, Sieghart W, Tietz EI. Benzodiazepine-mediated regulation of alpha1, alpha2, beta1-3 and gamma2 GABA(A) receptor subunit proteins in the rat brain hippocampus and cortex. *Neuroscience* (1999) 93(1):33–44. doi:10.1016/S0306-4522(99)00118-9
  85. Gur RE, Cowell PE, Latshaw A, Turetsky BI, Grossman RI, Arnold SE, et al. Reduced dorsal and orbital prefrontal gray matter volumes in schizophrenia. *Arch Gen Psychiatry* (2000) 57(8):761–8. doi:10.1001/archpsyc.57.8.761
  86. Lewis DA, Volk DW, Hashimoto T. Selective alterations in prefrontal cortical GABA neurotransmission in schizophrenia: a novel target for the treatment of working memory dysfunction. *Psychopharmacology (Berl)* (2004) 174(1):143–50. doi:10.1007/s00213-003-1673-x
  87. Jensen K, Chiu CS, Sokolova I, Lester HA, Mody I. GABA transporter-1 (GAT1)-deficient mice: differential tonic activation of GABA(A) versus GABA(B) receptors in the hippocampus. *J Neurophysiol* (2003) 90(4):2690–701. doi:10.1152/jn.00240.2003
  88. Enomoto T, Tse MT, Floresco SB. Reducing prefrontal gamma-aminobutyric acid activity induces cognitive, behavioral, and dopaminergic abnormalities that resemble schizophrenia. *Biol Psychiatry* (2011) 69(5):432–41. doi:10.1016/j.biopsych.2010.09.038
  89. Sawaguchi T, Matsumura M, Kubota K. Delayed response deficits produced by local injection of bicuculline into the dorsolateral prefrontal cortex in Japanese macaque monkeys. *Exp Brain Res* (1989) 75(3):457–69. doi:10.1007/BF00249897
  90. Goto N, Yoshimura R, Kakeda S, Moriya J, Hori H, Hayashi K, et al. No alterations of brain GABA after 6 months of treatment with atypical antipsychotic drugs in early-stage first-episode schizophrenia. *Prog Neuropsychopharmacol Biol Psychiatry* (2010) 34(8):1480–3. doi:10.1016/j.pnpbp.2010.08.007
  91. Kelemen O, Kiss I, Benedek G, Keri S. Perceptual and cognitive effects of antipsychotics in first-episode schizophrenia: the potential impact of GABA concentration in the visual cortex. *Prog Neuropsychopharmacol Biol Psychiatry* (2013) 47:13–9. doi:10.1016/j.pnpbp.2013.07.024
  92. Marsman A, Mandl RC, Klomp DW, Bohlken MM, Boer VO, Andreychenko A, et al. GABA and glutamate in schizophrenia: a 7 T (1)H-MRS study. *Neuroimage Clin* (2014) 6:398–407. doi:10.1016/j.nicl.2014.10.005
  93. Rowland LM, Kontson K, West J, Edden RA, Zhu H, Wijtenburg SA, et al. In vivo measurements of glutamate, GABA, and NAAG in schizophrenia. *Schizophr Bull* (2012) 39(5):1096–104. doi:10.1093/schbul/sbs092
  94. Rowland LM, Krause BW, Wijtenburg SA, McMahon RP, Chiappelli J, Nugent KL, et al. Medial frontal GABA is lower in older schizophrenia: a MEGA-PRESS with macromolecule suppression study. *Mol Psychiatry* (2016) 21(2):198–204. doi:10.1038/mp.2015.34
  95. Wang J, Tang Y, Zhang T, Cui H, Xu L, Zeng B, et al. Reduced gamma-aminobutyric acid and glutamate+glutamine levels in drug-naïve patients with first-episode schizophrenia but not in those at ultrahigh risk. *Neural Plast* (2016) 2016:3915703. doi:10.1155/2016/3915703
  96. Yoon JH, Maddock RJ, Rokem A, Silver MA, Minzenberg MJ, Ragland JD, et al. GABA concentration is reduced in visual cortex in schizophrenia and correlates with orientation-specific surround suppression. *J Neurosci* (2010) 30(10):3777–81. doi:10.1523/JNEUROSCI.6158-09.2010
  97. Kegles LS, Mao X, Stanford AD, Girgis R, Ojeil N, Xu X, et al. Elevated prefrontal cortex gamma-aminobutyric acid and glutamate-glutamine levels in schizophrenia measured in vivo with proton magnetic resonance spectroscopy. *Arch Gen Psychiatry* (2012) 69(5):449–59. doi:10.1001/archgenpsychiatry.2011.1519
  98. Tayoshi S, Nakataki M, Sumitani S, Taniguchi K, Shibuya-Tayoshi S, Numata S, et al. GABA concentration in schizophrenia patients and the effects of antipsychotic medication: a proton magnetic resonance spectroscopy study. *Schizophr Res* (2010) 117(1):83–91. doi:10.1016/j.schres.2009.11.011
  99. Ongur D, Prescott AP, McCarthy J, Cohen BM, Renshaw PF. Elevated gamma-aminobutyric acid levels in chronic schizophrenia. *Biol Psychiatry* (2010) 68(7):667–70. doi:10.1016/j.biopsych.2010.05.016
  100. Schür RR, Draisma LW, Wijnen JP, Boks MP, Koevoets MG, Joëls M, et al. Brain GABA levels across psychiatric disorders: a systematic literature review and meta-analysis of 1H-MRS studies. *Hum Brain Mapp* (2016) 37(9):3337–52. doi:10.1002/hbm.23244
  101. Goto N, Yoshimura R, Moriya J, Kakeda S, Ueda N, Ikenouchi-Sugita A, et al. Reduction of brain gamma-aminobutyric acid (GABA) concentrations in early-stage schizophrenia patients: 3T proton MRS study. *Schizophr Res* (2009) 112(1–3):192–3. doi:10.1016/j.schres.2009.04.026
  102. Hedman AM, Van Haren NE, Van Baal CG, Kahn RS, Hulshoff Pol HE. IQ change over time in schizophrenia and healthy individuals: a meta-analysis. *Schizophr Res* (2013) 146(1–3):201–8. doi:10.1016/j.schres.2013.01.027
  103. Lisman JE, Coyle JT, Green RW, Javitt DC, Benes FM, Heckers S, et al. Circuit-based framework for understanding neurotransmitter and risk gene interactions in schizophrenia. *Trends Neurosci* (2008) 31(5):234–42. doi:10.1016/j.tins.2008.02.005

**Conflict of Interest Statement:** The authors declare that the research was conducted in the absence of any commercial or financial relationships that could be construed as a potential conflict of interest.

Copyright © 2017 De Jonge, Vinkers, Hulshoff Pol and Marsman. This is an open-access article distributed under the terms of the Creative Commons Attribution License (CC BY). The use, distribution or reproduction in other forums is permitted, provided the original author(s) or licensor are credited and that the original publication in this journal is cited, in accordance with accepted academic practice. No use, distribution or reproduction is permitted which does not comply with these terms.



# Antigliadin Antibodies (AGA IgG) Are Related to Neurochemistry in Schizophrenia

Laura M. Rowland<sup>1\*</sup>, Haley K. Demyanovich<sup>1</sup>, S. Andrea Wijtenburg<sup>1</sup>, William W. Eaton<sup>2</sup>, Katrina Rodriguez<sup>2</sup>, Frank Gaston<sup>1</sup>, Daniela Cihakova<sup>3</sup>, Monica V. Talor<sup>3</sup>, Fang Liu<sup>1</sup>, Robert R. McMahon<sup>1</sup>, L. Elliot Hong<sup>1</sup> and Deanna L. Kelly<sup>1</sup>

<sup>1</sup>Maryland Psychiatric Research Center, Department of Psychiatry, University of Maryland School of Medicine, Baltimore, MD, United States, <sup>2</sup>Department of Mental Health, Johns Hopkins Bloomberg School of Public Health, Baltimore, MD, United States, <sup>3</sup>Immunologic Disorders Laboratory, Department of Pathology, Johns Hopkins University School of Medicine, Baltimore, MD, United States

## OPEN ACCESS

### Edited by:

Anouk Marsman,  
Copenhagen University Hospital  
Hvidovre, Denmark

### Reviewed by:

Jeffrey A. Stanley,  
Wayne State University School  
of Medicine, United States

Fei Du,  
Harvard Medical School,  
United States

### \*Correspondence:

Laura M. Rowland  
lrowland@mprc.umaryland.edu

### Specialty section:

This article was submitted to  
Neuroimaging and Stimulation,  
a section of the journal  
Frontiers in Psychiatry

Received: 31 January 2017

Accepted: 29 May 2017

Published: 19 June 2017

### Citation:

Rowland LM, Demyanovich HK,  
Wijtenburg SA, Eaton WW,  
Rodriguez K, Gaston F, Cihakova D,  
Talor MV, Liu F, McMahon RR,  
Hong LE and Kelly DL (2017)  
Antigliadin Antibodies (AGA IgG)  
Are Related to Neurochemistry  
in Schizophrenia.  
*Front. Psychiatry* 8:104.  
doi: 10.3389/fpsy.2017.00104

Inflammation may play a role in schizophrenia; however, subgroups with immune regulation dysfunction may serve as distinct illness phenotypes with potential different treatment and prevention strategies. Emerging data show that about 30% of people with schizophrenia have elevated antigliadin antibodies of the IgG type, representing a possible subgroup of schizophrenia patients with immune involvement. Also, recent data have shown a high correlation of IgG-mediated antibodies between the periphery and cerebral spinal fluid in schizophrenia but not healthy controls, particularly AGA IgG suggesting that these antibodies may be crossing the blood-brain barrier with resulting neuroinflammation. Proton magnetic resonance spectroscopy (MRS) is a non-invasive technique that allows the quantification of certain neurochemicals *in vivo* that may proxy inflammation in the brain such as myoinositol and choline-containing compounds (glycerophosphorylcholine and phosphorylcholine). The objective of this exploratory study was to examine the relationship between serum AGA IgG levels and MRS neurochemical levels. We hypothesized that higher AGA IgG levels would be associated with higher levels of myoinositol and choline-containing compounds (glycerophosphorylcholine plus phosphorylcholine; GPC + PC) in the anterior cingulate cortex. Thirty-three participants with a DSM-IV diagnosis of schizophrenia or schizoaffective disorder had blood drawn and underwent neuroimaging using MRS within 9 months. We found that 10/33 (30%) had positive AGA IgG ( $\geq 20$  U) similar to previous findings. While there were no significant differences in myoinositol and GPC + PC levels between patients with and without AGA IgG positivity, there were significant relationships between both myoinositol ( $r = 0.475, p = 0.007$ ) and GPC + PC ( $r = 0.36, p = 0.045$ ) with AGA IgG levels. This study shows a possible connection of AGA IgG antibodies to putative brain inflammation as measured by MRS in schizophrenia.

**Keywords:** gluten, gliadin, antibody, myoinositol, GPC + PC, schizophrenia, neuroimaging, inflammation

## INTRODUCTION

Several emerging lines of evidence suggest that the etiology and pathophysiology of schizophrenia may be related to inflammatory processes. Data contributing to this hypothesis include prenatal maternal infection and the subsequent pro-inflammatory response (1–3). Also, multiple studies have demonstrated increased levels of various peripheral cytokines to be elevated in people with

first-episode or multi-episode schizophrenia (1, 2, 4–8). In addition, positron emission tomography (PET) studies have demonstrated increased binding to the 18-kDa translocator-protein (TPSO; a marker of microglial activation) in the brains of people with schizophrenia (9–11). Finally, several genome-wide association studies have documented the presence of single-nucleotide polymorphisms in the major histocompatibility complex, genes related to immune function, that are associated with increased risk of schizophrenia (12–17).

A subset of individuals with schizophrenia may be particularly sensitive to inflammation due to immune activation to specific antigens, and this may contribute to the illness pathophysiology. This is in line with the fact that studies on inflammatory markers are not elevated in all people with schizophrenia and why inconsistent results have been shown in cross-sectional cytokine studies. The exacerbation of systemic or brain immune activation could be due to increased permeability of the mucosal epithelial tight junctions in the intestine and blood–brain barrier (18–21). Increased permeability permits entrance of pathogens, toxins, and antigens that could lead to subsequent immune response and reaction; a postulated mechanism of the brain to gut relationship mediated by inflammation. Partial support comes from a recent study indicating increased blood–cerebral spinal fluid (CSF) permeability coupled with antibody response to dietary proteins in first-episode schizophrenia (22). This study found a high correlation of IgG-mediated antibodies (e.g., antibodies to gliadin) between the periphery and CSF in schizophrenia but not healthy controls.

Positivity to immunoglobulin G antibodies to gliadin (AGA IgG) are observed in about 20–30% of people with schizophrenia compared to less than 10% in healthy controls (23–25). This potentially reflects gluten sensitivity (GS), which is a newly characterized syndrome defined by some intestinal but mostly extra-intestinal symptoms related to the ingestion of gluten-containing food (i.e., wheat, barley, or rye) distinct from celiac disease (CD) and wheat allergy (26, 27). High levels of AGA IgG have also been observed in brain conditions such as ataxia (28–30). This provides further support for the gut–brain inflammation linkage. It is plausible that there is a subset of about one-quarter to one-third of the schizophrenia population that may be highly susceptible to GS-mediated peripheral and central inflammation.

Proton magnetic resonance spectroscopy (MRS) is a non-invasive technique that allows the quantification of certain neurochemicals *in vivo*. These neurochemicals reflect a wide variety of mechanisms that range from neuronal function to neurotransmission. MRS biochemicals such as myoinositol and glycerophosphorylcholine (GPC) plus phosphorylcholine (PC) referred to as “GPC + PC” may serve as a proxy for inflammation. Myoinositol is localized primarily in glial cells (31) and is elevated in conditions characterized by central nervous system inflammation (32) such as hepatitis C virus-associated encephalopathy in occipital and parietal gray and white matter (33) and multiple sclerosis in white and cortical gray matter (34, 35). GPC + PC levels putatively reflect cellular membrane metabolism, both synthesis and breakdown (36, 37), and increased levels are observed in neuroinflammatory diseases (32). Hence, spectroscopic measures of myoinositol and GPC + PC could provide insight into

brain inflammation. With respect to schizophrenia, results are inconsistent regarding alterations in myoinositol and GPC + PC levels in various brain regions (38, 39). However, the majority of studies on schizophrenia did not examine the immune or measures related to inflammation except for one study that reported higher medial temporal lobe myoinositol in a subset of patients with elevated S100B (40).

The objective of this exploratory study was to examine the relationship between serum AGA IgG levels and MRS neurochemical measurements of the anterior cingulate cortex (ACC) in schizophrenia. Given that AGA IgG antibodies may cross the blood–brain barrier in schizophrenia (22), we hypothesized that those who tested positive for AGA IgG would have higher levels of ACC myoinositol and GPC + PC compared to those who tested negative for AGA IgG. Furthermore, we hypothesized that higher AGA IgG levels would be associated with higher levels of ACC myoinositol and GPC + PC. The ACC was the focus since it is involved in the pathophysiology of schizophrenia, as strongly supported by MRS, other neuroimaging modalities, and postmortem research (41, 42).

## MATERIALS AND METHODS

Participants were recruited from the Maryland Psychiatric Research Center. Three hundred sixty-six patients with a DSM-IV-TR diagnosis of schizophrenia or schizoaffective disorder participated in a study to measure serum AGA IgG. Of those who completed the antibody screening, 33 participants were able to also complete an MRS session; inclusion criteria for the MRS portion consisted of those between the ages of 18 and 55, and without contraindications for MR scanning (e.g., claustrophobia, metal contained in their bodies). Participants had the MRS scan and blood draw on separate occasions averaging approximately 8.8 months apart and no patient was on a gluten-free diet. All participants were evaluated for their capacity to provide informed consent before giving written consent prior to participation. The University of Maryland Baltimore Institutional Review Board approved this study.

### Anti-Gliadin Antibodies

Blood was drawn and serum stored at  $-80^{\circ}\text{F}$  for batched analysis at the Johns Hopkins University Immune Disorders Laboratory. The sera were analyzed for AGA IgG using the INOVA kit #708650, which is an ELISA measure for native gliadin, not a deaminated version of gliadin (linked to CD). We utilized positivity of AGA IgG according to the manufacturer cutoff of AGA IgG levels  $\geq 20$  U. We have also independently replicated the cutoff value in a sample of over 370 people with schizophrenia compared to 80 healthy controls with no psychiatric or medical comorbidities. Ninety percent of healthy controls fall below the cutoff and the distribution in schizophrenia is bimodal showing means in those not positive to be  $< 10$  U and the mean values of those who are positive to be  $> 40$  U (Cihakova et al., under review).

### MRS Acquisition and Analysis

MR scanning was conducted on a 3-T Siemens Tim Trio equipped with a 32-channel head coil. Head position was fixed with foam

padding to minimize movement. Anatomical T1-weighted images were acquired for spectroscopic voxel placement with a “MP-RAGE” sequence. Spectroscopic methods have been previously described (43). The spectroscopic voxel was 4.0 cm × 3.0 cm × 2.0 cm prescribed on the midsagittal slice and positioned parallel to the genu of the corpus callosum and scalp with the midline of the voxel corresponding to the middle of the genu of the corpus callosum. The voxel contained a mixture of rostral and dorsal ACC. Spectra were acquired with a phase rotation STEAM: TR/TM/TE = 2,000/10/6.5-ms, VOI ~24 cm<sup>3</sup>, NEX = 128, 2.5-kHz spectral width, 2,048 complex points, and phases: φ1 = 135°, φ2 = 22.5°, φ13 = 112.5°, φADC = 0°. The test-retest reproducibility of this sequence is excellent, as reported in both healthy volunteers (44) and participants with schizophrenia (45). A water reference (NEX = 16) was also acquired for phase and eddy current correction as well as quantification. LCModel (6.3-0D) was used for spectral quantification (46) with a simulated basis set that contained alanine (Ala), aspartate (Asp), creatine (Cr), γ-aminobutyric acid (GABA), glucose (Glc), glutamate (Glu), glutamine (Gln), glutathione (GSH), glycine (Gly), glycerophosphocholine (GPC), lactate (Lac), myo-Inositol (mI), N-acetylaspartate (NAA), N-acetylaspartylglutamate (NAAG), phosphocholine (PC), phosphocreatine (PCr), phosphorylethanolamine (PE), scyllo-Inositol (SI), and taurine (Tau). Metabolite levels are reported in institutional units, and metabolites with Cramer Rao Lower Bounds ≤20% were included in further analyses. The spectroscopic voxel was segmented into gray, white, and CSF tissues using SPM8 and in house MATLAB code, and the metabolite levels were corrected for the proportion of gray, white, and CSF tissue proportions (44). The following metabolites were quantified and reported: total choline (glycerophosphorylcholine + phosphorylcholine), myoinositol,

glutamine, glutamine, glutamate + glutamine, glutathione, N-acetylaspartate, and total creatine (creatine + phosphocreatine). Spectroscopic voxel location and corresponding spectrum are illustrated in **Figure 1**.

## Statistical Analyses

Data were not normally distributed and therefore non-parametric statistical analyses were conducted. The differences in MRS measures between those patients who were “positive” (i.e., >20 U) vs. “negative” for the AGA IgG antibodies were examined with the Kruskal-Wallis test. Spearman’s correlations were performed between the MRS measures and AGA IgG levels on all participants.

## RESULTS

A description of the clinical and demographic information is listed in **Table 1**. Briefly, the mean age of the participants was 33.8.36 ± 12.4 (SD), 52% were African-American, and 48% were Caucasian. Of these, there were 18 males (55%) and 15 females (45%). Participants were of mixed illness duration with the majority ( $N = 28$ ) having been ill for more than 2 years. Ten of the 33 participants were positive for AGA IgG GS (30%). There were no significant differences in demographic information of those with and without positivity to IgG AGA. The overall mean IgG AGA level in the group was 17.03 ± 24.29 U. The mean AGA IgG in the positive group was 44.61 ± 29.09 vs. 5.04 ± 4.02 U in the AGA IgG negative group ( $t = 20.30$ , df = 1,  $p < 0.0001$ ).

Two participants moved during MR scanning and therefore spectral quality was poor and not included in the analysis. Contrary to hypothesis, there were no significant differences in myoinositol or GPC + PC between participants who were AGA

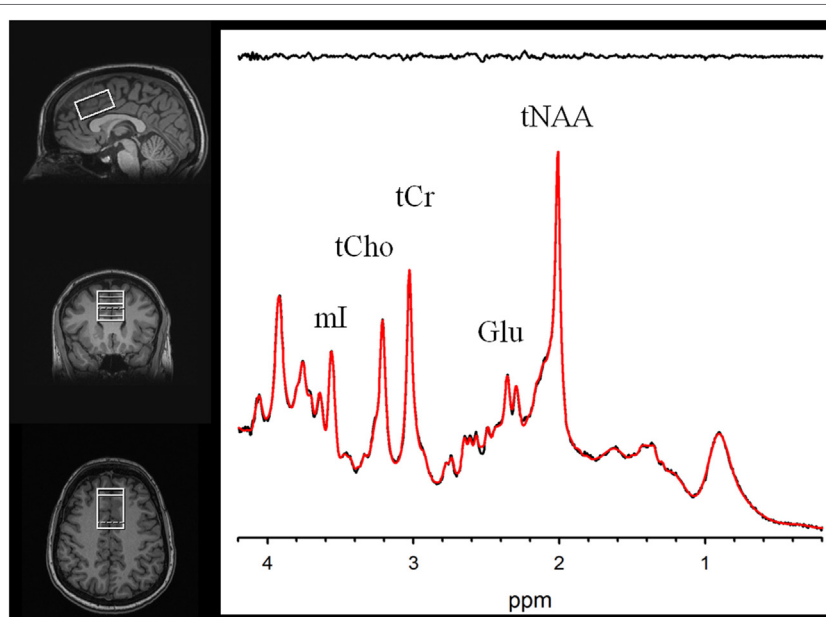


**FIGURE 1** | Voxel images and a representative spectrum (black line), LCModel fit (red line), residual (black line at top). Myoinositol (mI), Phosphocreatine+Creatine (tCr), Phosphorylcholine+Glycerophosphorylcholine (tCho), Glutamate (Glu), and N-Acetylaspartate (tNAA).

**TABLE 1** | Demographic and clinical information.

Variable	Overall group (N = 33)	AGA Ig positive group (N = 10)	AGA IgG negative group (N = 23)	Statistic between groups
Mean age (years)	33.8 ± 12.4	32.01 ± 11.3	34.6 ± 13.1	T = 0.30, p = 0.58
Sex (male)	18 (55%)	6 (60%)	12 (52%)	$\chi^2 = 0.17, p = 0.68$
Race				
African-American	17 (52%)	6 (60%)	11 (48%)	$\chi^2 = 0.41, p = 0.52$
Caucasian	16 (48%)	4 (40%)	12 (52%)	
Schizophrenia vs. schizoaffective diagnosis	25 (76%) 8 (24%)	7 (70%) 3 (30%)	18 (78%) 5 (22%)	$\chi^2 = 0.26, p = 0.61$
Duration of illness (years)	16.2 ± 14.8 (N = 31)	12.4 ± 12.1 (N = 9)	16.2 ± 14.8 (N = 22)	T = 0.7, p = 0.5
Mean AGA IgG (U)	17.0 ± 24.3	44.6 ± 29.1	5.0 ± 4.0	T = 20.3, p < 0.0001

IgG positive compared to those who were IgG negative. There were no differences in the other metabolites between AGA IgG-positive and -negative groups. The correlation analyses between AGA IgG and the metabolites are reported in **Table 2**. Results revealed significant relationships between AGA IgG levels and both myoinositol ( $r = 0.475, p = 0.007$ ) and GPC + PC ( $r = 0.36, p = 0.045$ ) (see **Figures 2 and 3**). There were no significant correlations noted for glutamate, glutamine, glutathione, N-acetylaspartate, or creatine ( $p > 0.1$ , **Table 2**).

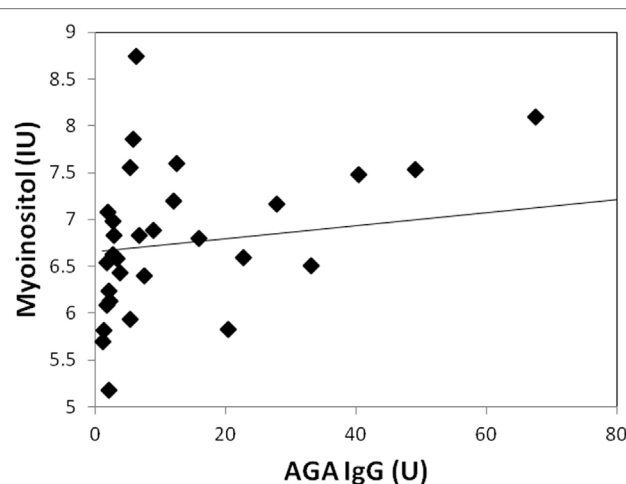
## DISCUSSION

Despite the accumulating evidence of the evidence of AGA IgG antibodies in a subset of schizophrenia, little work has shown the connection of these antibodies with brain inflammation. To the best of our knowledge, this is the first study to show a relationship between peripheral AGA IgG and ACC myoinositol and GPC + PC levels. Our results also replicate the estimated prevalence of AGA IgG positivity in approximately one-third of people with schizophrenia.

Magnetic resonance spectroscopy measures of brain myoinositol and GPC + PC are thought to reflect inflammation in the brain. Myoinositol is a glial cell marker (31) and is elevated in conditions characterized by CNS inflammation such as HCV-associated encephalopathy, HIV, and multiple sclerosis (33–35, 47). Choline-containing compounds such as GPC + PC reflect cellular membrane synthesis and breakdown (37), and high levels of GPC + PC have been observed in multiple sclerosis with active lesions (48, 49) and HIV infection (50). One study reported higher MRS myoinositol and GPC + PC levels coupled with higher microglial activation measured with PET in patients with hepatitis C (51). The combination of these studies provides good support that MRS measures of myoinositol and GPC + PC proxy neuroinflammation (32). Therefore, the association between higher levels of AGA IgG and brain myoinositol and GPC + PC suggests a link between AGA IgG and CNS inflammation in schizophrenia. It is important to note that the relationships between AGA IgG and the brain metabolites were specific to myoinositol and GPC + PC only, further supporting the AGA IgG neuroinflammation link. These results are also consistent with a study showing a high-positive correlation between blood AGA IgG and CSF AGA IgG in schizophrenia patients but not healthy controls (22), suggesting greater CNS permeability and likely inflammation.

**TABLE 2** | Spearman's correlations between magnetic resonance spectroscopy measures and AGA IgG in schizophrenia patients.

Metabolite	Mean (IU)	SD	r-Value	p-Value
Glutamate (N = 31)	9.12	0.87	0.104	0.58
Glutamine (N = 30)	2.18	0.39	-0.1048	0.58
Glutamate + glutamine (N = 31)	10.97	1.21	0.006	0.97
Glutathione (N = 31)	2.11	0.35	0.01	0.96
N-acetylaspartate (N = 31)	9.91	0.90	0.006	0.97
Total creatine (N = 31)	8.87	0.92	0.25	0.18
Myoinositol (N = 31)	6.76	0.77	0.48	0.007
Glycerophosphorylcholine + phosphorylcholine (N = 31)	1.81	0.27	0.36	0.045

**FIGURE 2** | Correlation plot showing a strong positive relationship ( $r = 0.48, p = 0.007$ ) between AGA IgG and myoinositol levels. 31/33 of the participants had data available.

The ACC was the focus of this study because of its involvement in the pathophysiology of schizophrenia supported by postmortem and imaging research (41, 42). Volumetric MRI studies suggest that both dorsal and rostral ACC gray matter is reduced in schizophrenia (41), and proton MRS studies suggest ACC glutamatergic and GABAergic alterations in schizophrenia (42, 52, 53). Postmortem work parallels these imaging findings as indicated by reduced ACC neuropil and altered GABAergic and glutamatergic neurons (41) in schizophrenia. If inflammation is a contributing factor to these ACC alterations is not clear, as studies focused on

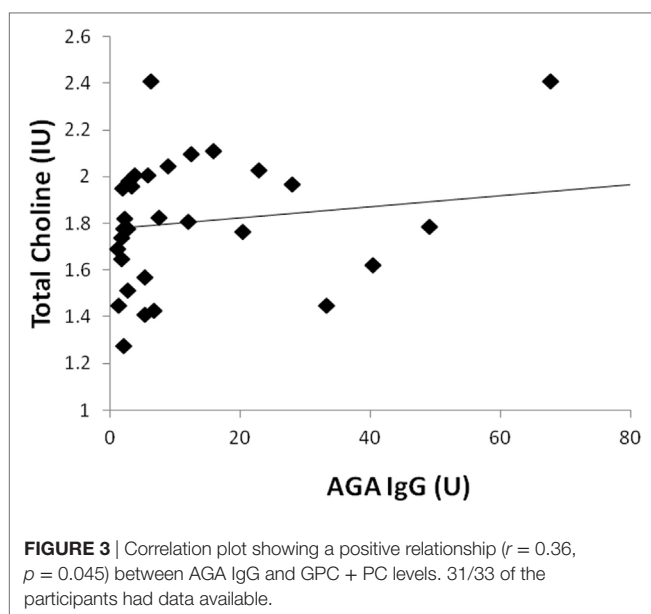


**FIGURE 3 |** Correlation plot showing a positive relationship ( $r = 0.36$ ,  $p = 0.045$ ) between AGA IgG and GPC + PC levels. 31/33 of the participants had data available.

inflammatory postmortem and PET markers in cortical regions including the ACC have been inconsistent (54). Moreover, the majority of MRS studies of the ACC in schizophrenia did not report alterations in myoinositol or GPC + PC (38); however, previous studies also did not examine specific immune parameters. It is also unclear how the current study's findings translate to other brain regions. Future studies are necessary to determine if AGA IgG is related to MRS myoinositol and GPC + PC in other brain regions.

Several study limitations are worth mentioning. First, the blood draw for AGA IgG was not on the same day as the imaging procedures; however, due to a long half-life of serum IgG antibodies (~20 days) (55) and long-term stability of AGA IgG in patients with schizophrenia (<15% change in 6 months) (Kelly, unpublished data), we do not anticipate significant changes of AGA IgG levels. Second, as with the majority of studies in schizophrenia, all patients were taking antipsychotic medications, which could impact the results. We do not have the specific antipsychotic medication to include in the report. However, data support that immune involvement is independent of antipsychotic treatment (56–66). Additionally, antipsychotic medication treatment in rodents does not change GPC + PC or myoinositol levels (67). Third, we do not have clinical symptom status at the time of blood

draw to link to symptomatology and the groups were too small to do subanalysis by gender, age, or illness duration. Only one brain region was examined, therefore brain region specificity cannot be discussed. Fourth, since causation cannot be determined from this data, it remains unknown if this sensitivity to gluten causes neuroinflammation or if antibodies are high based on neuroinflammatory process present in this group. Preclinical research is needed to determine potential causative factors related to these linked phenomena. Finally, it is not possible to ascertain if higher GPC + PC reflects cell membrane formation or breakdown, so the results should be interpreted with caution.

In conclusion, these results suggest a possible connection of AGA IgG antibodies to putative brain inflammation as measured by MRS in schizophrenia. More research is needed to help delineate the group of people at risk for GS, which is likely a subset of schizophrenia. It is possible that interventions targeted to reduce the immune response to gluten, such as a gluten-free diet, could prove beneficial to ameliorating neuroinflammation and possibly illness symptoms.

## ETHICS STATEMENT

All participants were evaluated for their capacity to provide informed consent before giving written consent prior to participation. This study was approved by the University of Maryland Baltimore Institutional Review Board.

## AUTHOR CONTRIBUTIONS

LR, DK, SW, WE, KR, and DC conceptualized and designed the project. HD, SW, MT, DK, and LH acquired the data. FG, FL, SW, LR, RM, DC, KR, and DK analyzed the data. LR, HD, SW, WE, KR, FG, DC, MT, FL, RM, LH, and DK interpreted the study results, drafted the manuscript and revised it critically, and gave final approval.

## ACKNOWLEDGMENTS

We thank the patient participants who kindly volunteered for this project.

## FUNDING

This work is supported by National Institutes of Health (R01MH094520, R01MH085646, and R34MH100776).

## REFERENCES

- Meyer U, Schwarz MJ, Muller N. Inflammatory processes in schizophrenia: a promising neuroimmunological target for the treatment of negative/cognitive symptoms and beyond. *Pharmacol Ther* (2011) 132(1):96–110. doi:10.1016/j.pharmthera.2011.06.003
- Fineberg AM, Ellman LM. Inflammatory cytokines and neurological and neurocognitive alterations in the course of schizophrenia. *Biol Psychiatry* (2013) 73(10):951–66. doi:10.1016/j.biopsych.2013.01.001
- Moieni M, Irwin MR, Jevtic I, Breen EC, Eisenberger NI. Inflammation impairs social cognitive processing: a randomized controlled trial of endotoxin. *Brain Behav Immun* (2015) 48:132–8. doi:10.1016/j.bbi.2015.03.002
- Potvin S, Stip E, Sepehry AA, Gendron A, Bah R, Kouassi E. Inflammatory cytokine alterations in schizophrenia: a systematic quantitative review. *Biol Psychiatry* (2008) 63(8):801–8. doi:10.1016/j.biopsych.2007.09.024
- Miller A, Phillips A, Gor J, Wallis R, Perkins SJ. Near-planar solution structures of mannose-binding lectin oligomers provide insight on activation of lectin pathway of complement. *J Biol Chem* (2012) 287(6):3930–45. doi:10.1074/jbc.M111.320341
- Fillman SG, Cloonan N, Catts VS, Miller LC, Wong J, McCrossin T, et al. Increased inflammatory markers identified in the dorsolateral prefrontal cortex of individuals with schizophrenia. *Mol Psychiatry* (2013) 18(2):206–14. doi:10.1038/mp.2012.110

7. Hope TMH, Seghier ML, Leff AP, Price CJ. Predicting outcome and recovery after stroke with lesions extracted from MRI images. *Neuroimage Clin* (2013) 2:424–33. doi:10.1016/j.nicl.2013.03.005
8. Hope TA, Kvitting JPE, Hope MD, Miller DC, Markl M, Herfkens RJ. Evaluation of Marfan patients status post valve-sparing aortic root replacement with 4D flow. *Magn Reson Imaging* (2013) 31(9):1479–84. doi:10.1016/j.mri.2013.04.003
9. van Berckel BN, Bossong MG, Boellaard R, Kloet R, Schuitemaker A, Caspers E, et al. Microglia activation in recent-onset schizophrenia: a quantitative (<sup>11</sup>C)-[PK11195 positron emission tomography study. *Biol Psychiatry* (2008) 64(9):820–2. doi:10.1016/j.biopsych.2008.04.025
10. Doorduin J, de Vries EFJ, Willemsen ATM, de Groot JC, Dierckx RA, Klein HC. Neuroinflammation in schizophrenia-related psychosis: a PET study. *J Nucl Med* (2009) 50(11):1801–7. doi:10.2967/jnumed.109.066647
11. Bloomfield PS, Selvaraj S, Veronese M, Rizzo G, Bertoldo A, Owen DR, et al. Microglial activity in people at ultra high risk of psychosis and in schizophrenia: an [<sup>11</sup>C]PBR28 PET brain imaging study. *Am J Psychiatry* (2016) 173(1):44–52. doi:10.1176/appi.ajp.2015.14101358
12. Shi J, Levinson DF, Duan J, Sanders AR, Zheng Y, Pe'er I, et al. Common variants on chromosome 6p22.1 are associated with schizophrenia. *Nature* (2009) 460(7256):753–7. doi:10.1038/nature08192
13. Stefansson H, Ophoff RA, Steinberg S, Andreassen OA, Cichon S, Rujescu D, et al. Common variants conferring risk of schizophrenia. *Nature* (2009) 460(7256):744–7. doi:10.1038/nature08186
14. Bergen SE, O'Dushlaine CT, Ripke S, Lee PH, Ruderfer DM, Akterin S, et al. Genome-wide association study in a Swedish population yields support for greater CNV and MHC involvement in schizophrenia compared with bipolar disorder. *Mol Psychiatry* (2012) 17(9):880–6. doi:10.1038/mp.2012.73
15. Zhang JP, Malhotra AK. Genetics of schizophrenia: what do we know? *Curr Psychiatr* (2013) 12(3):24–33.
16. Schizophrenia Working Group of the Psychiatric Genomics Consortium. Biological insights from 108 schizophrenia-associated genetic loci. *Nature* (2014) 511(7510):421–7. doi:10.1038/nature13595
17. Sekar A, Bialas AR, de Rivera H, Davis A, Hammond TR, Kamitaki N, et al. Schizophrenia risk from complex variation of complement component 4. *Nature* (2016) 530(7589):177–83. doi:10.1038/nature16549
18. Axelsson R, Martensson E, Alling C. Impairment of the blood-brain barrier as an aetiological factor in paranoid psychosis. *Br J Psychiatry* (1982) 141:273–81. doi:10.1192/bj.p.141.3.273
19. Torrey EF, Albrecht P, Behr DE. Permeability of the blood-brain barrier in psychiatric patients. *Am J Psychiatry* (1985) 142(5):657–8. doi:10.1176/ajp.142.5.657
20. Bauer K, Kornhuber J. Blood-cerebrospinal fluid barrier in schizophrenic patients. *Eur Arch Psychiatry Neurol Sci* (1987) 236(5):257–9. doi:10.1007/BF00380949
21. Kirch DG, Alexander RC, Suddath RL, Papadopoulos NM, Kaufmann CA, Daniel DG, et al. Blood-CSF barrier permeability and central nervous system immunoglobulin G in schizophrenia. *J Neural Transm Gen Sect* (1992) 89(3):219–32. doi:10.1007/BF01250674
22. Severance EG, Gressitt KL, Alaiedini A, Rohleder C, Enning F, Bumb JM, et al. IgG dynamics of dietary antigens point to cerebrospinal fluid barrier or flow dysfunction in first-episode schizophrenia. *Brain Behav Immun* (2015) 44:148–58. doi:10.1016/j.bbi.2014.09.009
23. Dickerson F, Stallings C, Origoni A, Vaughan C, Khushalani S, Leister F, et al. Markers of gluten sensitivity and celiac disease in recent-onset psychosis and multi-episode schizophrenia. *Biol Psychiatry* (2010) 68(1):100–4. doi:10.1016/j.biopsych.2010.03.021
24. Sidhom O, Laadhar L, Zitouni M, Ben Alaya N, Rafrati R, Kallel-Sellami M, et al. Spectrum of autoantibodies in Tunisian psychiatric inpatients. *Immunol Invest* (2012) 41(5):538–49. doi:10.3109/08820139.2012.685537
25. Okusaga O, Yolken RH, Langenberg P, Sleemi A, Kelly DL, Vaswani D, et al. Elevated gliadin antibody levels in individuals with schizophrenia. *World J Biol Psychiatry* (2013) 14(7):509–15. doi:10.3109/15622975.2012.747699
26. Fasano A. Surprises from celiac disease. *Sci Am* (2009) 301(2):54–61. doi:10.1038/scientificamerican0809-54
27. Catassi C. Gluten sensitivity. *Ann Nutr Metab* (2015) 67(Suppl 2):15–26. doi:10.1159/000440990
28. Hadjivassiliou V, Green MH, James RF, Swift SM, Clayton HA, Green IC. Insulin secretion, DNA damage, and apoptosis in human and rat islets of Langerhans following exposure to nitric oxide, peroxynitrite, and cytokines. *Nitric Oxide* (1998) 2(6):429–41. doi:10.1006/niox.1998.0203
29. Hadjivassiliou M, Davies-Jones GA, Sanders DS, Grunewald RA. Dietary treatment of gluten ataxia. *J Neurol Neurosurg Psychiatry* (2003) 74(9):1221–4. doi:10.1136/jnnp.74.9.1221
30. Mittelbronn M, Krober SM, Wersebe A, Weller M, Hewer W, Meyermann R, et al. A 63-year-old man with dementia, ataxia and VI nerve palsy. *Brain Pathol* (2007) 17(4):466–7. doi:10.1111/j.1750-3639.2007.00091\_3.x
31. Brand A, Richter-Landsberg C, Leibfritz D. Multinuclear NMR studies on the energy metabolism of glial and neuronal cells. *Dev Neurosci* (1993) 15(3–5):289–98. doi:10.1159/000111347
32. Chang L, Munsaka SM, Kraft-Terry S, Ernst T. Magnetic resonance spectroscopy to assess neuroinflammation and neuropathic pain. *J Neuroimmune Pharmacol* (2013) 8(3):576–93. doi:10.1007/s11481-013-9460-x
33. Bokemeyer M, Ding XQ, Goldbecker A, Raab P, Heeren M, Arvanitis D, et al. Evidence for neuroinflammation and neuroprotection in HCV infection-associated encephalopathy. *Gut* (2011) 60(3):370–7. doi:10.1136/gut.2010.217976
34. Bagory M, Durand-Dubief F, Ibarrola D, Comte JC, Cotton F, Confavreux C, et al. Implementation of an absolute brain <sup>1</sup>H-MRS quantification method to assess different tissue alterations in multiple sclerosis. *IEEE Trans Biomed Eng* (2012) 59(10):2687–94. doi:10.1109/TBME.2011.2161609
35. Kirov II, Tal A, Babb JS, Herbert J, Gonen O. Serial proton MR spectroscopy of gray and white matter in relapsing-remitting MS. *Neurology* (2013) 80(1):39–46. doi:10.1212/WNL.0b013e31827b1a8c
36. Maddock RJ, Buonocore MH. MR spectroscopic studies of the brain in psychiatric disorders. *Curr Top Behav Neurosci* (2012) 11:199–251. doi:10.1007/7854\_2011\_197
37. Harris JL, Yeh HW, Swerdlow RH, Choi IY, Lee P, Brooks WM. High-field proton magnetic resonance spectroscopy reveals metabolic effects of normal brain aging. *Neurobiol Aging* (2014) 35(7):1686–94. doi:10.1016/j.neurobiolaging.2014.01.018
38. Schwerk A, Alves FD, Pouwels PJ, van Amelsvoort T. Metabolic alterations associated with schizophrenia: a critical evaluation of proton magnetic resonance spectroscopy studies. *J Neurochem* (2014) 128(1):1–87. doi:10.1111/jnc.12398
39. Plitman E, de la Fuente-Sandoval C, Reyes-Madrigal F, Chavez S, Gomez-Cruz G, Leon-Ortiz P, et al. Elevated myo-inositol, choline, and glutamate levels in the associative striatum of antipsychotic-naïve patients with first-episode psychosis: a proton magnetic resonance spectroscopy study with implications for glial dysfunction. *Schizophr Bull* (2016) 42(2):415–24. doi:10.1093/schbul/sbv118
40. Rothermundt M, Ohrmann P, Abel S, Siegmund A, Pedersen A, Ponath G, et al. Glial cell activation in a subgroup of patients with schizophrenia indicated by increased S100B serum concentrations and elevated myo-inositol. *Prog Neuropsychopharmacol Biol Psychiatry* (2007) 31(2):361–4. doi:10.1016/j.pnpbp.2006.09.013
41. Fornite A, Yucel M, Dean B, Wood SJ, Pantelis C. Anatomical abnormalities of the anterior cingulate cortex in schizophrenia: bridging the gap between neuroimaging and neuropathology. *Schizophr Bull* (2009) 35(5):973–93. doi:10.1093/schbul/sbn025
42. Marsman A, van den Heuvel MP, Klomp DW, Kahn RS, Luijten PR, Hulshoff Pol HE. Glutamate in schizophrenia: a focused review and meta-analysis of (<sup>1</sup>H)-MRS studies. *Schizophr Bull* (2013) 39(1):120–9. doi:10.1093/schbul/sbr069
43. Rowland LM, Summerfelt A, Wijtenburg SA, Du X, Chiappelli JJ, Krishna N, et al. Frontal glutamate and gamma-aminobutyric acid levels and their associations with mismatch negativity and digit sequencing task performance in schizophrenia. *JAMA Psychiatry* (2016) 73(2):166–74. doi:10.1001/jamapsychiatry.2015.2680
44. Wijtenburg SA, Gaston FE, Spieker EA, Korenic SA, Kochunov P, Hong LE, et al. Reproducibility of phase rotation STEAM at 3T: focus on glutathione. *Magn Reson Med* (2014) 72(3):603–9. doi:10.1002/mrm.24959
45. Bustillo JR, Rediske N, Jones T, Rowland LM, Abbott C, Wijtenburg SA. Reproducibility of phase rotation stimulated echo acquisition mode at 3T in schizophrenia: emphasis on glutamine. *Magn Reson Med* (2016) 75(2):498–502. doi:10.1002/mrm.25638
46. Provencher SW. Estimation of metabolite concentrations from localized in vivo proton NMR spectra. *Magn Reson Med* (1993) 30(6):672–9. doi:10.1002/mrm.1910300604

47. Harezlak J, Buchthal S, Taylor M, Schifitto G, Zhong J, Daar E, et al. Persistence of HIV-associated cognitive impairment, inflammation, and neuronal injury in era of highly active antiretroviral treatment. *AIDS* (2011) 25(5):625–33. doi:10.1097/QAD.0b013e3283427da7
48. Arnold DL, Matthews PM, Francis GS, O'Connor J, Antel JP. Proton magnetic resonance spectroscopic imaging for metabolic characterization of demyelinating plaques. *Ann Neurol* (1992) 31(3):235–41. doi:10.1002/ana.410310302
49. Bitsch A, Kuhlmann T, Stadelmann C, Lassmann H, Lucchinetti C, Bruck W. A longitudinal MRI study of histopathologically defined hypointense multiple sclerosis lesions. *Ann Neurol* (2001) 49(6):793–6. doi:10.1002/ana.1053
50. Young AC, Yiannoutsos CT, Hegde M, Lee E, Peterson J, Walter R, et al. Cerebral metabolite changes prior to and after antiretroviral therapy in primary HIV infection. *Neurology* (2014) 83(18):1592–600. doi:10.1212/wnl.0000000000000932
51. Grover VP, Pavese N, Koh SB, Wylezinska M, Saxby BK, Gerhard A, et al. Cerebral microglial activation in patients with hepatitis C: in vivo evidence of neuroinflammation. *J Viral Hepat* (2012) 19(2):e89–96. doi:10.1111/j.1365-2893.2011.01510.x
52. Rowland LM, Krause BW, Wijtenburg SA, McMahon RP, Chiappelli J, Nugent KL, et al. Medial frontal GABA is lower in older schizophrenia: a MEGA-PRESS with macromolecule suppression study. *Mol Psychiatry* (2016) 21(2):198–204. doi:10.1038/mp.2015.34
53. Wijtenburg SA, Wright SN, Korenic SA, Gaston FE, Ndubuiwu N, Chiappelli J, et al. Altered glutamate and regional cerebral blood flow levels in schizophrenia: a 1H-MRS and pCASL study. *Neuropsychopharmacology* (2017) 42(2):562–71. doi:10.1038/npp.2016.172
54. Trepanier MO, Hopperton KE, Mizrahi R, Mechawar N, Bazinet RP. Postmortem evidence of cerebral inflammation in schizophrenia: a systematic review. *Mol Psychiatry* (2016) 21(8):1009–26. doi:10.1038/mp.2016.90
55. Brekke OH, Sandlie I. Therapeutic antibodies for human diseases at the dawn of the twenty-first century. *Nat Rev Drug Discov* (2003) 2(1):52–62. doi:10.1038/nrd984
56. Beumer W, Drexhage RC, De Wit H, Versnel MA, Drexhage HA, Cohen D. Increased level of serum cytokines, chemokines and adipokines in patients with schizophrenia is associated with disease and metabolic syndrome. *Psychoneuroendocrinology* (2012) 37(12):1901–11. doi:10.1016/j.psyneuen.2012.04.001
57. Guo J, Clausen DM, Beumer JH, Parise RA, Egorin MJ, Bravo-Altamirano K, et al. In vitro cytotoxicity, pharmacokinetics, tissue distribution, and metabolism of small-molecule protein kinase D inhibitors, kb-NB142-70 and kb-NB165-09, in mice bearing human cancer xenografts. *Cancer Chemother Pharmacol* (2013) 71(2):331–44. doi:10.1007/s00280-012-2010-z
58. Drexhage RC, Knijff EM, Padmos RC, Heul-Nieuwenhuijzen LVD, Beumer W, Versnel MA, et al. The mononuclear phagocyte system and its cytokine inflammatory networks in schizophrenia and bipolar disorder. *Expert Rev Neurother* (2010) 10(1):59–76. doi:10.1586/ern.09.144
59. Drexhage RC, Hoogenboezem TA, Cohen D, Versnel MA, Nolen WA, van Beveren NJ, et al. An activated set point of T-cell and monocyte inflammatory networks in recent-onset schizophrenia patients involves both pro-and anti-inflammatory forces. *Int J Neuropsychopharmacol* (2011) 14(6):746–55. doi:10.1017/S1461145710001653
60. Leonard BE, Schwarz M, Myint AM. The metabolic syndrome in schizophrenia: is inflammation a contributing cause? *J Psychopharmacol* (2012) 26 (5 Suppl):33–41. doi:10.1177/0269881111431622
61. Miller BH, Zeier Z, Xi L, Lanz TA, Deng S, Strathmann J, et al. microRNA-132 dysregulation in schizophrenia has implications for both neurodevelopment and adult brain function. *Proc Natl Acad Sci U S A* (2012) 109(8):3125–30. doi:10.1073/pnas.1113793109
62. Mondelli V, Howes O. Inflammation: its role in schizophrenia and the potential anti-inflammatory effects of antipsychotics. *Psychopharmacology (Berl)* (2014) 231(2):317. doi:10.1007/s00213-013-3383-3
63. Severance EG, Alaeddini A, Yang S, Halling M, Gressitt KL, Stallings CR, et al. Gastrointestinal inflammation and associated immune activation in schizophrenia. *Schizophr Res* (2012) 138(1):48–53. doi:10.1016/j.schres.2012.02.025
64. Severance EG, Gressitt KL, Stallings CR, Origoni AE, Khushalani S, Leweke FM, et al. Discordant patterns of bacterial translocation markers and implications for innate immune imbalances in schizophrenia. *Schizophr Res* (2013) 148(1):130–7. doi:10.1016/j.schres.2013.05.018
65. Steiner J, Bogerts B, Sarnyai Z, Walter M, Gos T, Bernstein H-G, et al. Bridging the gap between the immune and glutamate hypotheses of schizophrenia and major depression: potential role of glial NMDA receptor modulators and impaired blood-brain barrier integrity. *World J Biol Psychiatry* (2012) 13(7):482–92. doi:10.3109/15622975.2011.583941
66. Stojanovic A, Martorell L, Montalvo I, Ortega L, Monseny R, Vilella E, et al. Increased serum interleukin-6 levels in early stages of psychosis: associations with at-risk mental states and the severity of psychotic symptoms. *Psychoneuroendocrinology* (2014) 41:23–32. doi:10.1016/j.psyneuen.2013.12.005
67. Bustillo J, Barrow R, Paz R, Tang J, Seraji-Bozorgzad N, Moore GJ, et al. Long-term treatment of rats with haloperidol: lack of an effect on brain N-acetyl aspartate levels. *Neuropsychopharmacology* (2006) 31(4):751–6. doi:10.1038/sj.npp.1300874

**Conflict of Interest Statement:** The authors declare that the research was conducted in the absence of any commercial or financial relationships that could be construed as a potential conflict of interest.

Copyright © 2017 Rowland, Demyanovich, Wijtenburg, Eaton, Rodriguez, Gaston, Cihakova, Talor, Liu, McMahon, Hong and Kelly. This is an open-access article distributed under the terms of the Creative Commons Attribution License (CC BY). The use, distribution or reproduction in other forums is permitted, provided the original author(s) or licensor are credited and that the original publication in this journal is cited, in accordance with accepted academic practice. No use, distribution or reproduction is permitted which does not comply with these terms.

# Advantages of publishing in Frontiers



## OPEN ACCESS

Articles are free to read for greatest visibility and readership



## FAST PUBLICATION

Around 90 days from submission to decision



## HIGH QUALITY PEER-REVIEW

Rigorous, collaborative, and constructive peer-review



## TRANSPARENT PEER-REVIEW

Editors and reviewers acknowledged by name on published articles



## REPRODUCIBILITY OF RESEARCH

Support open data and methods to enhance research reproducibility



## DIGITAL PUBLISHING

Articles designed for optimal readership across devices



FOLLOW US  
@frontiersin



IMPACT METRICS  
Advanced article metrics track visibility across digital media



EXTENSIVE PROMOTION  
Marketing and promotion of impactful research



LOOP RESEARCH NETWORK  
Our network increases your article's readership

### Frontiers

Avenue du Tribunal-Fédéral 34  
1005 Lausanne | Switzerland

Visit us: [www.frontiersin.org](http://www.frontiersin.org)

Contact us: [info@frontiersin.org](mailto:info@frontiersin.org) | +41 21 510 17 00